

Technical Report Documentation Page

1. REPORT No.

CA-DOT-TR-1115-1-73-02

2. GOVERNMENT ACCESSION No.

3. RECIPIENT'S CATALOG No.

4. TITLE AND SUBTITLE

Detectors for Automatic Fog-Warning Signs

5. REPORT DATE

November 1973

7. AUTHOR(S)

W.R. Juergens

6. PERFORMING ORGANIZATION

13-351-601115

8. PERFORMING ORGANIZATION REPORT No.

CA-DOT-TR-1115-1-73-02

9. PERFORMING ORGANIZATION NAME AND ADDRESS

Traffic Branch
California Division of Highways
Sacramento, CA 95807

10. WORK UNIT No.

11. CONTRACT OR GRANT No.

12. SPONSORING AGENCY NAME AND ADDRESS

California Department of Transportation
Sacramento, California 95807

13. TYPE OF REPORT & PERIOD COVERED

Final Report

14. SPONSORING AGENCY CODE

15. SUPPLEMENTARY NOTES

16. ABSTRACT

This report discusses efforts to provide fog warning signs to alert motorists of reduced visibility ahead during foggy conditions. Fog sensors were connected to changeable message signs to provide notice to the motorist of dense fog ahead. The fog study was coordinated with California Highway Patrol.

17. KEYWORDS

Fog, automatic fog detectors, fog detectors, fog warning system

18. No. OF PAGES:

18

19. DRI WEBSITE LINK

<http://www.dot.ca.gov/hq/research/researchreports/1973/73-51.pdf>

20. FILE NAME

73-51.pdf

4775

HIGHWAY RESEARCH REPORT

LIBRARY COPY

Transportation Laboratory

DETECTORS FOR AUTOMATIC

FOG-WARNING SIGNS

PART 1

73-51
DND

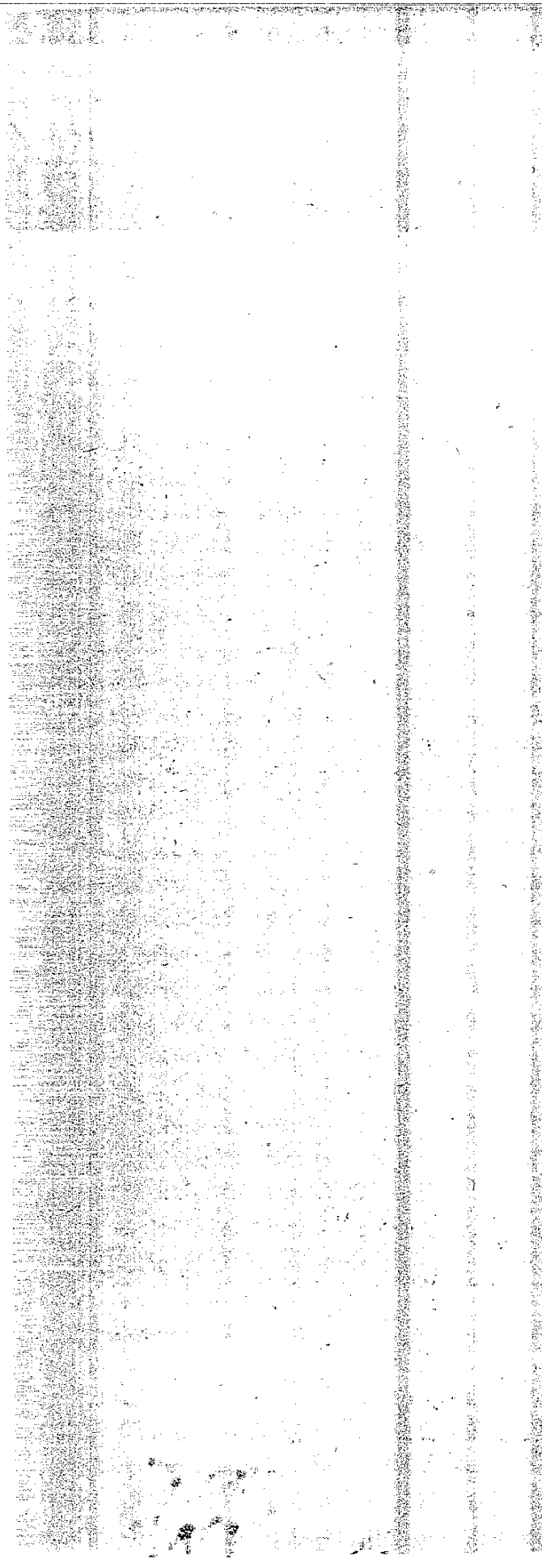
STATE OF CALIFORNIA
Business and Transportation Agency
Department of Transportation
Division of Highways

TRAFFIC BRANCH
A. C. ESTEP, Traffic Engineer
Research Report
CA-DOT-TR-1115-1-73-02

Prepared by: W. R. Juergens

November, 1973

73-51
DND



1. Report No.		2. Government Accession No.		3. Recipient's Catalog No.	
4. Title and Subtitle Detectors for Automatic Fog-Warning Signs				5. Report Date November 1973	
				6. Performing Organization Code 13-351-601115	
7. Author(s) W. R. Juergens				8. Performing Organization Report No. CA-DOT-TR-1115-1-73-02	
				10. Work Unit No.	
9. Performing Organization Name and Address Traffic Branch California Division of Highways Sacramento, CA 95807				11. Contract or Grant No.	
				13. Type of Report and Period Covered Final Report	
12. Sponsoring Agency Name and Address California Department of Transportation Sacramento, California 95807				14. Sponsoring Agency Code	
				15. Supplementary Notes	
16. Abstract This report discusses efforts to provide fog warning signs to alert motorists of reduced visibility ahead during foggy conditions. Fog sensors were connected to changeable message signs to provide notice to the motorist of dense fog ahead. The fog study was coordinated with the California Highway Patrol.					
17. Key Words Fog, automatic fog detectors, fog detectors, fog warning system			18. Distribution Statement unlimited		
19. Security Classif. (of this report) Unclassified		20. Security Classif. (of this page) Unclassified		21. No. of Pages 18	22. Price

[The page contains extremely faint and illegible text, likely a document or report, with significant noise and artifacts.]

DEPARTMENT OF TRANSPORTATION
DIVISION OF HIGHWAYS
1120 N Street
Sacramento, California 95814



Final Report
601115

Mr. J. A. Legarra
Deputy State Highway Engineer

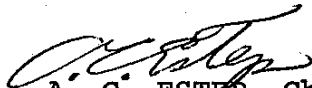
Dear Sir:

Submitted herewith is a final research report titled:

"DETECTORS FOR AUTOMATIC FOG-WARNING SIGNS"

By

W. R. Juergens


A. C. ESTEP, Chief
Traffic Branch

Approval Recommended:

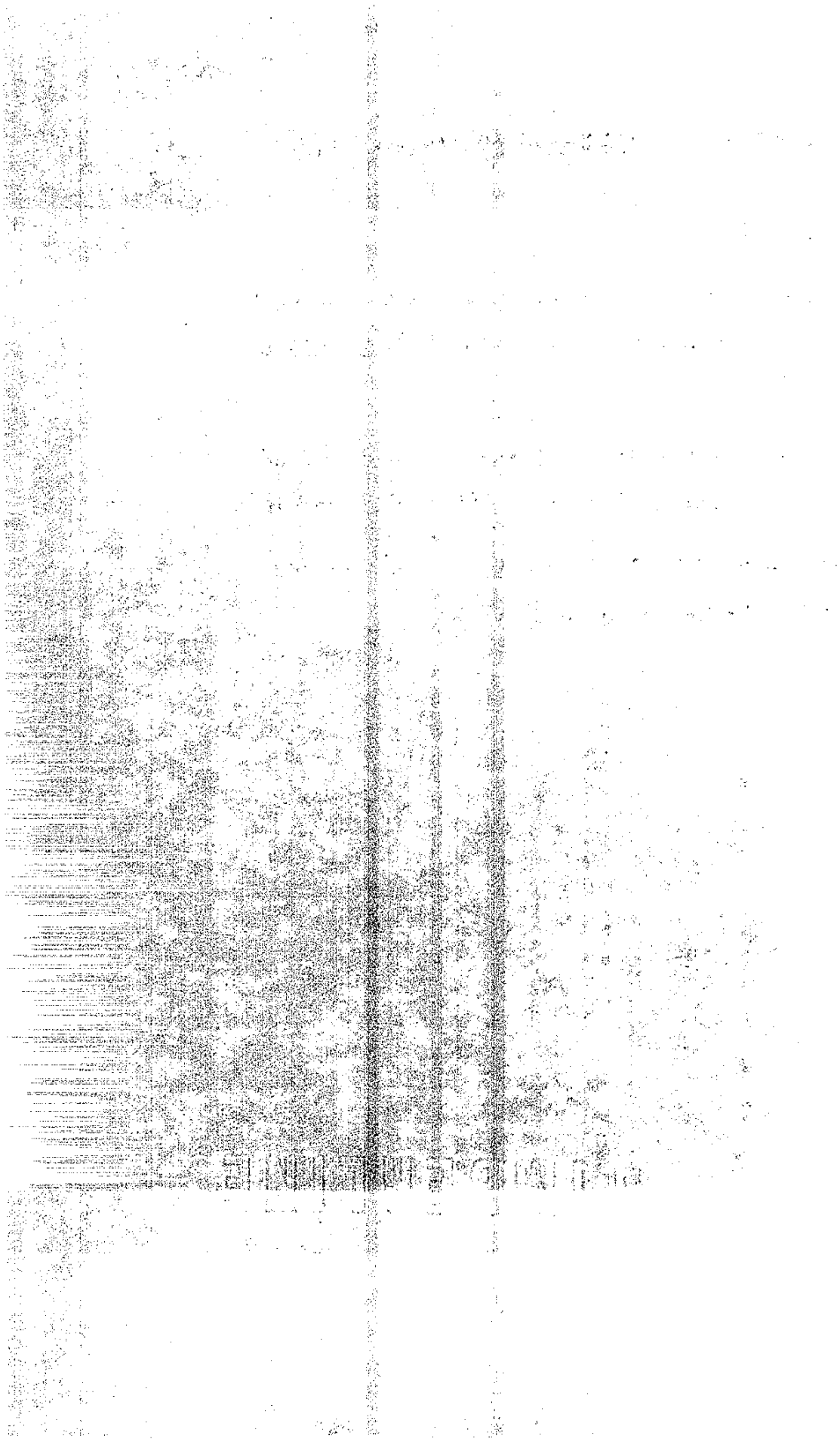

G. L. RUSSELL, Chief
Office of System Operations

Attachment

DETECTORS FOR AUTOMATIC FOG-WARNING SIGNS

PURPOSE OF STUDY:

1. To evaluate various fog detectors and recorders in detecting and measuring the reduction in highway visibility due to fog.
2. To evaluate the ability of the detectors to activate fog-warning messages on changeable message signs.
3. To determine the effect the signs and various warning messages have on drivers.



DETECTORS FOR AUTOMATIC FOG-WARNING SIGNS

The failure of drivers to assess his visual range in fog, and to relate that range to his stopping distance can lead to the chain-type accident.

The situation of driving in light fog (visibility greater than 500 feet) and encountering fog areas of lesser visibility exists in several areas in California. The question is--"How do you notify the motorist of a heavier fog pocket ahead?".

Our approach to investigating this situation was to connect a fog sensor to a changeable message sign. When the visibility was reduced to 300 feet, the message "Dense Fog Ahead" was displayed to the motorist giving notice of conditions ahead.

Several studies have been conducted in California to prevent the multiple vehicle accidents associated with driving in fog. This study focused on one phase of the fog accident problem-- evaluation of fog detectors. Part I of this report is a narrative of the study; Part II describes a preliminary evaluation of the fog detectors.

Our research program on fog studies was advanced a few years when the Environmental Technology Center of Lear Siegler, Inc., Englewood, Colorado, offered for \$1 to provide and install one SM4 transmissometer and recorder in California to detect and

measure the reduction in highway visibility due to fog.

We readily accepted their offer. The Division was to provide at the test site a 20-foot by 150-foot moderately level area enclosed by 6-foot chain link fence with barbed wire around the top.

The California Highway Patrol and Transportation District 10 personnel (1) field-reviewed several possible locations in order to select a test location. The location selected is approximately 50 miles south of Sacramento on Highway 99 in San Joaquin County between Arch Road on the north and Austin Road on the south, a distance of 9.7 miles. The average daily traffic on this section is approximately 30,000 vehicles, of which approximately 15 percent are trucks.

The heaviest of the County's fog pockets is about 6 miles long in this area. The fog is heaviest there because of the low-lying flat valley floor area (elevation 40 to 50 feet) and the proximity to the river. Different from the coastal fog that rolls in from the ocean, the valley is plagued with tule fog, a low-lying fog (radiation type) which rises from the ground when vapors from moist earth are transformed into tiny fog droplets by cool air.

The California Highway Patrol initiated Operation Fog Bound in the Stockton area in 1970. Phase five of their program

was enforcement and the resulting problem of traffic control during dangerous fog periods. A system of caravanning vehicles through dangerous fog areas was developed, utilizing Highway Patrol vehicles as the "pilot" cars; and was given the identification title of "Round Robin". This type of patrol was implemented as necessary when fog conditions restricted normal visibility to a dangerous level.

Data from Operation Fog-Bound Statistics (2) indicated:

Fog Season	68/69	69/70	70/71	71/72
Fog Hours	171	235	217	1,036

Fog hours are defined as all hours in which visibility was restricted due to fog at any location within the area.

The winter season (1972/73) we picked for research of fog detectors had only 163 fog hours. However, we got 23.95 inches of rain instead of the normal 13.37 inches. This was the 4th rainiest year on record.

The compound for the SM4 transmissometer and other detectors was located at the Lathrop Road Interchange. This site was selected because of:

- . Available space
- . Available power
- . Available telephone lines
- . Near the center of the area to be monitored

We received offers from other companies to evaluate their fog detectors. These offers were accepted and a standard agreement for \$1 each was signed with AeroVironment, Inc., Pasadena, California (Highway Fog Monitor); Kahl Scientific Instrument Corp., El Cajon, California (Videograph); and Meteorology Research, Inc., Altadena, California (Fog Visiometer).

The fog detectors are discussed in Part 2 of the report "Detectors for Automatic Fog-Warning Signs" by Bemis, Pinkerman, Shirley, and Skog, July 1973 (CA-DOT-TL-7121-1-73-22).

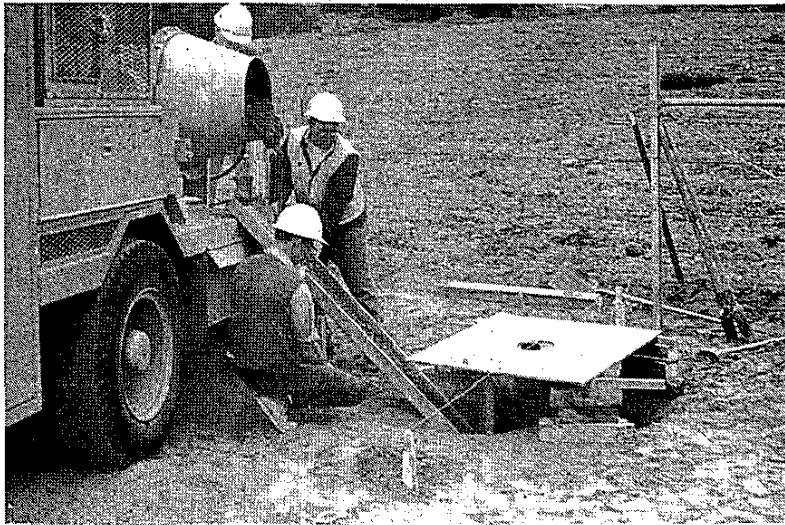


Figure 1
Construction of base for SM4 transmissometer



Figure 2
View of enclosure for fog sensors.
Looking north from Lathrop Road Overcrossing

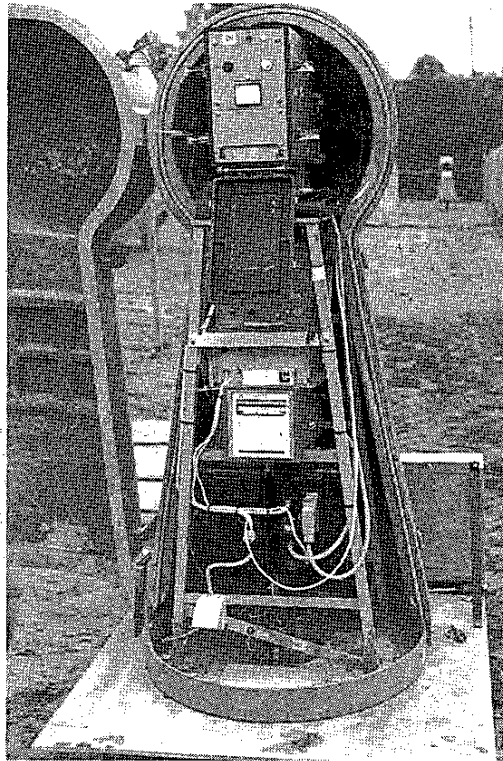


Figure 3 - SM4 Transmissometer

Our next task was to provide a changeable message sign to connect to the fog sensor. We had neither the lead time nor the money to provide a sign bridge over the roadway (this is what we should have provided).

A changeable message display sign (3) manufactured by Display Technology Corporation, Cupertino, California, was selected. It was provided on a monthly rental basis for the period of the fog study.

This sign had not been used on our highway system and we wanted to evaluate its capabilities.

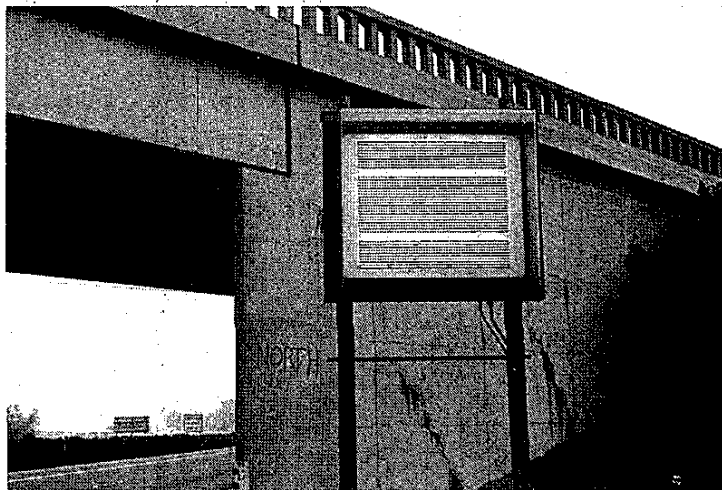


Figure 4
A view of the changeable message sign without any message display

Rather than displaying a blank sign to the motorist for 99 percent of the time during the study period, a safety message was selected, "BUCKLE UP FOR SAFETY".

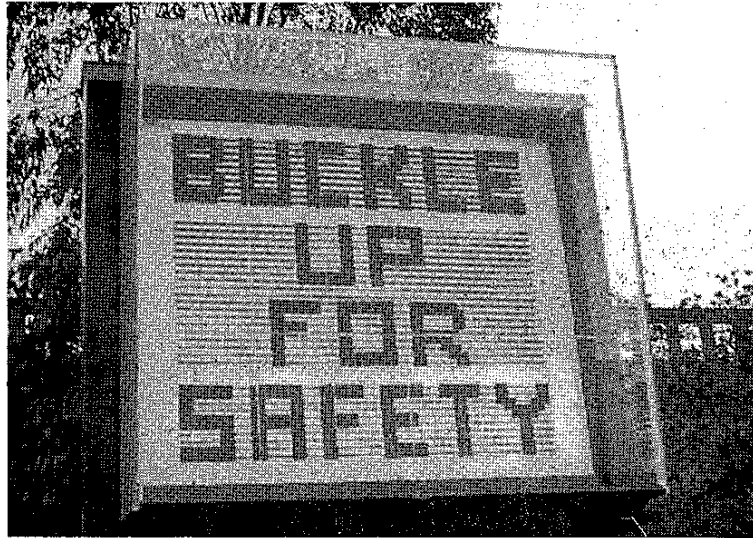


Figure 5

This safety message was displayed until interrupted by a notice of dense fog or notice of accident ahead. The message was cycled to flash every 15 seconds. All messages on the signs were 13-inch letters except the words "WRECK" and "FOG" which were 26 inches,

The signs were connected to the fog sensors using telephone lines.

The fog detector and sign systems were to function as follows:

1. When the visibility dropped to 300 feet, the message "DENSE FOG AHEAD" would be displayed to the motorist giving notice of conditions ahead.



Figure 6

This message was to stay on the sign until the visibility improved to 450 feet. At that time, the message would revert to "BUCKLE UP FOR SAFETY".

2. A console showing sign messages displayed on southbound and northbound signs was placed in the Stockton Highway Patrol Office by Display Technology, Inc. The console

was adequate, easy to use and understand. Buttons were lighted, indicating what message was displayed on each sign.

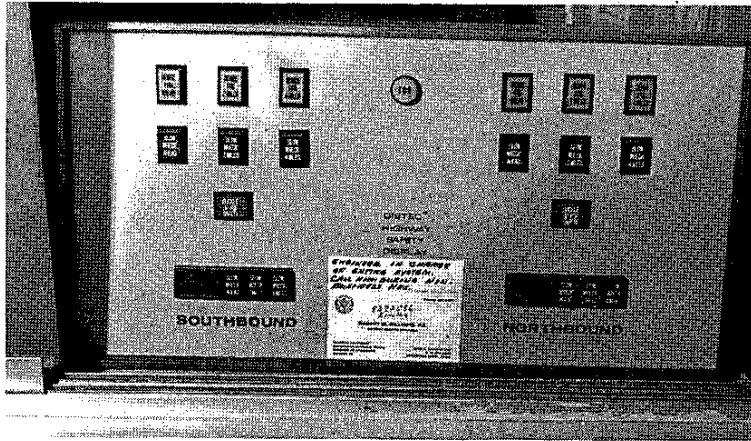


Figure 7
Display Technology Console in Stockton Office
of California Highway Patrol

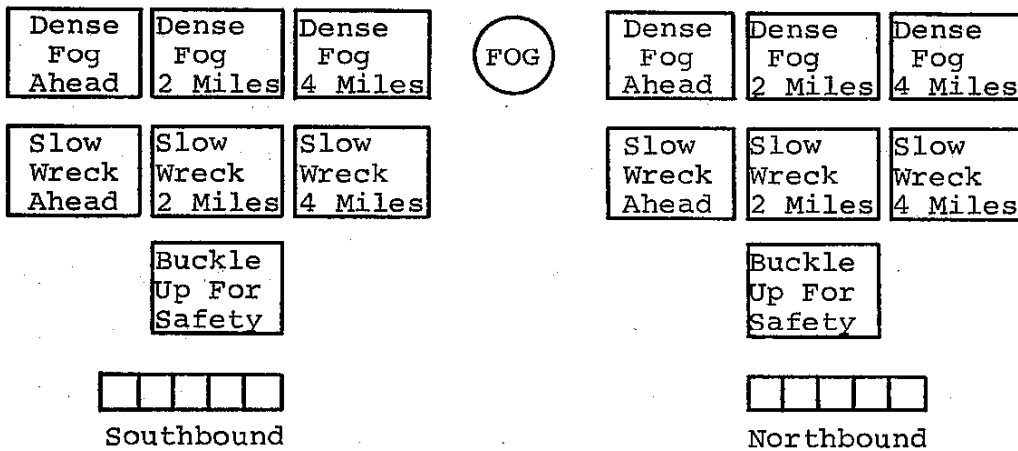


Figure 8
Arrangement of Console with messages available

3. Numerals were painted on each shoulder indicating the mileage along the highway from each fog sign.



Figure 9

Mile Number on Highway

For example, if a dense fog occurred over a short section of highway, the patrol unit would radio the approximate location to the Patrol office. The button "DENSE FOG 2 MILES" for the southbound sign would be pushed to activate the sign, while leaving the northbound sign to read "DENSE FOG AHEAD".

4. In the event a traffic accident occurred, the patrol unit (Figure 10) would radio the location to the officer on duty in the Stockton CHP office (Figure 11), who would activate the sign to read "SLOW! WRECK AHEAD" (Figure 12) or "SLOW! WRECK 2 MILES". If an accident occurred during the period of dense fog, the sign message would alternate "DENSE FOG AHEAD" - "SLOW! WRECK AHEAD".



Figure 10

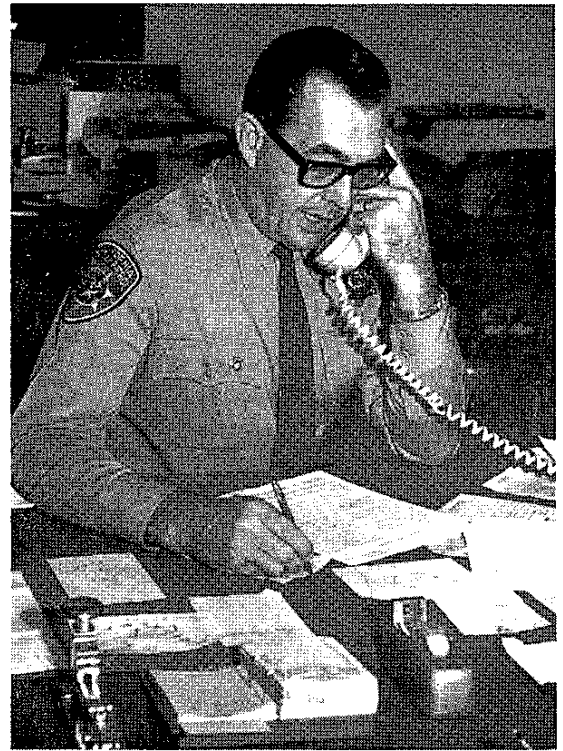


Figure 11



Figure 12

Due to well-coordinated efforts by participating agencies and individual personnel assigned, the study period was meaningful and no accidents occurred.

We learned several things:

- . The location and size of the signs were not effective enough to catch the drivers' eye. Signs should be placed overhead on structures or at more remote locations where other signs or highway features are not competing.
- . There was no evidence that speed was reduced in the control zones while the signs were in operation warning of heavy fog ahead.
- . In a permanent location, consideration should be given to the use of a microwave interconnect between sign and fog detector. Using telephone lines is too costly.
- . A speed advisory system capable of informing drivers of other vehicles' speed beyond the drivers' available sight distance ahead might help in warning drivers of traffic congestion and stoppages ahead.

- (1) Acknowledgment is due to many who contributed substantially to this research project:

From the California Highway Patrol:

Captain C. W. Wynn, Commander, Stockton
Captain G. D. Risenhoover, Commander, Stockton
Sergeant Doug Taylor
Officer Elmer Harper

From Transportation District 10 - Stockton:

Bill Gillespie, District Traffic Engineer
Jack Lobenberg, Asst. District Traffic Engineer
Wilbur Elias, Asst. District Traffic Engineer

- (2) Item 5 of Information Bulletin by California Highway Patrol dated July 1972.
- (3) For more information on types of changeable message signs, please refer to Special Report 129 by the Highway Research Board on "The Changeable Message Concept of Traffic Control". This Special Report contains papers presented at a conference held on July 1971 on the design, operation, and use of changeable message signs.

UBJ 12/22/72

Memorandum

To : Mr. R. J. Dattel
Attention: Mr. A. C. Estep
Traffic Engineer

Date: December 15, 1972
File : 06-Operation Fogbound

From : Department of Public Works—Division of Highways
Fresno - District 6 Traffic

Subject:

At one of the meetings with the California Highway Patrol, Captain Behringer of the Kern County area requested that some sort of a system be devised to help the drivers of the Operation Fogbound vehicles to locate the off-ramps during dense fog. The officers were concerned about having to slow down in order to find the off-ramps - thereby increasing the probability of a rear-end type of accident.

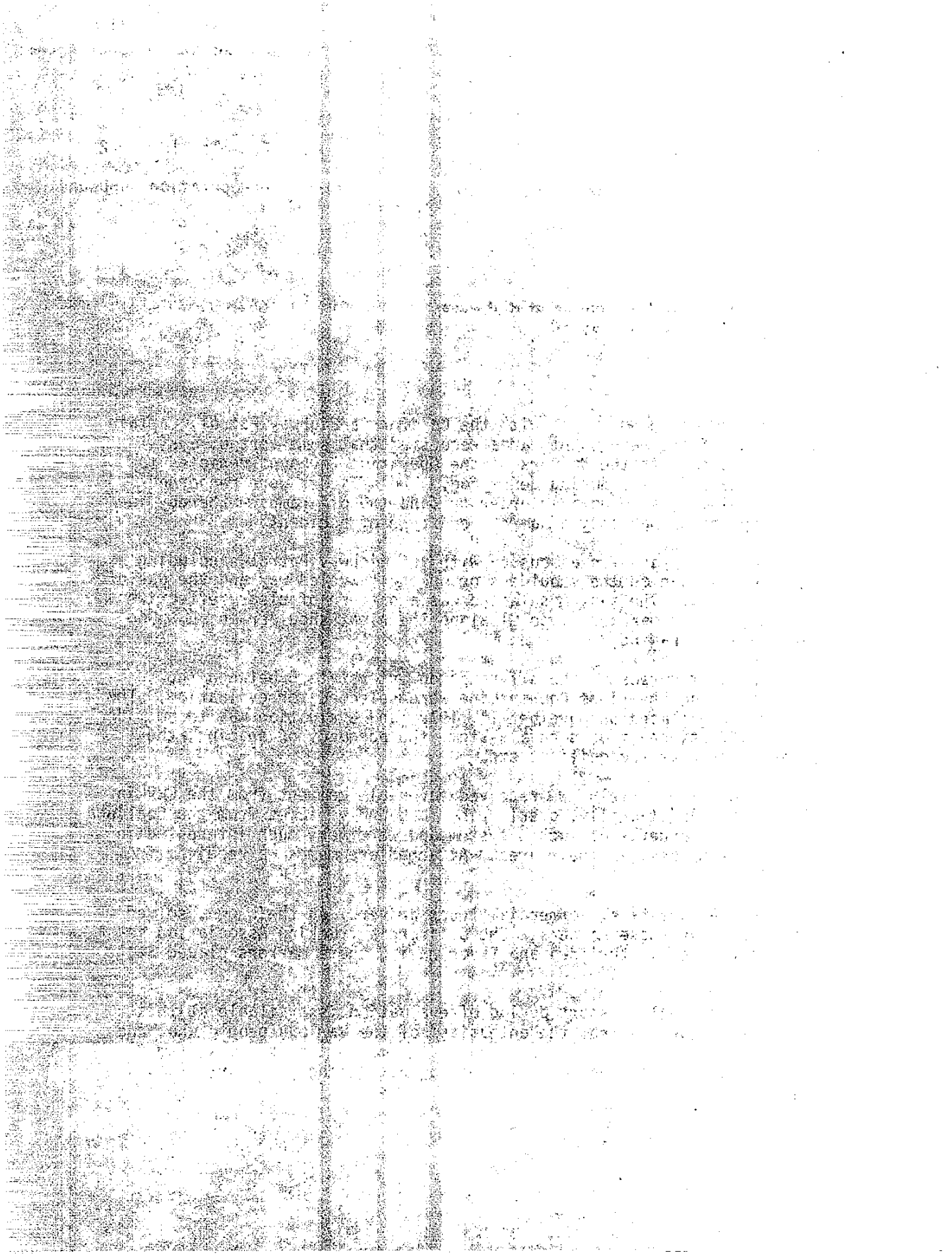
Several ideas were discussed with the Highway Patrol, including striping pattern on the shoulders or on the traveled way and the use of guide markers. The system selected was a pattern of clear reflective raised pavement markers (Type G) along the right shoulder as shown on the attached drawing.

For test purposes, the off-ramps on Interstate 5 between the junction of 99 and the Kings County Line were selected for evaluation. The markers were placed on November 11, 1972, and evaluation was to be made on the effectiveness of such a system, the adequacy of spacing, the pattern for best recognition, etc.

Almost immediately, we received favorable comment from the CHP in that area. Additionally, overlapping fogbound vehicles from the Coalinga area saw the benefit of such a system and were very much interested in having the markers in their area. Attached are memos we received from the CHP.

At the same time, commercial truck drivers, on their own, solved the purpose of these markers. The California Trucking Association is enthusiastic about the idea and favor having these markers placed State-wide.

Although only a short period of evaluation is available at this time, it is obvious from the enthusiasm of the various people who benefited from the information provided by the markers that the system is working quite well - not only in the fog but during all hours of darkness.



Mr. R. J. Datel
Attn: Mr. A. C. Estep

-2-

December 15, 1972

We believe that the information these markers provide can also be helpful to the general public. Therefore, we propose to publicize the markers through the various local news media, the Automobile Clubs and through the Trucking Association magazine.

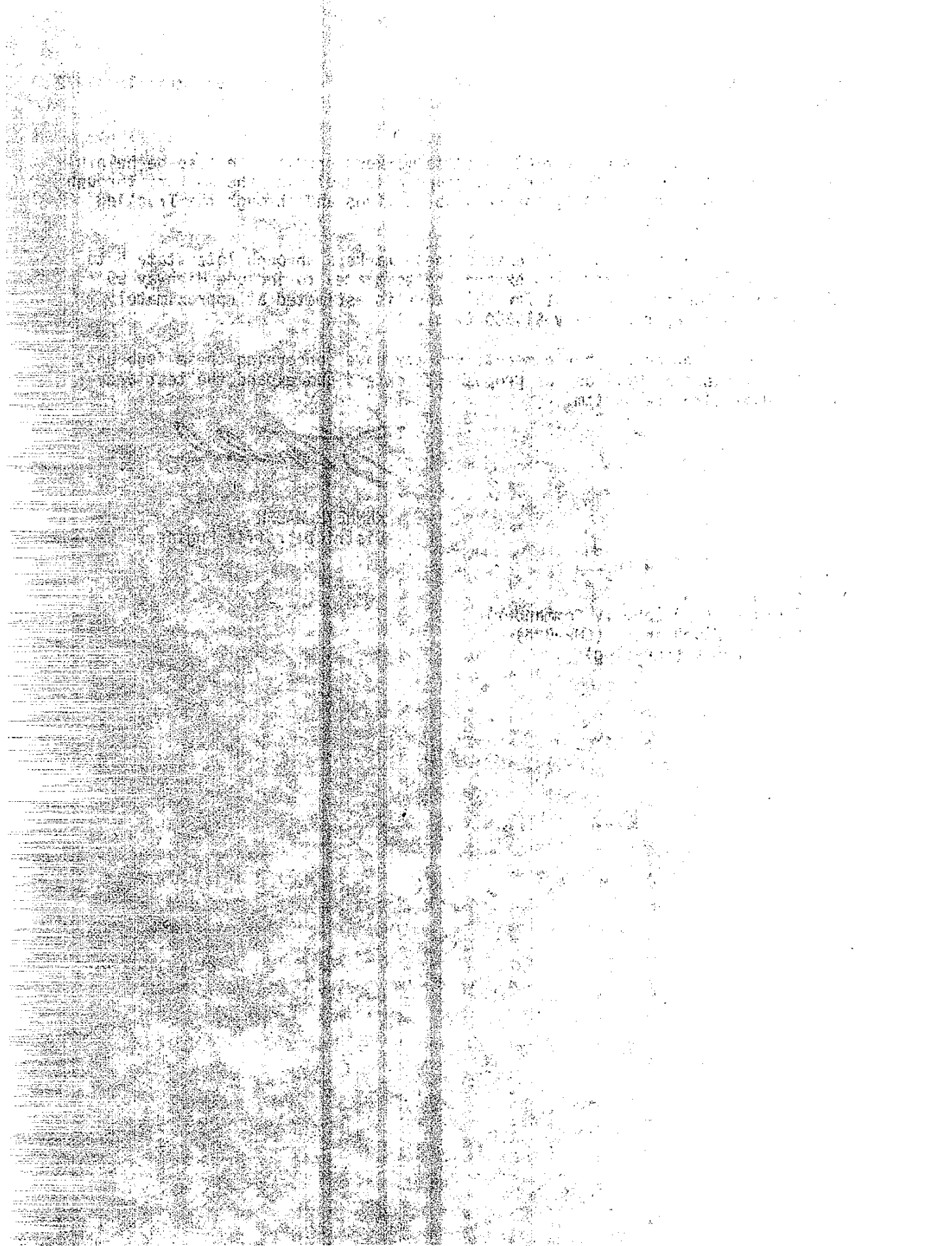
In addition, we propose to extend these markers through Interstate 5 to the Merced County Line and also expand the test area to include Highway 99 through Kern County. The cost for this work is estimated at approximately \$15 per ramp or approximately \$1,300 total.

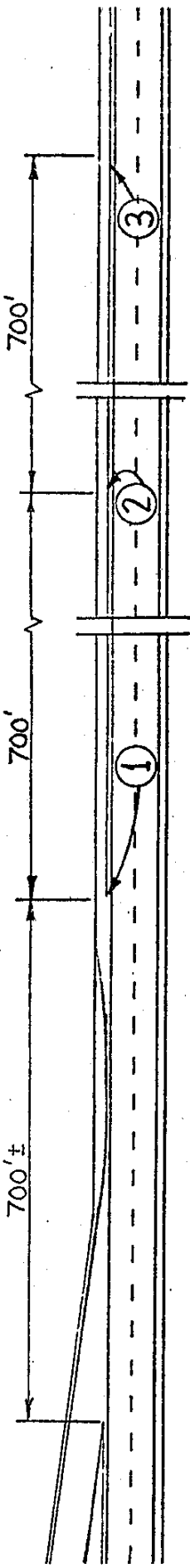
We would appreciate any comments you may have concerning these fogbound, off-ramp markers as well as our proposal to extend and expand the test area and to publicize the system.



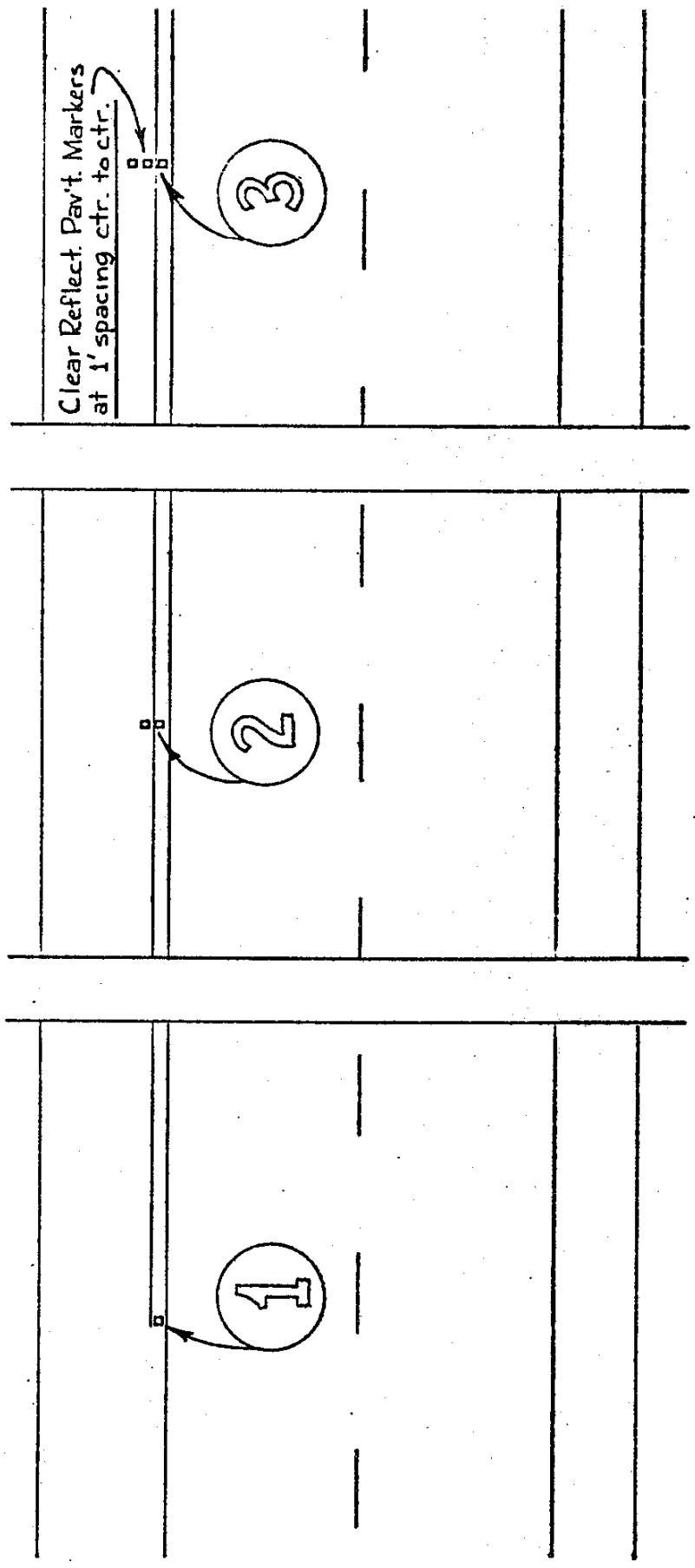
KENNETH WALSH
District Traffic Engineer

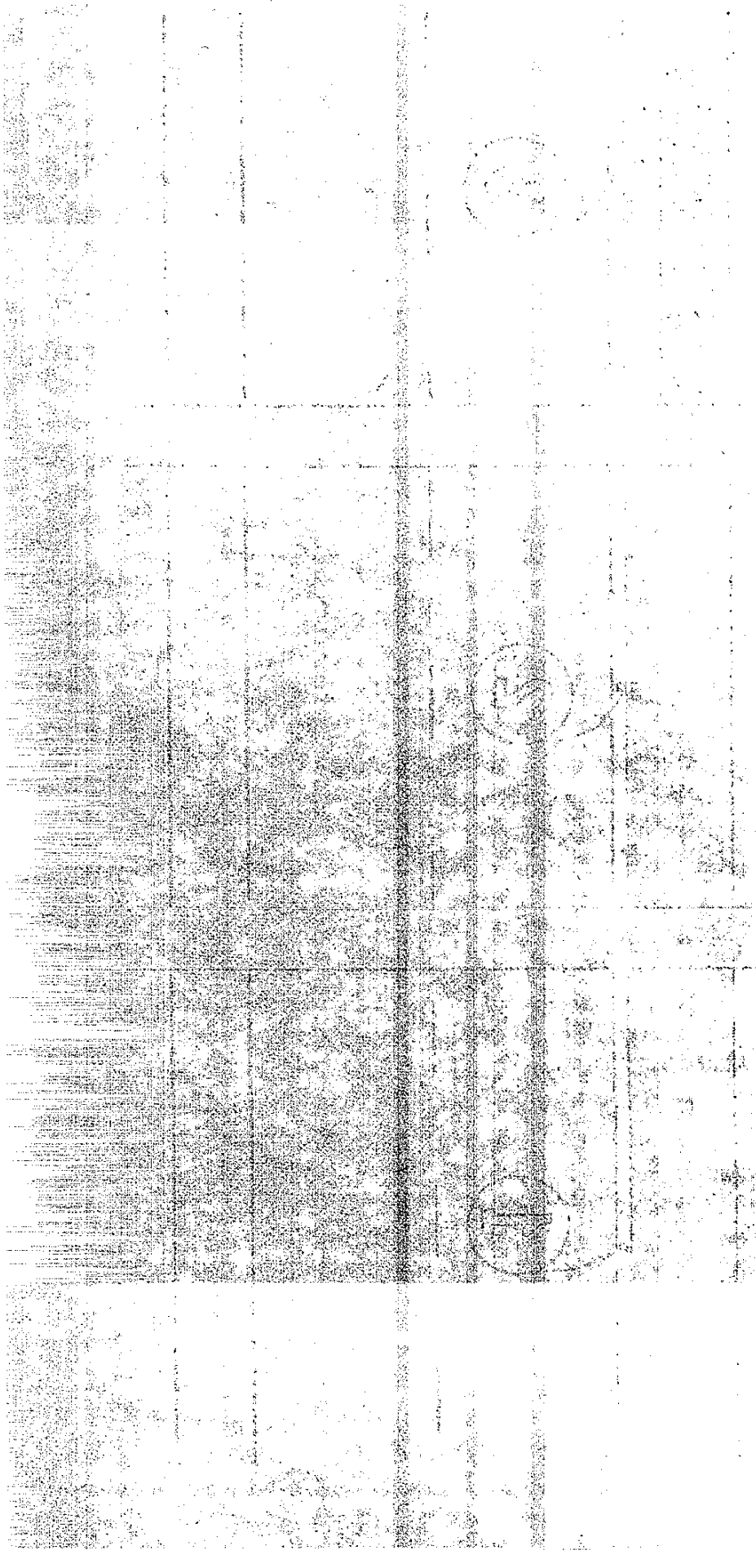
RTY:ga
Attachment
cc: TPHodges (CHP Zone IV Commander)
Captain RGBehringer (CHP-Bkd)
Lt. OERubey (CHP-C1ng)





Clear Reflect. Pav't. Markers
at 1' spacing ctr. to ctr.





HIGHWAY RESEARCH REPORT

DETECTORS FOR AUTOMATIC FOG-WARNING SIGNS

INTERIM REPORT

July, 1973

STATE OF CALIFORNIA
BUSINESS AND TRANSPORTATION AGENCY
DEPARTMENT OF TRANSPORTATION
DIVISION OF HIGHWAYS

TRANSPORTATION LABORATORY

RESEARCH REPORT

CA-DOT-TL-7121-1-73-22

NOTICE

OF THE

DEPARTMENT OF

AGRICULTURE

UNITED STATES

DEPARTMENT OF

AGRICULTURE

UNITED STATES

DEPARTMENT OF

AGRICULTURE

UNITED STATES

DEPARTMENT OF

TECHNICAL REPORT STANDARD TITLE PAGE

1. REPORT NO.		2. GOVERNMENT ACCESSION NO.		3. RECIPIENT'S CATALOG NO.	
4. TITLE AND SUBTITLE Detectors for Automatic Fog-Warning Signs				5. REPORT DATE July 1973	
				6. PERFORMING ORGANIZATION CODE 19701-762501-657121	
7. AUTHOR(S) Bemis, G.R., Pinkerman, K.O., Shirley, E.C. and Skog, J.B.				8. PERFORMING ORGANIZATION REPORT NO. CA-DOT-TL-7121-1-73-22	
9. PERFORMING ORGANIZATION NAME AND ADDRESS Transportation Laboratory California Division of Highways Sacramento, CA 95819				10. WORK UNIT NO.	
				11. CONTRACT OR GRANT NO.	
12. SPONSORING AGENCY NAME AND ADDRESS California Department of Transportation Traffic Branch Sacramento, CA 95807				13. TYPE OF REPORT & PERIOD COVERED Interim Report	
				14. SPONSORING AGENCY CODE	
15. SUPPLEMENTARY NOTES					
16. ABSTRACT The feasibility of using automatic fog detectors in a fog-hazard warning system was investigated. Three fog sensors were installed and evaluated on a comparative basis. Due to atypical meteorology, there was insufficient dense fog for adequate testing. Of the three instruments tested, only the Fog Visiometer supplied by Meterology Research, Incorporated showed promise.					
17. KEY WORDS Fog, automatic fog detectors, fog detectors, fog warning system			18. DISTRIBUTION STATEMENT Unlimited		
19. SECURITY CLASSIF. (OF THIS REPORT) Unclassified		20. SECURITY CLASSIF. (OF THIS PAGE) Unclassified		21. NO. OF PAGES 18	22. PRICE



Interim Report
Trans. Lab. 45311

1958

This is an interim research report titled:

FACTORS FOR AUTOMATIC FOG-WARNING SIGNS

BY

Paul R. Benia, P.E. and Kenneth O. Hankeman
Co-Investigators

Paul C. Shirley, P.E.
Principal Investigator

Under the supervision of
John B. Egan, P.E.

1958

ACKNOWLEDGEMENT

The assistance of Mr. Bill Juergens of the Division of Highways Traffic Branch, who administered the contract, is appreciated. Also, the assistance of the District 10 Traffic Department, who prepared the test site and maintained the instruments, is acknowledged.

The cooperation of Lear Siegler, Inc., Meteorology Research, Inc., Kahl Scientific Instrument Corporation, and AeroVironment, Inc. in providing the automatic Instruments is appreciated.

The contents of this report reflect the views of the Transportation Laboratory which is responsible for the facts and the accuracy of the data presented herein. The contents do not necessarily reflect the official views or policies of the State of California. This report does not constitute a standard, specification, or regulation.

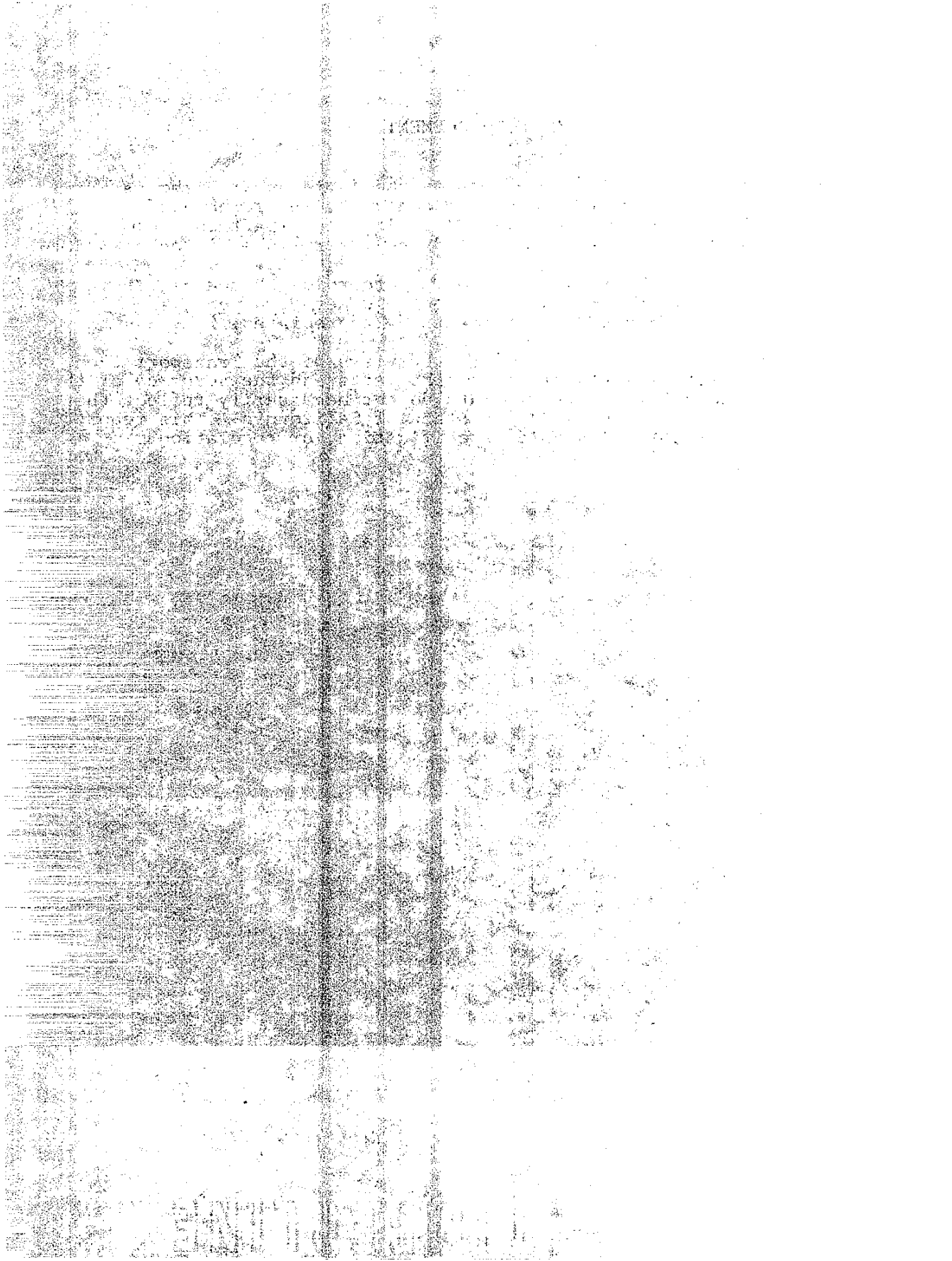
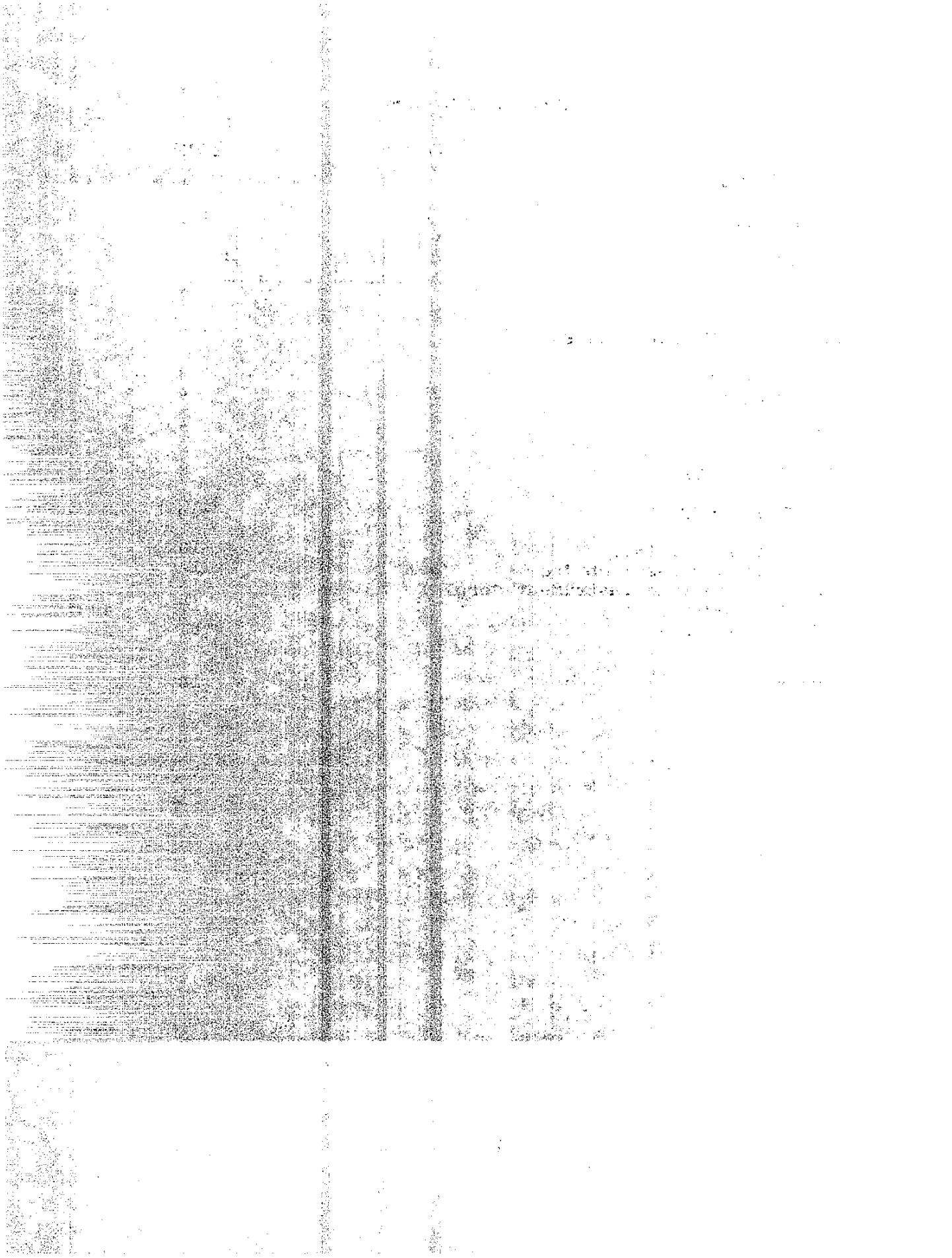


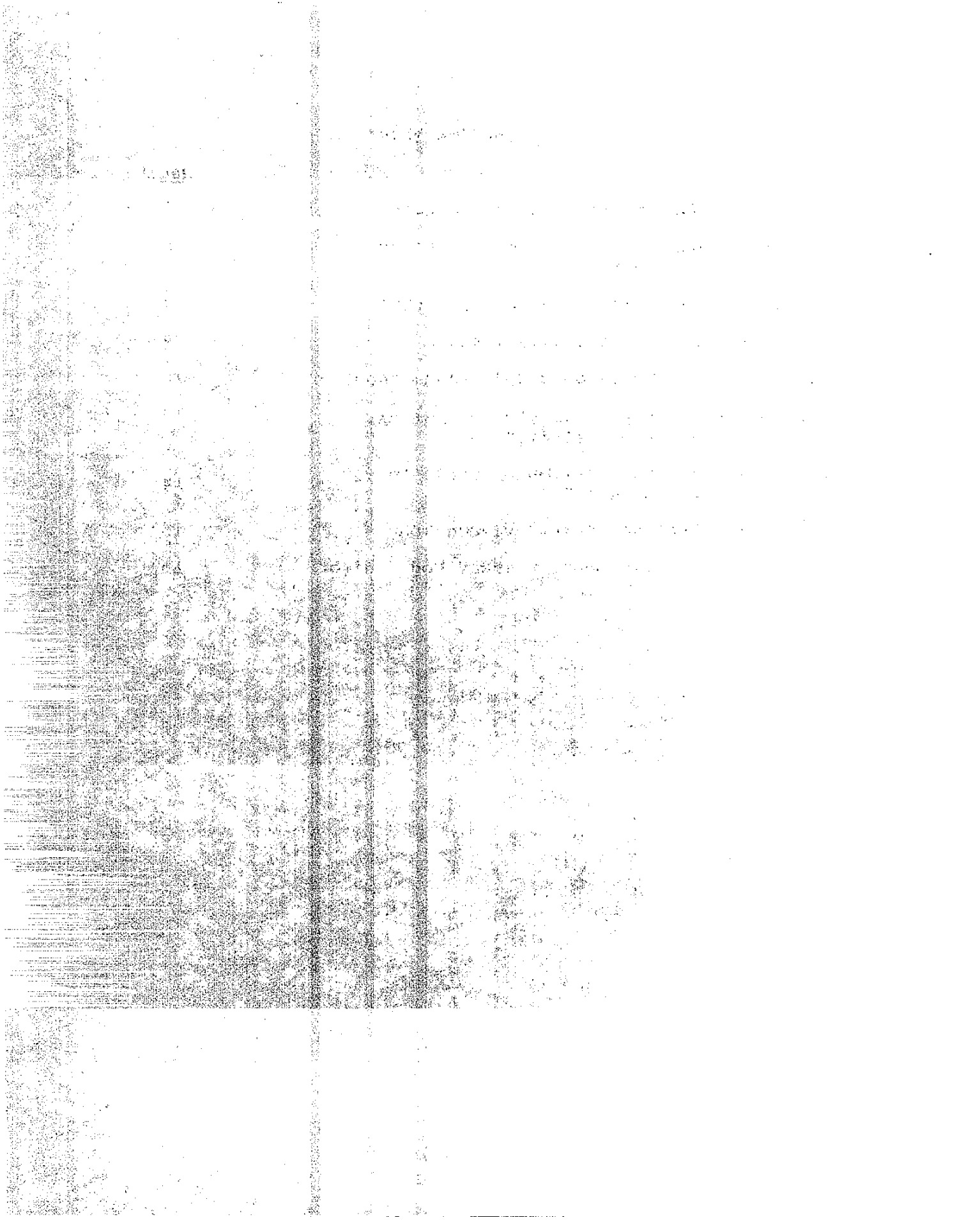
TABLE OF CONTENTS

	<u>Page</u>
ACKNOWLEDGMENT	i
ILLUSTRATIONS	iii
INTRODUCTION	1
CONCLUSIONS	2
A HIGHWAY FOG WARNING SYSTEM	3
Fog Detector	3
Warning Sign	4
TEST PROCEDURE	7
VISIBILITY TARGET	8
INSTRUMENTS TESTED	9
Lear Siegler, Inc.	10
Meteorology Research Inc.	12
Kahl Scientific Instrument Corp.	14
AeroVironment, Inc.	15
Future Studies	16
REFERENCES	18



ILLUSTRATIONS

	<u>Page</u>
Figure 1 - Warning Sign (Close Range)	5
Figure 2 - Warning Sign from several hundred feet distance	5
Figure 3 - Tail Light Visibility target	8
Figure 4 - Unlit Visibility Target	9
Figure 5 - Lear Siegler's SM4 Transmissometer	10
Figure 6 - MRI Fog Visiometer output vs. various visibilities	13
Figure 7 - MRI Fog Visiometer prior to installation	14
Figure 8 - Kahl Scientific Videograph	15
Figure 9 - AeroVironment Highway Fog Monitor	16



INTRODUCTION

Fog has been a persistent problem for both automotive and air-borne traffic for many years. It can be a particularly serious hazard in many places in the State of California, especially where discrete pockets of very dense "radiation" fog form in the Central Valley. As a result, considerable thought and effort has been given to ideas and devices designed to improve traffic safety.

This report describes a preliminary evaluation of an automatic fog warning system that could be used to warn motorists of hazardous driving conditions due to reduced visibility in fog. The study was conducted by the Division of Highways, Transportation Laboratory in cooperation with the Division of Highways, Traffic Branch.

CONCLUSIONS

The lack of dense fog precluded the analysis of a statistical relationship between the estimated visibility and the parameters measured by the automatic fog sensors. Of the instruments examined in this study, it appears that the instrument supplied by Meteorology Research Incorporated has the greatest potential. It was not determined how well visibilities measured by the various instruments were related to visibilities on the highway.

A HIGHWAY FOG WARNING SYSTEM

Various state agencies have been interested in the fog-related highway accident problem for some time. Previously, studies were conducted by the Division of Highways Maintenance Branch to see if it is possible to improve visibility in fog by applying a dispersal agent[1]. Also, the Division of Highways Traffic Branch has studied the effect of changeable signs which displayed the safe driving speed[2]. The California Highway Patrol (CHP) has developed "Operation Fogbound" where the motorist is warned via commercial radio of hazardous driving conditions during periods of dense fog (November through February in the Stockton area). The CHP also leads groups of cars through the fog at a safe driving speed (the "Round Robin" part of Operation Fogbound). Their experience leads them to suggest the following definitions[3]:

Critical fog - visibilities of 200 feet or less.

Dangerous fog - visibilities of 200 feet to 500 feet.

Light fog - fog with a visibility greater than 500 feet.

A highway fog warning system should be composed of at least two warning signs and several automatic fog detectors. The warning signs should be activated when a drastic, dangerous reduction in visibility is encountered.

Fog Detector

Historically, automatic fog detectors have been developed for use at airports and at foggy waterways. They are not always directly suitable for use on the highway. For example, the minimum visibility of interest at airports is about 660 feet (1/8 mile) in increments of 660 feet (eighths of a mile). A highway fog detector should operate over a range of about 50 feet to 1000 feet, within an accuracy of ± 25 feet. A change in visibility of ± 25 feet would correspond to a change in safe driving speed of ± 3 miles per hour (on wet pavement) in the range of 30-60 mph[4]. Typically, the motorist finds himself in trouble when he encounters a rapid change in visibility within the fog. He is aware that he is in fog, but he must be warned of an abrupt and unexpected decrease in his safe driving speed. In order to locate these changes, several fog sensors are required. Ideally, a proper highway fog detector should be inexpensive enough so that several of the instruments could be deployed within a hazardous fog area.

A small, battery powered sensor which would look inconspicuous to the motorist or pedestrian would not need the security of a chain link enclosure if it were built to look like part of an existing piece of roadway equipment such as a guard rail post. Several instruments could be connected by telephone lines and used to activate signs, alert the CHP of possible problem areas, etc.

All of the fog sensors evaluated in this study would require some type of security such as a chain link enclosure. With the exception of the Fog Visiometer, the instruments are fairly large and distracting to the motorist. Although not a requirement, the transmissometer and the AeroVironment Fog Monitor are too large and bulky to be used for any type of mobile operation, but the Fog Visiometer and the Videograph are compact enough to be so employed.

Warning Sign

The warning sign should be large enough so that it is easily visible under adverse conditions. It should probably be in the form of a sign bridge so that it straddles the traffic lanes. Activating flashing yellow lights when a warning message is displayed on the sign would draw motorist's attention to the sign. Having multiple messages on the sign is not really necessary for fog warnings, but may be of value when used in conjunction with another mission (warning of an accident or congestion ahead, for example).

The sign used to alert motorists of adverse driving conditions was provided by Display Technology Corporation of Cupertino, California. The lack of lead time for the study called for the installation of two signs from existing stock. The sign chosen was not sufficiently large to be adequately visible in adverse weather. The locations of the signs were dictated by the requirements of power, guardrail protection, proximity to sensors, and availability of telephone lines which were connected to one of the fog sensors. Although the sign seems large at close range, it does not stand out from its surroundings in either foggy or clear weather.



Figure 1

View of Warning Sign at Close Range

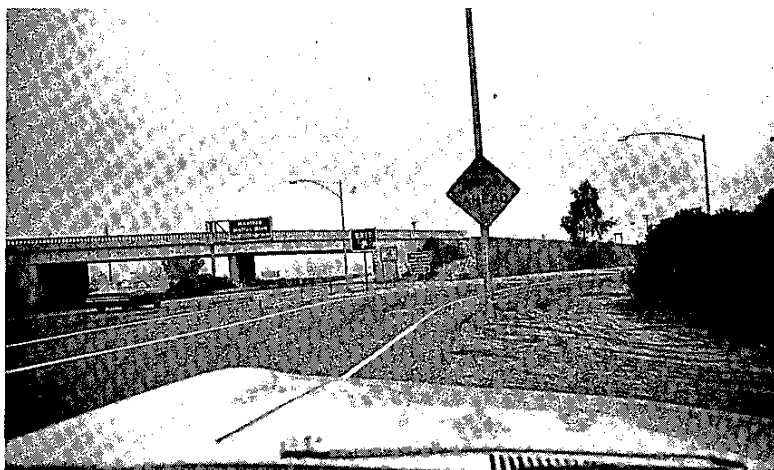


Figure 2

View of Warning Sign from Several Hundred Feet Distance

The message displayed on the signs during periods of adverse visibility is "Dense Fog Ahead". The words "dense" and "ahead" were 13 inches high while the word "fog" was 26 inches high. Since the letters of the words were not in the standard shapes or colors normally used on highways, standard graphs relating letter height to visibility could not be used:

The illumination of the sign was not proper for night time or fog conditions. Field alteration by the supplier led to a great improvement in visibility. During periods of heavy fog, however, the sign was still difficult to observe.

A control board was located at a nearby California Highway Patrol office. The CHP personnel had the option of overriding the automatic fog detectors. They could display fog warning messages and/or wreck ahead messages. They could also input the distance to the hazard.

TEST PROCEDURE

The fog sensors were located in a chain link enclosure about 50 feet from the highway, with the transmissometer placed parallel to the road. Since the enclosure is about 3 feet lower than the traveled way, the sensors were mounted at a 5 foot height in order to sample fog which was about 2 feet above the road.

The actual visibility was obtained by human observers. They approached a lighted tail light until it became visible. This distance was recorded, along with the time of the observation. The procedure was then repeated with an unlit object as the visibility target.

VISIBILITY TARGET

In dense fog with a relatively low background brightness (night time or a deep layer of fog during the day) the object which usually first becomes visible on the roadway is the automobile tail light. When the fog is shallow enough during daylight hours, solid, blocky objects first become visible. For these reasons, the intent of the study was to gather data using a dual definition of visibility:

1. Low background brightness:

Visibility - "that distance at which a person can just discern a 'standard' tail light mounted at an average height above ground".

2. High background brightness:

Visibility - "that distance at which a person can just discern a typical unlit object located adjacent to the highway" (such as a sign or a bridge).

The particular tail light that was chosen is considered to be of "typical" brightness and lighted area. It was mounted at a height of 29 inches above ground in a plywood test stand which was painted grey. The light was powered by a constant voltage power source at the design voltage of the bulb (14.0 volts). This tail light was obtained from a supply of lights evaluated for conformance to federal and state standards[5]. It is the opinion of the conformance testers that the brightness of the light and the lit cross sectional area of the light are typical.



Figure 3

Tail Light Visibility Target

The second visibility target was an unlit highway sign located adjacent to the test site. The tail light was placed next to the sign. The observers slowly traversed the distance between themselves and the targets, moving towards the targets. When the first target became visible (always the tail light in the few observations that were made) the distance was noted. The observers then proceeded until the second target became visible. The observers were driving adjacent to the highway shoulder in an automobile at a low rate of speed at the time they made their observations.



Figure 4

View of Unlit Visibility Target and General
Layout of Site

INSTRUMENTS TESTED

Four fog sensors were installed for the test within a chain-link enclosure. Each fog sensor utilizes a different principle of operation. All measure intensity of light and use a mathematical model to estimate "meteorological visual range". None measure visibility directly. It was felt that if a significant correlation could be obtained between the data outputs of the fog sensors and the actual visibility as measured by a human observer, a statistical equation relating the two could be derived for each of the fog

sensors. This would be possible only if the fog was more or less uniform (brightness, droplet size, etc.), and a different equation would be required if the fog parameters changed significantly.

The intent of the study was to travel to the site during periods of dense fog. At that time, the visibility would be estimated by observing both a "standard" tail light and a typical unlit object. The lack of dense fog at the test site kept us from obtaining data with which to generate the statistical relationships. It is felt that this relationship must be obtained before proceeding with the planning, design, or operation of a fog-hazard warning system.

The four fog sensors and their individual characteristics are described below:

Lear Siegler, Inc - SM4 Transmissometer

This is a double path instrument with a sender-receiver at one location and a reflector 37 meters away. To insure precise optical alignment, large bases must be prepared with a rigid foundation.



Figure 5
SM4 Transmissometer

Special baffles are installed in both units in an attempt to keep the air adjacent to the lenses calm, preventing dust from obscuring the lenses. A beeper was provided in order to keep birds from setting up home in the optical path. The light from the sender is first modulated by a light chopper and then split into two beams. One beam is retained in the unit as a reference beam and the other beam is passed through the fog and back to the receiver. The ratio of the intensities of the two light beams is the transmission:

$$T (\%) = \frac{\text{Final intensity of sample beam}}{\text{Intensity of reference beam}} \times 100$$

The light chopper insures that only the light emitted by the sender is analyzed. Other light sources such as automobile lights and fixed roadway lights do not interfere.

The measured transmission, T, was recorded on a strip chart recorder equipped with a data pen and an event marker. During the test period it became apparent that the instrument was probably out of calibration. Attempts at recalibration were made by the instrument supplier. Although the output should have been 20 mA on a clear day, initially the output was about 18.5 mA and improved to about 19.5 mA after recalibration. However, a check of the strip chart recorder showed that the pen of the recorder consistently recorded about 10% lower than the actual transmission as indicated by the milliamp dial (20 mA = 100% transmission). Ten data pairs (milliamps and strip chart readings) were observed. A regression equation relating the data is:

$$T (\%) = 11.36 + 91.39 \times (\text{chart reading})$$

From the above equation any chart reading may be converted to the appropriate percent transmission. However, any transmission level below about 11% would be recorded as zero. Since 11% transmission corresponds to a visibility of about 315 feet, visibilities below this level were not recorded. Also, the instrument was set to turn on the warning sign when the chart read 10% transmission and off when the chart reading improved to 17%. It was thought that this corresponded to visibilities of about 310 feet and 440 feet respectively. Actually, the transmission levels were 20.5% and 27% and the corresponding visibilities about 500 feet and 600 feet. It is felt that these difficulties can be corrected by a revision in the electrical components between the milliamp dial output and the strip chart recorder.

The range of the instrument depends upon the path length selected for use. At the optimum path length (about 37 meters) the instrument's range is about .05 kilometers (+160 feet) to about 5 kilometers (+16,000 feet). At the low range, a small change in transmission causes a large change in visibility. This means that the transmissometer is not very precise at visibilities below about 300 feet or so.

The cost of purchasing and installing this instrument may preclude its widespread use for highway monitoring.

Meteorology Research, Inc. - Fog Visiometer

This is a short path instrument that measures light scattered forward, sideward, and backward from the main light beam. The sample area is about 1.4 feet in length. The flash lamp is inclined in the forward direction. Electronics are used to compensate for light scattered at angles approaching zero and 180 degrees from the original path of the light beam.

This instrument comes from the factory with instructions for obtaining the following visibilities[6]:

1. Runway Visibility (RVV) - the distance that an observer would observe visually in a given direction using as targets either dark objects against the horizon sky during daytime or unfocused lights of moderate intensity at night. RVV (meters) = $\frac{2.9}{b}$, where b = scattering coefficient as measured by the MRI Fog Visiometer.

2. Meteorological Range (L_{vd}) - the greatest distance at which a sufficiently large black object can be seen against the daytime horizon sky, assuming the eye is able to distinguish differences in contrast of 2%.

$$L_{vd} \text{ (meters)} = \frac{3.9}{b}, \text{ where } b \text{ is as previously defined.}$$

The relationship of either of these visibilities to the visibilities encountered on the highway is not clear. A graph relating highway visibility to the scattering coefficient was published in a report prepared by the California Division of Highways. The visibility target used in this case consisted of actual automobile tail lights[1]. It can be seen from Figure 6 that highway visibility (TSD) is significantly different than either L_{vd} or RVV.

The Fog Visiometer normally is set at a visibility range (L_{vd}) of 260 feet to 20,000 feet, but can be easily calibrated to read 100 feet to 10,000 feet. This second range can be halved or quartered to obtain readings down to 50 feet or 25 feet respectively. This would require the manufacturer to establish another calibration point but would greatly increase the usability of the instrument.

The Fog Visiometer seemed to operate properly once the installation was completed. It was not possible to obtain observations of highway visibility while the Fog Visiometer was installed due to a lack of dense fog at the test site.

MRI FOG VISIOMETER OUTPUT VS VARIOUS VISIBILITIES

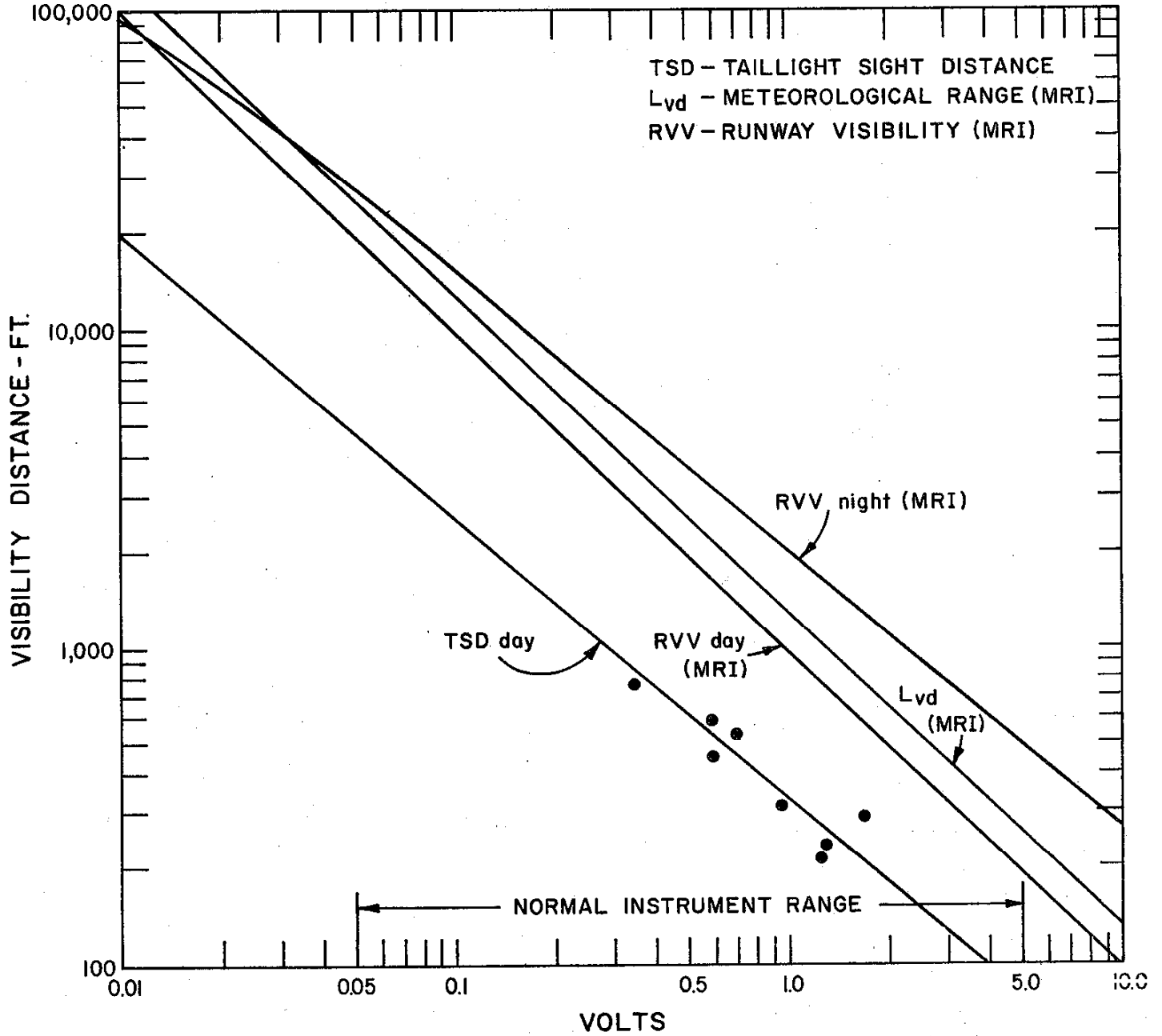


Figure 6
(from Reference I)

When connected to the sign, the CHP felt that the Fog Visiometer was not turning on the fog sign when it should have been. However, the CHP had probably become accustomed to seeing the sign turn on at 500 feet while connected to Lear Siegler's instrument. The Fog Visiometer was set to turn on the sign when the visibility dropped to 300 feet and turn the sign off when the visibility improved to 450 feet.

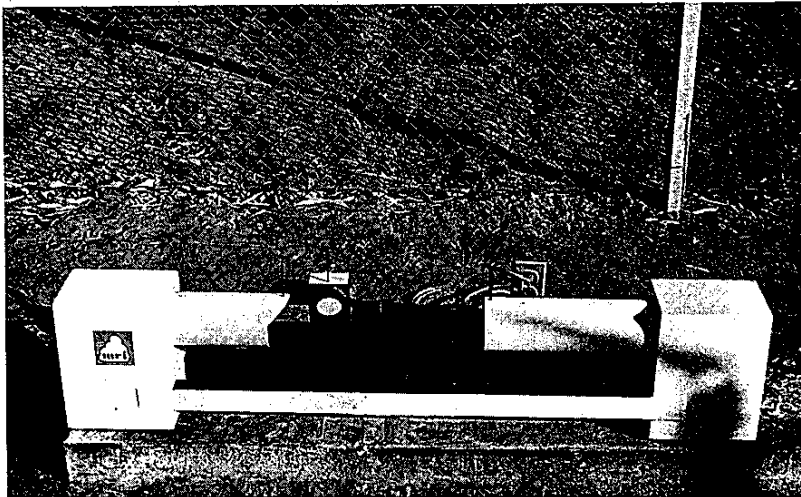


Figure 7

Fog Visiometer before Final Installation
on Pole

During the period of study, no operational problems were observed. The instrument was operated with proper exposure only for two months.

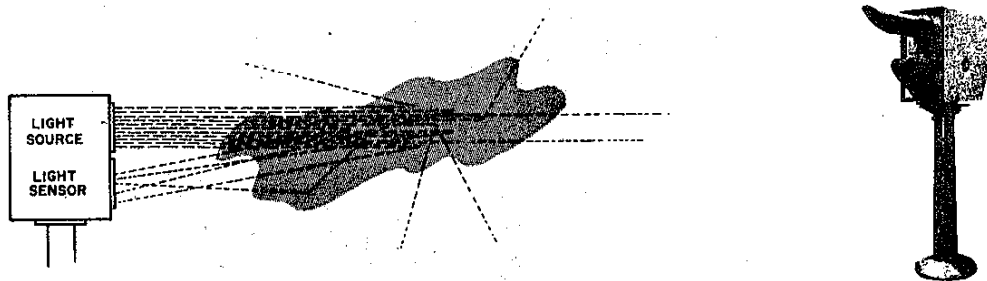
Kahl Scientific - Videograph

The Videograph as supplied by Kahl Scientific is not applicable for use on the highway. The instrument is able to measure a minimum visibility of .06 mile (316 feet). Readings are obtainable only in increments of about 100 feet (or more) since the instrument is graduated in the nearest 5/100 mile at the lower visibilities. Above 0.20 miles, the graduations are in 1/10 mile increments. The maximum range is 6 miles.

The Videograph is a backscatter device which has both the flash unit and the receiver unit mounted on the same stand. The

light that reflects off the fog and back towards the flasher unit is called backscatter light. There is a possibility for backscatter devices to overestimate visibility in a dense fog since absorption losses of light can be significant in this case. Kahl Scientific does not feel that the instrument can be made to function properly below .06 miles [7].

No operational difficulties were encountered. However, the short duration of field exposure (1 month) was not sufficient to demonstrate the instrument's durability



39AM300 VIDEOGRAPH (BACK-SCATTER VISIBILITY MONITORING)

Figure 8

Kahl Scientific Videograph

AeroVironment, Inc. - Highway Fog Monitor

AeroVironment installed a Model 150 Highway Fog Monitor for evaluation. This instrument measures light that is scattered in the forward direction with the direct path of the light blocked by a dark object. The path of the light follows the surface of two cones placed back-to-back with the light scattering from fog in a donut-shaped region where the bases of the cones meet. This donut-shaped region is the sample volume since the geometry of the device only allows light scattered in this region to be sensed at the receiving end.

The light source is near the ground and shines upward a distance of about 4 feet. The instrument flashes the light at a slow rate when the visibility is above 1000 feet and increases the rate of flashing when the visibility drops below 1000 feet.

This instrument was observed to be flashing at the slow rate when the visibility was low (around 250 feet). When notified of this problem, the supplier removed the instrument for servicing and did not return the instrument to the test site. Since this was a prototype instrument, the supplier was not able to replace it with another instrument.

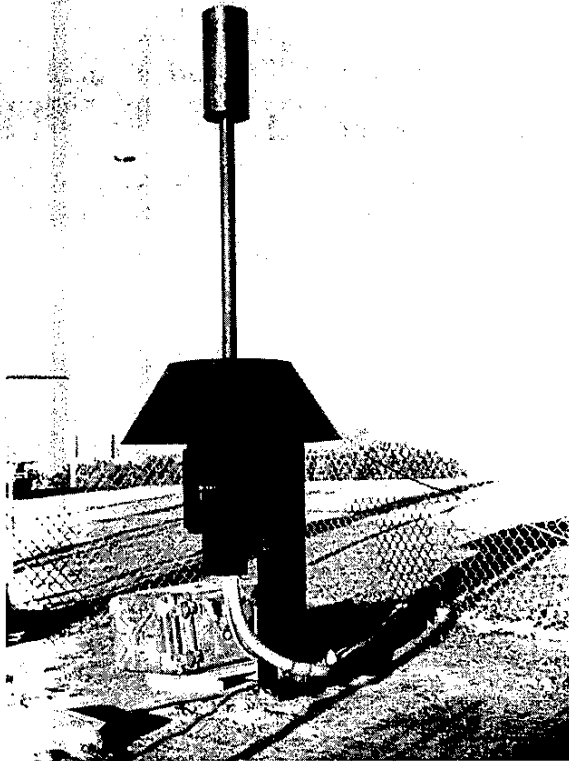


Figure 9

AeroVironment Highway Fog Monitor

Future Studies

It appears that there is a sufficient need for an automatic fog warning system. Much effort has been expended by various agencies in an effort to successfully warn the motorist of unseen dangers. It does not seem feasible at this time to warn the motorist of stopped vehicles (via loop detectors or radar for example). Warning the motorist of reductions in safe driving speed which are beyond his visibility range seems to be the most feasible alternative.

To warn the motorist of changes in driving conditions ahead, it is necessary to have several fog sensing devices. The sensors should be placed in locations that historically experience the most dense fog conditions. Since many automatic fog sensors would be required for this type of system, they must be fairly inexpensive. Extensive field installation would also not be feasible.

Two automatic fog detectors which were not tested, but which may have a great potential are:

- 1) Closed circuit television - This could be directed towards targets placed at incremental distances along the roadway. A count of the number of targets visible (this could be done electronically) would directly yield the existing visibility. The camera also could be directed towards the traffic to inform the Highway Patrol or Traffic Branch of onroad conditions.
- 2) Small Sized Backscatter Device - This device would be very small (about 6" to 8" in greatest dimension) and could be inconspicuously mounted on a guard rail post. It would be operated by a dry cell battery and would emit a low energy light. This instrument would be fairly inexpensive and could be installed in greater numbers than larger, more expensive devices. The feasibility of using a large number of devices would offset the relatively small sample volume.

To overcome difficulties encountered during this period of study with regard to relating actual visibility to instrument visibility, time lapse photography could be used to measure the actual visibility. This would insure that all periods of fog were observed, whether it occurred during working days or not. One of the fog sensors could trigger the camera so that it only operated during periods of reduced visibility. The visibility targets could be square, black objects with lights mounted on one corner. They could be spaced out at 50 feet increments and the number of targets visible would indicate the visibility. Care must be taken to insure that the visibility reduction is due to fog and not dirt on the lens or some other interference. Also, a camera and the human eye do not always perceive contrast in a like manner.

REFERENCES CITED

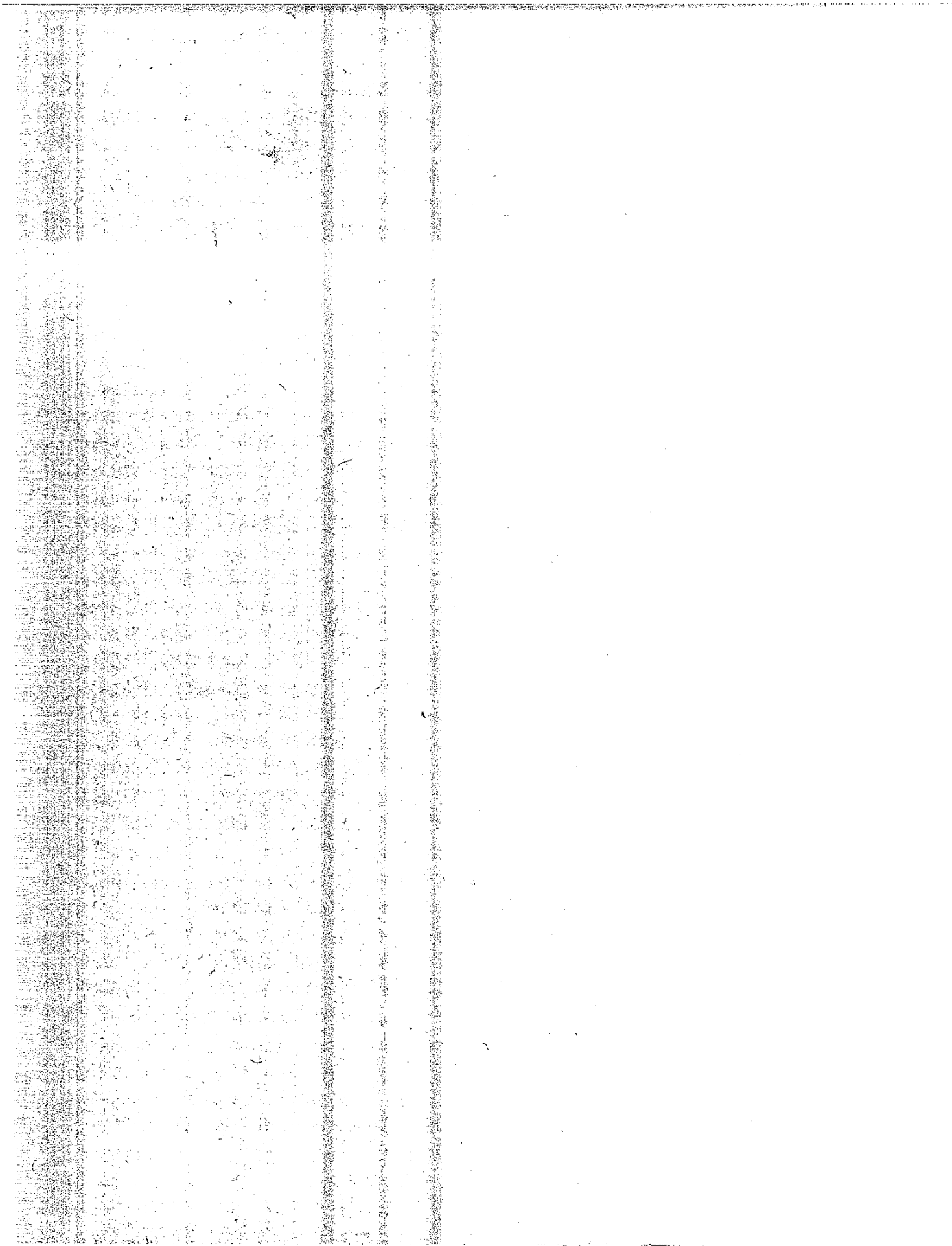
1. Beaton, et al, Stockton Fog Dispersal Study, California Division of Highways, Report No. CA-HWY-MR 657107-1-72-24.
2. Tamburri, T. N., Theobald, D. J., et. al. Reduced Visibility (Fog) Study, California Division of Highways, Headquarters Traffic Department, March 1967.
3. Wynn, C. W., Captain, "Operation Fogbound - Accident Reduction Plan". California Highway Patrol, Stockton area, October 1972,
4. AASHO, "A Policy on Geometric Design of Rural Highways - 1965" American Association of State Highway Officials, 1966.
5. Standards Conformity Evaluation Report No. 2135. California Division of Highways Materials and Research Department, October 1972.
6. "MRI Fog Visiometer Instruction Manual", Fog Visiometer Model 1580, Altadena, California, 1971.
7. Phone conversation with Mr. Gene Jerzewski of Kahl Scientific, February 13, 1973.

REFERENCES UNCITED

8. National Cooperation Highway Research Report 95, Highway Fog, Highway Research Board, 1970.

RECEIVED SACRAMENTO
DIVISION OF HIGHWAYS
MAILS & RES. DEPT.

1973 DEC 20 AM 3 10



STATE OF CALIFORNIA
BUSINESS AND TRANSPORTATION AGENCY
DEPARTMENT OF PUBLIC WORKS
DIVISION OF HIGHWAYS
BRIDGE DEPARTMENT



STRUCTURAL BEHAVIOR
OF A
FLEXIBLE METAL CULVERT
UNDER A DEEP EARTH EMBANKMENT
USING METHOD A BACKFILL

73-50
DND

1. Report No.	2. Government Accession No.	3. Recipient's Catalog No.	
4. Title and Subtitle Structural Behavior of a Flexible Metal Culvert Under a Deep Earth Embankment Using Method A Backfill		5. Report Date June 1973	6. Performing Organization Code 14030
		8. Performing Organization Report No. CA-Hy-BD-624111-73-6	
7. Author(s) David W. Spannagel, Asst. Bridge Engineer Raymond E. Davis, Sr. Bridge Engineer Alfred E. Bacher, Sr. Bridge Engineer		10. Work Unit No.	
9. Performing Organization Name and Address California Division of Highways Bridge Department Research & Development Unit P.O. Box 1499, Sacramento, CA 95807		11. Contract or Grant No. D-4-24	
12. Sponsoring Agency Name and Address U.S. Department of Transportation Federal Highway Administration Washington, D.C.		13. Type of Report and Period Covered Research Final Report 6/65 - 6/73	
		14. Sponsoring Agency Code	
15. Supplementary Notes			
<p>16. Abstract</p> <p>A culvert consisting of twin 108-inch-nominal-diameter structural steel plate pipes was buried under 160 feet of highway embankment at Apple Canyon using Method A backfill. Two cross-sections were heavily instrumented to determine soil pressures, displacements, strains, and settlements at various fill heights and following construction completion.</p> <p>Results indicated that the soil pressures were linear functions of fill height and produced fairly uniform peripheral distributions. Displacements were small. Stresses exceeding the specified minimum yield were observed without apparent structural distress.</p> <p>Theoretical analysis procedures were applied to the installation to determine their relative merit. The finite element procedure proved the best, although sufficient soil property data were not available to predict accurately pipe displacements and stresses.</p> <p>Comparisons were made between this installation and a similar structural plate pipe at Chadd Creek using Method B (baled straw) backfill. The Method A backfill technique was found to be superior to Method B due to the uniformity of pressures, stresses and moments obtained.</p>			
17. Key Words <u>Culverts (Flexible), Design, Earth Pressure, Soil Mechanics, Structural Plate Pipe, Stresses</u>		18. Distribution Statement Unlimited	
19. Security Classif. (of this report) Unclassified	20. Security Classif. (of this page) Unclassified	21. No. of Pages	22. Price

**79-50
OND**

00:27
01:40

ACKNOWLEDGMENTS

The research reported herein was financed in part and conducted in cooperation with the United States Department of Transportation, Federal Highway Administration. The work was performed under the direction of the California Division of Highways, Bridge Department, Research and Development Section. Instrumentation of the field prototype and data acquisition were performed by the California Division of Highways, Materials and Research Department.

The tested prototype was designed by the Bridge Department under the supervision of Mr. A. E. Bacher, Senior Bridge Engineer and co-principal investigator.

Acknowledgment is gratefully extended to Messrs. E. E. Evans, H. D. Nix, G. C. Castleton and L. R. Patterson, of the Bridge Department, for their assistance in computer programming and data reduction; to F. G. Gillenwaters who designed the prototype culvert; to Messrs. W. W. Chow, A. Sequeira, W. Weber and other members of the Materials and Research Department staff for their efforts in providing the data; and to Messrs. W. E. Schaefer, H. Heckerroth, J. J. Webster, T. H. Muhich and their staffs, of District 07, for valuable assistance during the planning and construction phases of this project.

The contents of this report reflect the views of the authors, who are responsible for the facts and the accuracy of the data presented herein. The contents do not necessarily reflect the official views or policies of the

Federal Highway Administration or the California Division of Highways. This report does not constitute a standard, specification or regulation.

TABLE OF CONTENTS

<u>Item</u>	<u>Page No.</u>
Abstract	i
Key Words.	i
Acknowledgments.	ii
Table of Contents.	iv
List of Tables	v
List of Figures.	vii
Introduction	1
Objectives	1
Description of Prototype	3
Instrumentation.	5
Results of Field Observations.	8
A. Culvert Displacements	8
1. Relative Shape Changes	8
2. Absolute Movements	11
B. Settlements	12
C. Soil Pressure Data.	12
D. Culvert Strains	21
Assessment of Current Analytical and Design Techniques	25
A. General	25
B. Marston-Spangler Theory	25
C. Ring Compression Theory	37
D. Flexibility Factor.	39
E. Neutral Point Method.	40
F. Finite Element Method	43

TABLE OF CONTENTS (Continued)

<u>Item</u>	<u>Page No.</u>
Comparison of Method A and Method B Backfill.	52
A. General.	52
B. Relative Shape Changes	52
C. Soil Pressure and Effective Density.	54
D. Culvert Strains.	55
Summary of Observations	58
A. Experimental Results for Method A Backfill . .	58
B. Theoretical Analyses	59
C. Comparison of Method A and Method B Backfill.	61
Conclusions	61
Recommendations for Future Research	63
Statement of Implementation	64
Bibliography.	66

LIST OF TABLES

<u>No.</u>	<u>Description</u>
1	Data Acquisition Schedule
2	Increases in Soil Pressure at Various Times During Construction
3	Increases in Effective Density at Various Times During Construction
4	Crown Pressures by Marston's Theory, Positive Projecting Conduits, Station 10+00
5	Crown Pressures by Marston's Theory, Negative Projecting Conduits, Station 10+00

LIST OF TABLES (Continued)

<u>No.</u>	<u>Description</u>
6	Crown Pressures by Marston's Theory, Positive Projecting Conduits, Station 7+25
7	Crown Pressures by Marston's Theory, Negative Projecting Conduits, Station 7+25
8	Comparison of Spangler's Elongations and Experimental Values
9	Values of E' Calculated by Spangler's Theory
10	Comparison of Moments and Thrusts Produced by Method A and Method B Backfill
11	Comparison of Moment Gradients Produced by Method A and Method B Backfill
12	Material Properties
13a	SR-4 Gauge Positions Exhibiting Strains in Excess of Actual Yield Level
13b	Specified Minimum Yield Level
13c	Actual Yield Stress Level
13d	Specified Minimum Yield Level

LIST OF FIGURES

<u>No.</u>	
1	Apple Canyon Culvert Site Prior to Fill Construction
2	Plan and Elevation of Apple Canyon Installation
3	Soil Pressure Meter Layout
4	Strain Gauge Layout
5	Culvert Deformation Scheme
6	Settlement Platform Layout
7	Survey Monument Layout, Stationing and Elevations
8-9	Changes in Culvert Diameter Dimensions
10-11	Culvert Deformations vs Fill Height and Time
12	Displaced Shapes at Various Times
13-14	Changes in Longitudinal Deformations
15	Lateral Movements
16	Culvert Invert Settlements
17-28	Soil Settlement vs Fill Height and Time
29-55	Soil Pressures vs Fill Height and Time
56	Soil Pressure Profiles at Various Times
57	Effective Density Profits at Various Times
58-67	Circumferential Strain Cross Sections
68-83	Observed Strains vs Fill Height and Time
84	Conversion of Strain to Stress
85	Conditions for Positive Projecting Conduits
86	Conditions for Negative Projecting Conduits

LIST OF FIGURES (Continued)

<u>No.</u>	
87-90	Comparison of Observed Crown Pressure and Pressures Calculated by Marston's Theory
91	Spangler's Assumed Pressure Distribution for Flexible Culverts
92-93	Comparison of Experimental Thrusts and Those Due to the Ring Compression Theory
94-95	Moment Profiles Calculated by Neutral Points
96	Finite Element Mesh for Apple Canyon
97-98	Comparison of Experimental Soil Pressure Distributions and Pressures from Finite Elements
99-100	Moment Profiles Computed by Finite Elements
101	Plan and Elevation of Chadd Creek Installation
102-107	Comparison of Diameter Changes Due to Method A and Method B Backfill
108-111	Soil Pressures vs Fill Height and Time at Chadd Creek
112-117	Comparison of Soil Pressures Due to Method A and Method B Backfill
118-119	Comparison of Effective Density Profiles for Method A and Method B Backfill
120	Comparison of Moment and Thrust Profiles for Method A and Method B Backfill

LIST OF APPENDICES

Appendix

Description

A

Non-Linear Stress Dependent Soil
Properties

INTRODUCTION

In recent years the advent of heavy earth-moving equipment has made it economically feasible to span deep chasms with earth embankments rather than bridge structures. This procedure also solves the earth disposal problem created by nearby cuts. Generally, some type of drainage facilities must be placed within these fills to carry surface runoff. The culverts used for this purpose are subjected to enormous loads and must be designed accordingly.

Two construction techniques are commonly used for installing culverts in deep embankments. The first consists entirely of soil backfill from the foundation to the final grade and is referred to as Method A. The construction technique suggested by Dean Anson Marston, called Method B or the "imperfect trench" method, is also employed. The latter method is an attempt to reduce culvert overburden by introducing a compressible inclusion over the culvert crown. A research project to assess the effects of Method B backfill on a 114-inch diameter, elliptical, structural plate pipe at Chadd Creek was reported by Davis (1)*. This report describes the results of a similar research project conducted at Apple Canyon in California to determine the effects of Method A backfill on a twin 108-inch diameter, elliptical, structural plate pipe culvert embedded in a 160-foot deep embankment.

Objectives

The primary objectives of this project fell into

*Numbers in parentheses refer to the bibliography.

three categories. The first was the determination of the behavior of a structural plate pipe embedded in a deep embankment. This was accomplished by: (1) determining the magnitudes of deformations, lateral movements, longitudinal dilatation and settlement of the prototype culvert; (2) evaluating the soil pressure distributions and effective densities surrounding the culvert; and (3) determining the strains and stresses within the pipe, calculating membrane moments and thrusts and relating these data to the observed soil pressures.

The second objective was the assessment of current analytical and design techniques, comparing them with observed pipe behavior. Among the theories evaluated were: (1) the Marston-Spangler Theory of Loads on Buried Conduits; (2) the Ring Compression theory; and (3) the Flexibility Factor. Internal moments, thrusts and stresses were determined from the external soil pressures using the Neutral Point Analysis reported by Davis (1). In addition, the capabilities of the finite element method for predicting soil pressures and pipe stresses were assessed.

Finally, the behaviors of the Chadd Creek and Apple Canyon installations, using Method B and Method A backfill conditions, respectively, were compared. Soil pressure profiles, internal strains and stresses and pipe deformations were compared in order to determine the suitability of each type of backfill for flexible culverts. As a result of this project, design specifications and analytical techniques for structural plate pipe culverts may be revised.

Description of the Prototype

The tested culvert was constructed at Apple Canyon, on Interstate Freeway 5 in Los Angeles County. The site is about eight miles south of the town of Gorman. A photograph of the canyon prior to backfilling and with culvert in place comprises Figure 1. A plan view of the culvert installation and an embankment cross-section are depicted in Figure 2.

The culvert installation consists of twin, 108-inch nominal diameter, structural steel plate pipes. Both pipes were elongated vertically 5 percent to provide a major vertical axis of 113 inches and a minor horizontal axis of 105 inches prior to installation. The elongation was accomplished by rolling the proper curvature into the pipe plates during fabrication. The pipe plates were galvanized steel conforming to AASHO M-167, ASTM A-442 fastened with ASTM A-325, 7/8-inch diameter, high strength steel bolts. Each 8-foot pipe length was assembled from 6 pipe segments with continuous longitudinal seams on the horizontal diameter, and having corrugations of 6-inch pitch and 2-inch depth. The total culvert length measured 1,072 feet.

The pipe thickness varied along the length of the culvert. Figure 2 contains a table of plate gage transitions. Pipe segments at the two heavily instrumented stations, 7+25 and 10+00, were of different gage. At Station 7+25, Number 1 gage plates were assembled using 6 bolts per foot. Pipe at Station 10+00 consisted of 3/8-inch plates with 8 bolts per foot.

The pipes were placed in a shallow, trapezoidal

shaped trench. The original ground along the bottom of the canyon and adjacent to the natural stream bed was sub-excavated to form a trench 40 feet wide at the top, 24 feet wide at the bottom and 11 feet deep. A layer of structure backfill, about one foot deep was placed in the bottom of the trench and compacted to 95 percent relative compaction. The structure backfill comprised 3 inch maximum aggregate with not less than 35 percent passing a Number 4 sieve and a specified sand equivalent greater than 30. The bottom of the trench was shaped to conform to the pipe curvature, the bedding angle being 90 degrees. The plates comprising the invert were installed in the shaped bedding, and the remaining plates were bolted in place. Structure backfill was placed in the trench to a height of one foot above the pipe crown. Backfill was to be brought up uniformly around the pipe in 8-inch lifts; however, it was noted that the backfill elevation differed by as much as three feet on opposite sides of the pipes at some locations. Ninety-five percent relative compaction of the structure backfill material was achieved using small, manually operated vibratory rollers. Water was added to aid in compaction with no special moisture control.

Apple Canyon was originally "U" shaped. The final embankment was 900 feet long by 155 feet wide at the top by 168 feet high measured from original ground. Overfills at the two heavily instrumented stations were 68 feet and 160 feet at Stations 7+25 and 10+00, respectively. The

embankment material was a clayey, sandy gravel common to the area. It was quite friable and tended to break down during compaction.

Construction of the embankment began in late 1965. Inclement weather slowed the installation of the instrumentation during January, 1966, but the pipes were fully instrumented and installed by mid-February. The embankment reached 10 feet above the crown on March 1, at which time the datum was established for all instrumentation readings. The highway subbase elevation was reached on May 5, 1966.

Instrumentation

Five sections along the culvert were instrumented. Two stations, 7+25 and 10+00, were extensively instrumented as follows:

(1) Eight modified Carlson soil stressmeters were placed in the embankment at the octant points of the left pipe. Two additional meters were placed at the ends of the horizontal diameter of the right pipe. The meters were embedded 6 inches from the periphery of the pipe and tangent to it. Standard Carlson stressmeter blanks were purchased and fitted with linear, variable, differential transformers to reduce susceptibility to damage often experienced with the more protruding Carlson strainmeter ordinarily employed as the transducer element. Figure 3 depicts the soil meter layout.

(2) Five similar meters were placed in the fill surrounding the culverts. Two were placed at the

elevation of the pipe horizontal diameter and 45 feet on either side of the installation centerline. The remaining meters were placed about 16-1/2 feet above the horizontal diameter, one directly over the crown of the left pipe and the others 45 feet on either side of the centerline. These meters are also depicted in Figure 3.

(3) SR-4 cross gauges were placed in quadruplets around the pipe periphery. Each quadruplet comprised 4 gauges whose elements were oriented longitudinally and circumferentially and placed on the inner and outer corrugation crowns and valleys. Quadruplets were located at the three upper and three lower octant points. Additional groups were placed 12 inches above and below both longitudinal seams at the horizontal diameter to avoid the double pipe thickness at the joint (see Figure 4).

(4) Three-quarter-inch steel spheres were welded to the inside of the pipe periphery at the octant points to determine pipe displacements. A second set of spheres were placed at the ends of the horizontal and vertical diameters two corrugations (12 inches) away from the first set to assess local culvert elongations. Chord lengths between the octant points were measured with an extensometer, elongations, with a large outside micrometer. Figure 5 depicts the deformation measurement scheme.

(5) Fluid type settlement platforms were placed within the embankment as shown in Figure 6 to assess settlement ratios and the height of the "plane of equal settlement."

The three remaining test stations 7+90, 8+55 and 9+20, contained only four Carlson soil stressmeters; one at the crown and three about 16-1/2 feet above the horizontal diameter, as described in (2) above. Unfortunately, lack of a properly designed slip joint in the conduit used to convey the upper embankment meter leads into the pipe resulted in shearing of the leads during construction, so that no valid pressure readings were obtained from these meters. Figure 3 also depicts the stressmeter layout at these stations.

In addition to the above instrumentation, survey monuments were placed at intervals along the culvert. Periodic level and tape surveys were made to determine changes in pipe camber, pipe lengthening due to transverse embankment dilatation and lateral movements. The locations of the survey monuments are depicted in Figure 7.

The data acquisition period spanned almost 40 months. Initial readings were made at the time of culvert installation. Since some initial loading is required in order to produce accurate soil pressure readings, the datum for all instrumentation was chosen at a fill height of 10 feet above the culvert crown. Subsequent readings were taken at intervals during fill construction and for

36 months thereafter. A schedule of data acquisition times is presented in Table 1.

Results of Field Observations

A. Culvert Displacements

1. Relative Shape Changes

The culvert displacement field was determined by measuring the lengths of fourteen chords defined by steel spheres welded to the pipe as shown in Figure 5. The Cartesian coordinates and their changes were calculated for each sphere. In this analysis, the diameter connecting the crown and invert spheres was assumed to remain vertical with the origin at the center of the invert sphere. Chord length changes and coordinates were calculated with respect to an initial set of readings taken at the datum elevation. In addition, since the measurement of chord lengths is not subject to the initial loading requirements of soil stressmeters, readings taken prior to the fill height reaching the datum elevation are also valid. Therefore, the chord measurement data were also reduced with respect to the true initial shape of the pipe prior to beginning the structure backfill operation.

Curves representing the relative changes in the horizontal and vertical diameters versus fill height and time are depicted in Figures 8 and 9. The radial displacements of individual spheres with respect to the initial, unloaded shape versus fill height and time are presented in Figures 10 and 11.

The vertical diameter increased initially as fill was placed around the culvert barrels, reaching a maximum when the fill reached the crown elevation. As the fill elevation increased, the vertical diameter began to decrease, returning to its original length with 15 to 20 feet of overfill, and continuing to decrease throughout the remainder of the construction period. The horizontal diameter changes exhibited opposite behavior. The magnitudes of the horizontal changes were smaller than those of the vertical diameter, probably due to passive pressures generated as the pipe moved laterally into the fill. This phenomenon is evidenced by the fact that the horizontal diameters did not return to their original lengths until about 25 feet of overfill had been placed. Both the horizontal and vertical diameter dimensions stabilized soon after fill completion.

Radial displacements of each octant point, Figures 10 and 11, demonstrate the flexibility of the culvert barrel. The origin of the Cartesian coordinate system was placed at the culvert invert; hence, the crown displacements are identical to the aforementioned changes in the vertical diameter. Displacements of the remaining octant points are referenced to the culvert center. The horizontal octant point displacements exhibit behavior consistent with the above described diameter changes. At Station 10+00 both horizontal octant points displaced outward after the fill reached the crown elevation, while at Station 7+25 the left horizontal octant point exhibited

almost all of the outward movement, the right side remaining essentially unchanged with respect to the culvert center.

All octant points exhibited reversals in the direction of radial displacement during the initial stages of construction. Following this initial reversal, no other changes of direction occurred throughout the data acquisition period. At both test stations the three upper octant points initially displaced outward and then moved inward, the upper right octant point displacing farther than the upper left. The remaining octant points exhibited initial inward displacements and subsequent outward movements with the lower left sphere moving farthest outward. All displacements stabilized soon after fill completion. Figure 12 compares the displaced shape at the two test stations for various times during the data acquisition period.

Longitudinal elongation measurements between spheres placed two corrugations apart at each test station (see Figures 13 and 14) indicate maximum elongations of up to 0.07 inch per foot after 36 months. Station 10+00, near the center of embankment dilatation, exhibited an average total elongation of 0.01 inch per foot, while Station 7+25 exhibited a total average elongation of about 0.02 inch per foot. Measurements at both test stations indicate superimposed upward and sidewise movements. Elongation is evidenced at Station 10+00, although some anomaly occurred at higher fill elevations where the crown and invert elongated and both sides shortened.

2. Absolute Movements

The chord changes discussed above were relative to an assumed origin at the pipe invert. Absolute movements of the culvert were assessed by periodic chain and level surveys through the installation. Movements of the monuments were later related to the steel balls at the invert of each test station.

Lateral movements are depicted graphically in Figure 15. The lateral motion is erratic with a maximum of about 2-1/2 inches at Station 10+00, where the fill was highest. Maximum invert settlement of over two feet was also observed at that station (see Figure 16).

The total elongation of the pipes, measured along tangents, was approximately 4 inches, or a little less than 0.004 inch per foot. The increase in length of a straight chord joining the two ends of the culvert, which is a more representative measure of the embankment dilatation, was approximately 9 inches over a distance of 962 feet, or about 0.009 inch per foot. The discrepancy between the two apparent elongations suggests inclusion of a rotational component in the chord length, due to lateral movements, which tends to straighten the pipes. The elongation along the tangents may be compared with the local elongations shown in Figures 12 and 13. At Station 7+25, the average of the four local elongations is 0.016 inch (per foot), four times as great as the overall average elongation noted above. At Station 10+00, the average value of the four local elongations is 0.002 inch (per foot), or about half the overall average,

reflecting the proximity of this station to the center of dilatation, where no elongation would be expected.

B. Settlement

The settlement data obtained from Apple Canyon are plotted in Figures 17 through 28. The curves represented in these plots were originally very erratic and for this reason the obviously erroneous points, represented by triangles, have been omitted from the regression analysis. The position of each platform was as shown in Figure 6.

The purpose for collecting settlement data was two-fold: (1) to determine the theoretical loads on the culvert by Marston's Theory; and (2) to serve as a check on the accuracy of the finite element method of analysis. Both of these techniques will be discussed in detail later.

During the fill construction, the settlement platforms at the upper elevations of Station 10+00 were disconnected in order to allow the contractor to install a drainage structure through the fill. After completion of the drainage installation, most of the reconnected settlement platforms failed, and subsequent readings from those platforms have not been plotted.

C. Soil Pressure Data

As noted previously, much desirable soil pressure information was lost due to shearing of the stressmeter leads at the end of a conduit leading into the culvert due to embankment settlement during construction. Only those embankment meters placed above Station 7+25 provided valid

pressure readings. In addition, the meters placed level with the horizontal diameter at Station 10+00 on the right also failed to provide valid readings. The invert meter at Station 7+25 provided very low pressure readings. An inspection hole cut in the invert of the pipe at that point revealed the presence of a void which had formed subsequent to placement of the meter, so that pressures obtained may or may not be representative of the general pressure field at that level.

Soil pressures from the modified Carlson soil stressmeters are plotted against fill height and time in Figures 29 through 55. The datum for all soil stressmeters was established when the fill reached 10 feet over the crown for those meters at or below the crown elevation and was placed at 21 feet above the crown for the upper embankment meters. Pressures below these datum planes were determined from prior readings and polynomial extrapolation. A Fourier analysis was employed to generate the plots. Curves of effective density, representing the equivalent fill density which would produce the measured pressure under hydrostatic conditions, are also shown on the figures. The effective density curves are derived by the relationship:

$$ED = \frac{\Delta P}{\Delta H} \times C \quad (1)$$

where: ED is the effective density

ΔP is the change in soil pressure (psi);

ΔH is the change in fill height (ft);

C is a constant required for units conversion,

$144 \frac{\text{in}^2}{\text{ft}^2}$ in this case.

The interpolated pressures given by the Fourier analysis were used to generate the effective densities in order to produce smooth curves.

The soil pressure-fill height curves appear as smooth, non-linear functions. No relative maxima or minima occurred during the construction period in any of the soil pressure plots. The resulting effective density functions are nearly linear during the construction period but become non-linear after the maximum overfill is reached at each station. Soil pressures acquired prior to the assumed datum elevation were used in polynomial extrapolation procedures to generate the pressure-fill height functions with respect to the actual meter elevations.

The pressure-fill height plots for Station 10+00, Figures 29 through 40, indicate small discrepancies between the interpolating function values and the actual zero pressure. The magnitudes of these discrepancies serve as a measure of the accuracy of the interpolating functions used to generate the plots. The first section of each plot represents the variation in soil pressure during embankment construction. The non-linear behavior is due to the nature of the soil mechanical properties which Kulhany, et al (2) have shown to be functions of both overburden and confining pressure. Since the construction period spanned only about four months, the plastic effects of cohesion and consolidation do not greatly affect the soil pressure functions.

The last portions of the plots represent soil pressures as functions of time, only. In general, the pressures continued to increase during the first few months

following fill completion, stabilized temporarily and then exhibited further pressure increases. The initial pressure increases can be attributed to continued embankment settlement as evidenced by the settlement platform data, roadway construction at the top of the fill and, to some extent, to consolidation. The period of relatively stable pressures began between 3 and 6 months after embankment completion and lasted for about 18 to 24 months; during which time the pressures were somewhat erratic, tending to remain constant or increase slightly. Mean pressures during the stable period were 8 to 76 percent higher than at the time of embankment completion; with an average mean increase of 39 percent. Final readings taken 36 months after completion showed further pressure increases ranging from 36 to 103 percent above the values at the time of construction completion.

Figures 41 through 55, representing the soil pressure-fill height relationships at Station 7+25, also show small discrepancies at the zero level. The plots indicate the soil pressure behavior during and following embankment construction and, additionally, the pressures recorded between the time the fill reached its maximum elevation at this station and the time of embankment completion. During the initial stage pressure functions exhibited non-linear behavior similar to that of meters at Station 10+00.

While construction of the embankment continued elsewhere, most pressure meters registered increases but at a slower rate. This behavior indicates definite longitudinal

distribution of pressure which has been observed in other flexible pipe installations and, to some extent, in rigid arch culverts. Only one meter, at the upper right octant, registered any pressure decrease. These pressure changes occurred over approximately one month and ranged from a 5 percent decrease for the above mentioned meter to a 64 percent increase for the adjacent meter at the right end of the horizontal diameter. The average pressure increase was 35 percent.

Following embankment completion, the pattern of continued pressure increase, subsequent, temporary stabilization and then further increases was also evident for many meters at Station 7+25. As at the previous station, the period of relatively stable pressures commenced 3 to 6 months after completion and continued for 18 to 24 months. The pressures during the stable period also tended to be erratic; exhibiting mean increases ranging from 43 to 96 percent higher than the embankment completion values. The average increase in mean stable period pressures was 61 percent. After 36 months most indicated pressures had risen, registering increases of between 37 and 143 percent, with an average of 82 percent, higher than the embankment completion pressures. Table 2 contains comparisons of the soil pressure readings at various times during the data acquisition period.

Profiles of soil pressure at various times during the data acquisition period are depicted in Figure 56. Due to the above mentioned void discovered at the invert meter position at Station 7+25, the profiles contain dashed lines which indicate possibly erroneous data.

The pressure distributions for the two test stations differ significantly. At Station 10+00 the distributions were fairly uniform, having a single relative minima at the upper right octant point. Station 7+25 exhibited two relative minima, one at the left and the second at the right upper octant points and a less uniform distribution. Maximum lateral pressure occurred at the right end of the horizontal diameter for all cases at Station 10+00 but at Station 7+25, maximum lateral pressures during fill construction occurred at the left side. The general shape of the pressure profiles at each station remained essentially unchanged throughout the data acquisition period.

The asymmetric nature of the pressure distributions is typical of other prototype installations studied in California (7, 8, 9). Soil pressure meters are subject to many inaccuracies due to their position and manner of placement, local fill heterogeneity and idiosyncracies in operation. This is graphically demonstrated in the case of the invert meter at Station 7+25. Notwithstanding this, however, the validity of the pressure profiles and variations between the two test stations may be explained in several ways.

The absence of anomalies in the pressure-fill height functions supports the assumption of valid readings. All meters indicated the same general characteristics relative to fill height and time. Data scatter which occurs in the time portions of the pressure plots may be attributed, in part, to seasonal variations in soil moisture content. In addition, the pressures registered by adjacent meters agree

with one another. None of the meters exhibited readings which were vastly different from others of similar orientation.

Asymmetry of pressures can be partially explained by the fact that there are two pipes in this installation. If a plane of symmetry were to exist, it would occur midway between the pipes and corresponding meters on the two pipes would indicate identical pressures. Comparison of appropriate meters revealed that such symmetric pressures were not present at Station 7+25 but did occur at Station 10+00.

The displacement study, discussed above, provides an explanation for this asymmetric behavior. Station 7+25 exhibited significant leftward movement and, if both pipes move at nearly the same rate, passive pressures are generated at the left side of each barrel while active pressures are developed on the right sides. The larger pressures on the left sides and smaller pressures on the right sides tend to confirm this hypothesis. At Station 10+00 lateral motion was only about 25 percent of that at Station 7+25, probably due to its proximity to the center of embankment dilatation and its distance from bends in the pipe, and horizontal asymmetry was significantly reduced.

A further explanation for the discrepancies between the horizontal meters at Station 7+25 is found in the displaced shape of the pipe. From Figure 12 the right end of the horizontal diameter remained virtually undeformed with respect to the invert while the left end exhibited almost all of the horizontal movement. Thus, passive pressures would be developed at the left side while the right side meter would

register at-rest values. This behavior, coupled with the action due to lateral motion, would produce high pressures at the left sides of each pipe, a low value at the right side of the left pipe and, depending on the displacement characteristics of the right pipe, its right side pressure may be larger than or equal to that of the left pipe. At Station 7+25, this behavior was noted with the right side of the right pipe indicating a pressure initially smaller and ultimately larger than the right side of the left pipe.

Effective densities are also depicted on the soil pressure-fill height plots, Figures 29 through 55. Relative maximum densities were recorded at the beginning of fill construction in most cases (see Table 3). At Station 10+00 effective densities decreased slightly during the construction phase, with an average decrease of about 11 percent. Subsequent readings taken after fill completion show increased densities commensurate with the pressure increases occurring following embankment completion. Effective densities in excess of the actual density as determined by compaction tests were observed in the majority of cases after 36 months. The highest recorded density, 238 pcf, was measured at the lower left octant point. The average density increase between the time of fill completion and 36 months thereafter was 54 percent.

At Station 7+25 the effective density decreases averaged 27 percent during embankment construction. In the interval between the time maximum overfill was reached at this station and the completion of construction, most of the effective densities increased by an average of 28 percent.

Following embankment completion the effective densities continued to increase as the soil pressure increased. The densities calculated at 36 months after fill completion averaged 86 percent above those at the time of reaching maximum overfill.

Typical profiles of effective density around the left pipe are depicted in Figure 57. The octant point values were determined from the soil pressure-fill height functions, and Fourier analysis was used to construct the profiles. These plots differ from those previously published in Reference 17 due to subsequent refinements in the method of data reduction and plot generation.

In general, the profiles exhibit shapes similar to those for pressure. At Station 10+00 crown vertical densities are nearly equal to the soil hydrostatic density, 120 pcf. The invert vertical density is somewhat higher, probably caused by passive soil pressure generated as the fill and pipe settled into the foundation material. The maximum effective density was oriented laterally and occurred at the right end of the horizontal diameter where the two pipes are closest. This density, averaging 153 pcf during fill construction was also probably caused by passive soil pressures. The asymmetric density distributions are directly attributable to the pressure distributions discussed previously.

Effective density distributions for Station 7+25 exhibit a somewhat symmetrical nature but are much less uniform than those of Station 10+00. The largest observed

density, 191 pcf, occurred at the crown and was about 1.6 times larger than the maximum density determined by compaction tests. The invert density, however, was quite low due to the above mentioned void between the pipe and bedding. The highest density occurred at the lower left octant, averaging 179 pcf during construction of overfill at this station. The high density present at the upper left octant of Station 10+00 was not noted, indicating, for lack of suitable evidence to the contrary, that one of the two corresponding meters may not have yielded representative pressures.

The exterior prism effective densities are also of interest. At Station 7+25, where all soil stressmeters functioned, the exterior prisms exhibited lower vertical effective densities than did the crown or interior prism. Only one exterior prism soil stressmeter functioned at Station 10+00 and it also indicated a lower vertical effective density than did the crown meter. These readings indicate a differential settlement such as may be expected when the relative rigidities of the soil and culvert are such that the culvert crown settles less than the exterior prism consolidates.

D. Culvert Strains

The strain gauges at Apple Canyon functioned well over the three-year span of data acquisition even though the gauges were placed in a moist earth environment and in many cases were submerged under water. None of the gauges failed during the construction period, and only six gauge circuits had shorted out two years after embankment completion.

Evidence of the reliability of the strain gauge data is seen in the linearity of the strain patterns across the corrugated wall at every section.

Transverse embankment dilatation which produced spreading of the joints in concrete pipes and arch culverts and stretching of flexible culverts in previous tests was also evident at Station 7+25. In general, each of the inner and outer longitudinal crown gauge elements exhibited compressive strains while the corresponding valley elements exhibited tension. This pattern was not evident at Station 10+00 until the fill had reached 120 feet above the culvert crown.

Strain cross-sections for Station 10+00 at a fill height of 55 feet above the crown are depicted in Figures 58 through 67. The linearity of circumferential strain patterns is evident and typifies the patterns for both test stations throughout the data acquisition period.

Figures 68 through 83 depict typical variations in strain as functions of fill height and time. The smooth, non-linear strain behavior is readily apparent.

Circumferential and longitudinal stresses in the pipe walls were calculated using the equations,

$$f_c = E (\epsilon_c + \mu \epsilon_L) \quad (2)$$

$$f_L = E (\mu \epsilon_c + \epsilon_L) \quad (3)$$

where: f_c and f_L are the circumferential and longitudinal stress, respectively; ϵ_c and ϵ_L are the circumferential and longitudinal strains; E is Young's modulus which was assumed to be 29,000,000 psi for the analysis and μ is Poisson's ratio, having an assumed value of 0.285. The effects of

local yielding were not included in the strain data reduction. The equations for stress and circumferential pipe moments and thrusts are presented in Figure 84.

Tensile tests performed on coupons obtained from the corrugated pipe material are summarized in Table 12a. Half of the specimens were tested prior to being cold-rolled to form the pipe curvature, the remainder being tested after rolling. The tested coupons exhibited yield stresses in excess of the specified ultimate strength. Actual ultimate strengths ranged from 38 to 70 percent higher than the specified minimum value. The effects of work hardening induced in the material due to cold-rolling are demonstrated by average yield and ultimate strength increases of 33 percent and 14 percent, respectively. Ultimate elongations ranged from 15 percent larger to 28 percent smaller than the specified minimum value.

Table 13a presents a record of those strain gauge positions at which yield strains were recorded during the data acquisition period. Strains commensurate with the actual yield stress level were recorded at Station 10+00, only. Initial yield in the circumferential direction was observed at the invert when the maximum overfill was reached. Subsequently, circumferential yield spread to the lower left octant point, the right horizontal diameter and the crown. Longitudinally, yield strains were observed at the crown at various times following embankment completion.

Strains commensurate with the specified minimum yield stress were measured at both test stations during

embankment construction. Table 13b presents a record of where such strains were observed. At Station 7+25, such strains were first recorded in the circumferential direction just below the left horizontal diameter with about 50 feet of overfill and at the invert with about 52 feet of fill. These points correspond to areas which exhibited large displacements. Subsequently, yielding spread to nearly the entire plate depth at these points and toward adjacent octants. Some strain redistribution was observed as the specified yield occurred at adjacent points. Longitudinally, specified yield strains first occurred at the lower left octant point after the maximum fill was reached but prior to embankment completion. Such strains were confined to the lower left octant and the invert throughout the data acquisition period. The remaining octant points maintained strain levels below the minimum yield level although some strains approached that value.

At Station 10+00 strains first approach the minimum yield stress value simultaneously at the invert and lower right octant with about 63 feet of overfill. Strain levels continued to increase at all octant points, the entire circumference reaching the specified yield level within 18 months after construction was completed. Longitudinally, specified yield strains first occurred at the crown with about 120 feet of fill, and at the invert within 2-1/2 months after fill completion. Thirty-six months after construction completion, longitudinal strains in the yield range were still confined to the three upper octants, the invert and lower right octant point.

Pipe section and material properties were used in conjunction with the strain data to compute circumferential moments and thrusts. Section properties were calculated from the dimensions of the corrugated pipe walls. Specifications required a minimum seam strength of 250,000 lbs. which was well above the maximum calculated thrust of 167,883 lbs. Maximum recorded moment was -145,182 in-lbs, at 36 months after construction completion.

ASSESSMENT OF CURRENT ANALYTICAL AND DESIGN TECHNIQUES

A. General

Current design techniques include methods for predicting overburden pressure and deflection, for developing adequate seam strengths, for providing a sufficiently rigid section to maintain their shape during transport and installation and for predicting deflections from a theoretical soil-structure model. Any or all of these methods may be used during the design phase. The following is a comparison of the result of each method with the experimental data obtained at the Apple Canyon installation. In addition, two analytical techniques, the Neutral Point Analysis and the method of Finite Elements will be applied to the culvert installation.

B. Marston-Spangler Theory

Dean Anson Marston of the Iowa Engineering Experiment Station developed a theory for loads on underground conduits. Professor M. G. Spangler, also of the Iowa Engineering Experiment Station has utilized this theory to predict deflections in flexible culverts. These theories are often used in conjunction in the design of culverts;

loads calculated from Marston's theory being used to predict deflections by Spangler's method.

Marston's theory considers the differential settlements of the interior and exterior soil prisms above the conduit and the resulting transfer of load by shear along the prism interfaces. Culverts are classified according to their bedding and backfill conditions and subclassified based on two abstract quantities, the "settlement ratio" and the "plane of equal settlement." Marston's theory is well documented in the literature (3,4,5) and will not be reiterated here.

The classifications of interest in this report are the positive and negative projecting conduits. Positive projecting conduits rest on bedding material at the original ground level and an embankment is built over them. Figure 85 depicts this condition. Negative projecting conduits are installed in relatively shallow, narrow trenches excavated in original ground and fill is added above the original ground elevation (see Figure 86).

Conduit subclassifications are complete and incomplete ditch and projection conditions. "Complete" and "incomplete" refer to the position of the "plane of equal settlement"; that elevation above which the soil directly over the culvert (interior prism) settles the same amount as the soil on either side (exterior prisms). For the incomplete condition the plane occurs within the fill. An imaginary plane above the top of the fill characterizes the complete condition.

For positive projecting conduits the projection condition occurs when the top of the conduit settles less than the soil surrounding the culvert. This behavior is characterized by a positive "settlement ratio" which is "the ratio of the difference between the settlement of the critical plane (the horizontal plane at the conduit crown in this case) and the top of the conduit to the deformation of the fill material adjacent to the conduit." A negative settlement ratio signifies a ditch condition.

A slightly different definition of settlement ratio is used for negative projecting conduits. In this case the critical plane occurs at the top of the shallow trench in which the pipe is installed and the settlement ratio is the ratio of the difference between the settlement of the critical plane and the top of the pipe to the consolidation of the interior prism below the critical plane. Only complete and incomplete ditch conditions apply for negative projecting conduits.

The Apple Canyon culvert was placed in a shallow trench having sloping sides excavated in original ground. Ordinarily, this type of construction would be classified as a negative projecting conduit. However, since the trench was very shallow and quite wide, the positive projecting conduit case may be more applicable. When such conditions are found during design, the case which predicts the smaller crown load governs. Therefore, vertical crown loads were calculated for both cases.

Generally, Marston's theory is applied to single conduits. However, at Apple Canyon two pipes were installed having four feet of fill between them. The proximity of the pipes makes it difficult to analyze each one separately. Therefore, to apply the theory to this culvert, a representative value for the conduit width had to be chosen. There are only three logical choices available:

1. The width of one pipe;
2. The width of two pipes;
3. The width of two pipes plus the soil fill between them.

The second choice yielded the best correlation with the experimental data. Therefore, the culvert width was set at eighteen feet.

The positive projecting conduit equations applied at Station 10+00 yielded a plane of equal settlement at between 12 and 14 feet above the crown and a positive settlement ratio, indicating that for fill heights below 12 feet the complete projection condition controls while above 14 feet the incomplete projection condition is applicable. Table 4 presents the results of the positive projecting conduit analysis and a comparison with experimental loads assuming a zero datum 10 feet above the crown. The differences between the adjusted theoretical solution and the experimental loads averaged -21.5 psi for points below the top of the embankment. After embankment completion the theoretical loads remained nearly constant while the

experimental loads continued to increase as discussed above. Theoretical and experimental data are compared graphically in Figure 87.

The negative projecting conduit incomplete ditch condition equations applied at Station 10+00 produce very good correlations. Tabulated results are given in Table 5. The plane of equal settlement is assumed to occur at the top of the trench, about one foot above the culvert crown, as a result of the zero settlement ratio. The average difference between the theoretical and experimental crown loads was only 1.4 psi. The readings taken after embankment completion do not correlate since the theoretical solution is a function of increasing fill height, which height remains constant after construction. Figure 88 depicts the experimental and theoretical crown loads as functions of fill height and time.

At Station 7+25 the positive projecting conduit case incomplete ditch condition yielded valid crown loads for the fill construction period. After embankment completion, the incomplete ditch condition controls but does not predict the loads accurately. During construction of the embankment over this station the average difference between theoretical and measured loads was -3.8 psi. Between the time the maximum overfill was reached at Station 7+25 and the embankment completion date, no fill was added over the crown and, consequently, the theoretical loads, which are a linear function of fill height, remained nearly constant

throughout the remainder of the embankment construction period while experimental loads increased. Following construction completion, the theoretical loads are quite erratic due to anomalies in the settlement ratio value produced by erratic settlement readings and do not correlate with the measured crown loads. The results of this case are given in Table 6 and depicted graphically in Figure 89.

As was the case at Station 10+00, Station 7+25 shows good correlation between experimental and theoretical loads using the negative projecting conduit equations for the period of fill construction over this station. The average difference between theoretical and measured crown pressure was 4.1 psi. Following maximum overfill at Station 7+25 the theoretical loads remained constant and correlations become very poor. Table 7 lists the results of this case. Comparisons of measured and theoretical crown pressures are depicted in Figure 90.

As illustrated in the aforementioned figures, Marston's theory may be used to predict crown pressures which occur during fill construction. However, post embankment completion pressure changes do not correlate with experimental values. For pipe sections under side slopes, crown load predictions are invalid after the fill has reached its maximum elevation over that station but prior to embankment completion. This is primarily due to the linear relationship between fill height and theoretical crown load as discussed above.

Once crown loads have been predicted for the maximum overfill applied to the culvert, Spangler's method

may be used for determining the appropriate wall thickness of the culvert. Spangler's theory is based on the premise that culvert deflections should control the design of flexible culverts since excessive deflection produces pipe collapse without accompanying rupture or buckling of the barrel. Such failures have been found to occur after the deflection reaches about 20 percent of the nominal pipe diameter. Suggested design criteria require that the deflection be limited to about 5 percent of the nominal pipe diameter, thereby producing a safety factor of 4.

The basic assumptions embodied by Spangler's deflection theory are: (1) the pipe is initially circular; (2) loads are applied symmetrically about the horizontal and vertical axes; and (3) thin ring theory is applicable to flexible metal culverts; and (4) the radii of curvature of the unloaded and loaded rings are nearly equal. With these assumptions and Spangler's hypothetical distribution of peripheral pressure on the culvert, as depicted in Figure 91, the horizontal deflection of the culvert can be calculated by the formula,

$$\Delta X = D_L \frac{K W_C r^3}{EI + 0.061 E' r^3} \quad (4)$$

where: ΔX is the horizontal displacement of one end of the horizontal diameter; D_L is the deflection lag factor (the ratio between instantaneous and final deflection under a given load); K is a constant whose value depends on the angle the shaped bedding makes with the pipe vertical axis; W_C is the crown load calculated by Marston's theory; r is the nominal pipe radius; E is Young's Modulus for the pipe

material; I is the moment of inertia per unit length of the cross-section of the pipe wall and E' is the modulus of soil reaction of the enveloping earth. The constant K is evaluated by the expression,

$$K = 0.5 \sin \alpha - 0.082 \sin^2 \alpha + 0.08 \frac{\alpha}{\sin \alpha} - 0.16 \sin \alpha (\pi - \alpha) - 0.04 \frac{\sin 2\alpha}{\sin \alpha} + 0.318 \cos \alpha - 0.208 \quad (5)$$

where: α is the angle of bedding. Suggested values for the deflection lag factor, D_L , range from 1.25 to 1.50. Spangler (6) suggested that a value for E' of 700 psi be used if at least 90 percent of the standard Proctor density can be achieved in the side-fill soil for at least two pipe diameters on each side of the pipe. The Federal Highway Administration design criteria uses $D_L = 1.5$ and $E' = 700$ psi for good backfill at 85 percent of standard Proctor density and $D_L = 1.25$ and $E' = 1400$ psi for excellent backfill at 95 percent of standard Proctor density. Data from other published tests (6) indicate a wide variation in the values of E' ranging from 230 psi to 8000 psi.

The installation at Apple Canyon does not meet all the criteria established by the assumptions pertinent to Spangler's theory. The loading conditions applied to the pipe cannot be symmetrical about the vertical axis of a single culvert barrel since, if a plane of symmetry were to occur, it would fall midway between the two pipes. Furthermore, there is nothing to suggest from past tests conducted in California (1,7,8,9) that a plane of symmetry occurs in a single barrelled culvert. In addition, the two culvert barrels were elongated by about 5 percent in the vertical

direction prior to installation.

Nonetheless, Spangler's theory will be applied to the Apple Canyon Culvert to determine the extent to which it agrees with the experimental data. For this analysis the Federal Highway Administration criteria for $\underline{D} = 1.50$ and $\underline{E}' = 700$ will be used. The bedding angle of 45° results in a \underline{K} value of 0.096. Crown pressure calculated from Marston's theory will be used as input. Spangler's equation contains total crown load, W_c , which may be related to crown pressure by,

$$P_v = \frac{W_c}{2r} \quad (6)$$

where P_v is the soil pressure acting vertically downward over the horizontal projection of the culvert. Appropriate substitution into Equation (4) yields,

$$\Delta X = \frac{2 D_L K P_v r^4}{EI + 0.061 E' r^3} \quad (7)$$

In addition, the modulus of soil reaction, E' , will be determined by two methods. The first involves rearranging Equation (7) to the form,

$$E' = \frac{2 D_L K P_v r^4 - EI \Delta X}{0.061 r^3 \Delta X} \quad (8)$$

The second method is derived from Spangler's assumed distribution of lateral loads as depicted in Figure 91 wherein the maximum lateral pressure, P_H , occurs at the horizontal diameter and has the form,

$$P_H = \frac{E' \Delta X}{2r} \quad (9)$$

where E' , ΔX and r are as defined above. Solving for E' yields,

$$E' = \frac{2 P_H r}{\Delta x} \quad (10)$$

Experimentally determined values for P_V , P_H and ΔX were used to calculate E' .

Table 8 presents a comparison of the elongations of the horizontal diameter as calculated by Spangler's theory and the experimental diameter changes measured at Apple Canyon. In this table, calculated ΔX values during the fill construction periods are based on a deflection lag factor of 1.0, since measured deflections are instantaneous values. Following embankment completion, a deflection lag factor of 1.25 is used. Loads developed for negative projecting conduits were used at Station 10+00, corresponding to the best fit with the experimental data. At Station 7+25, the positive projecting conduit loads, which best fit the experimental data, were used. Displacements calculated for Station 10+00 were 244 to 504 percent higher than the experimental displacements, with an average of 311 percent during construction, 268 percent following completion and an overall average of 292 percent. Theoretical displacements for Station 7+25 were also much larger than the experimental values, ranging from 280 to 699 percent higher. During placement of overfill at this station theoretical displacements averaged 560 percent larger, following completion at this station but prior to construction completion the average theoretical values were 400 percent higher and following construction Spangler's deflections were 288 percent higher with an overall average of 381 percent larger.

Application of Spangler's deflection equation yields very conservative results when an E' of 1400 psi is used. The direct application of this theory would predict a maximum deflection at Station 10+00 of 5.6 inches which represents about 5.2 percent of the nominal pipe diameter which is slightly greater than the design criterion of 5 percent deflection. The actual maximum horizontal deflection observed at Apple Canyon was only about 1.6 inches which suggests that the assumed value of E' , the only variable subject to significant change due to installation conditions, is probably too small.

Hence, the values of E' actually observed at Apple Canyon were calculated. Actual crown pressures and horizontal displacements were used. The deflection lag factor was assumed to be the average value of the ratio of horizontal displacements observed at the time of fill completion and 24 months thereafter, being 1.32. Table 9 contains the values of E' as calculated by the two methods discussed above.

Calculated values of E' using the deflection formula method were quite erratic. At Station 10+00, where both sides of the pipe moved outward, E' ranged from about 28,000 psi to over 46,000 psi, averaging 37,700 psi. At Station 7+25, where one end of the horizontal diameter exhibited almost all the observed movement, the resulting E' values do not appear to be valid since the right side exhibited values averaging 911,883 psi while the left side values were only 8,425 psi, or about 108 times smaller. Similar results were observed when the assumed pressure distribution equations were employed to calculate E' .

Since the behavior of the culvert barrel at Station 7+25 does not correspond to the type of motion hypothesized by Spangler, it is reasonable to disregard this station in determining the value of E' which should have been used for design. In addition, the data obtained do not include tangential pressures which are required in order to verify Spangler's hypothesis. Therefore, if it is assumed that Spangler's deflection theory could be used at Apple Canyon, an appropriate E' value would be between 37,700 psi and 23,500 psi, the low value resulting in the most conservative design.

It is believed that the large differences between theoretical and observed horizontal displacements and the large E' values can be attributed to the confinement afforded by the trench in which the culvert was placed. This confinement tended to limit horizontal displacement to a greater extent than would the normal positive projecting installation.

Initial pipe ellipticity may have been an additional factor in producing the discrepancies between theoretical and observed displacements. Spangler's original derivation of the Iowa Deflection Formula (4) assumes pipe radius, r , is a constant with respect to the angle of orientation as measured from the vertical, ϕ . Thus, the incremental pipe arc length, ds , is given by

$$ds = r d\phi$$

If r is a function of ϕ , as in the case of an ellipse, it can be represented by

$$r = r_0 + \Delta r f(\phi)$$

where r_0 is the nominal radius, Δr is the change in radius between a circle and the ellipse and $f(\phi)$ is some function of ϕ . Substituting into the equation for ds yields,

$$ds = r_0 d\phi + \Delta r f(\phi) d\phi$$

For small values of Δr , up to 5 or 6 percent of r_0 , the arc length of the ellipse and the nominal circle defined by r_0 can be considered equal. As this was the case at Apple Canyon, the effects of the initial vertical elongation are considered negligible. This is especially true when compared with the effects of loading asymmetry.

C. Ring Compression Theory

Another design method frequently used for flexible culverts was developed by White and Layer, called the "Ring Compression Theory." This technique approximates the stress in the culvert barrel as the total weight of the overfill above the culvert and requires that the ring be designed to carry this load. The equation for ring compression load per unit length is,

$$T = r\gamma H \tag{11}$$

where:

T is the ring compression load, per unit length;

r is the pipe radius;

γ is the soil density;

H is the overfill height.

A safety factor of 4 is usually applied to the ring compression load for design.

At Apple Canyon the measured vertical effective density was 120 pcf and the radius was 4.5 feet. Figures 92 and 93 represent the ring compression results and the experimentally determined vertical thrusts as functions of fill height and time. Station 10+00, Figure 92, indicates that ring compression yielded smaller thrusts than were actually measured. The discrepancy between the ring compression theory and experimental thrusts was -26.4 percent. Figure 93, for Station 7+25, shows that for the lower fill height, ring compression theory is conservative, averaging about 58 percent higher thrusts than were calculated from the measured strains.

An alternate analysis substituted the crown pressures calculated from Marston's theory for the fill height and soil density in equation, yielding,

$$T = r P_v \quad (12)$$

where:

T is the wall thrust;

r is the pipe radius;

P_v is the crown pressure from Marston's theory.

The theoretical thrusts using Marston's crown loads are also depicted in Figures 92 and 93. As in the previous analysis, theoretical thrusts at Station 7+25 were conservative, averaging 139 percent higher than the actual measured thrusts. At Station 10+00, however, theoretical thrusts were initially conservative for low fill heights but became progressively smaller with respect to the measured values for higher fill heights, resulting in a maximum thrust which

was about 48 percent lower than the measured values and an average theoretical thrust about 15 percent too low.

As a check on the suitability of the ring compression method, measured crown pressures were substituted for Marston's crown pressures in equation 12. The results, also depicted in Figures 92 and 93, are similar to those of the previous analyses. At Station 7+25, the ring compression method yields conservative thrusts at all fill heights, while at Station 10+00 the resulting thrusts are smaller than the measured values.

D. Flexibility Factor

Flexibility factors are used as indicators of rigidity of the culvert section. A maximum factor is considered necessary to insure that the culvert section will maintain its shape during handling and installation. For 6-inch by 2-inch corrugations, the recommended factor is 0.0200. The formula for flexibility factor is,

$$FF = \frac{D^2}{EI} \quad (13)$$

where:

D is the pipe diameter;

E is Young's modulus;

I is the moment of inertia of the cross-section.

The 3/8-inch plate sections at Station 10+00 had a flexibility factor of 0.00014, which is considerably smaller than the maximum allowable value. At Station 7+25, where Number 1 gage plates were used, the factor was 0.00020, again, well below the recommended maximum value.

E. Neutral Point Method

An analytical technique which may be used to verify design moments, thrusts and shears when the pipe geometry and external pressure distribution are known is the Neutral Point Method. External pressure distributions such as the one proposed by Spangler or resulting from experiments may be used.

The Neutral Point method is an extension of the "General Method of Indeterminate Structures," in which a culvert subjected to arbitrary external pressures is made statically determinate. The procedure involves cutting the pipe at its invert and subdividing it into a number of small segments called "voussoirs," each of length ds . One end of the cut ring is clamped to a rigid support, the other end being attached via a rigid bracket to the centroid of elastic weights, ds/EI , or "neutral point." External pressures are described by concentrated loads applied at the voussoir centroids. Restoration of compatibility after the loads are applied is achieved by the application of redundant forces at the neutral point. From these forces and the applied loading, moments, thrusts and shears may be calculated for each voussoir. Stresses are calculated from the moments and thrusts using elasticity theory. Displacements are determined from the voussoir rotations and do not reflect rigid body motion. The theoretical basis for the method has been reported in the literature (1,10). The number of arithmetic operations required makes a long-hand solution

by the neutral point method very tedious. Therefore, a computer program in Fortran IV language was used for the analysis.

Davis (1) has demonstrated that the neutral point procedure is quite sensitive to variations in geometry and applied pressure. Best geometric representations are obtained when two semi-ellipses are passed through the five octant points describing the left and right pipe halves. Field measured coordinates are used to describe the octant point positions.

Voussoir forces are determined by interpolation of a Fourier series passed through specified octant point pressures. For the analysis described herein, field measured pressures, based on the assumed datum, will be used. The asymmetric nature of the normal pressures resulted in a net unbalance in the horizontal and vertical pressures. To satisfy force equilibrium requirements, tangential forces must be applied at each voussoir, using actual tangential pressures, if known, or by approximation. The approximation used in the analysis is made by interchanging coefficients of the first sine and cosine terms of the Fourier series defining the normal pressures.

The pipe may be analyzed by assuming the entire fill to be in place prior to the analysis, called the "gravity turn-on" technique, or assuming the fill to be placed incrementally using successive pressure increases to model the construction. During an incremental analysis the pipe shape is modified prior to the addition of each

successive layer using either the calculated deformations or the available octant point coordinates. However, since calculated deformations may be inaccurate, the later shape modifications are preferred.

Distribution of internal moment calculated by three methods are compared with experimental moments based on the SR-4 gauge strains in Figures 94 and 95. Results of single layer, gravity turn-on analyses with and without assumed tangential pressures are depicted by dashed lines and solid lines, respectively. The pipe is not in equilibrium under either of these load cases; however, application of the assumed tangential force reduces the total force unbalance. Invert moment discontinuity which occurs in the analysis is reduced by the addition of tangential forces.

The third case depicted in each figure represents an incremental analysis, each layer having an assumed lateral pressure, the pipe shape being determined from prototype measurements. The incremental analysis further reduces the unbalanced force but does not significantly alter the calculated moment profile.

The neutral point analysis did not accurately predict the moment or thrust profiles at either test station. At Station 7+25, the incremental analysis produced the best correlations; the average discrepancies between theoretical and experimental values being + 462 percent for moments and + 87 percent for thrusts. The single layer analysis having assumed tangential forces used at Station 10+00 resulted in

average discrepancies of ± 647 percent and ± 19 percent for moments and thrusts, respectively.

The major reason for such large discrepancies between the Neutral Point method and the experimental data is probably the paucity of adequate pressure information. Since tangential pressures were not determined at Apple Canyon and the normal pressures, taken alone, did not produce static equilibrium, the Neutral Point method cannot be expected to yield satisfactory results when experimental data are used.

Attempts to increase the accuracy of the neutral point solutions by averaging the pressure profiles from both test stations and by forcing pressure symmetry through averaging pressures about the horizontal and vertical axes also proved fruitless. The reason for such failures is obvious, first because the shape changes at the two test stations are very different and secondly because pressure symmetry about the pipe axes cannot be expected at this installation. Since Spangler's pressure distribution is also symmetrical, attempts to use that distribution were not made.

F. Finite Element Method

The method of finite elements may be used to analyze embankments containing buried culverts. Several investigators (2, 11, 12, 13, 14) have successfully predicted the stress and displacement fields in dams and deep earth embankments using this method. The inclusion of a

culvert is an extension of the embankment analysis wherein shell elements are substituted for portions of the fill.

The finite element method provides an approximate solution to problems in continuum mechanics. Basically, the continuum (embankment and culvert in this case) is subdivided into discrete elements inter-connected at their nodes. Nodal point coordinates, element topology, material properties and boundary conditions are supplied as input. Equations are developed expressing the forces at each node in terms of the element stiffnesses and nodal point displacements. Solution of the resulting simultaneous equations yields displacements from which stresses and strains may be calculated. The theory and application of this method are well documented in the literature (2, 11, 15).

Finite element analyses have several distinct advantages over those previously discussed. A foreknowledge of the embankment displacements, required by Marston's theory, is not necessary since these are primary unknowns in the finite element analysis. Likewise, soil pressures distribution, assumed by Spangler may be calculated with the finite element method. Thus, this technique may be used to predict soil pressures, displacements, embankment stresses and pipe design parameters prior to construction. The only information necessary is a reasonable knowledge of the embankment geometry, the culvert properties and soil material properties.

Originally, it was intended that the Apple Canyon installation would be analyzed by the computer program PYPSIT developed by Brown (11). This program was designed to analyze

incrementally constructed embankments containing embedded culverts using either Method A or Method B backfill. However, numerical difficulties were encountered during the solution of the simultaneous equations, and the use of this program was discontinued.

A similar, incremental, plane-strain, finite element program developed by Herrmann (16) was obtained. Extensive modifications were made to include conduits within the fill and to calculate normal and tangential stresses at the soil-culvert interface. Numerical difficulties are not encountered since a different equation solver is used and the equations are formulated to reduce ill-conditioning.

Preliminary investigations, using a large mesh which simulated the entire embankment cross-section at Station 10+00, revealed that the embankment behaved symmetrically about a vertical plane midway between the two pipes. Displacements were essentially vertical at about 70 feet on either side of the plane of symmetry. Consequently, subsequent analyses were performed using a reduced mesh encompassing the fill bounded by the plane of symmetry midway between the pipes and a vertical plane 70 feet to the left as depicted in Figure 96. The foundation material was modeled to an elevation of 2,600 feet, about 22 feet below the culvert invert. Since foundation data were not available, the supporting soil was arbitrarily assumed to rest on a rigid foundation at that elevation. Boundary conditions applied to the mesh sides prevented lateral motion along both vertical boundaries. The embankment was analyzed in 6 increments, each coinciding with a

data acquisition elevation. The first layer ended 10 feet above the culvert crown and corresponds to the zero readings for all instrumentation. Subsequent layers terminated at 34, 55, 80, 122 and 160 feet above the crown.

Much effort was expended in attempting to correlate theoretical soil pressures and internal pipe moments and thrusts with field measured data. Initial analyses employed linear elastic properties for both the embankment and foundation materials. Foundation and fill moduli were assumed equal for the first trial. Other combinations of fill and foundation moduli were also tested. However, as will be discussed in detail later, the pressures calculated by the finite element method did not correlate well with the experimental values.

As a result of the trials using linear-elastic material properties, the finite element computer program was further modified to utilize a non-linear material representation. The particular procedure chosen was reported by Kulhany, et al., (2, 14) and has been used successfully in the analysis of embankments. The procedure determines Young's modulus and Poisson's ratio based on a hyperbolic idealization of the material stress-strain relationship and the state of stress existing in the continuum. The governing equations are,

$$E_i = \left[1. - \frac{R_f (1 - \sin \phi) (\sigma_1 - \sigma_3)}{2C \cos \phi + 2 \sigma_3 \sin \phi} \right]^2 K P_a \left(\frac{\sigma_3}{P_a} \right)^n \quad (14)$$

$$\mu_i = \frac{G - F \log \left(\frac{\sigma_3}{P_c} \right)}{P_c}$$

$$\left[\frac{d (\sigma_1 - \sigma_3)}{1. - \left[1. - \frac{R_f (1 - \sin \phi) (\sigma_1 - \sigma_3)}{2C \cos \phi + 2 \sigma_3 \sin \phi} \right] K P_a \left(\frac{\sigma_3}{P_a} \right)^n} \right]^2 \quad (15)$$

where:

- E_i - tangent modulus;
- μ_i - tangent Poisson's ratio;
- σ_1, σ_3 - major and minor principal stresses, respectively;
- C - soil cohesion;
- ϕ - angle of internal friction of the soil;
- K - initial modulus number (dimensionless);
- G - initial Poisson's ratio;
- n - exponent determining rate of variation with σ_3 ;
- R_f - ratio of ultimate deviator stress ($\sigma_1 - \sigma_3$) expressed by the pure hyperbolic stress-strain function to the deviator stress at failure;
- d - change in Poisson's ratio with confining pressure;
- F - change in Poisson's ratio with radial strain;
- P_a - atmospheric pressure expressed in appropriate units.

The parameters K , R_f , n , ϕ and C are determined from standard triaxial tests. Measurements of axial and volumetric strain must be made during the tests in order to evaluate G , F and d .

Unfortunately, the results of extensive soil sampling were lost due to the resignation of one of the University investigators. New samples were obtained from near the surface of the completed fill. The sample is not necessarily representative of the entire embankment but provides the only available information. Triaxial tests were performed on the new samples including measurement of axial and volumetric strains. The evaluation procedure and hyperbolic material parameters are described in Appendix A. Foundation material was not sampled.

Of the many analyses performed for the Apple Canyon installation, four are reported herein, two using linear-elastic material properties and two having non-linear properties. Enumeration of the reported trials is as follows:

- Trial 1 - Linear elastic material, foundation modulus equal to fill modulus;
- Trial 2 - Linear elastic material; foundation modulus equal to 1/4 fill modulus;
- Trial 3 - Non-linear material, foundation modulus equal to fill modulus;
- Trial 4 - Non-linear material, foundation modulus equal to 1/4 fill modulus.

The finite element data was reduced with respect to the prototype instrumentation datum, 10 feet above the crown. The results from each incremental analysis of each trial were compared with the experimental data for the corresponding elevation at Station 10+00. In addition, results from the third layer of each trial were compared with the data obtained at Station 7+25 for a fill height of about 52 feet. The soil pressures resulting from each trial are superimposed on experimentally determined pressure profiles for Stations 10+00 and 7+25 in Figures 97 and 98, respectively.

Trial 1, employing linear elastic materials, indicated good correlation of theoretical and observed pressures at the crown and both ends of the horizontal diameter for Station 10+00. The remaining octant points did not exhibit good agreement, with the poorest at the invert. The average pressure difference between calculated

and observed values was ± 18 percent. Theoretical lower octant pressures ranged from 21 to 25 percent below measured pressures. At Station 7+25, Trial 1 pressures correlated closely with measured values at the crown, left horizontal diameter and one lower octant point, the remaining octants exhibited significant discrepancies. The calculated pressures indicated an average discrepancy of ± 37 percent.

Pressure discrepancies at the invert were reduced by arbitrarily decreasing the foundation modulus to 25 percent of the embankment modulus. Other trials, not reported herein, showed that such a decrease might improve the overall pressure correlation. The invert pressure was significantly increased, reducing the discrepancy to about 12 percent at Station 10+00. The remaining octant pressures were also increased but to a lesser extent. The total pressure distribution was not significantly improved, the average error being ± 17.5 percent at Station 10+00. At Station 7+25 the average discrepancy was ± 43 percent.

Introduction of the non-linear material properties in Trial 3 tended to decrease the calculated octant point pressures. Only the crown and invert pressures indicated higher values. Excellent correlations were observed at the upper right quadrant; the discrepancy being about 1 percent. Invert pressure comparison was somewhat improved over the value from Trial 1. The average discrepancy for this trial was almost 18 percent at Station 10+00. A similar pressure distribution was observed at layer 3 (corresponding to a

data acquisition elevation at Station 7+25) but with poorer correlation.

Again, the foundation modulus was reduced to 25 percent of its Trial 3 value. As in the case of the linear material approximation, the average pressure discrepancy was reduced to + 16.7 percent.

Displacements, the primary unknowns, are also reported by the finite element program. Results from the four reported trials were compared with settlement platform readings, survey data and pipe octant point displacements. Foundation settlements were very small for Trials 1 and 3. Where the foundation modulus was reduced, Trials 2 and 4, the difference between experimental and calculated settlements was about 20 percent.

Settlement platform data for the fill above the pipe were also compared with the finite element output. The linear material model having low foundation modulus agreed with the experimental values to 16 percent. The remaining trials indicated differences of between 27 and 181 percent. Other investigators (12, 14) have achieved good correlations between theoretical and observed settlements using the finite element procedure. In these studies, the foundation configuration and material properties have been accurately assessed. Thus, the large differences observed at Apple Canyon were expected since these parameters can only be assumed.

Observed culvert deformations do not correlate with calculated displacements. This is also to be expected

due to the proximity of the culvert to the foundation material. All calculated pipe quantities are highly dependent on the foundation properties which are assumed in these analyses. In addition, the large lateral motions observed in the prototype were not evident in the computer analysis, probably due to variations in the soil backfill surrounding the barrel.

Pipe moments, shears and thrusts were also calculated by the finite element program. These quantities are determined from the pipe properties, geometry and computed nodal point displacements. Moments and thrusts generated during each trial were compared with the experimental values. Figures 99 and 100 indicate the experimental moment profile and the results of each finite element trial. In general, correlations are very poor. In many cases computed moments were of opposite sign from the experimental data. At Station 10+00, for a fill height of 160 feet, the four trials resulted in moment discrepancies averaging about \pm 950 percent. Correlations for Station 7+25, having a lower fill height were correspondingly smaller. The observed moment discrepancies may have been due to several factors: ill-condition of the stress matrices; lack of adequate soil property data and soil pipe interface idiosyncracies within the prototype. Since the calculated displacements did not accurately represent the actual prototype movements, the later factor would result in poor calculated moments. The computed thrusts were subject to errors due to ill-conditioning of the element output stiffness matrices. Hence, no valid

thrusts were obtained. Efforts to produce better correlations using calculated pressures in a neutral point analysis proved equally fruitless.

In summary, the finite element method, although a powerful analytical tool, is only as good as the input data. For cases where embedded pipes are analyzed, the material properties surrounding the pipe must be known. It should be emphasized that analyses by any of the above techniques presupposes uniform conditions. Construction practices employed will, in large measure, determine the actual behavior of the culvert and may bear little relationship to the structure as analyzed.

COMPARISON OF METHOD A AND METHOD B BACKFILL

A. General

A prototype culvert having Method B backfill was constructed at Chadd Creek, in Humboldt County, California (1). The culvert was a single, 114-inch nominal diameter, Number 1 gage, structural steel plate pipe. Method B backfill conditions were achieved by placing 3 to 5 feet of baled straw over the pipe crown. Three sections were instrumented in a manner similar to those at Apple Canyon. Figure 101 depicts the Chadd Creek installation.

B. Relative Shape Changes

Culvert deformations at Chadd Creek were determined in the same manner as at Apple Canyon. The reduced data may be found in the appendices to Reference 1. Figure 102 through 107, comparing the changes in horizontal and vertical diameters produced by Method A with those of Method B,

demonstrate the influence of a compressible inclusion above the culvert crown. Both installations exhibited horizontal diameter decreases and accompanying vertical elongations as fill is placed around the conduits. This behavior is due to the lack of confinement above the pipe. As the fill height increases, both conduits undergo shortening of the vertical diameter. However, Method B backfill exhibits a second reversal in trend after 20 to 40 feet of overfill had been placed, indicating that the baled straw has become effective in reducing vertical pressure while lateral pressures continue to increase with increasing fill height. This behavior is not present for Method A backfill. Instead, the vertical diameter continues to decrease as the overburden is increased.

The magnitudes of the vertical deformations for Method B backfill are considerably smaller than those of Method A. At the time of fill completion, one test station at Chadd Creek exhibited net vertical elongations of 0.19 inch, another showed no net vertical dimension change while the third exhibited a diameter decrease of about 0.35 inch. At a fill height of 60 feet, Method B backfill produced vertical elongations at two stations and shortening at a third. The magnitudes of these changes averaged 0.17 inch while at Apple Canyon both test stations exhibited vertical diameter decreases averaging 1.00 inch. Final deflections at Apple Canyon averaged about 2 percent, those at Chadd Creek, about 0.5 percent; neither of which exceed the 5 percent maximum value suggested by Spangler as a practical limit.

C. Soil Pressure and Effective Density

Typical soil pressures and effective densities for the Chadd Creek installations are plotted versus fill height and time in Figures 108 through 111. Comparisons of typical soil pressure data from the two prototypes are presented in Figures 112 through 117. The pressure and density functions depart radically from the linear nature observed at Apple Canyon. The effect of the baled straw over the crown is to reduce the effective overburden while allowing the lateral pressures to increase without restraint. Once the baled straw becomes sufficiently compressed, additional overburden is transmitted to the pipe producing pressure functions similar to those of Apple Canyon.

Effective density functions generated for Method B backfill are highly non-linear in contrast to the nearly constant functions evidenced for Method A. The meters located along the upper half of the pipe registered relative minimum densities for fill heights at or slightly below the top of the baled straw. Corresponding densities for the five meters at and below the horizontal diameter exhibit relative maxima. This behavior is symptomatic of Method B backfill wherein the compressible medium causes redistribution of vertical pressure toward the exterior prisms with a corresponding increase in lateral pressure due to Poisson's effect. As the fill elevation increases, upper octant densities increased and lower octant values remained constant or decreased slightly. Comparison of effective density profiles for Method A and Method B backfill are depicted in Figures 118 and 119.

Soil pressure meters located in the exterior prisms at Chadd Creek indicated superhydrostatic effective densities of about twice the actual embankment density. Corresponding meters at Apple Canyon exhibited subhydrostatic densities. This behavior indicated the transfer of overburden load to the exterior prisms under Method B and transfer of load to the pipe under Method A.

D. Culvert Strains

Strains in the Chadd Creek culvert were measured using SR-4 cross gauges placed in quadruplets as depicted in Figure 4. A compilation of the strain gauge data and computed stresses, moments and thrusts is contained in the appendices to Reference 1. Data from tensile tests performed on coupons obtained from the pipe material at Chadd Creek are listed in Table 12b.

Strains commensurate with the measured yield stress levels were observed at each test station at Chadd Creek and the positions exhibiting such strains are presented in Table 13c. Circumferential yield strains first occurred at the crown at each test station when the overfill reached 63 to 71 feet. At Station 0-96, where the maximum overfill was 81 feet, all gauge positions along the top and left sides and the invert indicated yield strains shortly after fill completion. At the remaining two stations, 0+44 and 1+00, where the maximum fill heights were 89 and 76 feet, respectively, yield strains were confined to the crown or crown and upper left octant. Longitudinally, yield strains occurred at the crown and just below the right

horizontal diameter when construction was completed at Station 0-96, only.

Had the pipe material properties conformed to the minimum specified yield and ultimate stress levels, the gauge positions exhibiting yield strains would have been as shown in Table 13d. Initial circumferential yield would have occurred at the crown at each test station when about 45 feet of overfill had been placed. At Stations 0-96 and 0+44, strains in excess of minimum yield strains were recorded at nearly all gauging positions after construction was completed. At Station 1+00, specified yield strains were exceeded along the left half of the culvert only. Longitudinal strains exceeded specified yield levels at Stations 0-96 and 1+00, only, with Station 0-96 exhibiting such strains at most gauge positions.

In contrast to Chadd Creek, specified minimum yield level strains, which were identical for both installations, did not occur until 52 feet of fill had been placed at Station 7+25, where the pipe properties are similar. Yielding was limited to the invert and left end of the horizontal diameter. Yield strains in the longitudinal direction at Station 7+25 did not occur until the maximum fill height had been reached and about 122 feet of fill was in place at Station 10+00.

Stresses calculated from the strain gauge data for both installations are compared in Table 10 for a fill height of 62 feet. These quantities are functions of pipe geometry and material properties as well as the state of

loading. Similar pipe properties are found at Station 7+25 at Apple Canyon. The stresses reported for the Chadd Creek culvert were averaged for the three test stations, and linear interpolation between stresses at fill height of 52 and 68 feet was used for the Apple Canyon data. Maximum positive circumferential stresses for Method B at Chadd Creek are about 35 percent larger than those at Apple Canyon, having Method A backfill. Maximum negative stresses are reduced by only 4 percent using Method A. The stress gradient, the difference between stress readings at adjacent octant points around the pipe, are given in Table 11 and averaged 43 percent lower for Method A, with a maximum of 46 percent lower.

In order to compare moments and thrusts, the effects of pipe diameter were eliminated. Experimental thrusts at Apple Canyon were adjusted by the ratio of the diameters of the two installations. Moments were adjusted by the ratio of the squared diameters. Table 10 presents the thrust and moment comparison for both culverts.

Method A backfill produced lower moments but larger thrusts than did Method B. Differences between maximum positive and maximum negative moments are negligible but the maximum moment gradient due to Method A is about 57 percent smaller than Method B. Thrusts, however, are significantly higher for Method A and the maximum thrust gradient was 45 percent larger. Typical moment and thrust profiles for both installations at a fill height of 62 feet are depicted in Figure 120.

Stresses, thrusts and moments at other fill heights and following embankment completion are not directly comparable due to differing conditions at the two installations. However, from the data obtained at these test sites it is apparent that the more uniform pressure distribution, lower stress gradients and small deflections produced by Method A backfill make this method of construction superior for flexible culverts. It is anticipated that, had a circular shape been used initially, substantial reductions in pipe stress and deflections may have been achieved since the initial deflections due to the placing of fill around the barrel would have been sufficient to produce initial ellipticity and the uniform pressure distribution would produce very small bending stresses.

SUMMARY OF OBSERVATIONS

A. Experimental Results for Method A Backfill

1. Vertical diameters increased as fill was placed around the culvert barrel but began to decrease as fill was added above the crown. Horizontal diameters behaved oppositely and exhibited smaller changes than the vertical diameter due to the development of passive pressures. Maximum vertical deflection was about 2 percent.
2. Soil pressures are smooth functions of fill height and time. During fill construction, pressure increases are nearly linear. Following embankment completion, pressures continued to increase to a relatively stable value lasting 18 to 24 months but

showed subsequent increases of 50 percent or more at between 24 and 36 months.

3. Profiles of effective density are fairly uniform with a maximum difference in density between any two octant points of about 46 percent. The magnitude of the horizontal and vertical densities are nearly equal.
4. Transverse strains indicated that plane sections remained plane throughout the data acquisition period.
5. Longitudinal and transverse strains vary non-linearly with fill-height and time.
6. Strains commensurate with the minimum specified yield stress occurred near the invert with between 50 and 80 feet of fill above the crown. Yield strains were confined to the invert region at Station 7+25 but progressed to the entire cross-section within 24 months after fill completion at Station 10+00. No structural distress was observed as a result of yielding.

B. Theoretical Analyses

1. Marston's theory of loads on buried conduits produced good correlations for experimental and theoretical vertical crown pressures, for the negative projecting conduit, incomplete projection condition. Following embankment completion, the theory failed to predict observed pressure increases.

2. Spangler's Iowa Deflection Formula for flexible culverts failed to predict the observed horizontal deflections. This fact was primarily due to the differences between the assumed pressure distribution developed by Spangler and the observed pressure profile.
3. Values of E' , the modulus of soil reaction, which would result in correct predicted deflections were very erratic but averaged about 37,700 psi for Station 10+00. This large value can probably be attributed to the confinement afforded by the shallow trench in which the pipe was installed. It is not believed that the initial pipe ellipticity was a significant factor in producing the large E' values.
4. The Ring Compression Theory underestimated the observed thrusts at Station 10+00 by an average of 26 percent but overestimated those at Station 7+25 by 58 percent. Theoretical thrusts do not include a safety factor.
5. The flexibility factors calculated for the Apple Canyon installation were well below the maximum allowable values.
6. Neutral point analyses using normal forces, only, did not produce equilibrium. The computed moments and thrusts did not correlate with the experimental values. Inclusion of assumed tangential loads

produced equilibrium but failed to produce accurate moments or thrusts.

7. Soil pressures calculated by the finite element method agreed with measured pressures to within 20 percent even though available material property data were limited. Calculated moments, thrusts and displacements did not correlate as well with experimental data.

C. Comparison of Method A and Method B Backfill

1. Vertical and horizontal diameter changes were smaller for Method B than for Method A backfill. Reversals in diameter changes occurred only once for Method A and twice for Method B.
2. Soil pressures due to Method A are more uniform functions of fill-height than those of Method B.
3. Superhydrostatic effective densities were observed in the exterior prisms for Method B and in the interior prism for Method A.
4. Stresses due to Method A were about 43 percent smaller than those of Method B for equivalent fill heights during construction. Yield strains were observed at lower fill heights for Method B. Moments were of approximately the same magnitude for both methods but the moment gradient for Method A was 57 percent lower. Method A produced larger thrusts and thrust gradients.

CONCLUSIONS

The nearly uniform pressure distribution, linear

pressure-fill height functions, and uniform moment gradients observed at Apple Canyon combine to produce favorable conditions for flexible metal culverts. Control of deflections, a critical criterion in culvert design, was adequate using Method A backfill although vertical deflections using Method B backfill were smaller. The pressure profiles produced by Method B backfill were much less uniform. With proper control of the pipe geometry, bedding, backfill and construction procedures, Method A backfill can result in a uniformly loaded pipe having very small bending moments and adequate deflection control.

The significance of high stresses at Apple Canyon was minimal. Stresses in excess of the minimum specified yield strength of the pipe material were noted but no structural damage was observed.

The methods of analysis presently available did not predict accurately the behavior exhibited by the Apple Canyon culvert. The post-completion behavior observed with both Method A and Method B backfill are not predicted by any of the techniques discussed herein. The ring compression theory provides a reasonable design approximation for flexible culverts. However, it is recommended that soil densities be increased by 70 percent to account for long-term effective density increases and that the safety factor of 4 be retained for design. The finite element procedure may provide an accurate analysis if sufficient information concerning the bedding, backfill and foundation are available. A more refined analysis considering soil consolidation theory to

assess soil properties as a function of time may be necessary to predict culvert behavior accurately. A three-dimensional analysis is required to determine the effects of longitudinal soil pressure distribution.

Based on the research at Apple Canyon and Chadd Creek, the use of Method B backfill for flexible culverts is not recommended. Observations at Apple Canyon suggested a uniform peripheral distribution of effective density as a basis for design. However, the very large fiber strains observed demonstrate that significant wall bending moments may result from small departures from a circular configuration. Such departures may exist initially or as a result of conformance of the pipe to a variable pressure distribution produced by embankment heterogeneity. Unconservative designs could result from an assumed uniform peripheral pressure distribution if some degree of shape irregularity were not considered. With adequate deflection control, an ultimate design concept can be implemented.

RECOMMENDATIONS FOR FUTURE RESEARCH

The research reported herein describes the behavior of a flexible metal pipe under service conditions only. The ultimate behavior of the pipe has not been investigated. Also, comparisons of Method A and Method B backfill conditions are hampered by the different conditions which occurred in the two discussed installations. It is recommended that further research be undertaken wherein an underdesigned, dummy flexible culvert is embedded in a deep embankment. Method A and Method B backfill conditions should be provided

to assess the behavior of these two types of construction under identical conditions. Other bedding and backfill conditions may also be studied.

On subsequent culvert research projects a method of determining tangential forces acting on the pipe should be developed so that equilibrium conditions can be assessed. Moreover, at least 2, and preferably 3, sets of pressure meters should be installed at each test station to account for soil heterogeneity or possible meter failure.

Prior to construction, extensive geological studies should be undertaken to determine the nature of the soil and rock strata underlying the installation. Soil samples and compaction tests should be made at each data acquisition level during fill construction in order to provide an accurate indication of the actual embankment properties. Triaxial testing, incorporating volumetric and axial strain measurements, must be made to provide data on the soil modulus and Poisson's ratio to facilitate analysis by the Finite Element Method.

An improved finite element procedure should be developed which will accurately assess the behavior of the culvert during construction and following embankment completion. A consolidation theory may be necessary to model post-embankment-completion conditions.

STATEMENT OF IMPLEMENTATION

The conclusions developed in this report are presently being implemented in the design of flexible culverts in California. Design is based on a uniform

peripheral effective density of 140 pcf, the ring compression theory and an ultimate design concept. Geologic investigations are now performed on all major culvert projects. The use of Method B backfill for flexible culverts has been discontinued. Future culvert installations having high fills or unusual configurations will be supplemented by results of finite element analyses.

The recommendations for future research are presently being implemented in a research project entitled, "Proof Testing of a Structural Plate Pipe with Various Bedding and Backfill Parameters". This project comprises an under-designed dummy pipe having Method A and various types of Method B backfill. Instrumentation will be similar to that of the Apple Canyon installation except that 3 sets of soil stressmeters are planned at each test zone. An extensive program of geologic investigations and soil sampling is planned. Theoretical analyses will be performed using the finite element technique. Improvements in the finite element program will be made in order to assess post-embankment-completion behavior.

BIBLIOGRAPHY

1. Davis, R. E., "Structural Behavior of a Flexible Metal Culvert Under a Deep Embankment Using Method B (Baled Straw) Backfill," California Division of Highways, Bridge Department, Report No. 4-69, 1969.
2. Kulhany, F. H., Duncan, J. M., Seed, H. B., "Finite Element Analysis of Stresses and Movements in Embankments During Construction," University of California, Berkeley, College of Engineering, Office of Research Services, Report No. S-69-8.
3. Spangler, M. G., "Field Measurements of the Settlement Ratio of Various Highway Culverts," Iowa Engineering Experimental Station, Bulletin No. 170, Ames, Iowa, 1950.
4. Spangler, M. G., "Soil Engineering," International Text Book Company, New York, 1951.
5. Spangler, M. G., "The Structural Design of Flexible Pipe Culverts," Iowa Engineering Experimental Station, Bulletin No. 153, Ames, Iowa, 1941.
6. National Cooperative Highway Research Program, "Structural Analysis and Design of Pipe Culverts," Report No. 116, Highway Research Board, 1971.
7. Davis, R. E., Patterson, L. R., "Structural Behavior of a Reinforced Concrete Arch Culvert - Phase II," California Division of Highways, Bridge Department, Report SSR 2-68, June, 1968.
8. Davis, R. E., Bacher, A. E., "Structural Behavior of a Concrete Pipe Culvert," California Division of Highways, Bridge Department, Report No. R&D 4-71, April, 1971.
9. Davis, R. E., "Structural Behavior of a Reinforced Concrete Arch Culvert," California Division of Highways, Bridge Department, Report No. SSR 3-66, September, 1966.
10. Grintner, L. E., "Theory of Modern Steel Structures," Vol. II, MacMillan Company, New York, 1949.
11. Brown, C. B., Green, D. R., Pawsey, S. F., "Flexible Culverts Under High Fills - Equilibrium Considerations," University of California, Berkeley, SESM Report No. 67-1, June, 1967.
12. Smith, T., Forsyth, R. A., Shirley, E. C., Chang, I. C., "Stresses and Deformations in Jail Gulch Embankment," Interim Report, California Division of Highways, Materials and Research Department, Report No. CA-HWY-MR632509-4-72-07, February, 1972.

13. Clough, R. W., Woodward, R. J., "Analysis of Embankment Stresses and Deformation," Journal of Structural Mechanics, ASCE, SM-4, July, 1972.
14. Kulhany, F. H., Duncan, J. M., "Stresses and Movements in Oroville Dam," Journal of the Structural Division, ASCE, SM-7, July, 1972.
15. Zienkiewicz, O. C., Cheng, Y. K., "The Finite Element Method in Structural and Continuum Mechanics," McGraw Hill, London, 1967.
16. Herrmann, L. R., Private Communications.
17. Davis, R. E., Bacher, A. E., "California's Culvert Research Program - Description, Current Status, and Observed Peripheral Pressures," Highway Research Record, No. 249, Highway Research Board, Washington, D.C.



TABLE 1

APPLE CANYON SPP

DATA AQUISITION SCHEDULE

Date	Sta 7+25		Sta 10+00	
	Elevation	Fill Height Over Crown	Elevation	Fill Height Over Crown
	2635	0	2630	0
2/28/66	2645	10	2640	10
3/09/66	2656	21	2656	26
3/16/66	2658	23	2664	34
3/29/66	2674	39	2674	44
4/05/66	2687	52	2685	55
4/08/66	2703	68	2703	73
4/12/66	2703	68	2710	80
4/15/66	2703	68	2730	100
4/22/66	2703	68	2752	122
4/29/66	2703	68	2775	145
5/05/66	2703	68	2790	160
7/19/66	2703	68	2790	160
10/06/66	2703	68	2790	160
3/16/67	2703	68	2790	160
6/27/67	2703	68	2790	160
11/15/67	2703	68	2790	160
5/22/68	2703	68	2790	160
4/23/69	2703	68	2790	160

TABLE 2

APPLE CANYON SPP

INCREASE IN SOIL PRESSURE AT VARIOUS TIMES DURING CONSTRUCTION
STATION 7+25

Meter	Embank. Compl. This Sta.	Constr. Compl.	% 1 Incr.	Post-Compl. Stable Period ²	% 1 Incr.	36 Mo After Constr. Compl.	% 1 Incr.
1	57.0	73.3	29	88.4	55	90.2	58
2	55.5	70.9	28	85.5	54	90.8	64
3	30.7	29.2	-5	44.5	45	50.0	63
4	34.5	56.7	64	67.6	96	83.7	143
5	42.7	57.5	35	74.9	75	88.6	108
6 ³	15.2	24.6	62	46.0	203	60.0	295
7	58.2	88.5	52	86.4	48	79.5	37
8	50.2	65.2	30	71.7	43	77.6	55
9	47.0	62.1	32	68.6	46	74.5	59
10	54.5	69.6	28	78.4	44	89.3	64
11	44.8	56.7	27	8.10	81	99.0	121
12	36.8	50.3	37	60.2	64	86.3	134
13	25.0	31.0	24	43.6	74	47.1	88
14	32.2	42.0	30	58.6	82	62.7	95
15	32.4	36.5	13	46.3	43	49.8	54
Avg. 3			35		61		82

1. Percentage increase based on pressures at point of maximum overflow at this station.
2. A period of relatively stable pressures occurred at between 3 and 24 months after construction completion.
3. Averages do not include contributions due to meter number 6.

TABLE 2 (Continued)
 APPLE CANYON SPP
 INCREASE IN SOIL PRESSURE AT VARIOUS TIMES DURING CONSTRUCTION
 STATION 10+00

Meter	Embank. Compl. This Sta.	Constr. Compl.	% Incr. 1	Post-Compl. Stable Period ²	% Incr. 1	36 Mo After Constr. Compl.	% Incr. 1
25	98.8	98.8	---	144.2	46	165.7	68
26	132.1	132.1	---	171.0	29	198.2	50
27	79.7	79.7	---	122.9	54	138.7	74
28	154.1	154.1	---	211.3	37	241.9	57
29	131.2	131.2	---	172.3	31	203.4	55
30	147.8	147.8	---	192.2	30	220.7	49
31	136.6	136.6	---	240.5	76	277.2	103
32	106.0	106.0	---	148.6	40	173.8	64
33	127.9	127.9	---	207.0	62	228.3	78
34	132.6	132.6	---	163.6	23	181.7	37
35	111.5	111.5	---	149.8	34	177.2	59
36	119.0	119.0	---	129.0	8	162.2	36
Avg.			--		39		56

1. Percentage increases based on pressures at point of maximum overflow at this station.
2. A period of relatively stable pressure occurred at between 3 and 24 months after construction completion.

TABLE 3

APPLE CANYON SPP

INCREASE IN EFFECTIVE DENSITY AT VARIOUS TIMES DURING CONSTRUCTION
STATION 7+25

Meter	Initial Density	Embank. Compl. This Sta.	% Increase ²	Constr. Compl.	% Increase ³	Post-Compl. Stable Period ⁴	% Increase ³	36-Mo After Constr. Compl.	% Increase ³
1	183	116	-37	145	25	176	51	179	54
2	182	121	-34	148	22	181	50	191	58
3	146	64	-56	64	0	92	44	104	63
4	99	72	-27	110	53	134	86	165	129
5	99	84	-15	112	33	142	69	167	99
6	52	29	-44	45	55	86	196	106	266
7	102	117	15	161	38	164	40	151	29
8	110	104	-5	130	25	142	36	154	48
9	97	102	5	130	27	143	40	155	52
10	157	113	-28	137	21	155	37	176	56
11	134	93	-31	118	27	161	73	194	108
12	85	77	-9	100	30	120	56	167	117
13	137	71	-48	87	23	121	70	127	79
14	174	92	-47	119	29	162	76	172	87
15	175	92	-47	100	9	128	39	137	39
Avg.			-27		28		64		86

1. Density observed at time of meter installation.
2. Density increase during placement of overfill at this station.
3. Density increase based on value at time of maximum overfill at this station.
4. A period of relatively stable pressures occurred between 3 and 24 months after construction completion.

TABLE 3 (Continued)

APPLE CANYON SPP

INCREASE IN EFFECTIVE DENSITY AT VARIOUS TIMES DURING CONSTRUCTION

STATION 10+00

Meter	Initial ₁ Density	Constr. Compl.	% Increase ₂	Post-Compl. Stable Period ₃	% ₄ Incr.	36 Mo After Constr. Compl.	% ₄ Incr.
25	106	86	-19	126	46	139	62
26	119	123	3	154	25	175	42
27	84	73	-13	110	51	119	63
28	164	142	-13	185	30	206	45
29	110	115	5	148	29	175	52
30	122	127	4	164	29	187	47
31	140	120	-14	207	85	238	98
32	120	98	-18	130	33	147	50
33	135	118	-13	184	56	198	68
34	137	120	-12	143	19	155	52
35	162	97	-40	131	35	144	48
36	101	104	3	113	8	131	26
Avg.			-11		37		54

1. Density observed at time of meter installation.

2. Density increase during construction of overfill at this station.

3. A period of relatively stable pressure occurred between 3 and 24 months after construction completion.

4. Density increase based on value at time of construction completion.

TABLE 4

APPLE CANYON

POSITIVE PROJECTION CONDUIT

Station 10+00

Fill Ht.	Crown Settle. $(S_f + d_c)$	Crit. Plane Consol. $(S_m + S_g)$	O.G. Settle. $S_f = S_g$	Ext. Prism Consol. S_m	Settle. ratio γ_{sd}	Plane of Equal Settle H_e	Load Coef. C_c	Load w	Adj Load	Exp. Data	Diff.
10	-.05	0.37	0.02	0.35	--	12.25	0.626	9.4	0.0	13	-4.7
26	0.28	0.53	0.18	0.35	.714	13.99	1.805	27.1	17.7	17	-10.5
34	0.30	0.63	0.28	0.35	.943	13.72	2.469	36.9	27.5	26	-12.8
44	0.45	0.74	0.42	0.32	.906	13.40	3.215	48.2	38.8	41	-10.1
55	0.62	0.87	0.58	0.29	.862	12.62	4.033	60.5	51.1	51	-19.7
73	0.91	1.10	0.85	0.25	.760	12.30	5.318	79.8	70.7	59	-18.6
80	1.02	1.20	0.95	0.25	.720	11.01	5.803	87.0	77.6	75	-33.8
100	1.32	1.44	1.23	0.21	.571	10.34	7.881	118.2	108.8	98	-20.8
122	1.60	1.72	1.48	0.24	.500	11.94	8.545	128.2	118.8	110	-38.6
145	1.77	2.02	1.63	0.37	.676	12.34	10.532	158.0	148.6	121	-45.6
160	1.81	2.23	1.65	0.58	.724		11.734	176.0	166.6		21.5
AVG											
2 1/2 Mo	2.04	2.41	1.86	0.55	.673	12.29	11.721	175.8	166.4	133	-33.4
5 Mo	2.05	2.53	1.87	0.66	.727	12.36	11.740	176.1	166.7	158	-8.7
10 Mo	2.08	2.64	1.89	0.75	.747	12.52	11.781	176.7	167.3	155	-12.3
18 Mo	2.11	2.72	1.92	0.80	.763	12.63	11.809	177.1	167.7	160	-7.7
24 Mo	2.17	2.77	1.98	0.79	.759	12.62	11.805	177.1	167.7	163	-4.7

K = 0.42118

p = 0.1503

TABLE 5

APPLE CANYON SPP

NEGATIVE PROJECTING CONDUIT

Station 10+00

Fill HT	Settle Ratio γ_{sd}	Plane of = Settle H_e	Load Coef. C_c	Load $W = 120\text{pcf}$ w	Adj Load	Exp. Data	Diff
10	0	1.35'	0.539	8.1	0.0		
26	0	1.35'	1.401	21.0	12.9	13	-0.1
34	0	1.35'	1.831	27.5	19.4	17	-2.4
44	0	1.35'	2.370	35.5	27.4	26	-1.4
55	0	1.35'	2.962	44.4	36.8	41	4.2
73	0	1.35'	3.931	59.0	50.9	51	0.1
80	0	1.35'	4.038	64.6	56.5	59	2.5
100	0	1.35'	5.384	80.8	72.7	75	2.3
122	0	1.35'	6.569	98.5	90.4	98	7.6
145	0	1.35'	7.807	117.1	109.0	110	1.0
160	0	1.35'	8.614	129.2	121.1	121	-0.1
Avg.							1.4
2½	0	1.35	8.614	129.2	121.1	133	
5	0	1.35	8.614	129.2	121.1	158	
10	0	1.35	8.614	129.2	121.1	155	
18	0	1.35	8.614	129.2	121.1	160	
24	0	1.35	8.614	129.2	121.1	163	

TABLE 6

APPLE CANYON SPP

POSITIVE PROJECTING CONDUIT

Station 7+25

Fill Ht.	Crown Settle. ($S_f + d_c$)	Crit. Plane Consol. ($S_m + S_g$)	O.G. Settle. $S_f = S_g$	Ext. Prism Consol. S_m	Settle. ratio γ_{sd}	Plane of Equal Settle H_e	Load Coef. C_c	Load w	Adj Load	Exp. Data	Diff.
10	0.02	0.21	0.00	0.21	0.904	13.71	0.625	9.4	0.0	0	
21	0.14	0.35	0.12	0.23	0.913	13.77	1.456	21.8	12.4	10	2.4
23	0.16	0.37	0.13	0.24	0.875	13.50	1.605	24.1	14.7	18	4.7
39	0.32	0.52	0.25	0.27	0.740	12.46	2.775	41.6	32.2	81	1.2
52	0.47	0.60	0.37	0.23	0.565	10.96	3.638	54.6	45.2	40	5.2
68	0.64	0.68	0.53	0.13	0.307	8.17	4.522	67.8	58.4	45	3.4
AVG.											3.8
77	0.69	0.76	0.57	0.19	0.368	8.92	4.592	68.9	59.5	49	5.5
96	0.80	0.86	0.66	0.20	0.300	8.08	4.514	67.7	58.3	51	7.3
117	0.86	0.93	0.72	0.21	0.333	8.55	4.549	68.2	58.8	58	0.8
140	0.90	0.95	0.76	0.19	0.263	7.58	4.466	67.0	57.6	56	1.6
155	0.93	0.94	0.77	0.17	0.059	3.64	4.104	61.6	52.2	60	-7.8
AVG.											1.5
2.5	0.97	0.93	0.81	0.12	-0.333					63	
5	1.00	0.85	0.83	0.02	-7.500					74	
10	1.04	0.85	0.86	-0.01	19.000					74	
18	1.03	0.79	0.89	-0.10	2.40					75	
24	1.06	0.79	0.89	-0.10	-2.700					77	

k = 0.42118

p = 0.1503

TABLE 7

APPLE CANYON SPP

NEGATIVE PROJECTING CONDUIT

Station 7+25

Fill Height	Settle Ratio γ_{sd}	Plane of = Settle H_e	Load Coef C_c	Load $W=120pcf$ w	Adj Load	Exp. Data	Diff.
10	0	1.35	0.539	8.1	0.0		
21	0	1.35	1.132	17.0	8.9	10	1.1
23	0	1.35	1.239	18.6	10.5	18	7.5
39	0	1.35	2.101	31.5	23.4	31	7.6
52	0	1.35	2.800	42.0	33.9	40	6.1
68	0	1.35	3.662	54.9	46.8	45	-1.8
Avg.							4.1
77	0	1.35	3.662	54.9	46.8	49	2.2
96	0	1.35	3.662	54.9	46.8	51	-4.2
117	0	1.35	3.662	54.9	46.8	58	11.2
140	0	1.35	3.662	54.9	46.8	56	9.2
155	0	1.35	3.662	54.9	46.8	60	13.2
Avg.							6.3
2.5	0	1.35	3.662	54.9	46.8	63	16.2
5	0	1.35	3.662	54.9	46.8	74	27.2
10	0	1.35	3.662	54.9	46.8	74	27.2
18	0	1.35	3.662	54.9	46.8	75	28.2
24	0	1.35	3.662	54.9	46.8	77	30.2

Table 8

Deflection by Spangler's Equation

Station 10+00				Station 7+25			
Fill Ht. & Time	Theo.	Exp.	% Diff.	Fill Ht. & Time	Theo.	Exp.	% Diff.
26	.728	--	--	21	1.251	--	--
34	.954	.158	504.	23	1.382	.173	699.
44	1.230	.286	330.	39	2.386	.375	536.
55	1.538	.377	308.	52	3.132	.531	490.
73	2.044	.495	313.	68*	3.890	.634	513.
80	2.240	.604	271.	68	3.952	--	--
100	2.800	.741	278.	68	3.884	.734	429.
122	3.414	.932	266.	68	3.912	.813	381.
145	4.058	1.109	266.	68	3.844	.818	370.
160	4.478	1.231	264.	68	3.534	.842	370.
2½**	5.598	1.402	299.	2½**	3.534	.892	296
5	5.598	1.445	287.	5	3.534	.898	294
10	5.598	1.515	270.	10	3.534	.911	288
13	5.598	1.535	265.	13	3.534	.912	288
18	5.598	1.563	258.	18	3.534	.919	285
24	5.598	1.586	253.	24	3.534	.929	280
36	5.598	1.629	244.	36	3.534	--	--

* Fill completed of this station

** Time after construction completion (months)

Table 9

Values of E' by Spangler's Theory

Fill Ht. & Time	Station 10+00			
	Method 1		Method 2	
	Right	Left	Right	Left
26	--	--	--	--
34	35716	45659	30488	25129
44	27994	37817	24455	20229
55	35086	46284	28100	25945
73	33139	43103	26862	22778
80	31106	40801	24940	21082
100	32796	42076	25192	21049
122	34259	44287	26523	21698
145	32507	40706	23346	19596
160	32094	39963	22467	19082
2½**	31007	38118	22192	18234
5	37132	44859	27240	23345
10	34303	40925	25153	20938
13	36353	42946	26330	21865
18	34660	41118	25700	21123
24	34931	40764	25408	20583
36	133354	23071	82890	13528

** Time after fill completion (months)

Table 9 (continued)

Values of E' by Spangler's Theory

Fill Ht. & Time	Station 7+25			
	Method 1		Method 2	
	Right	Left	Right	Left
21	--	--	--	--
23	43432	29735	13529	12916
39	620854	1364	124200	7023
52	1518557	6671	374220	7138
68*	2522179	5275	675277	6824
68	--	--	--	--
68	2872476	5489	864810	6925
68	711371	5543	236040	7090
68	435381	5000	140901	7134
68	635446	5723	242794	7219
2½**	393355	5697	131791	6916
5	510891	8470	186840	7649
10	602767	7800	225920	7427
13	556216	8478	209412	7346
18	723767	7895	271737	7327
24	626365	8265	249520	7665

* Fill completed at this station

** Time after fill completion (months)

TABLE 10

COMPARISON OF STRESS, MOMENT AND THRUST
FOR METHOD A AND METHOD B

FILL HEIGHT OVER CROWN = 62 FT.

Parameter	Method A	Method B	% Difference
Max. Positive Stress - Outer Crown (psi)	877	1320	34
- Inner Valley	609	944	35
- Outer Valley	427	733	42
- Inner Crown	704	996	29
Max. Negative Stress - Outer Crown (psi)	-1122	-1017	10
- Inner Valley	- 903	- 833	8
- Outer Valley	- 992	-1136	-13
- Inner Crown	-1219	-1509	-19
Max. Stress Grad. - Outer Crown (psi)	1370	2337	41
- Inner Valley	1119	1777	37
- Outer Valley	846	1869	54
- Inner Crown	1173	2505	53
Max. Positive Moment (in. - lb.)	59515	65532	9
Max. Negative Moment (in. - lb.)	-50999	-47488	- 4
Max. Moment Gradient* (in. - lb.)	49287	114029	57
Max. Thrust (lb.)	-28427	-21411	-33
Min. Thrust (lb.)	-6276	- 283	
Thrust Gradient* (lb.)	20780	14315	-45

* Gradient is defined as the difference between quantities at adjacent octant points.

TABLE 11

COMPARISON OF STRESS GRADIENTS*
FOR METHOD A & METHOD B BACKFILL

FILL HEIGHT OVER CROWN = 62 FT

Meter Positions	Outer Crown (psi)			Inner Valley (psi)		
	B	A	% Diff.	B	A	% Diff.
1 - 2	2771	792	250	1714	588	191
2 - 3	469	414	13	374	332	13
3 - 4	1172	279	320	903	233	288
4 - 5	341	57	498	805	45	1689
5 - 6	1083	1234	-12	279	960	-71
6 - 7	1023	1371	-25	786	1119	-30
7 - 8	232	639	-63	1144	393	-63
8 - 9	1342	883	52	1044	625	67
9 - 10	196	275	-28	142	205	-31
10 - 1	2337	767	205	1777	164	983
Avg.	1047	671	36	797	466	42

Meter Positions	Outer Valley			Inner Crown		
	B	A	% Diff.	B	A	% Diff.
1 - 2	1691	615	175	2290	831	176
2 - 3	439	295	49	556	408	36
3 - 4	913	214	327	1206	277	335
4 - 5	654	67	576	838	67	1151
5 - 6	431	656	-34	571	962	-40
6 - 7	837	846	-1	1085	1173	-7
7 - 8	161	573	-72	227	750	-70
8 - 9	1118	678	65	1504	877	71
9 - 10	325	239	36	385	262	46
10 - 1	1869	314	498	2505	454	451
Avg.	844	450	47	1118	606	46

* Gradient is defined as the difference in stress between adjacent octant points.

Table 12a				
Apple Canyon SPP				
Material Properties				
Sample No.	Sample Type	Yield Stress (psi)	Ultimate Stress (psi)	Elongation (%)
A-1	Straight	43,700	62,200	33.5
A-3	Straight	42,500	58,200	34.5
Avg		43,100	60,500	34.0
A-2	Curved	59,200	71,400	21.5
A-4	Curved	55,400	67,100	34.0
Avg		57,300	69,250	27.8
Specified		28,000	42,000	30.0

Table 12b				
Chadd Creek SPP				
Material Properties				
Sample No.	Sample Type	Yield Stress (psi)	Ultimate Stress (psi)	Elongation (%)
T1-1	Straight	41,900	51,100	30.0
T2-1	Straight	32,800	48,500	40.5
T3-1	Straight	33,000	48,500	39.0
Avg		35,900	49,367	36.5
T1-2	Curved	47,800	57,500	21.5
T2-2	Curved	44,500	55,800	28.0
T3-2	Curved	45,400	56,700	25.0
Avg		45,900	55,667	24.8
Specified		28,000	42,000	30.0

Table 13a

Apple Canyon SPP

SR-4 Gauge Positions Exhibiting Strains in Excess

of Actual Yield Level ***

Station 7+25			Station 10+00		
Fill Height	Circumferential	Longitudinal	Fill Height	Circumferential	Longitudinal
21			26		
23			34		
39			44		
52			55		
68*			73		
68			80		
68			100		
68			122		
68			145		
68			160*	6	
2.5**			2.5**	6, 9	1
5			5	5, 6, 9	1
10			10	5, 6, 9	
13.5			13.5	5, 6, 9	
18			18	1, 5, 6, 9	
24.5			24.5	1, 5, 6, 9	
36			36	1, 5, 6, 9	1

*Maximum overfill completed at this station

**Time after fill completion in months

*** $\sigma \geq \sigma_y = 57,300$ psi

Table 13b

Apple Canyon SPP

SR-4 Gauge Positions Exhibiting Strains in Excess

of Specified Minimum Yield Level ***

Station 7+25			Station 10+00		
Fill Height	Circumferential	Longitudinal	Fill Height	Circumferential	Longitudinal
21			26		
23			34		
39			44		
52	6,8		55	5	
68*	6,8		73	5,6	
68	6,8		80	5,6,9	
68	6,8		100	1,4,5,6,9	
68	6,8	7	122	1,4,5,6,9	1
68	6,8	7	145	1,4,5,6,9	1
68	6,8	7	160*	1,4,5,6,9	1
2.5**	5,6,8	7	2.5**	1,4,5,6,7,9	1,6
5	5,6,8	6,7	5	1,2,4,5,6,7,9	1,6
10	5,6,8	6,7	10	1,2,3,4,5,6,7,8,9	1,2,6
13.5	5,6,8	6,7	13.5	1,2,3,4,5,6,7,8,9	1,6
18	5,6,8	6,7	18	1,2,3,4,5,6,7,8,9,10	1,2,6,10
24.5	5,6,8	6,7	24.5	1,2,3,4,5,6,7,8,9,10	1,2,5,6,10
36	5,6,8	6,7	36	1,2,3,4,5,6,7,8,9,10	1,2,5,6,10

*Maximum overflow completed at this station

**Time after fill completion in months

*** $\sigma \geq \sigma_y$ (specified) = 28,000 psi

Table 13c

Chadd Creek SPP

SR-4 Gauge Positions Exhibiting Strains in Excess

of the Actual Yield Stress Level **

Station 1+00		Station 0+44		Station 0-96	
Fill Height	Circumferential	Fill Height	Circumferential	Fill Height	Circumferential
11		11		11	
20		20		20	
29		27		25	
38		36		35	
45		45		45	
56		55		55	
63	1	63	1	60	
76*	1	76	1	71	
76	1	79	1	72	
76	1	89*	1	81*	
4 mo.	1	4 mo.	1,10	4 mo.	1,2,3,4,6,10
					1,4
					1,4

* Maximum overfill at this station

** $\sigma \geq \sigma_y = 45,900$ psi

Table 13d

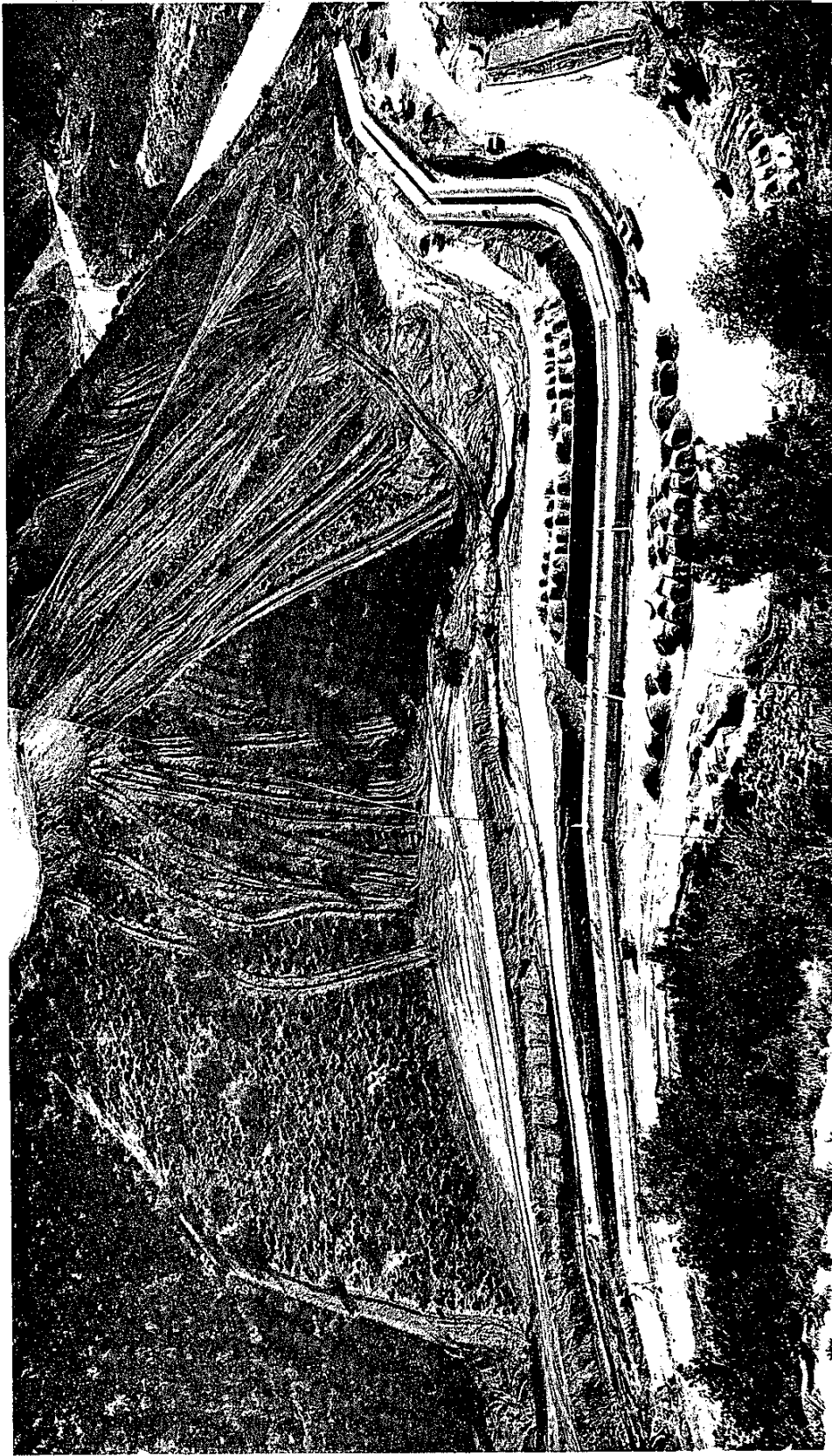
Chadd Creek SPP

SR-4 Gauge Positions Exhibiting Strains in Excess
of the Specified Minimum Yield Level **

Station 1+00			Station 0+44			Station 0-96		
Fill Height	Circumferential	Longitudinal	Fill Height	Circumferential	Longitudinal	Fill Height	Circumferential	Longitudinal
11			11			11		
20			20			20		
29			27			25		
38			36			35		
45			45	1,4		45	1,2,3,4,10	
56	1,2,8,9,10		55	1,4,10		55	1,2,3,4,5,6,8,10	
63	1,2,8,9,10		63	1,4,10		60	1,2,3,4,5,6,8,10	
76*	1,2,8,9,10	10	76	1,4,8,10		71	1,2,3,4,5,6,8,10	1,4,9,10
76	1,2,7,8,9,10	3,10	79	1,4,7,8,9		72	1,2,3,4,5,6,8,10	1,4,9,10
76	1,2,7,8,9,10	1,10	89*	1,2,4,6,7,8,9,10		81	1,2,3,4,5,6,8,10	1,2,3,4,9,10
4 mos	1,2,7,8,9,10	1,10	4 mo.	1,2,4,6,7,8,9,10		4 mo.	1,2,3,4,5,6,8,10	1,2,3,4,6,9,10

*Maximum overflow at this station

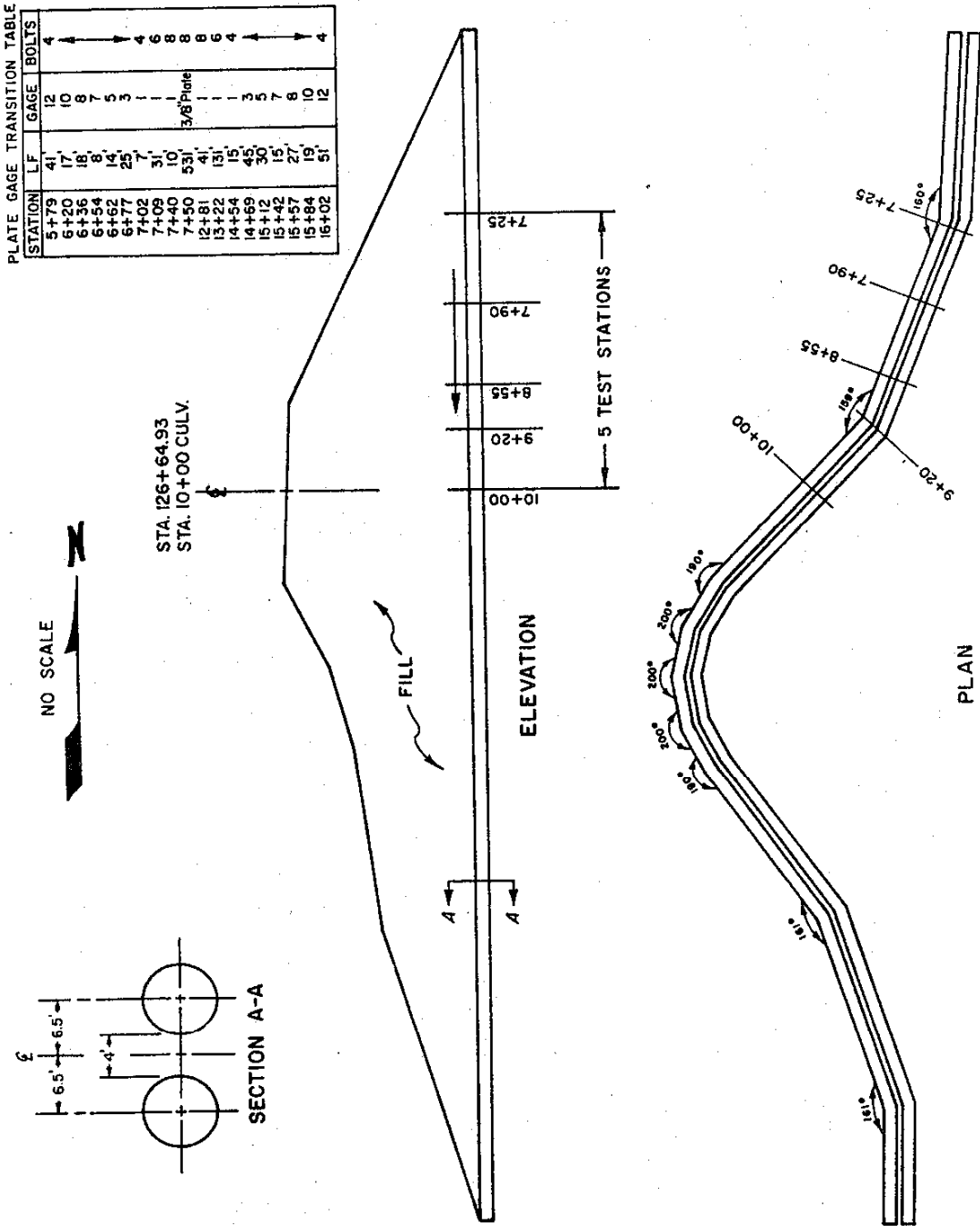
** $\sigma \geq \sigma_y = 28,000$ psi



APPLE CANYON CULVERT SITE PRIOR TO FILL CONSTRUCTION

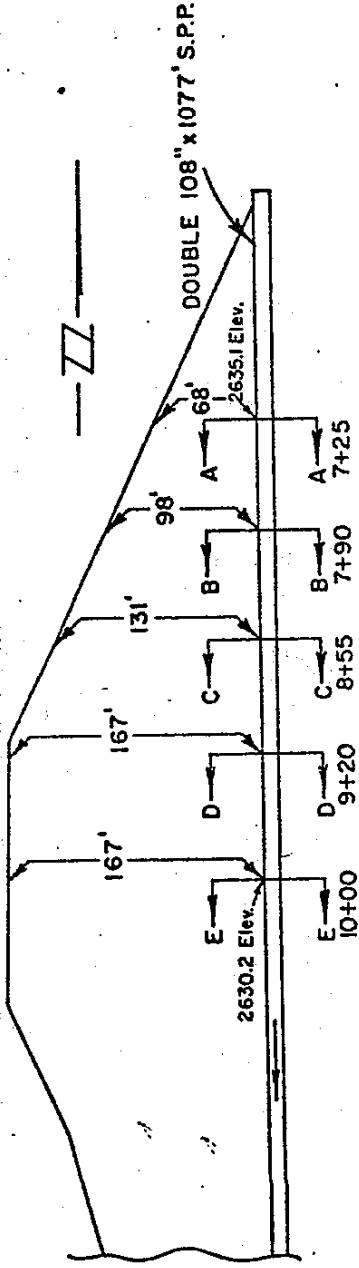
FIGURE 2

INSTALLATION AT APPLE CANYON OF
108" x 1077' TWIN PIPE CULVERT



APPLE CANYON SOIL PRESSURE METER IDENTIFICATION

07-LA-5-71.2/74.7



NO SCALE

≡ Soil pressure meter symbol

FIGURE 3

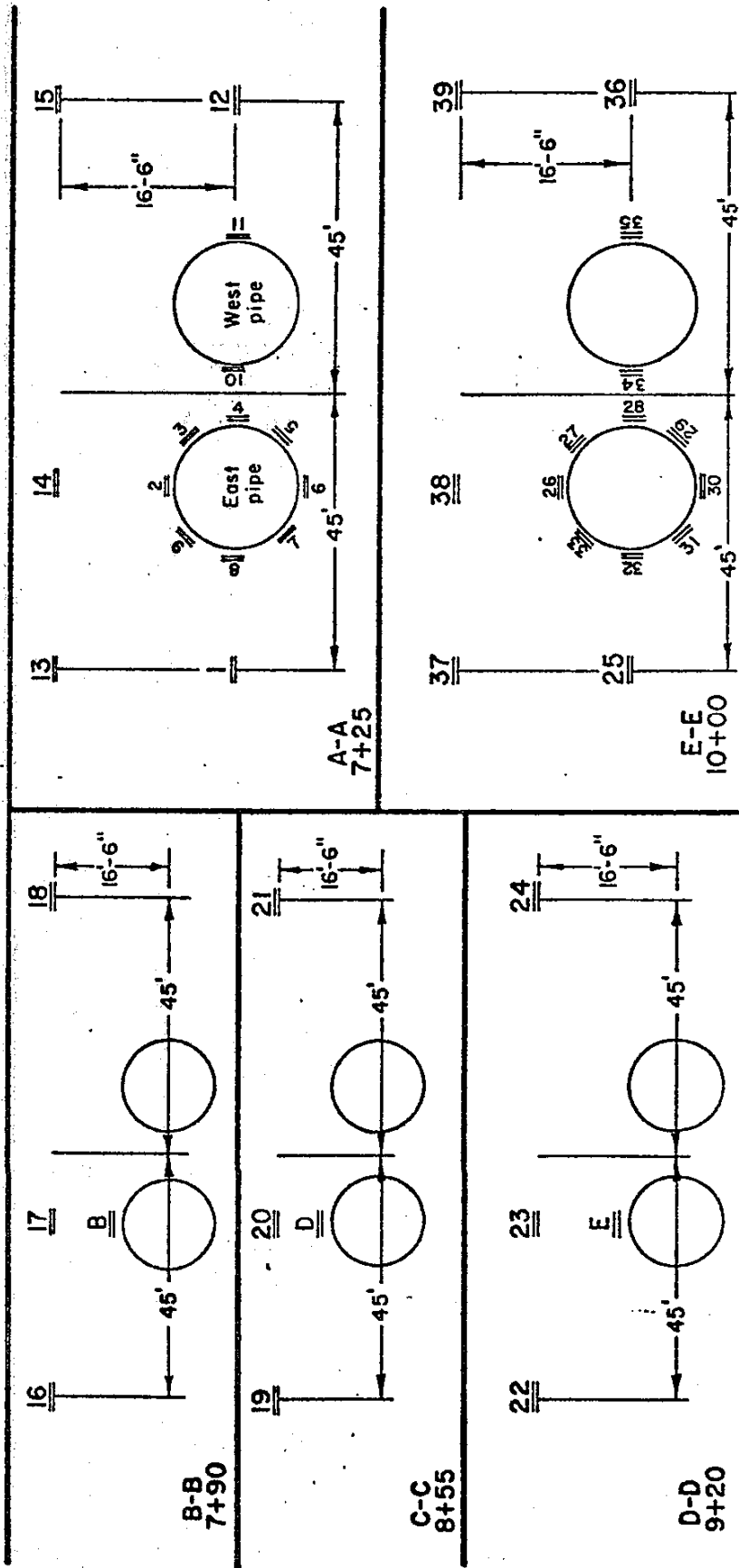


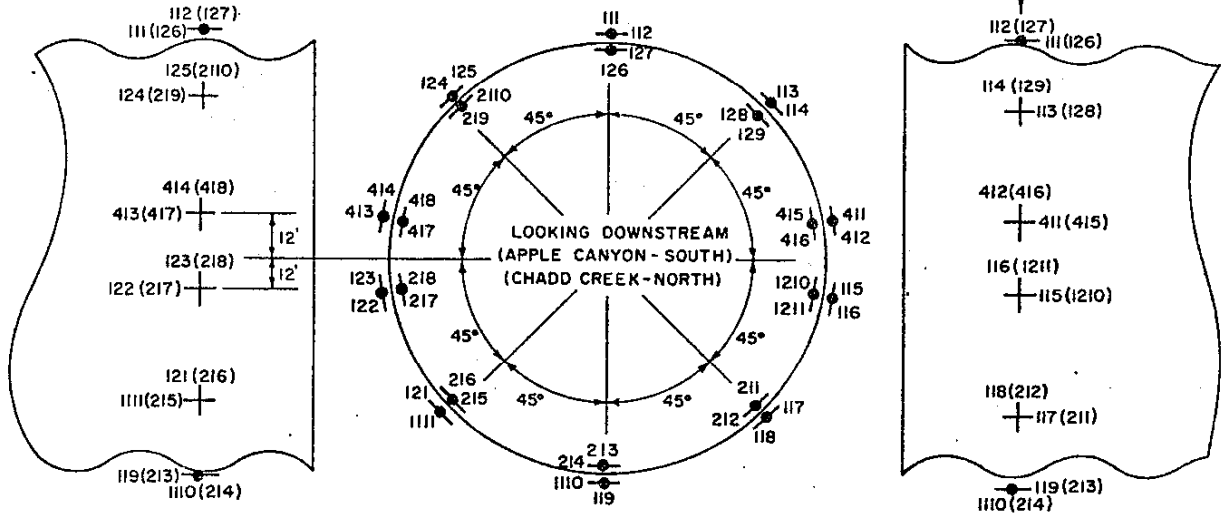
FIGURE 4

STRAIN GAGE NUMBER SYSTEM (identical at each sta.) FOR
CHADD CREEK AND APPLE CANYON CULVERTS

GAGE STATIONS	
CHADD CREEK	0-96, 0+44, 1+00
APPLE CANYON	7+25, 10+00

() DENOTES CORRESPONDING INTERIOR GAGE NUMBER

OUTSIDE GAGE LINE ON CORRUGATION CROWN.
INTERIOR GAGE LINE ON CORRUGATION VALLEY.



No Scale

— Longitudinal bolt line — located 12" circumferentially from strain gaged locations

OUTSIDE GAGE LINE ON CORRUGATION VALLEY.
INTERIOR GAGE LINE ON CORRUGATION CROWN.

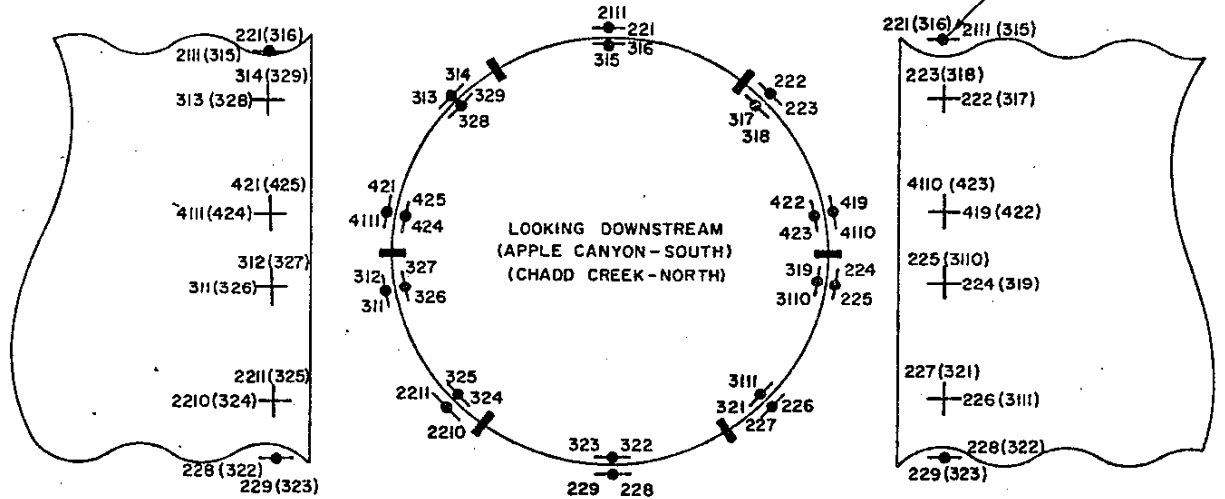
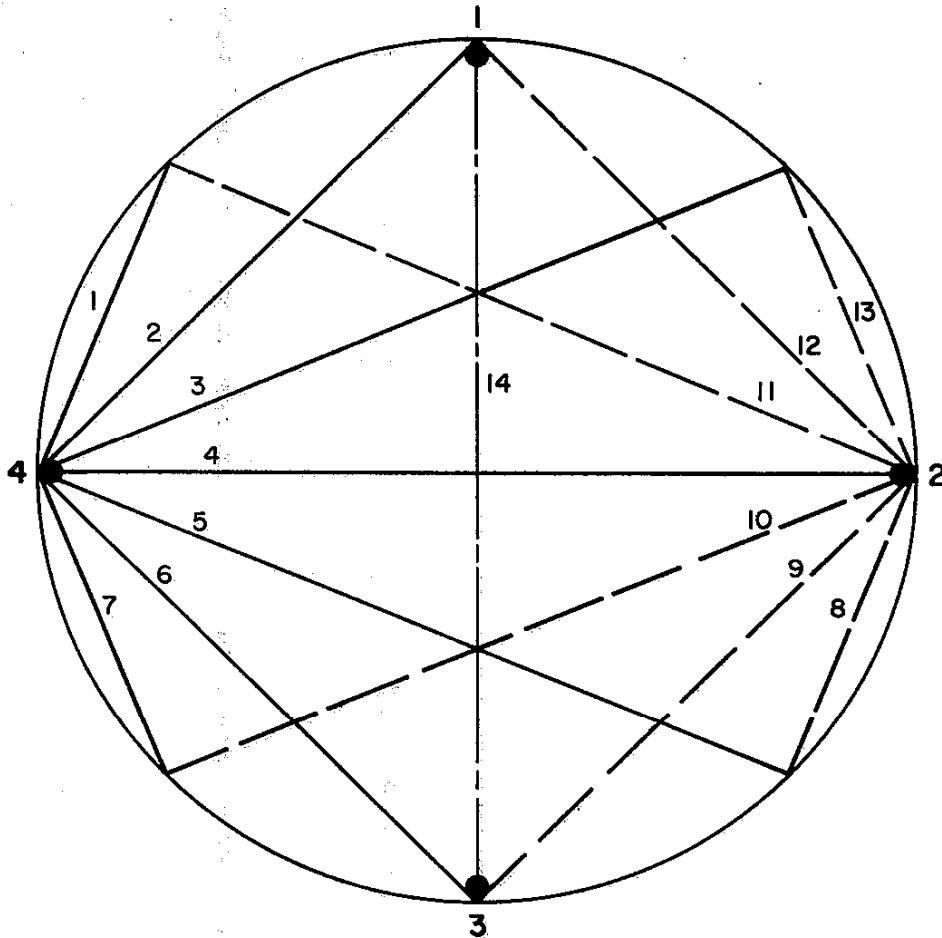


FIGURE 5

APPLE CANYON SPP
CULVERT DEFORMATION MEASUREMENTS

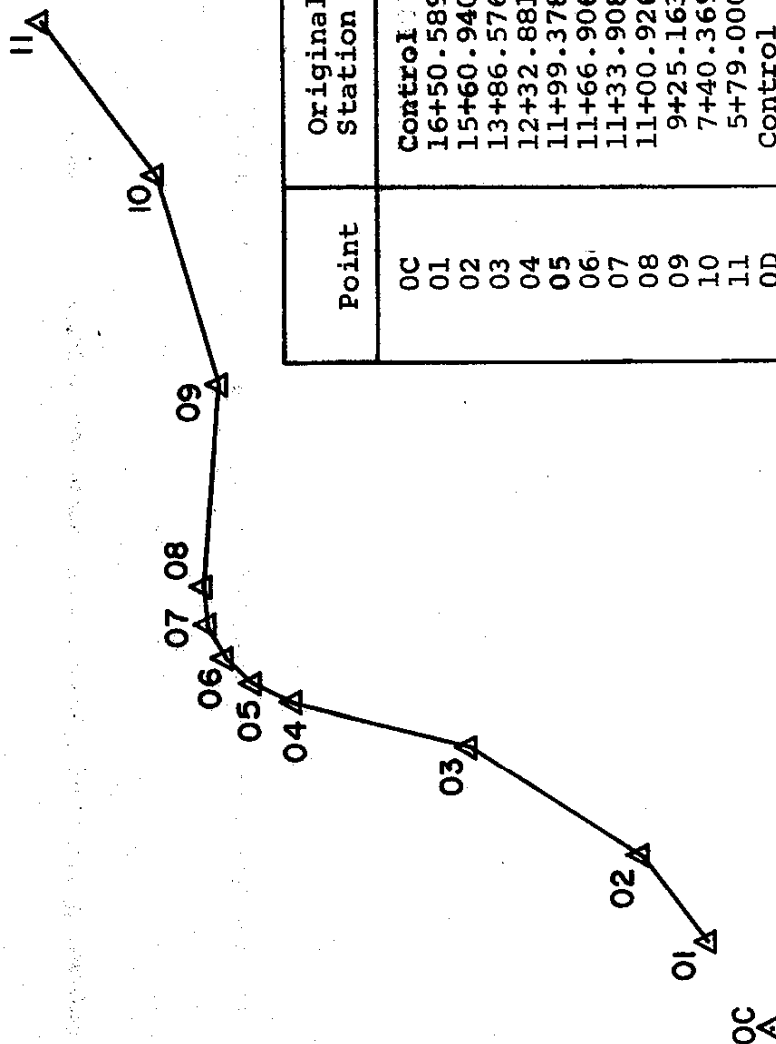


LEGEND

Chord Identity 4
Steel Spheres ●

FIGURE 7
 APPLE CANYON SPP
 SURVEY MONUMENT LAYOUT

OD



Point	Original Station	Original Elevation
OC	Control	2608.039
01	16+50.589	2610.089
02	15+60.940	2613.060
03	13+86.576	2616.389
04	12+32.881	2617.154
05	11+99.378	2617.967
06	11+66.906	2618.638
07	11+33.908	2619.342
08	11+00.926	2621.773
09	9+25.163	2622.708
10	7+40.369	2624.250
11	5+79.000	
OD	Control	

FIGURE 8

APPLE CANYON SPP
STATION 10+00
CHANGES IN CULVERT DIMENSIONS

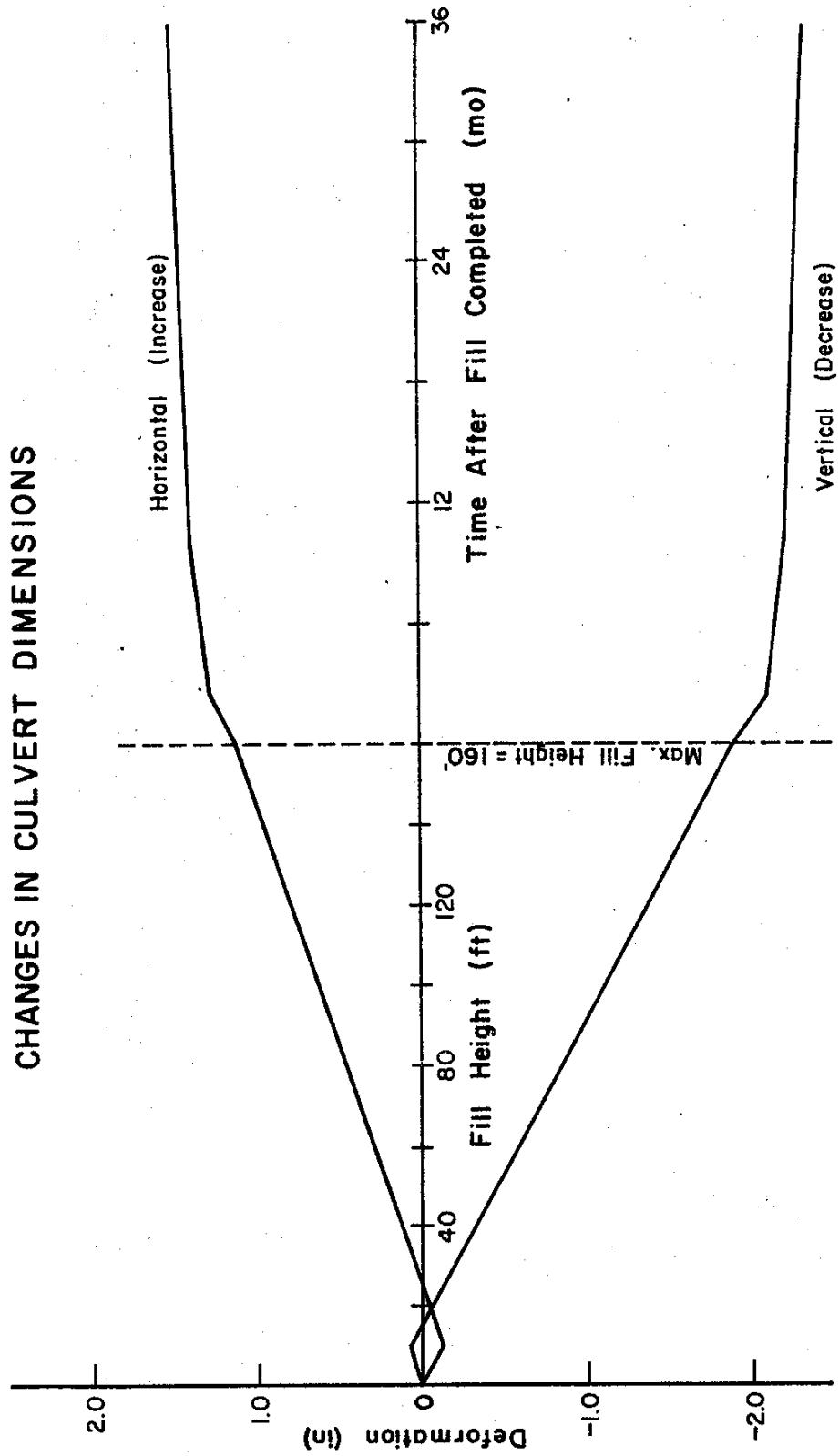


FIGURE 9

APPLE CANYON SPP
STATION 7+25
CHANGES IN CULVERT DIMENSIONS

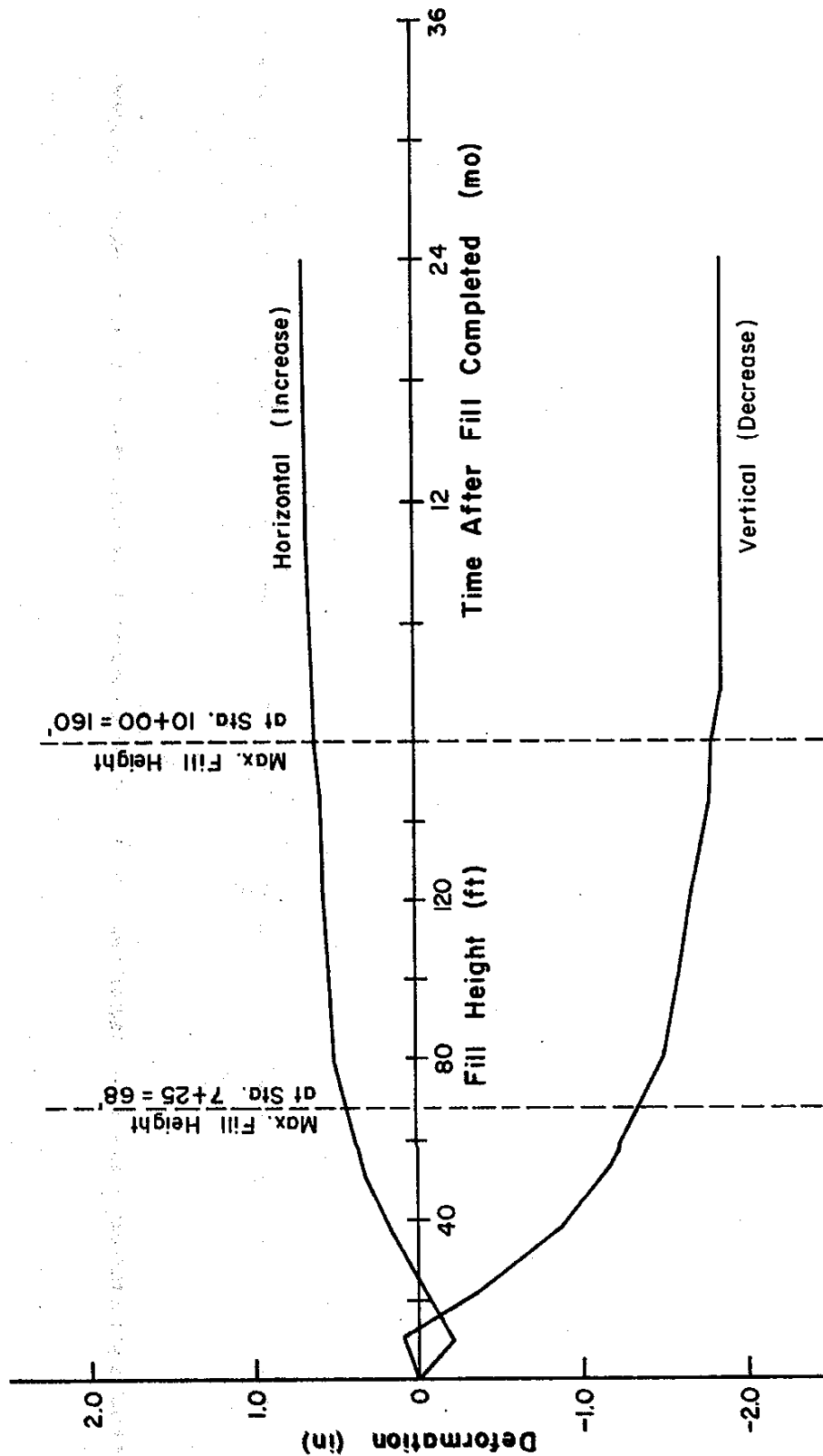


FIGURE 10

APPLE CANYON SPP
STATION 10+00
DISPLACEMENT VS. FILL HEIGHT

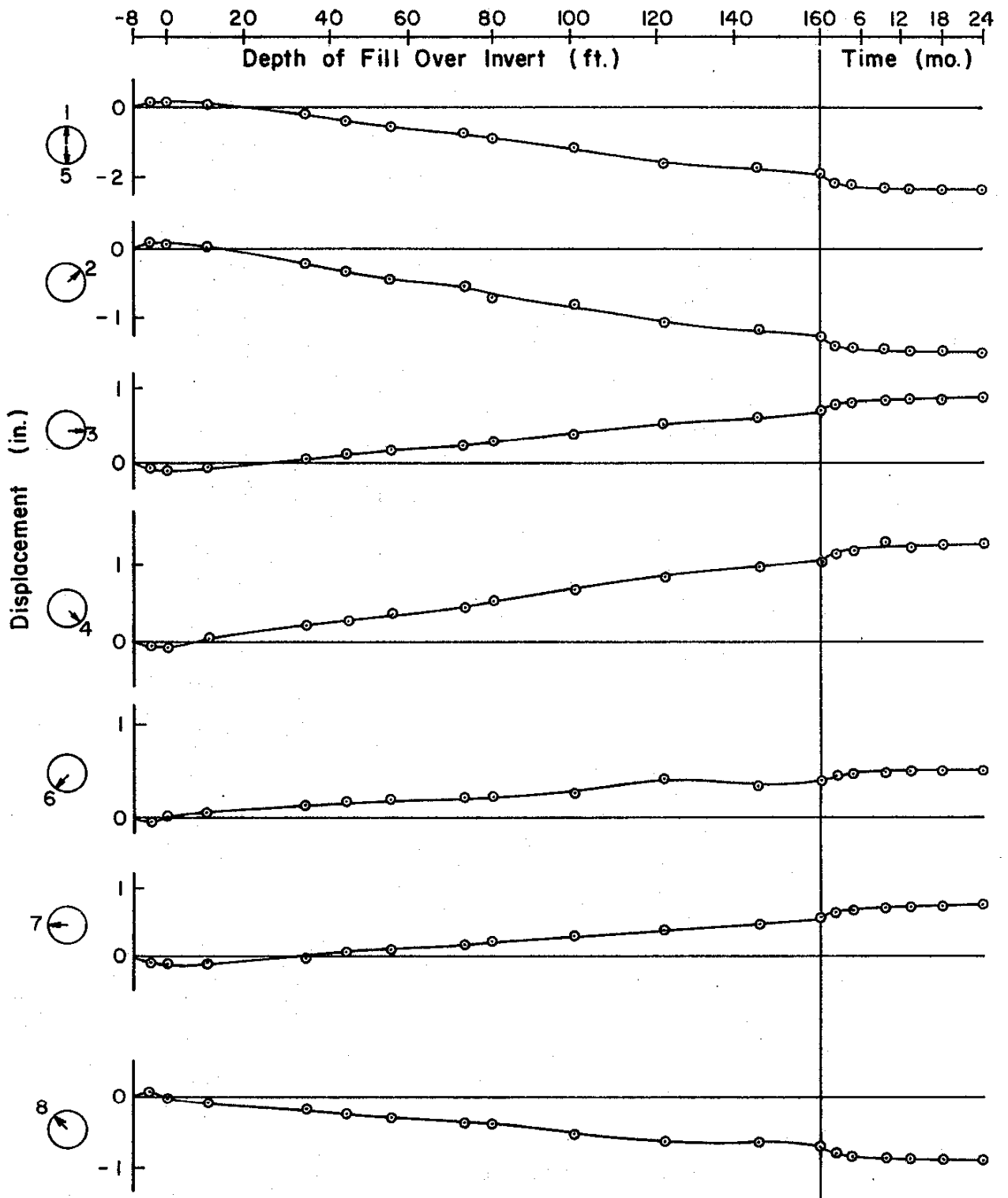


FIGURE 11

APPLE CANYON SPP
STATION 7+25
DISPLACEMENT VS. FILL HEIGHT

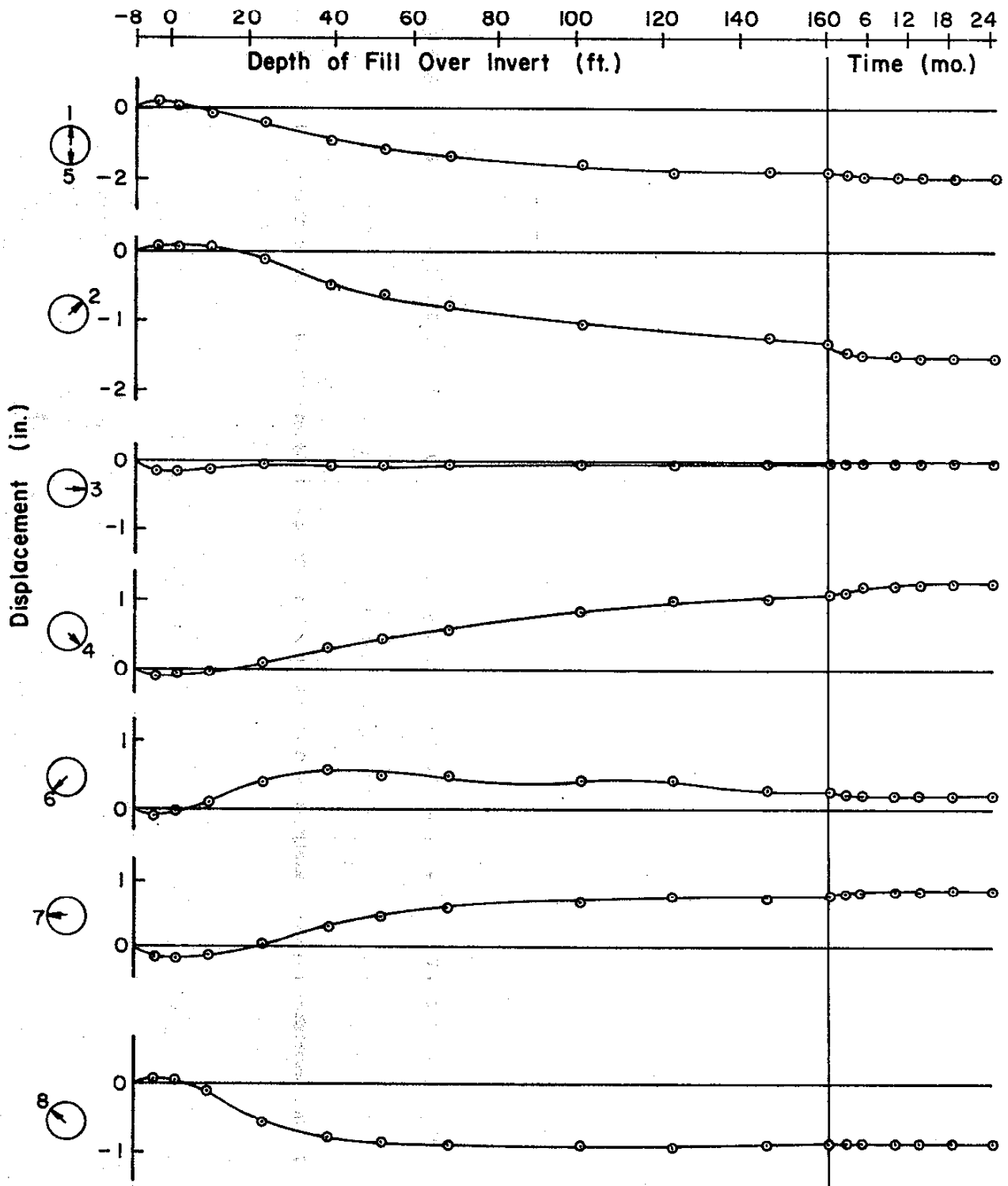
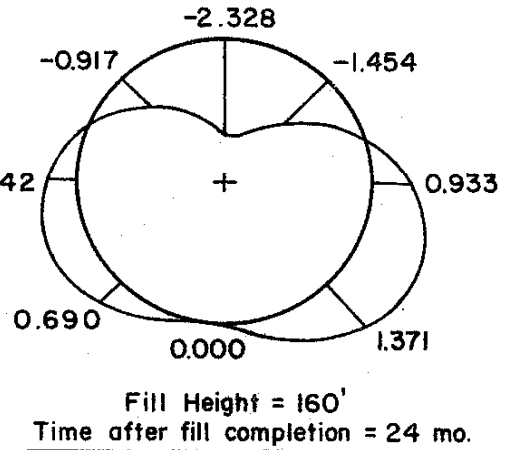
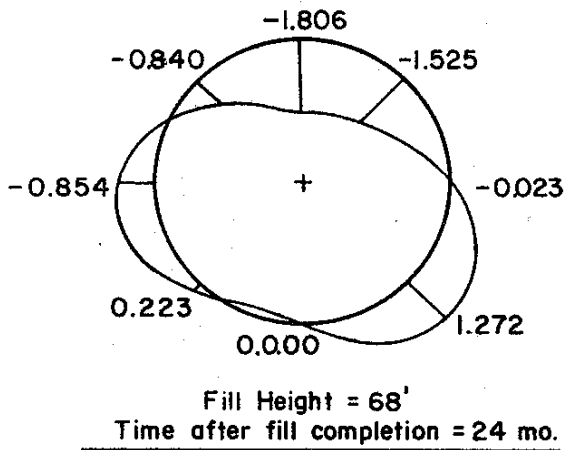
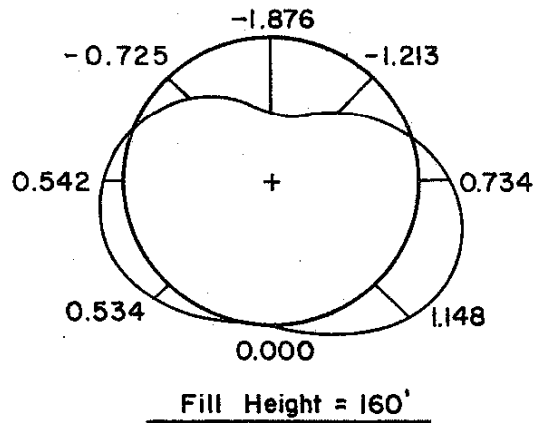
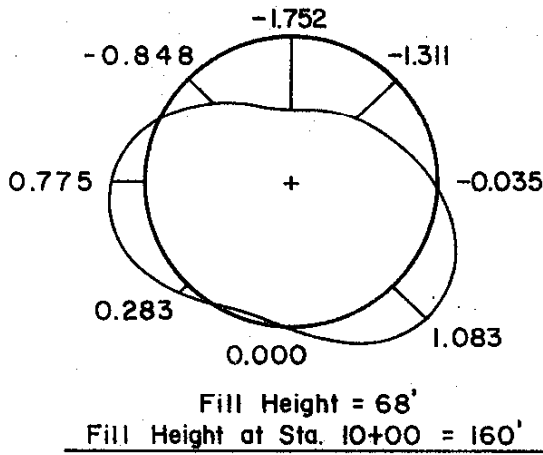
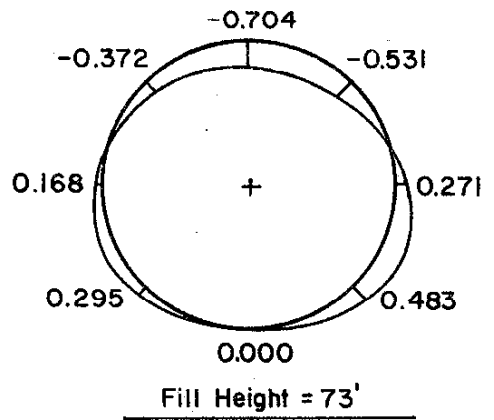
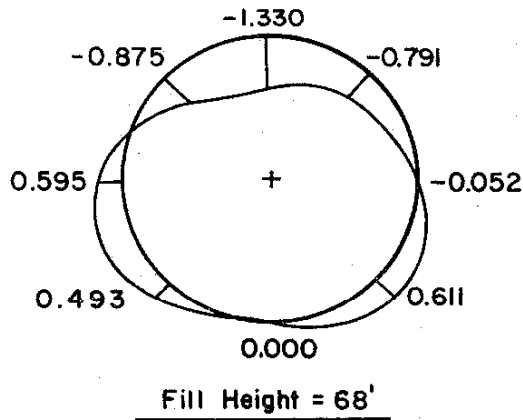


FIGURE 12

APPLE CANYON SPP
DISPLACED SHAPE AT VARIOUS TIMES



STATION 7+25

Scale:
0 1 2
in.

STATION 10+00

FIGURE 13

APPLE CANYON SPP
STATION 7+25

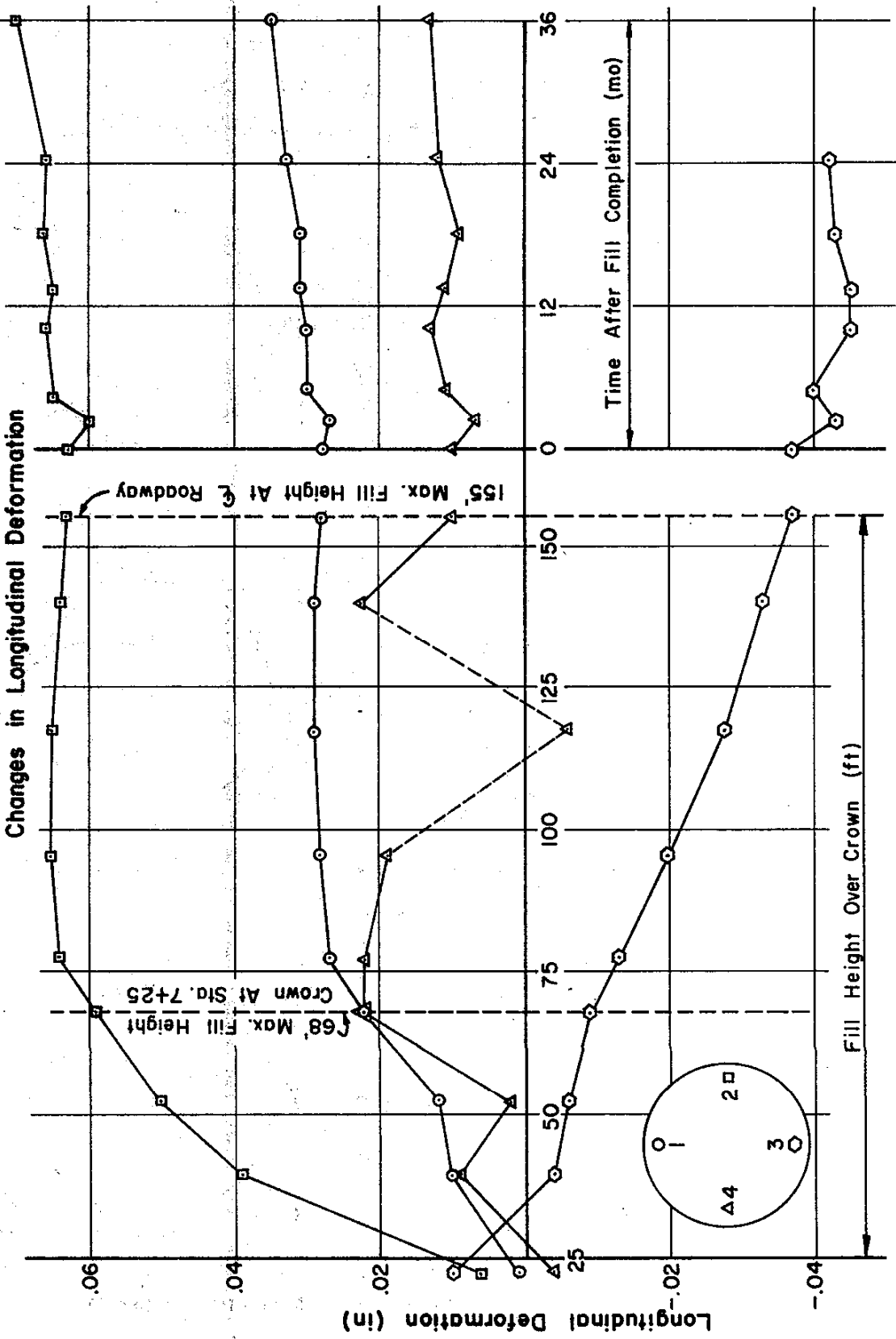


FIGURE 14

APPLE CANYON SPP
STATION 10+00

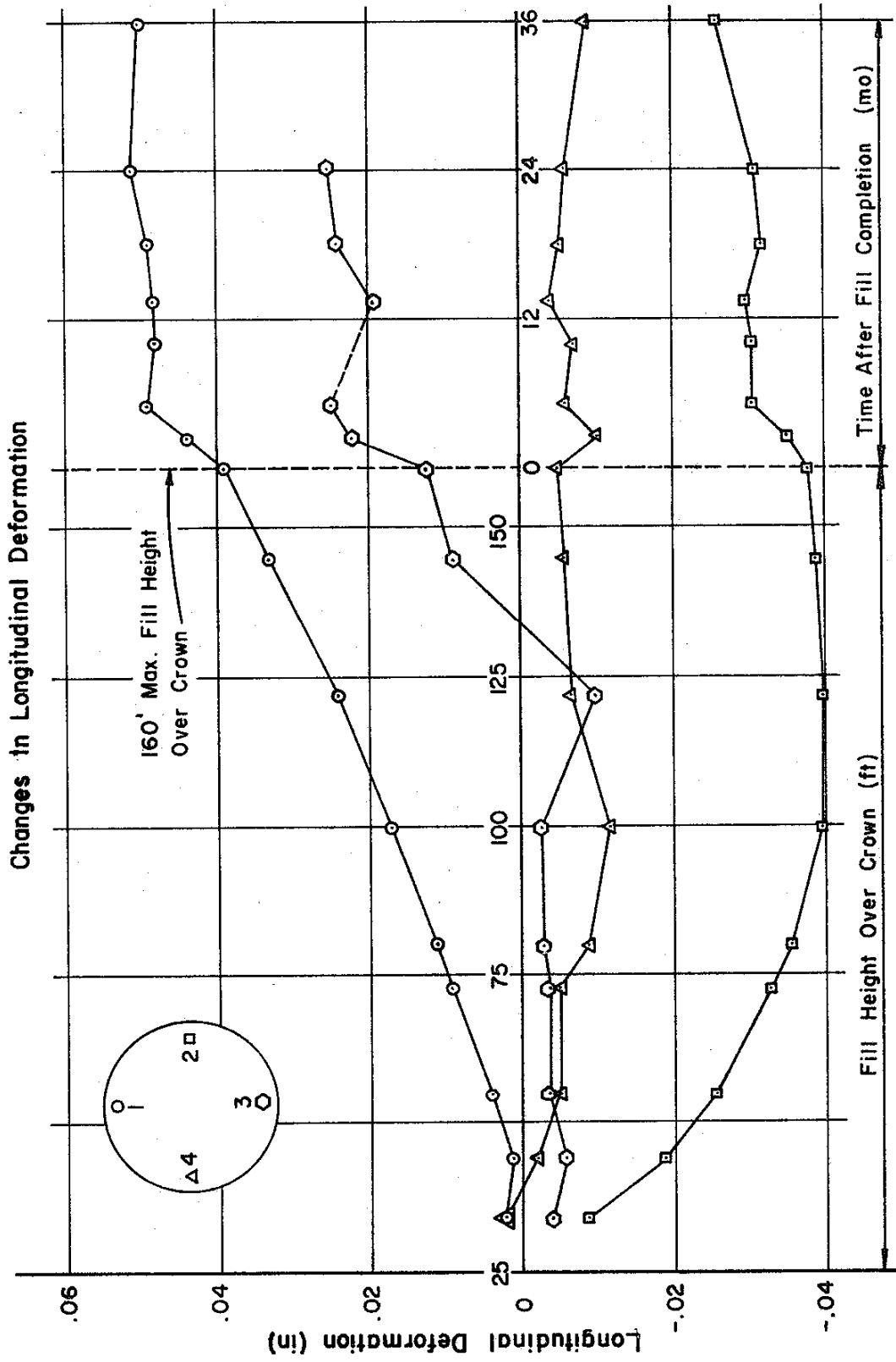


FIGURE 15

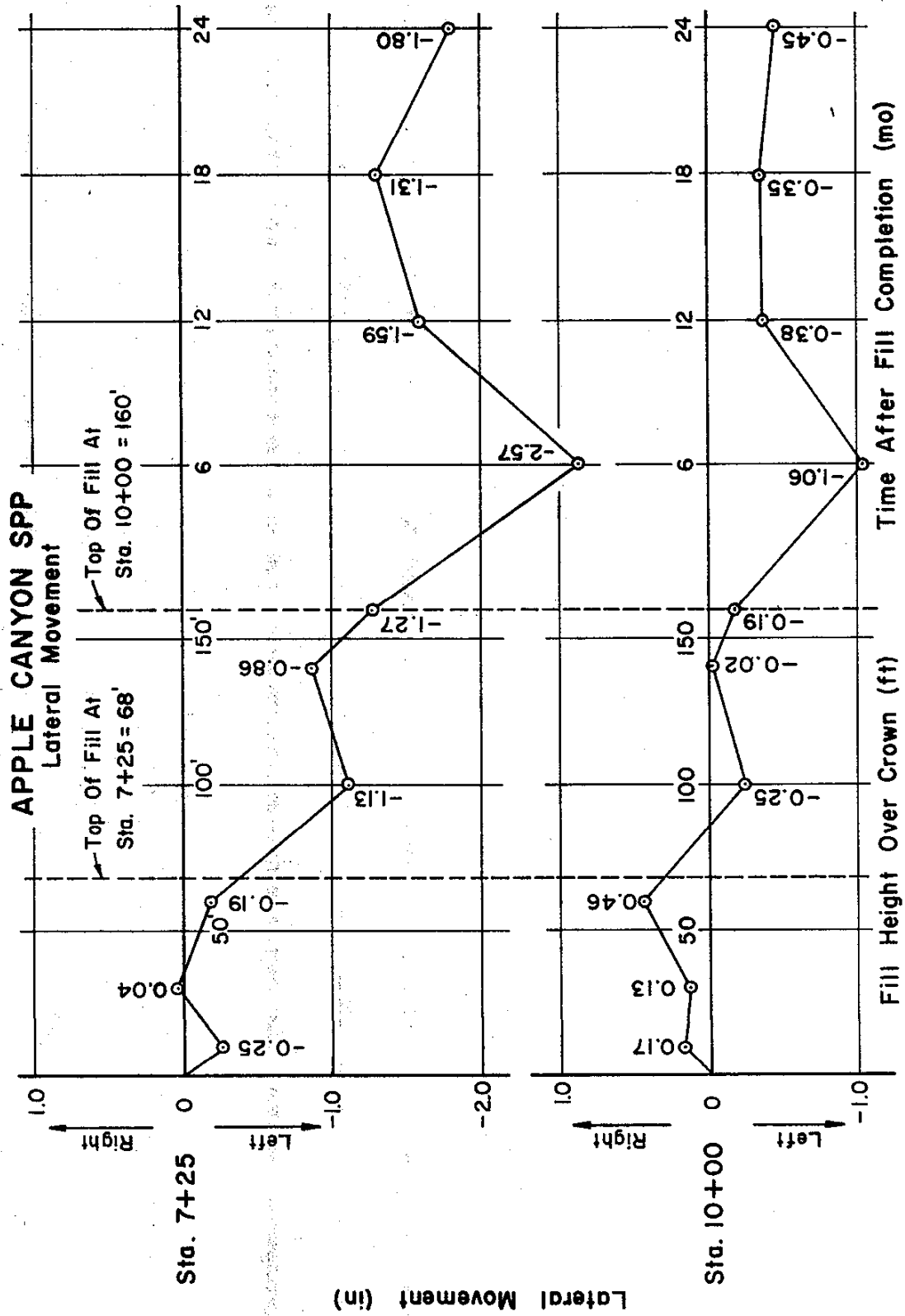
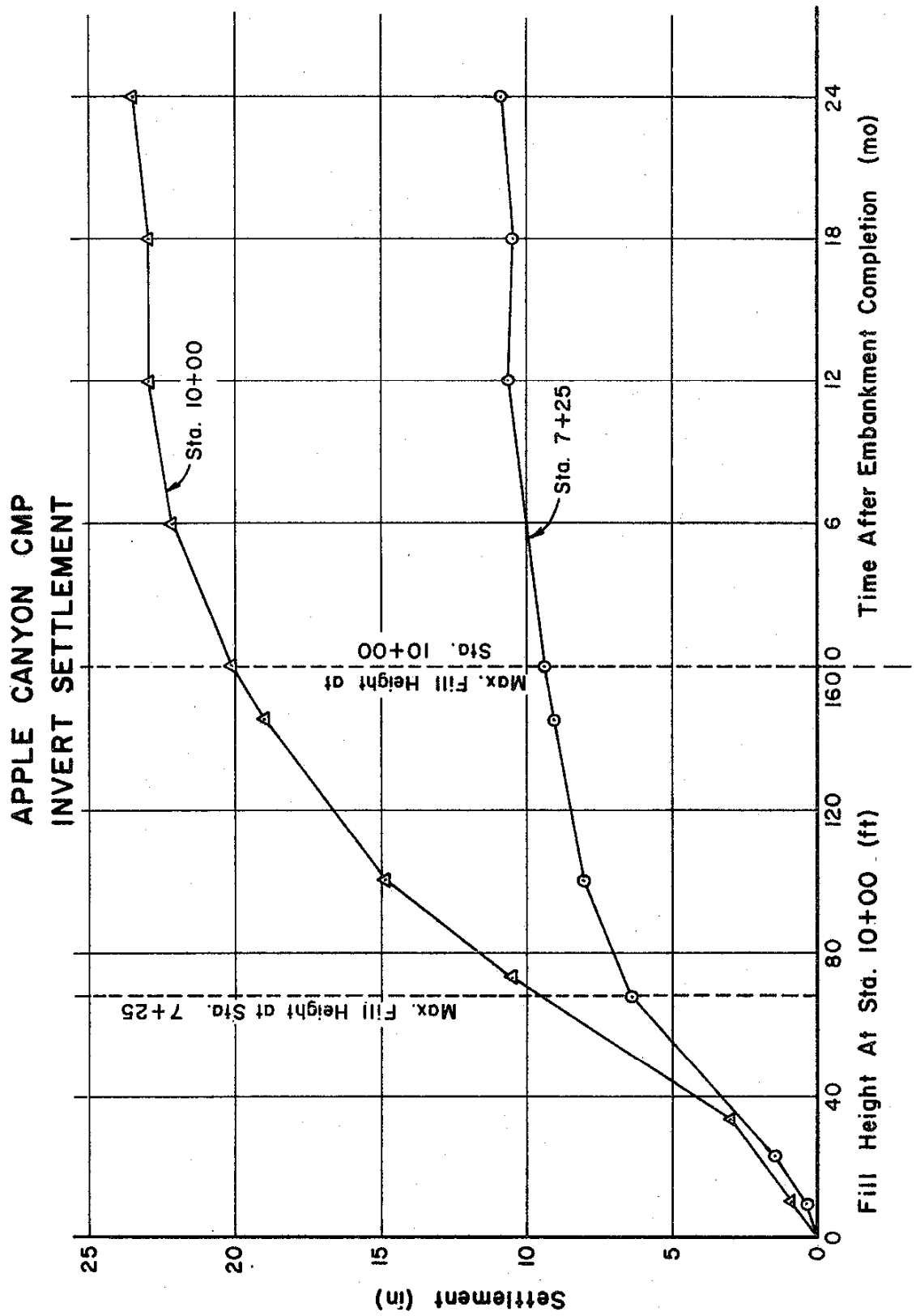


FIGURE 16



APPLE CANYON CMP - STATION 10+00
 METER NUMBER 40

⊙ SETTLEMENT PLATFORM READINGS
 — REGRESSION LINE THRU ⊙

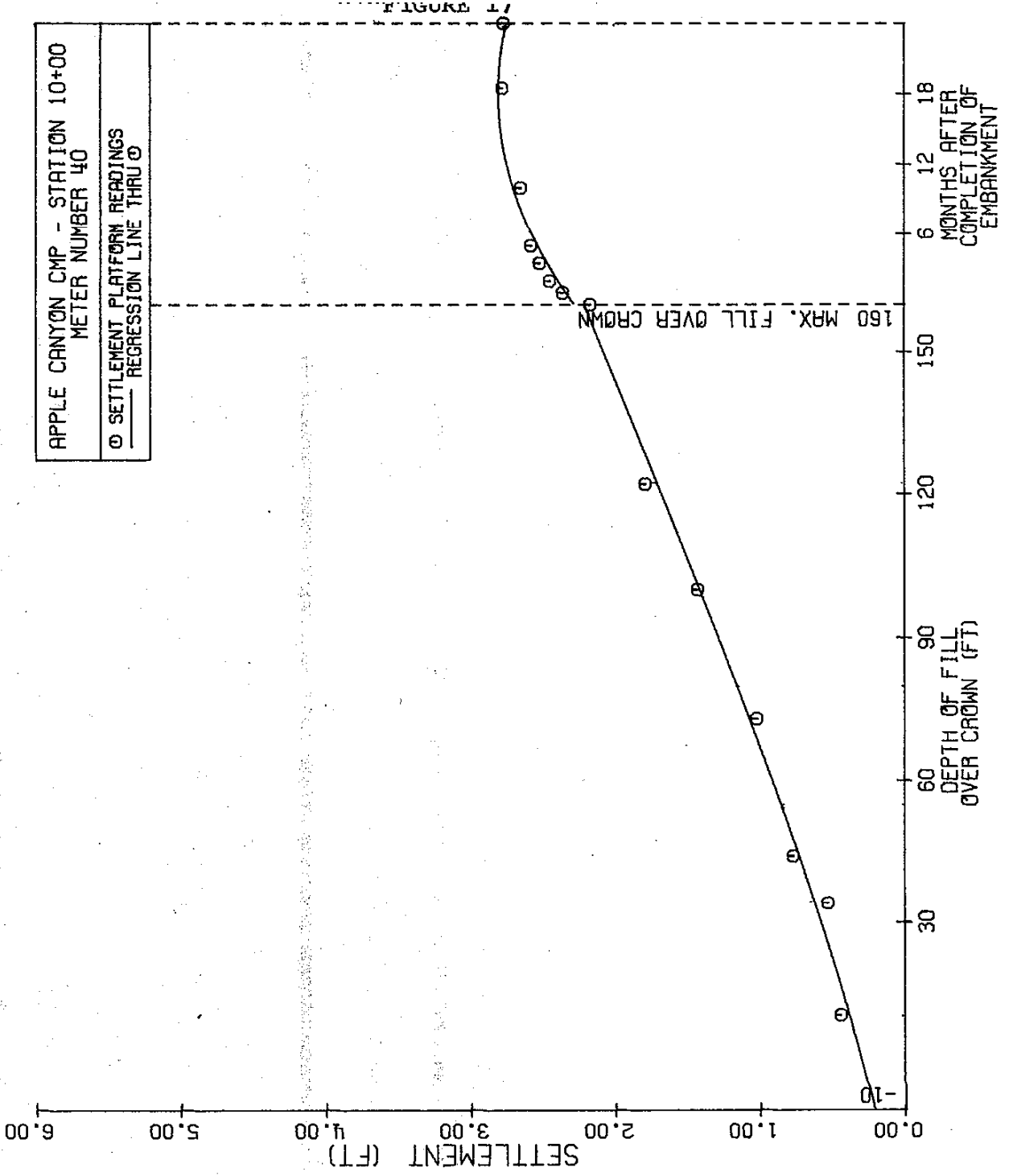


FIGURE 18

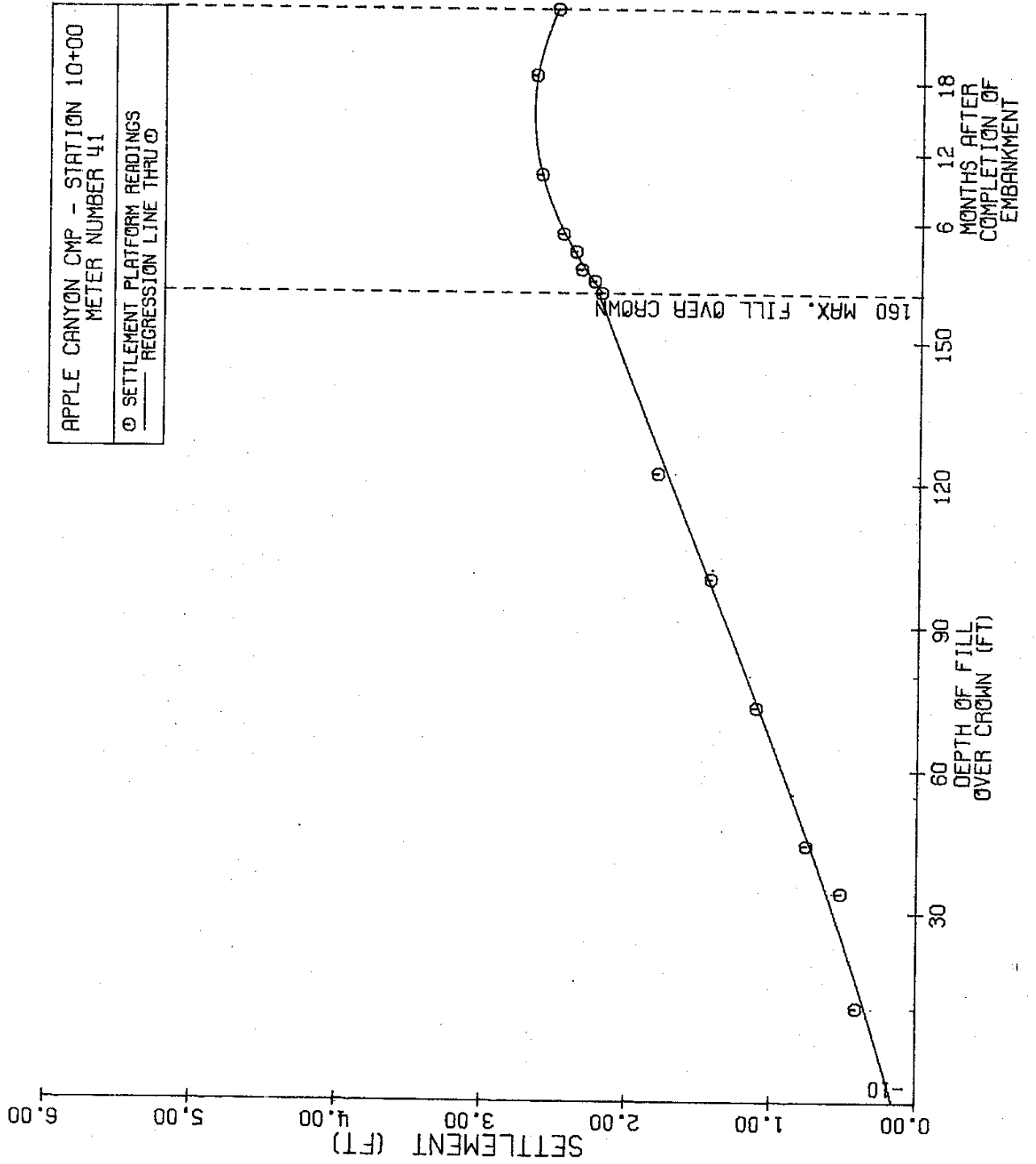


FIGURE 19

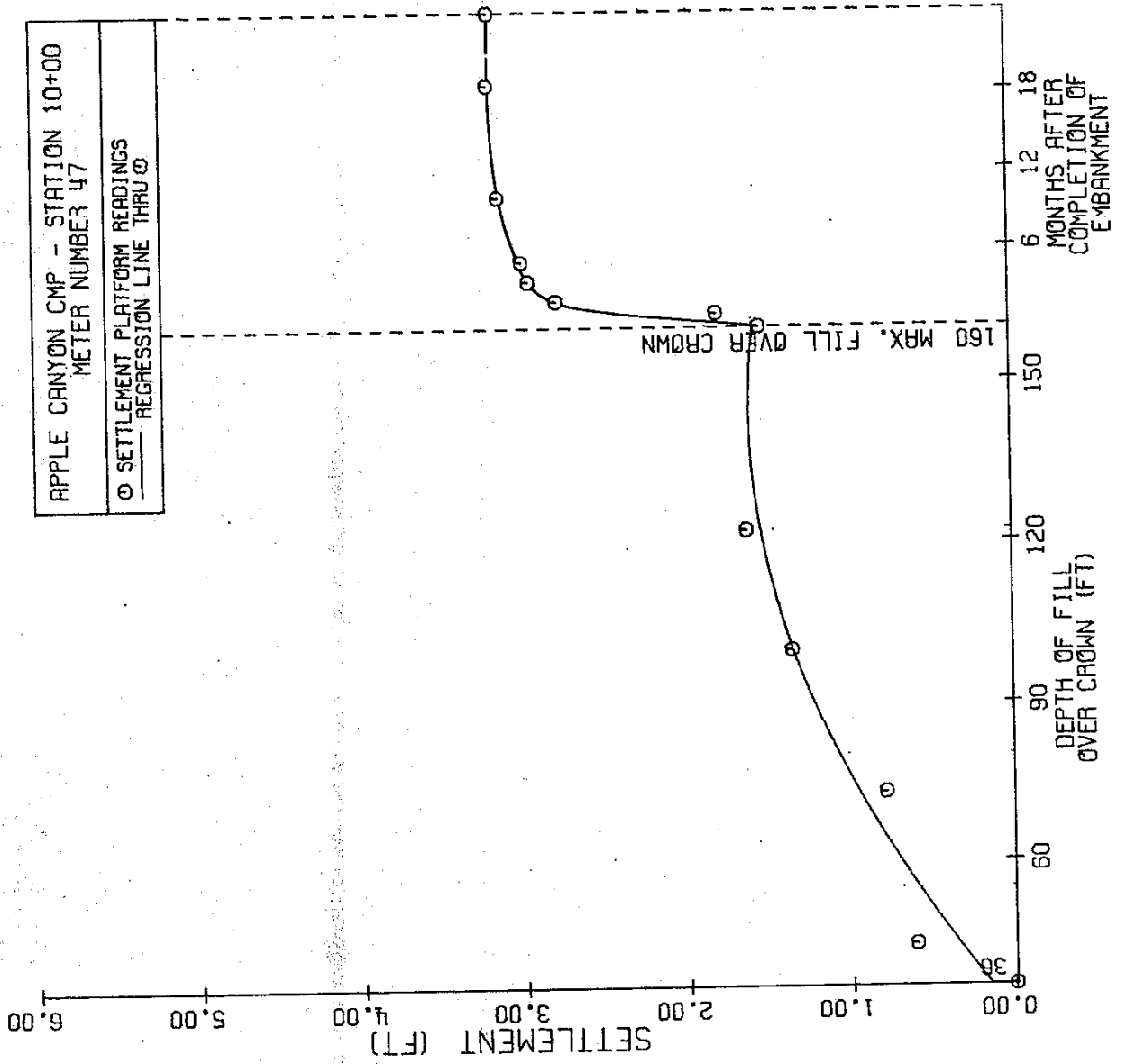


FIGURE 20

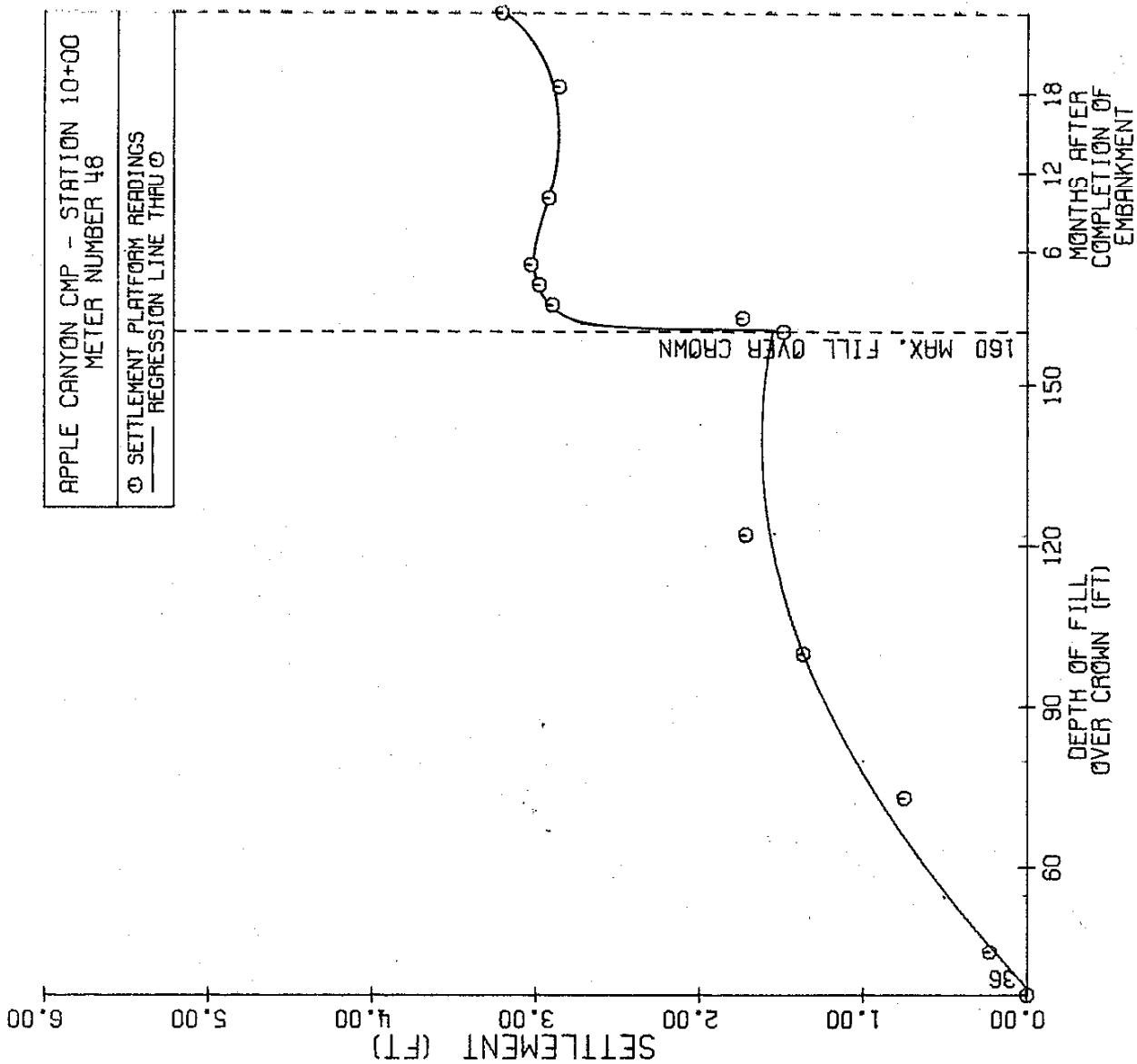
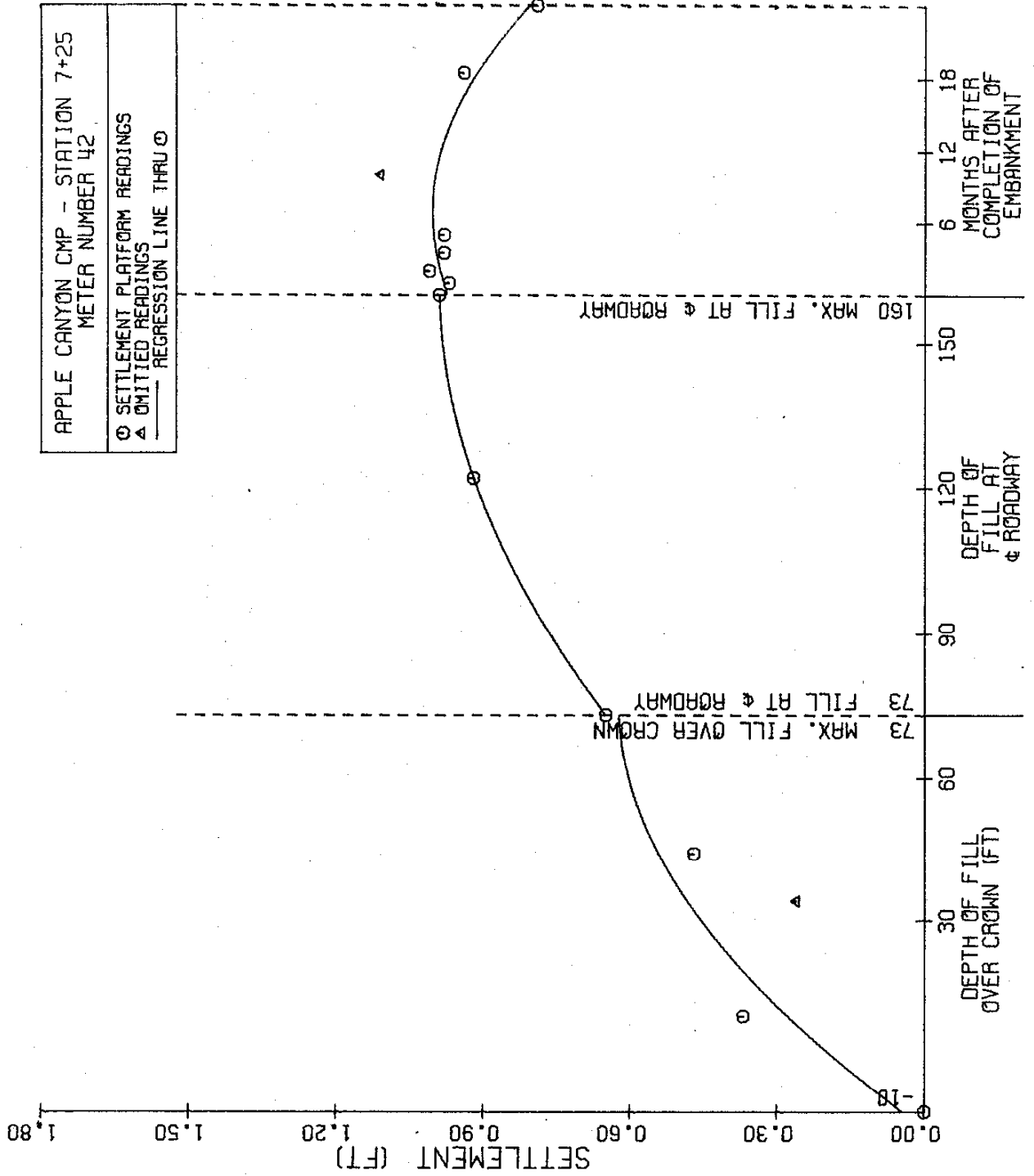


FIGURE 22



APPLE CANYON CMP - STATION 7+25
 METER NUMBER 42

○ SETTLEMENT PLATFORM READINGS
 ▲ OMITTED READINGS
 — REGRESSION LINE THRU ○

FIGURE 23

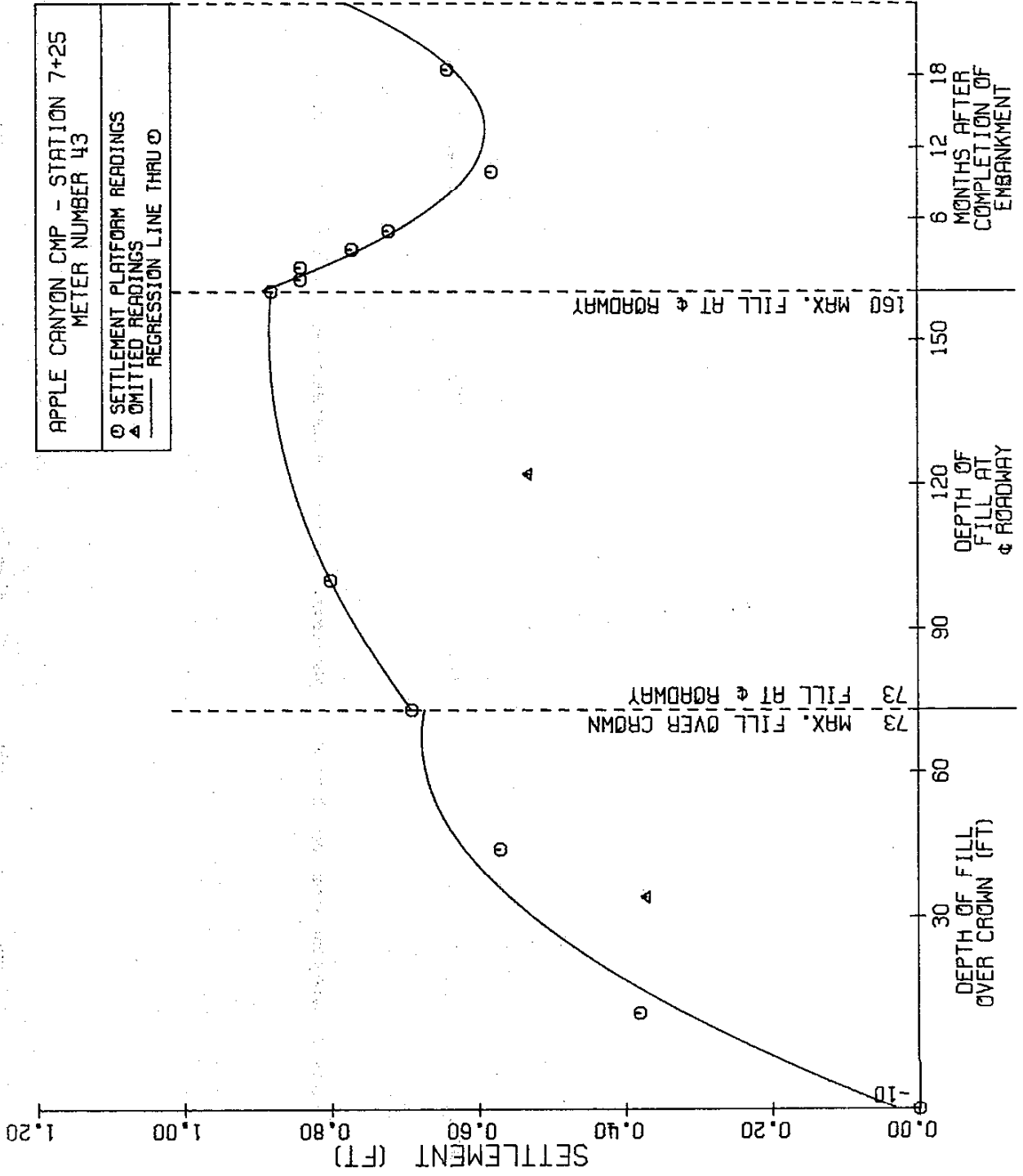


FIGURE 24

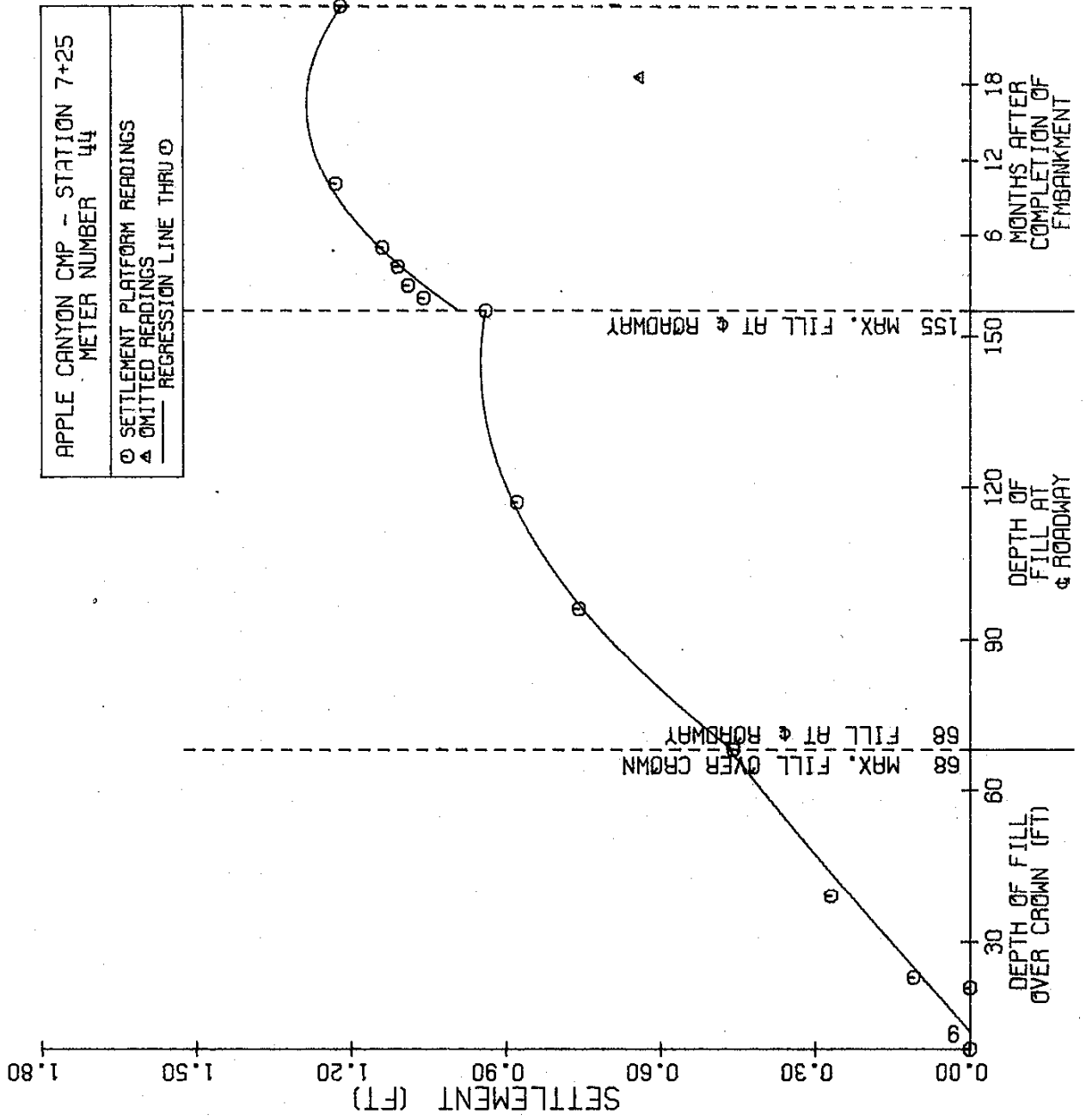


FIGURE 25

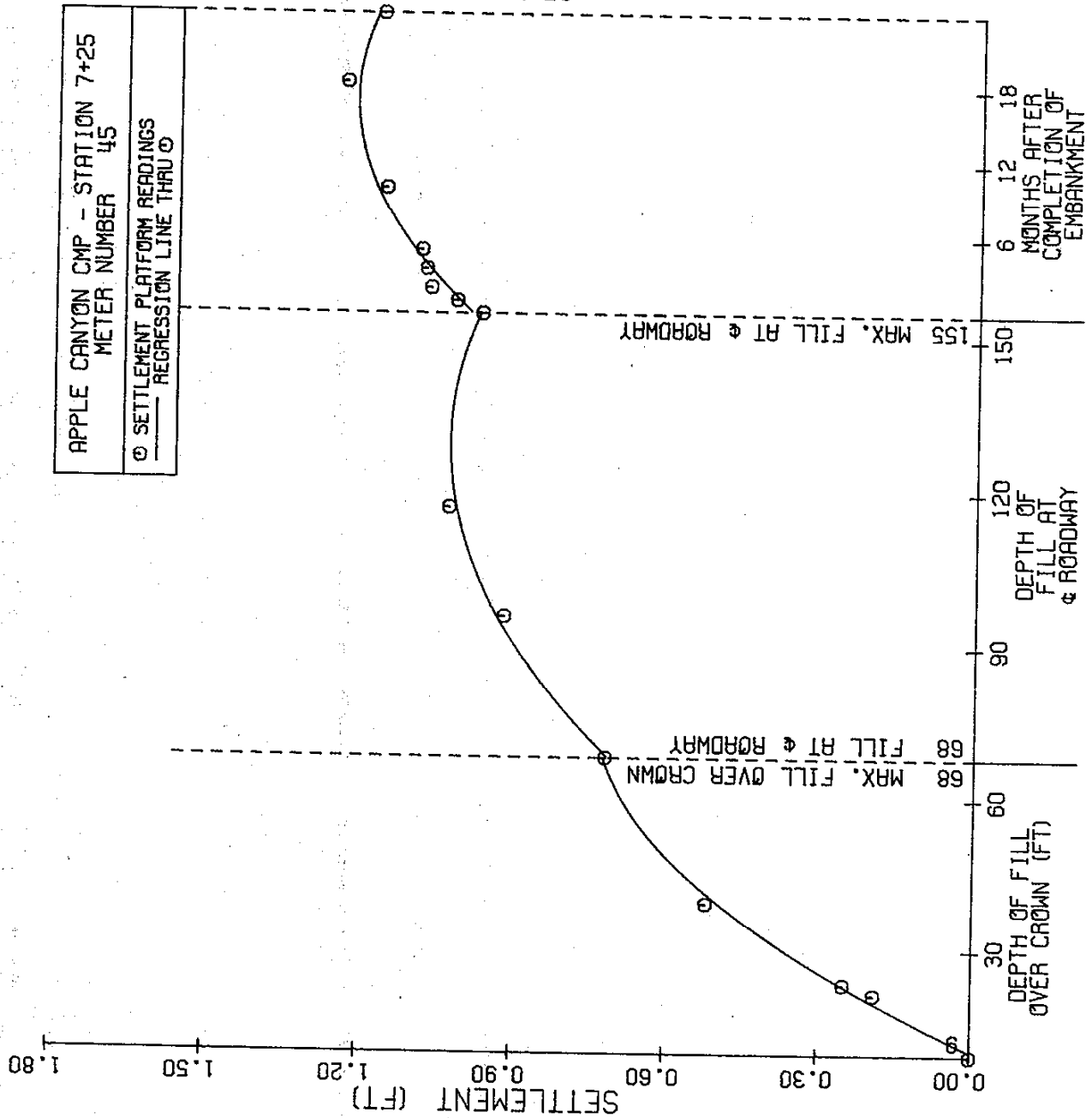


FIGURE 26

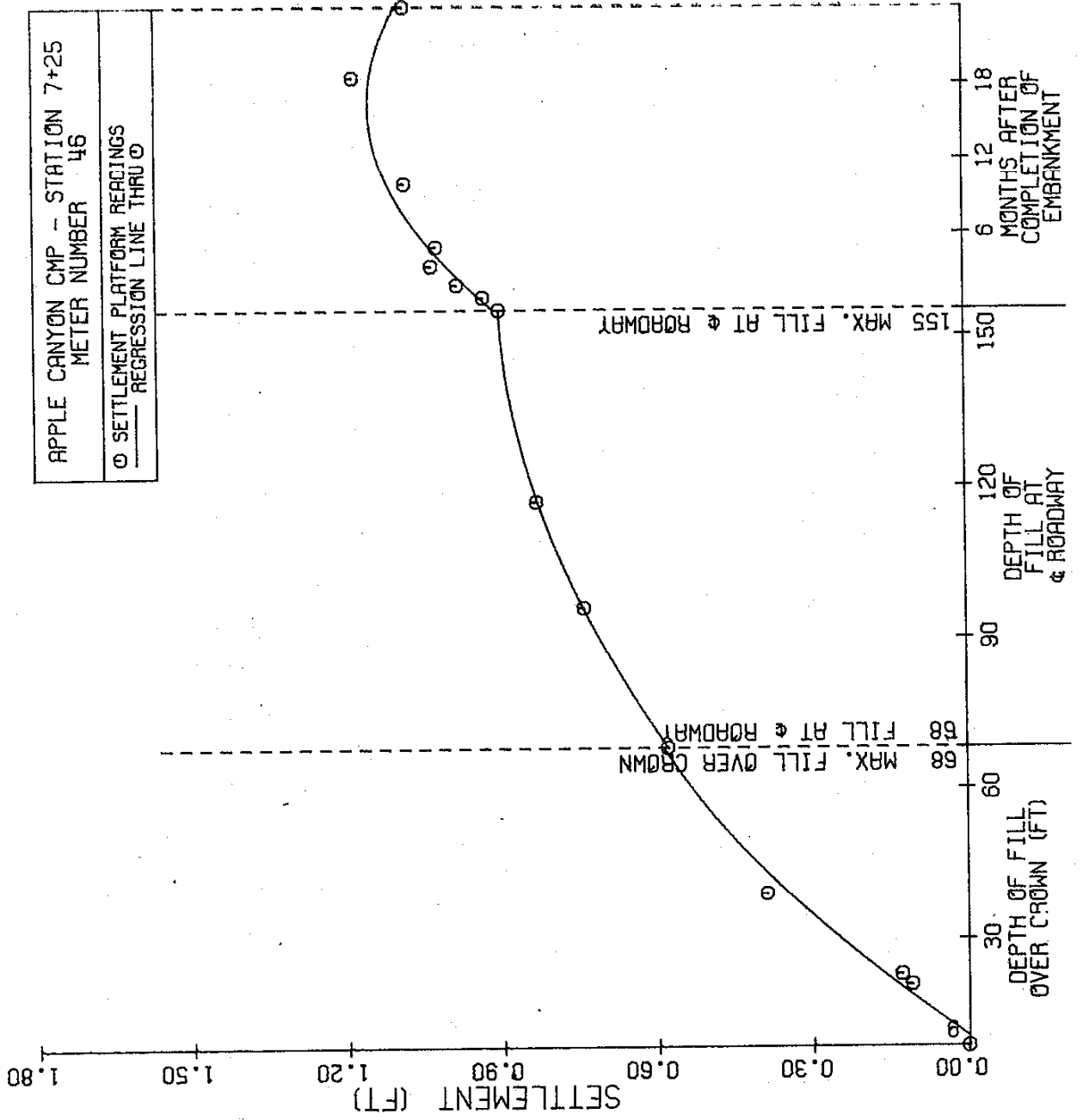


FIGURE 27

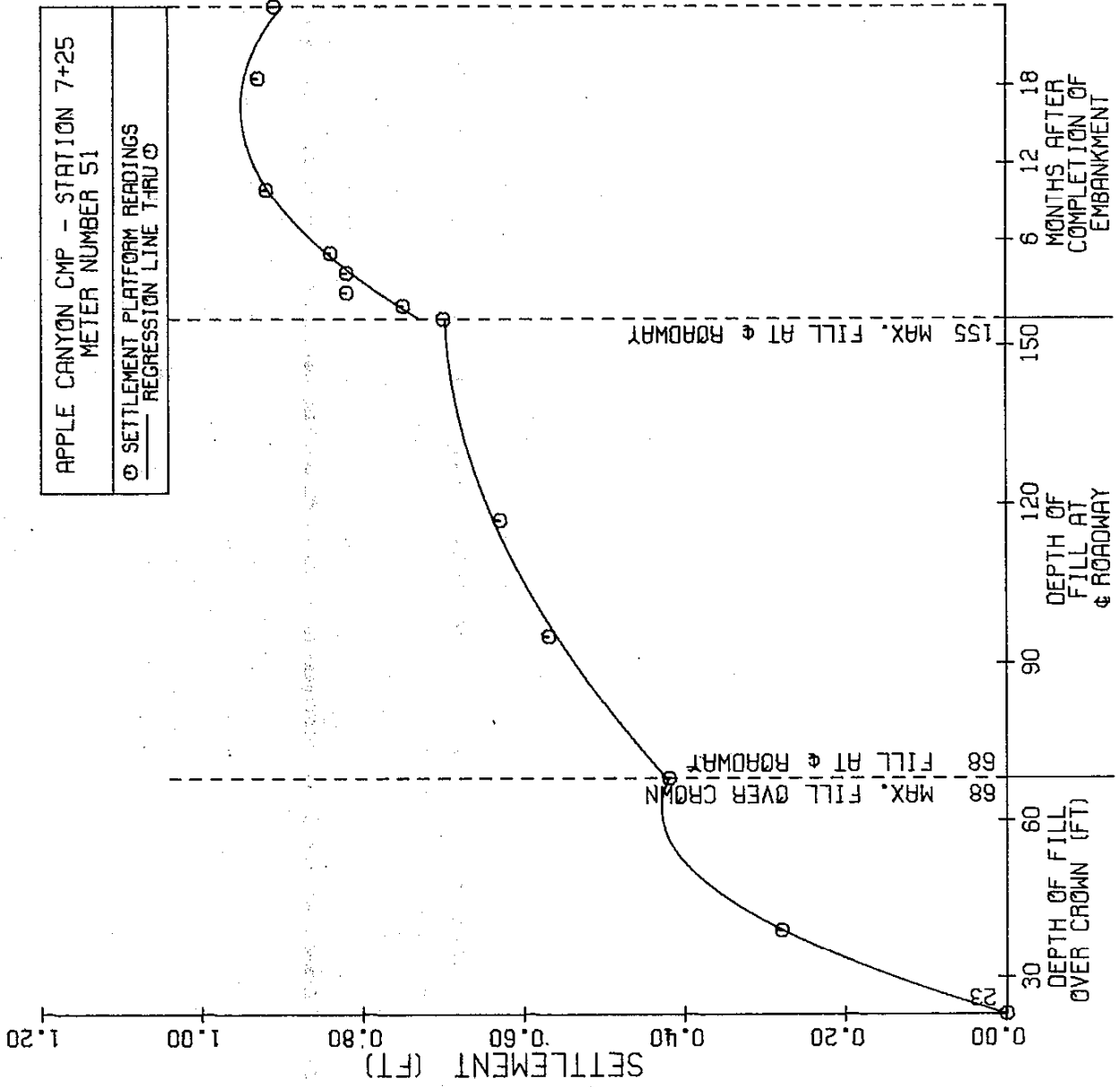


FIGURE 28

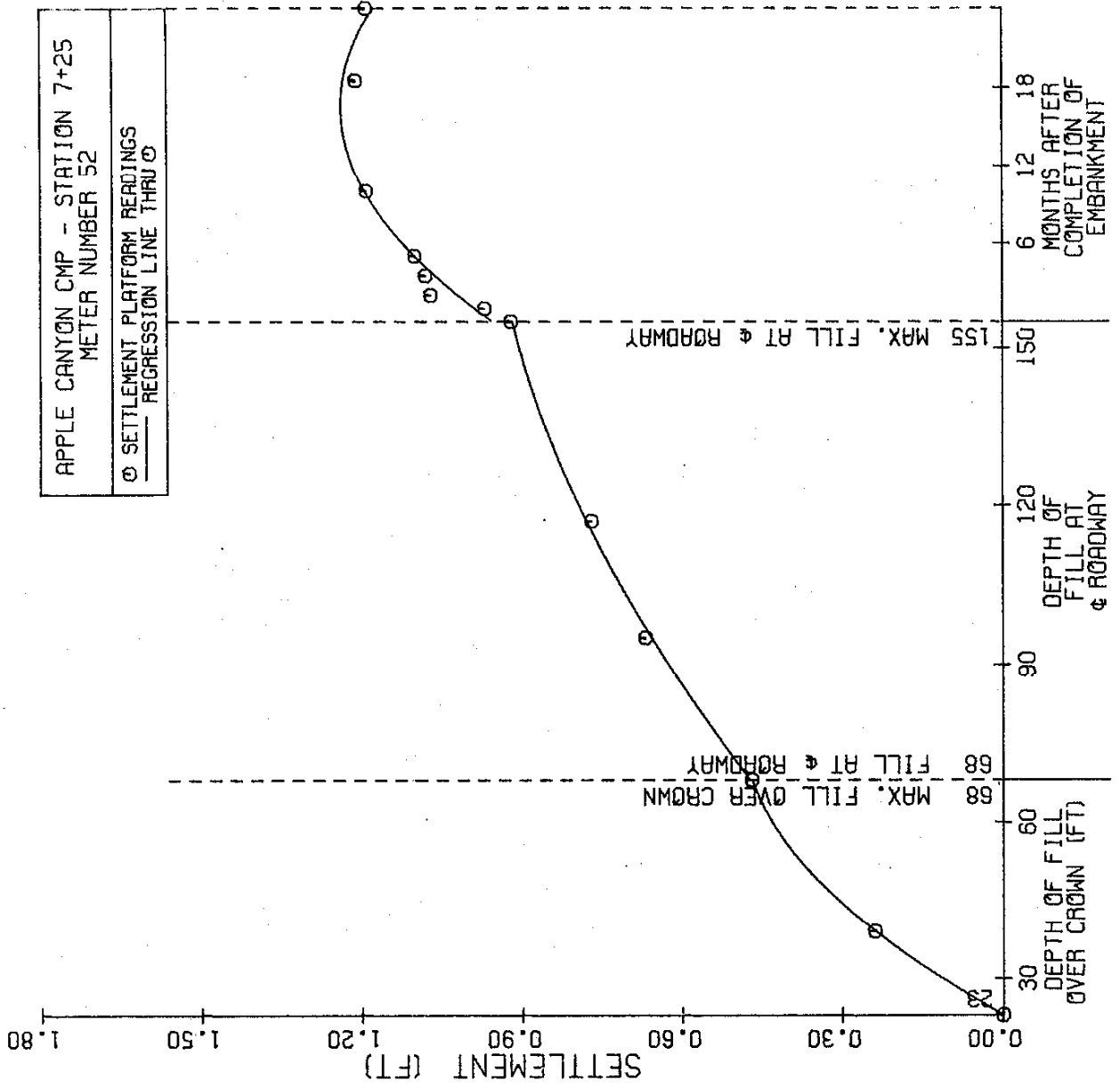


FIGURE 29

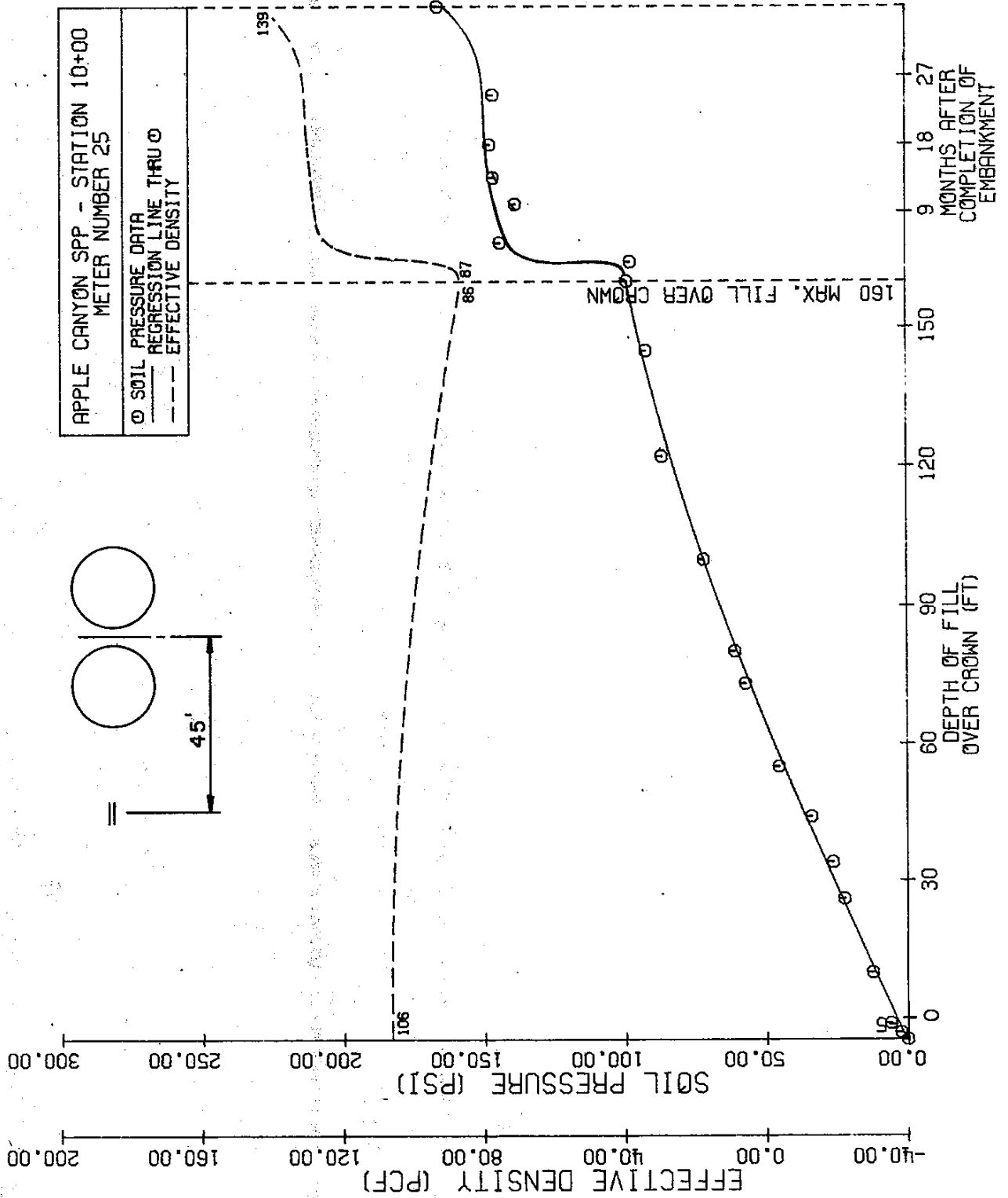


FIGURE 30

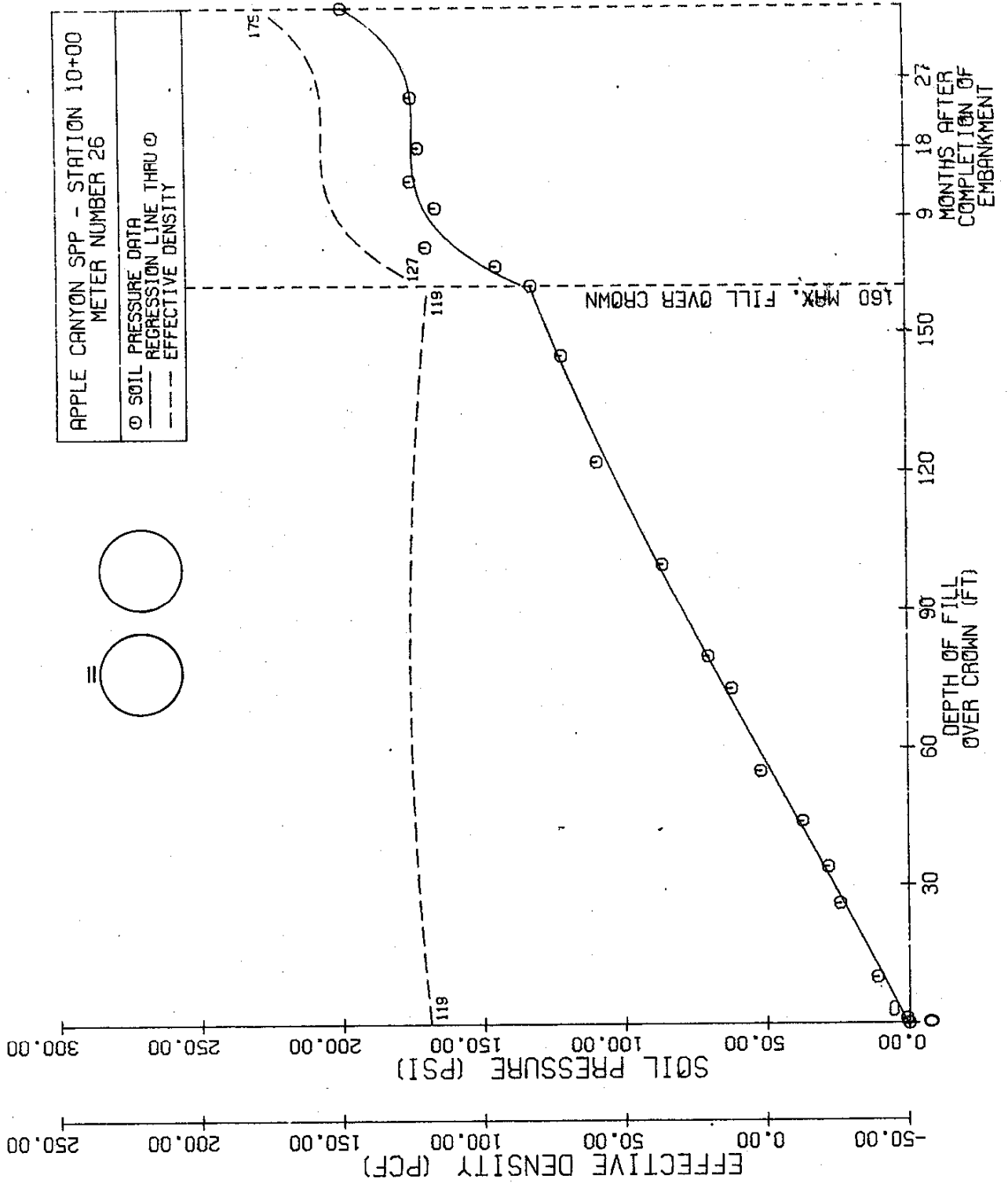
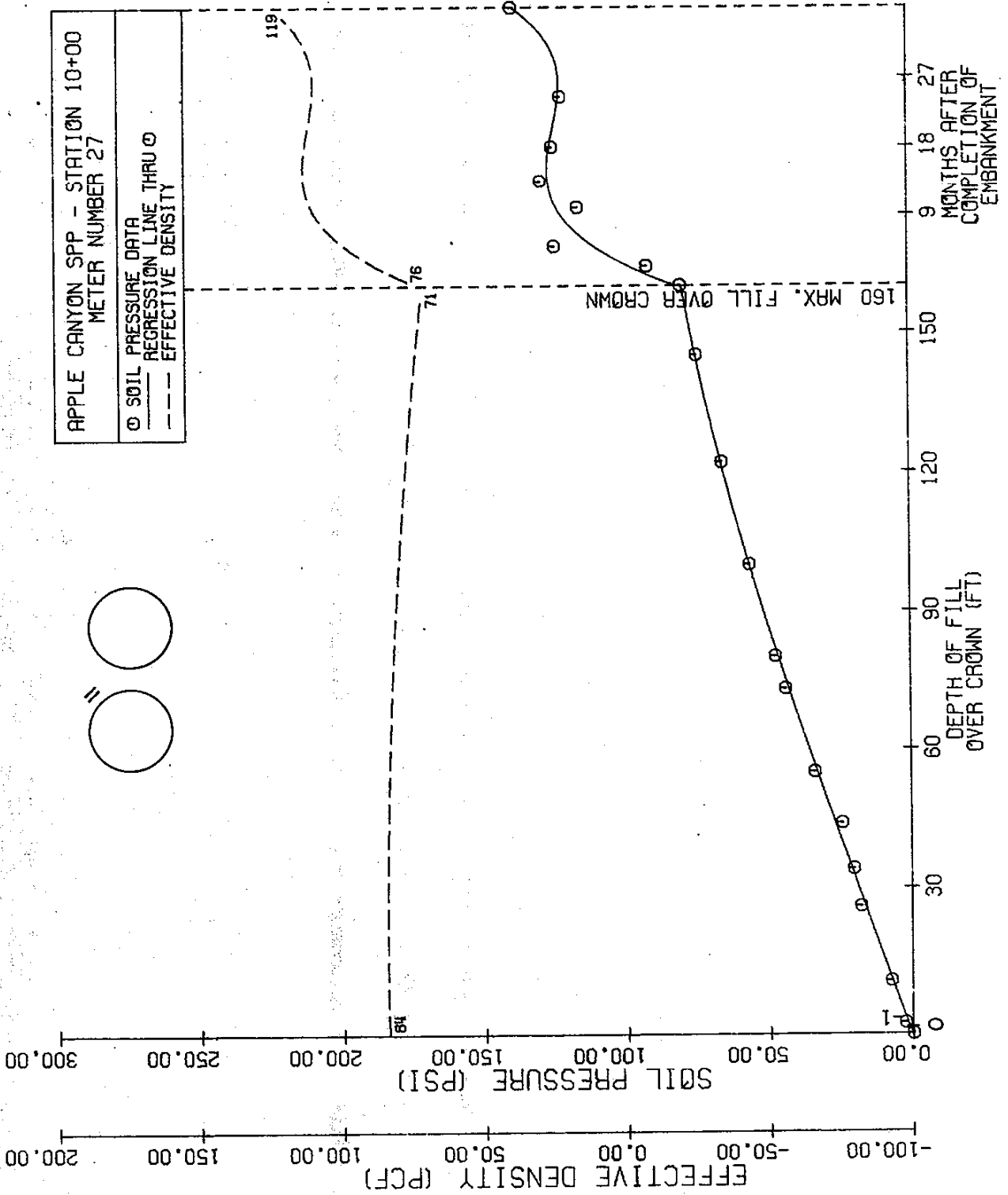
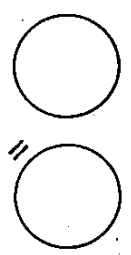


FIGURE 31



APPLE CANYON SPP - STATION 10+00
METER NUMBER 27



○ SOIL PRESSURE DATA
— REGRESSION LINE THROUGH ○
- - - EFFECTIVE DENSITY

FIGURE 32

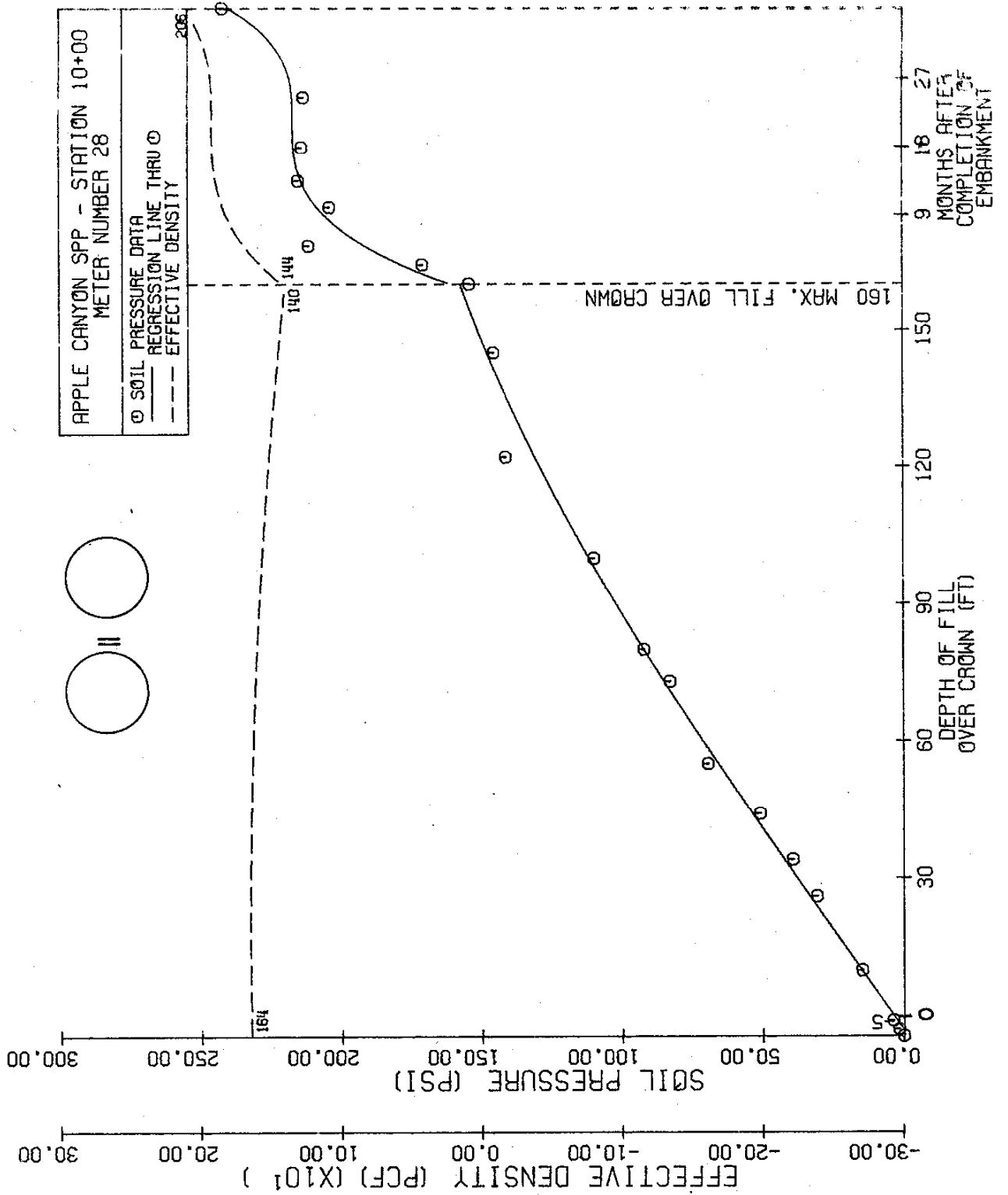


FIGURE 33

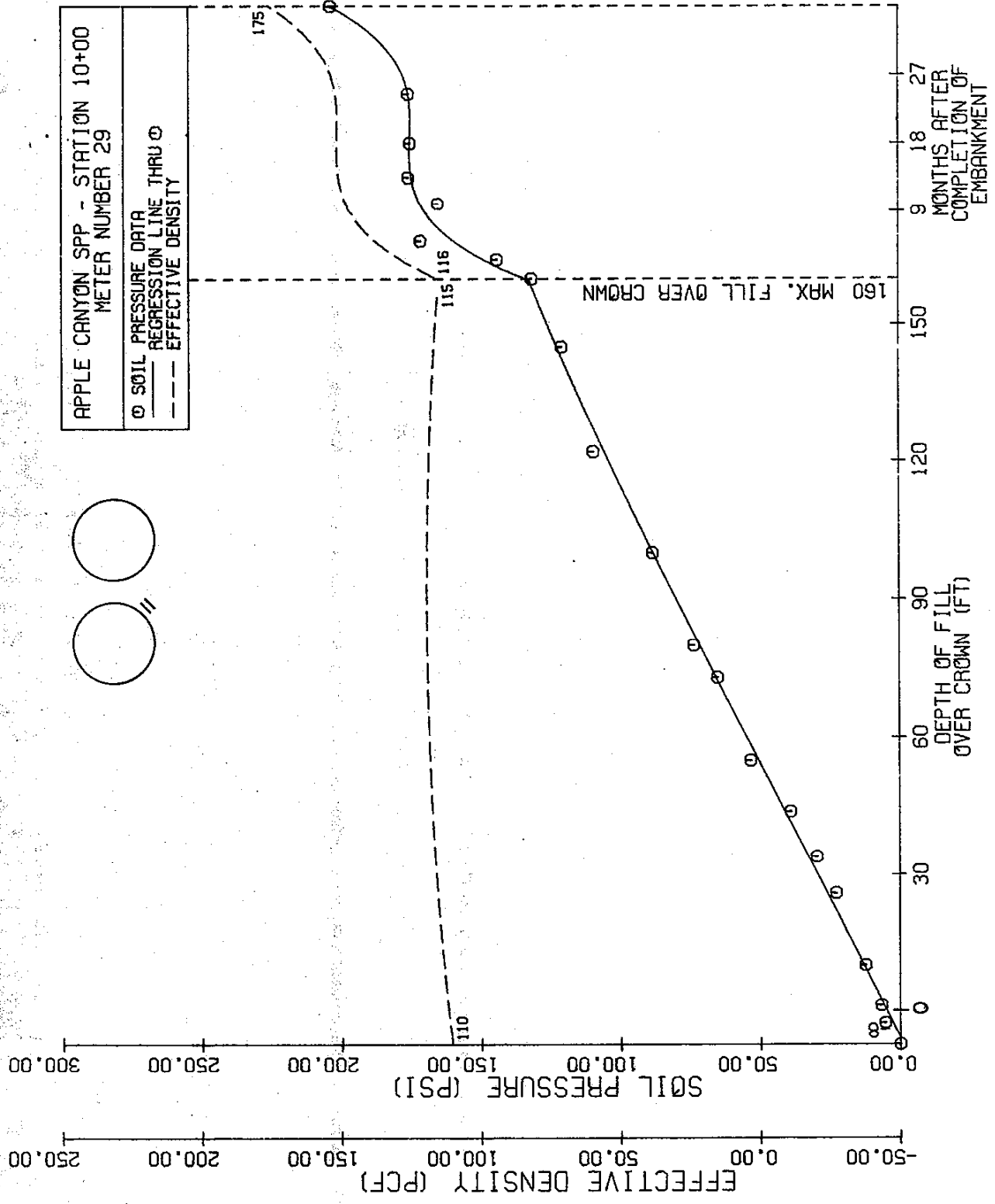


FIGURE 34

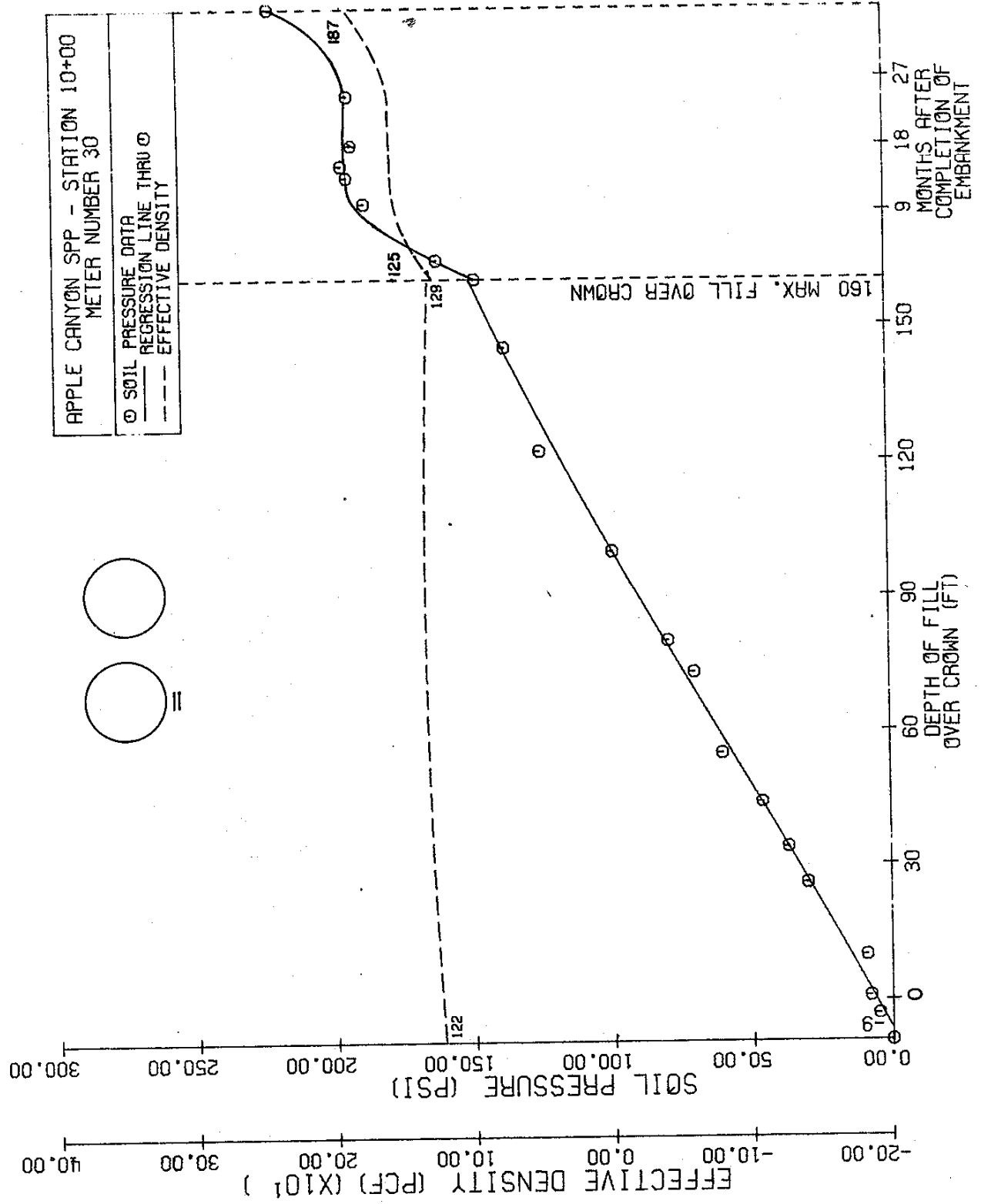


FIGURE 35

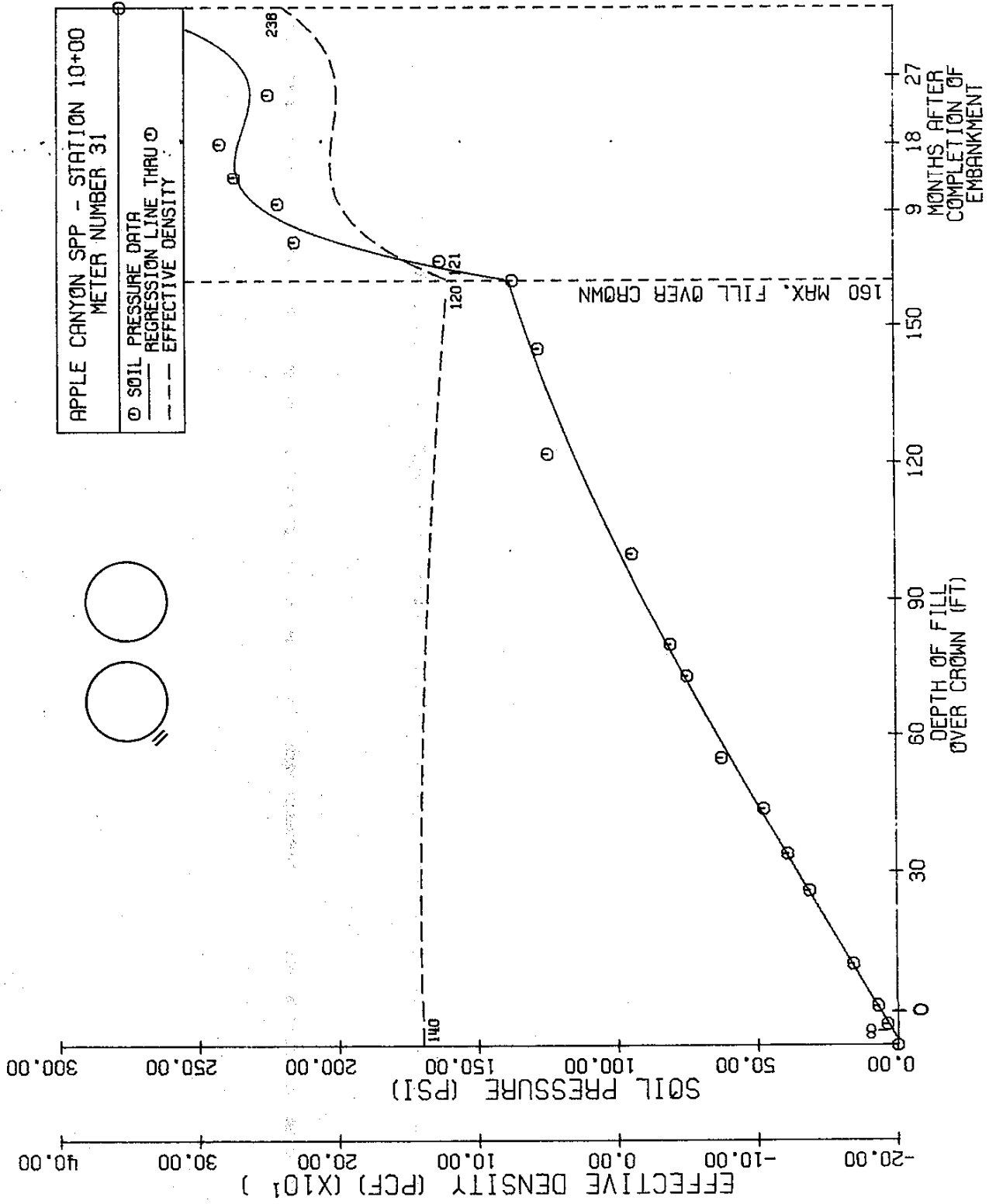


FIGURE 36

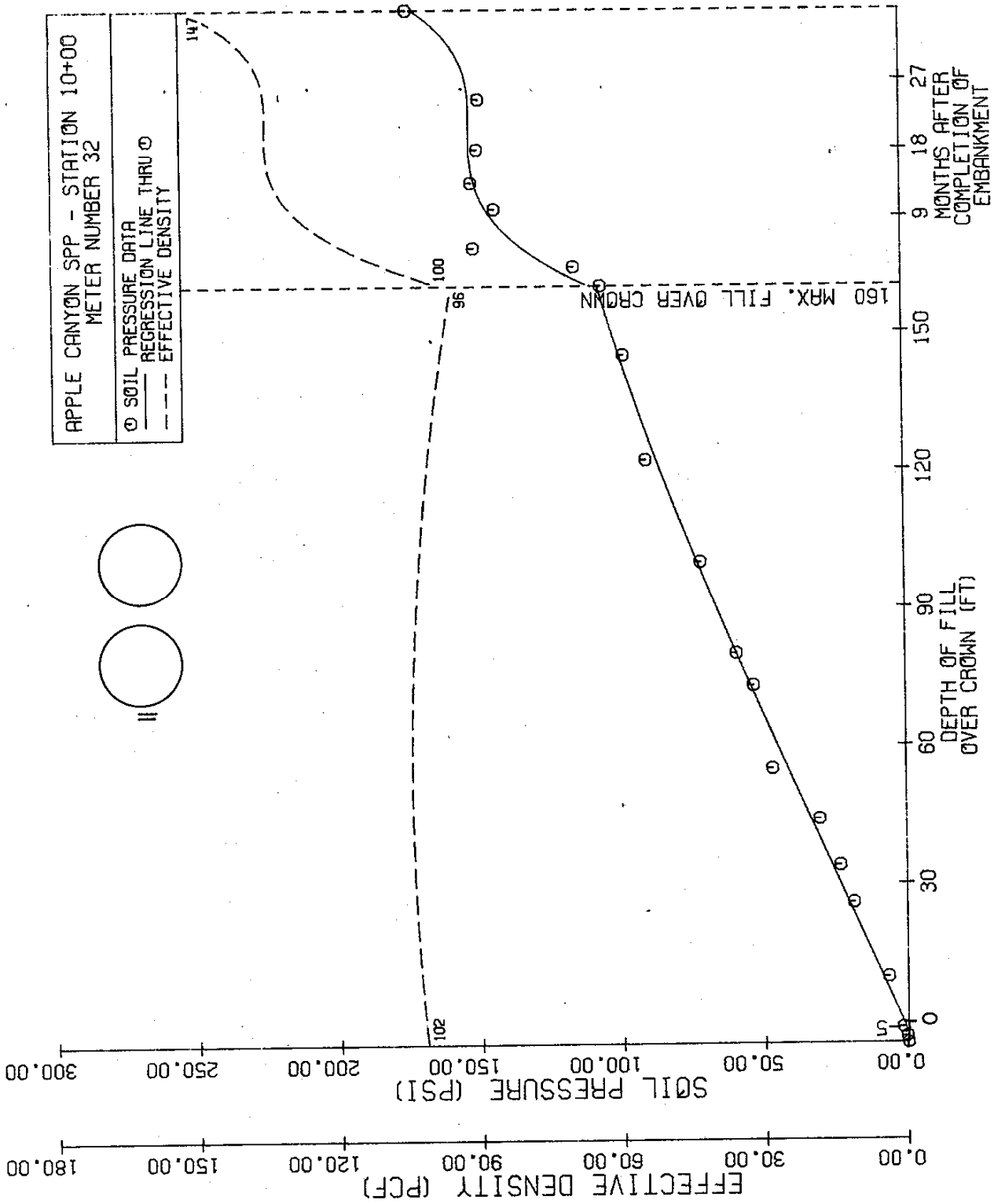


FIGURE 37

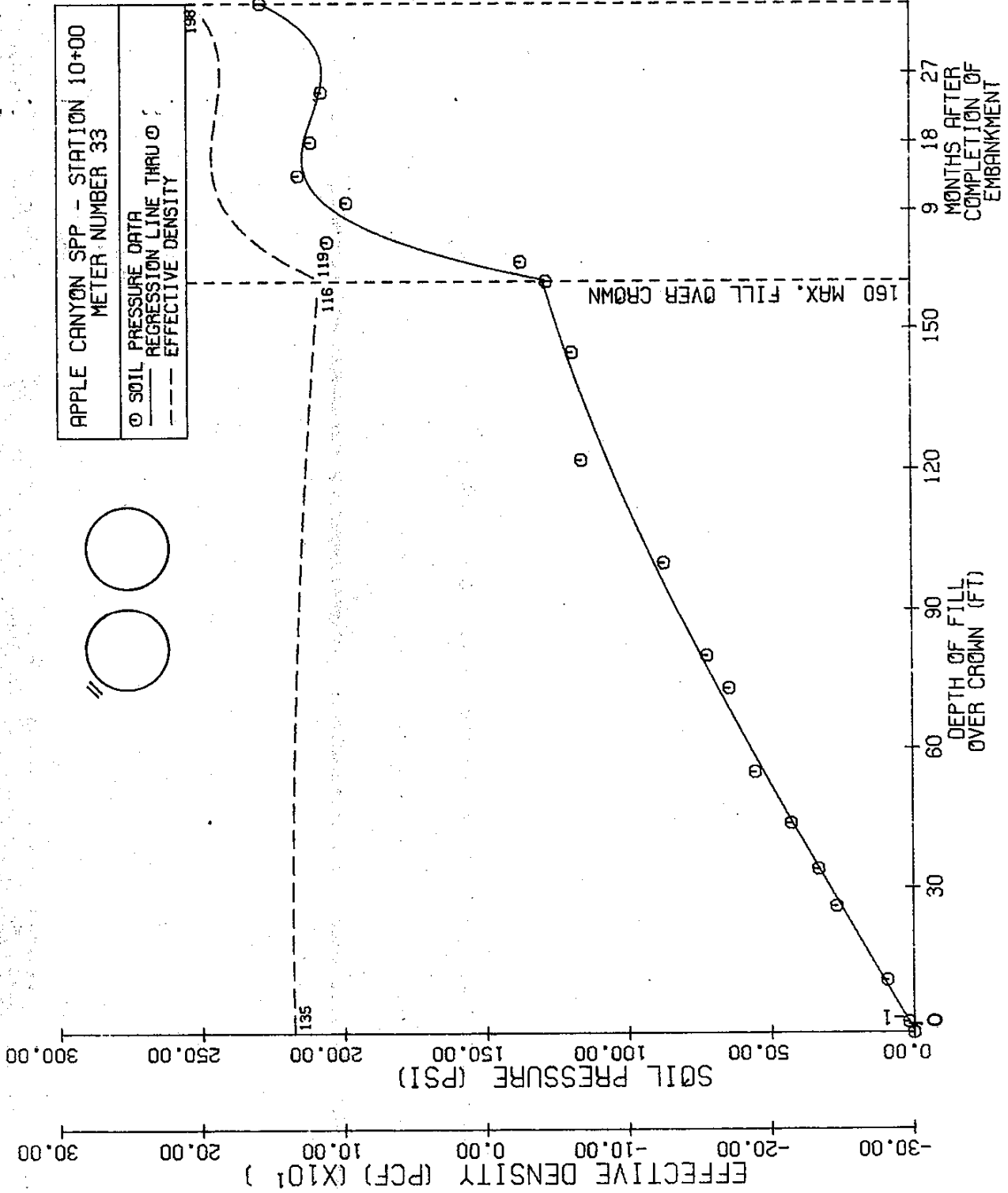


FIGURE 38

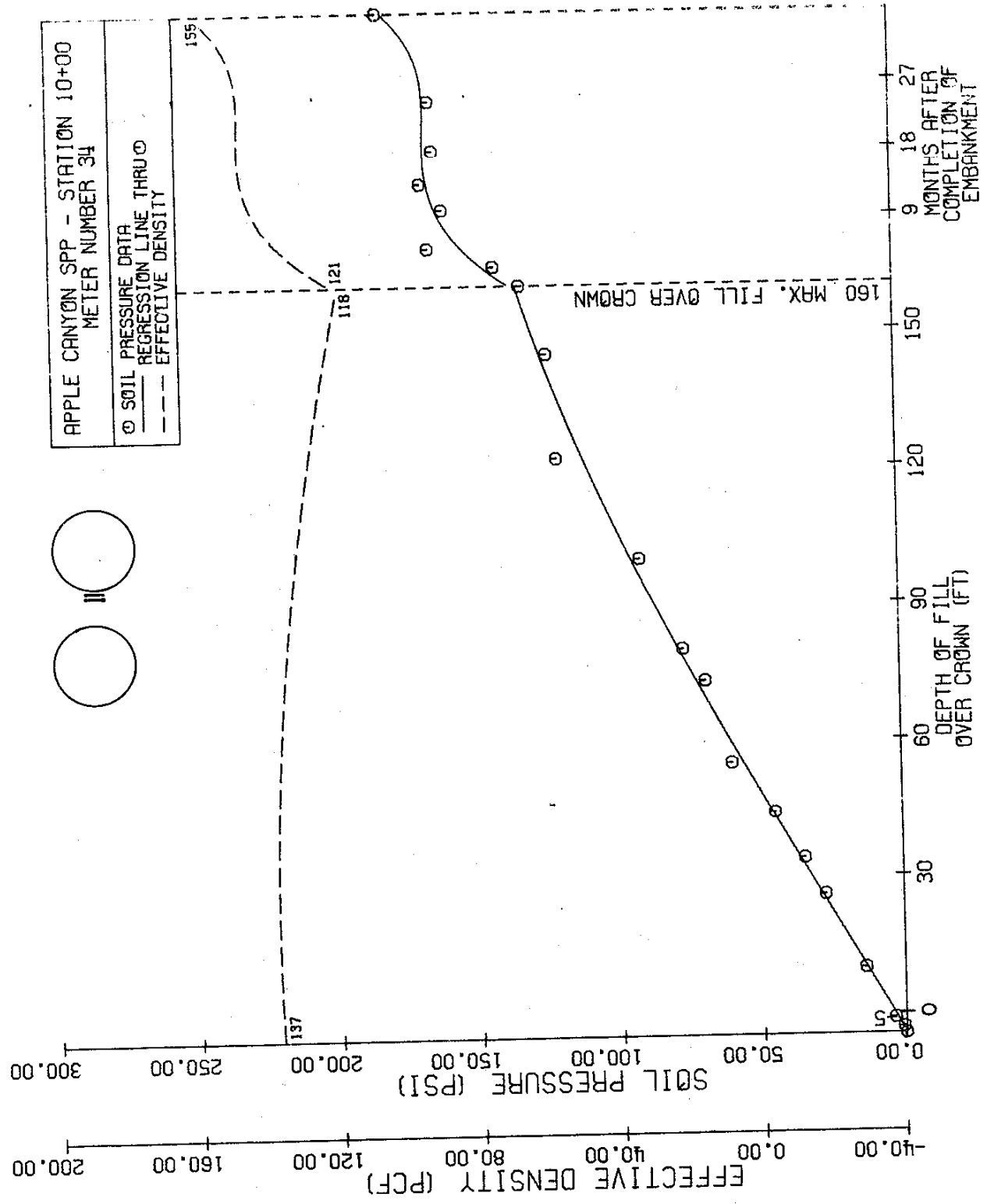


FIGURE 39

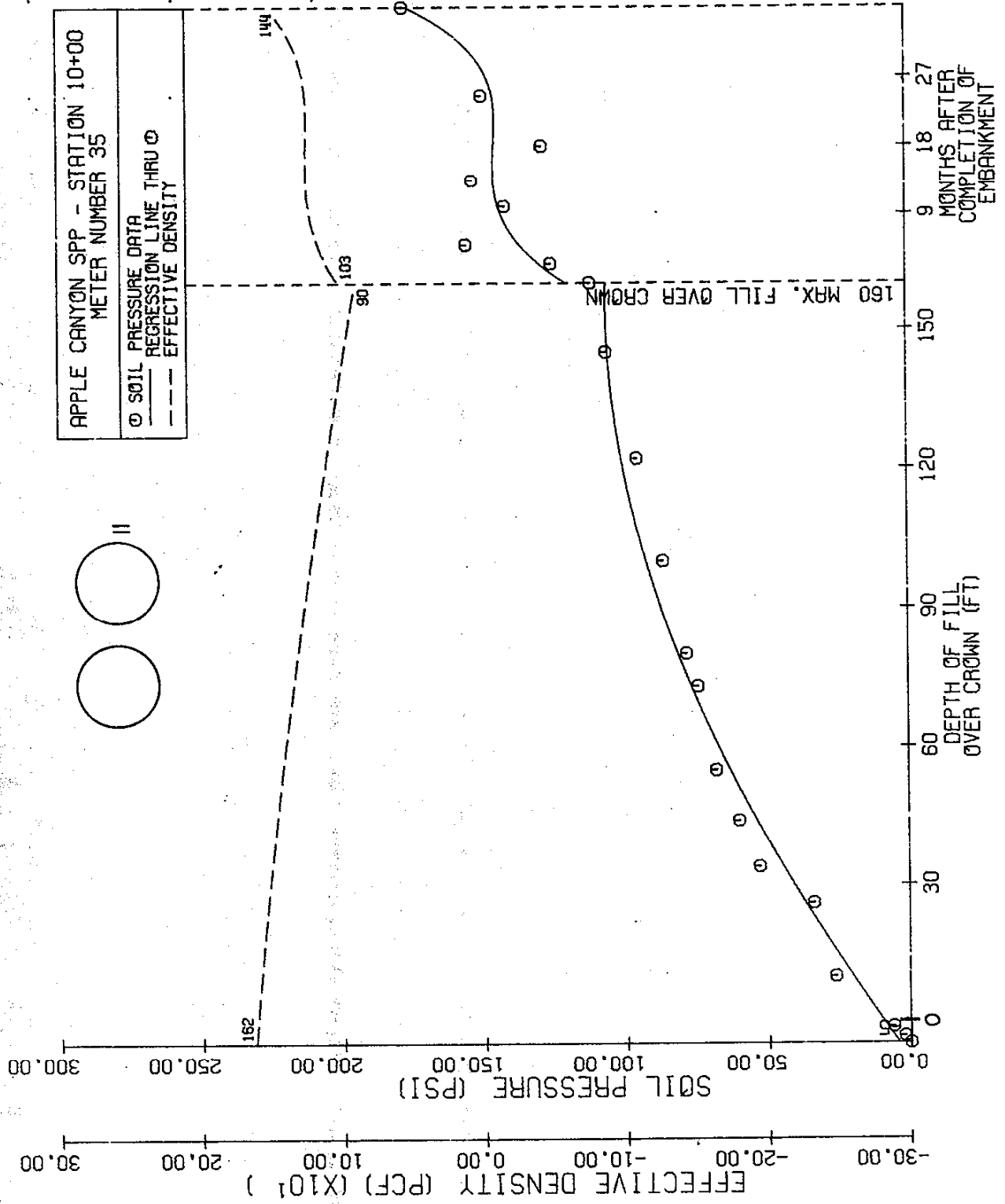


FIGURE 40

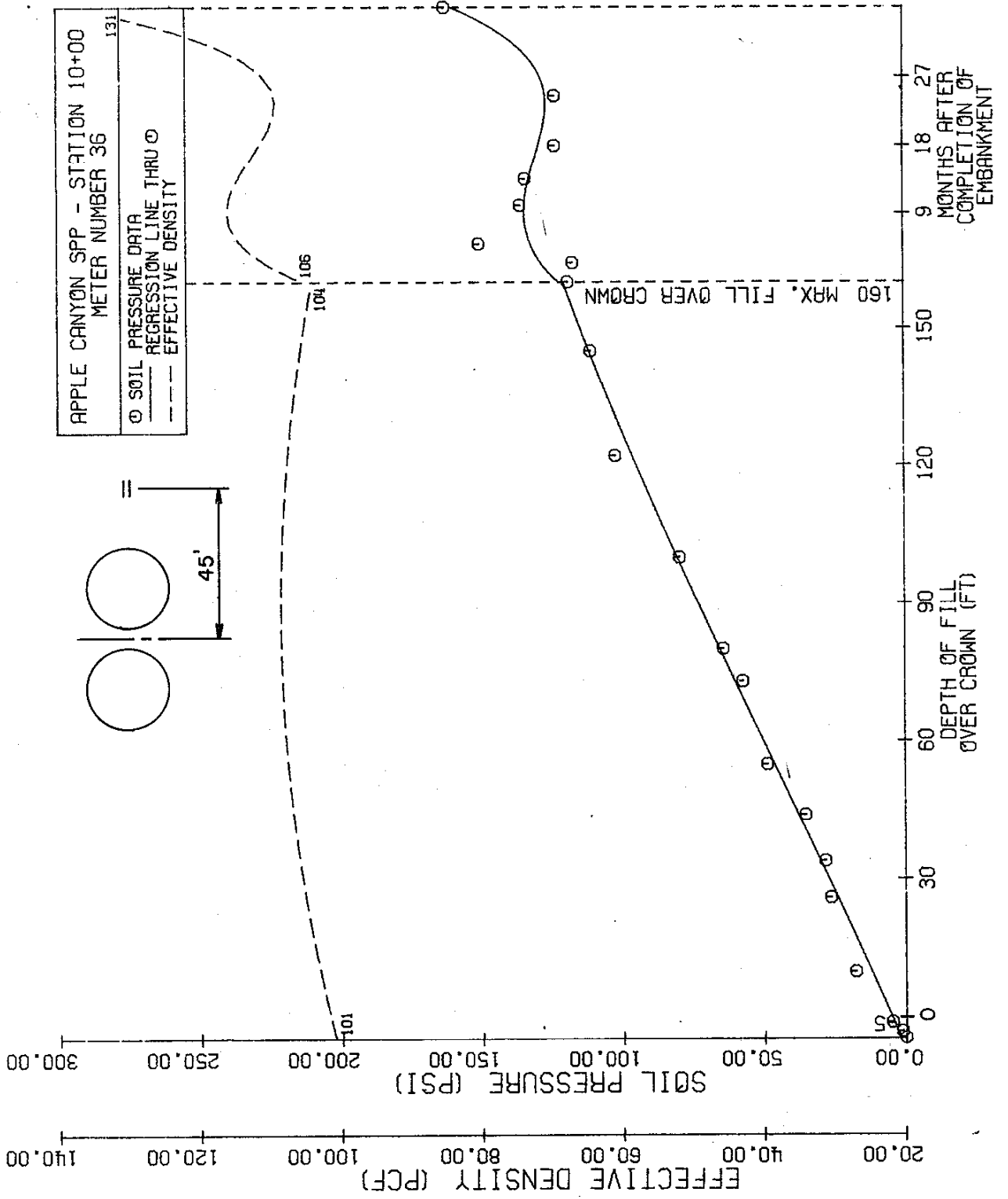


FIGURE 41

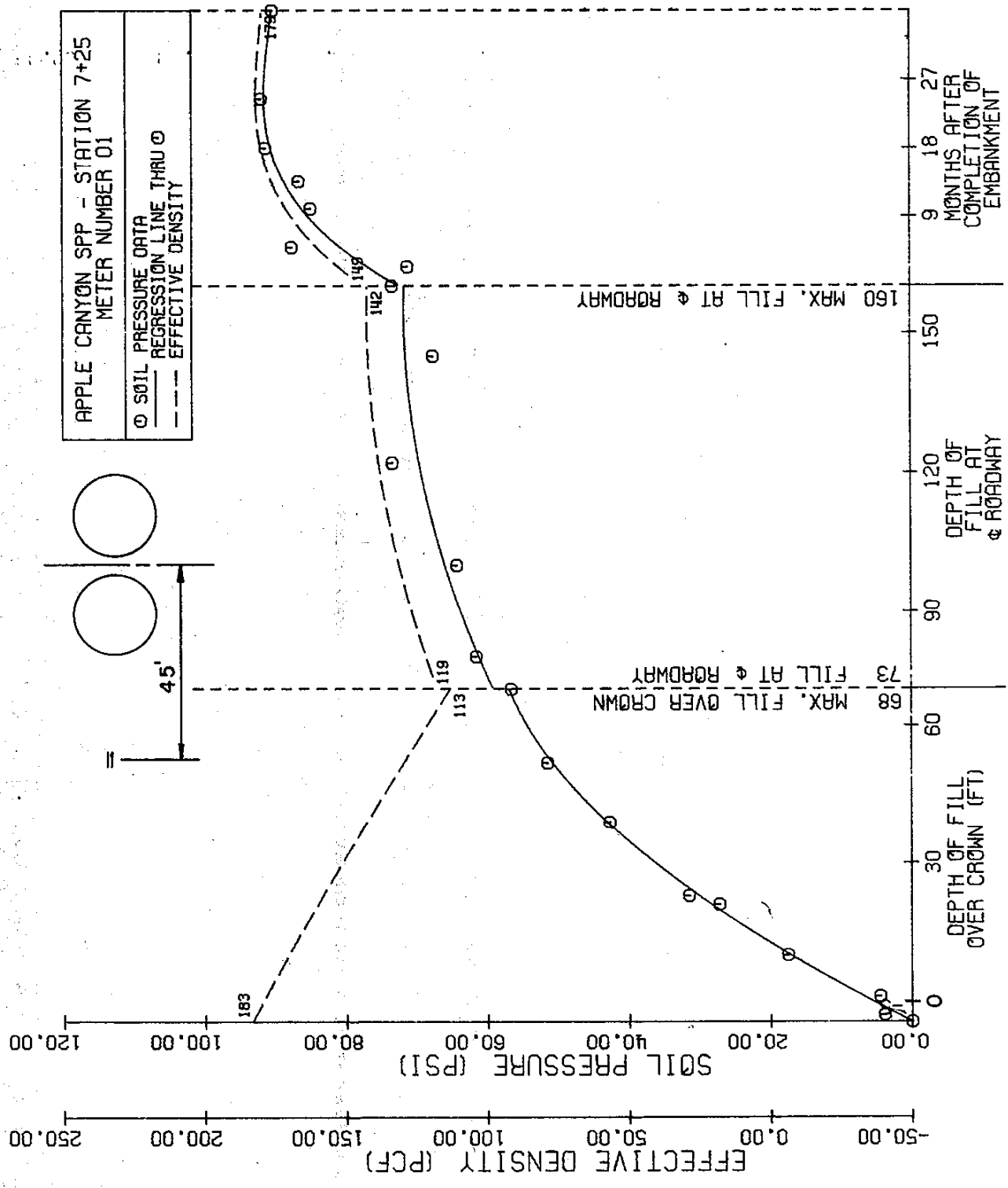


FIGURE 42

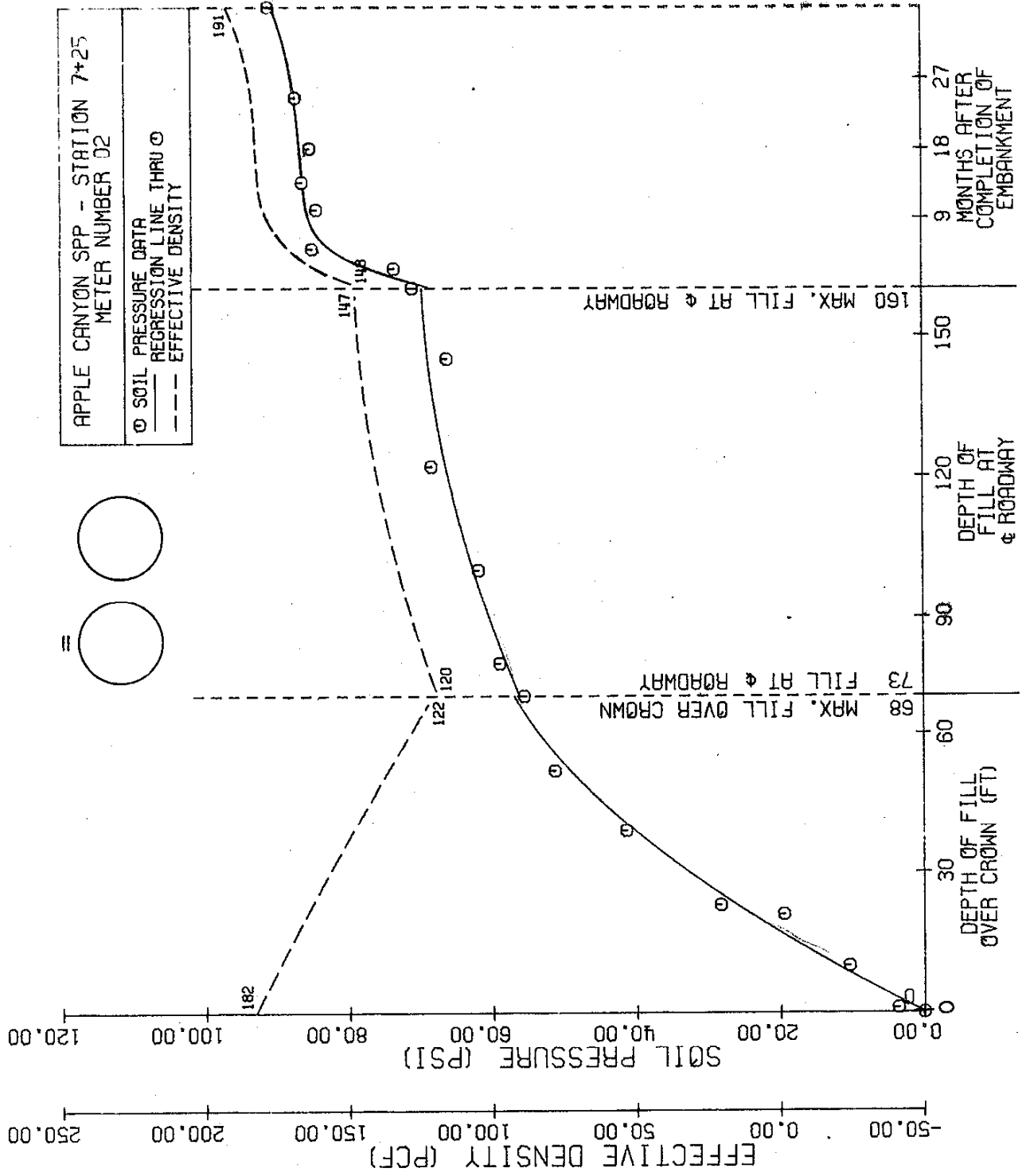


FIGURE 43

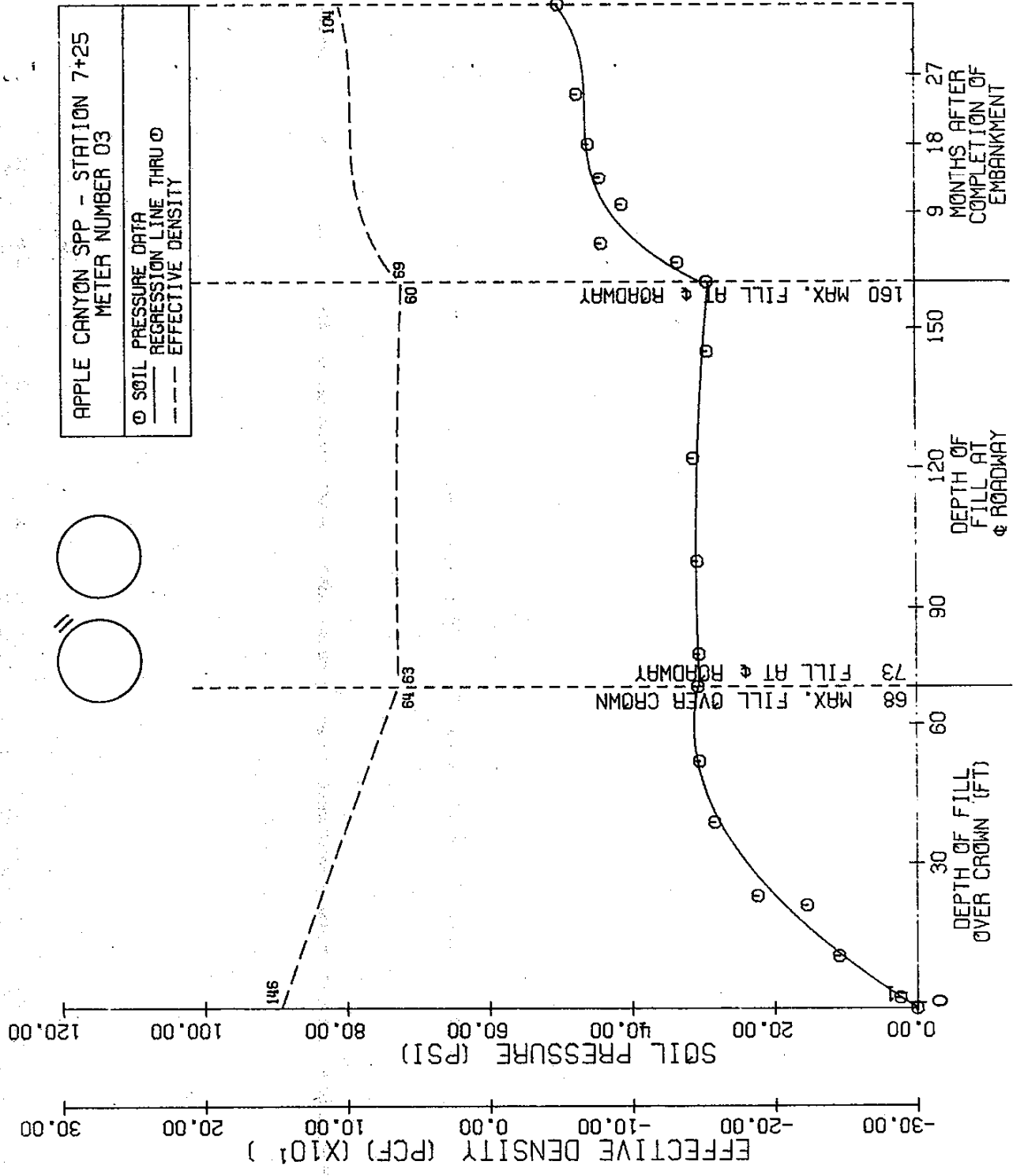


FIGURE 44

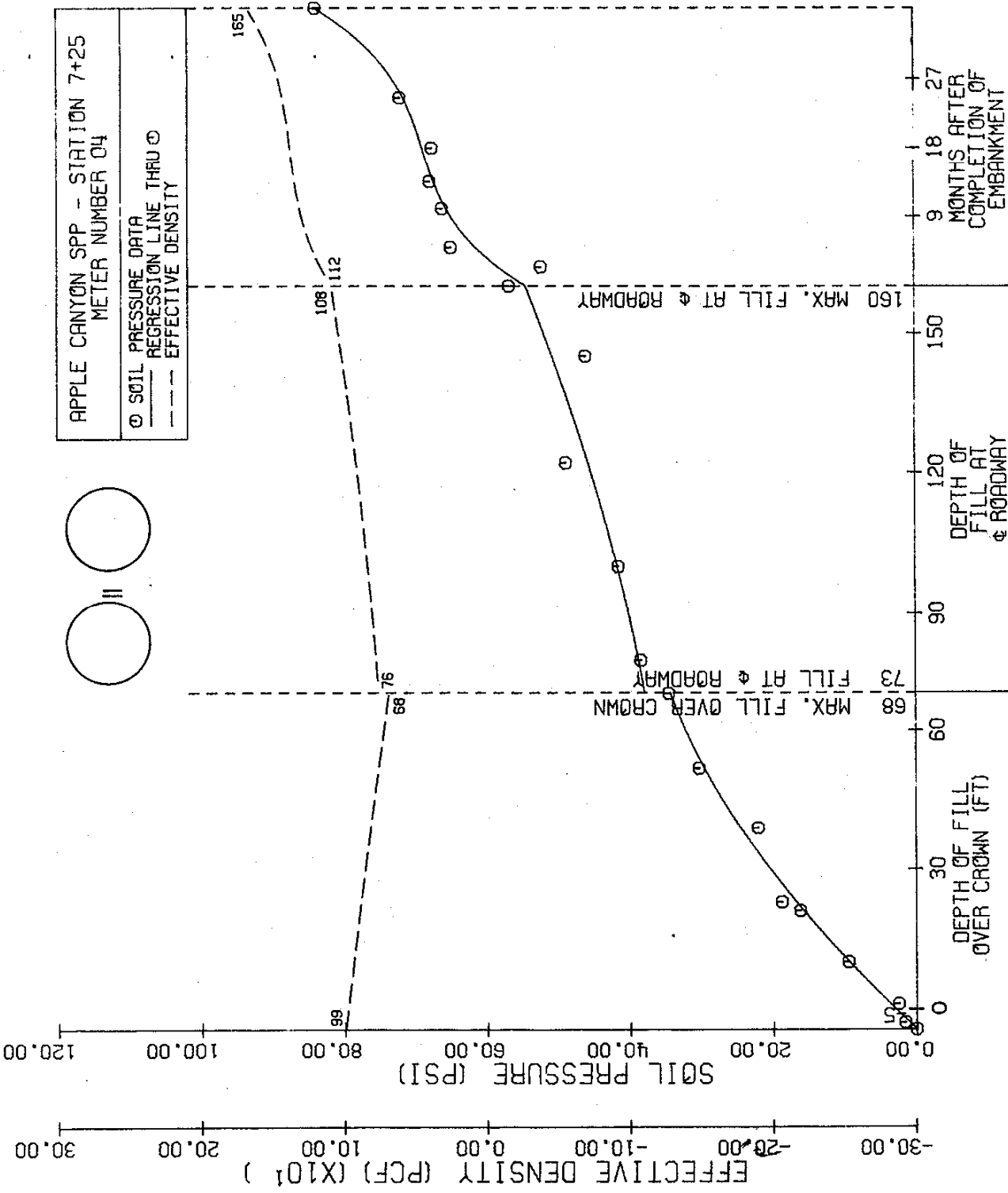


FIGURE 45

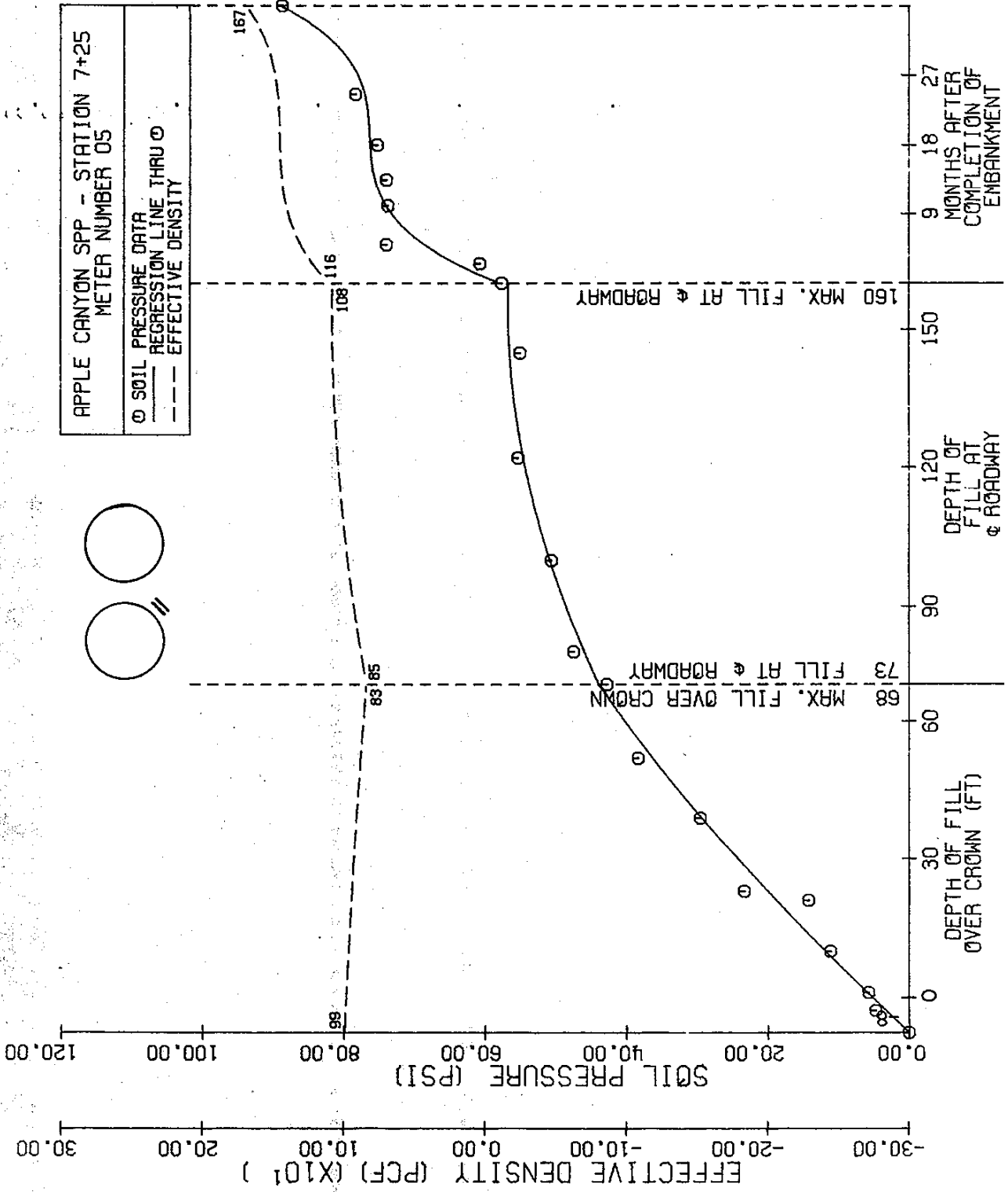


FIGURE 46

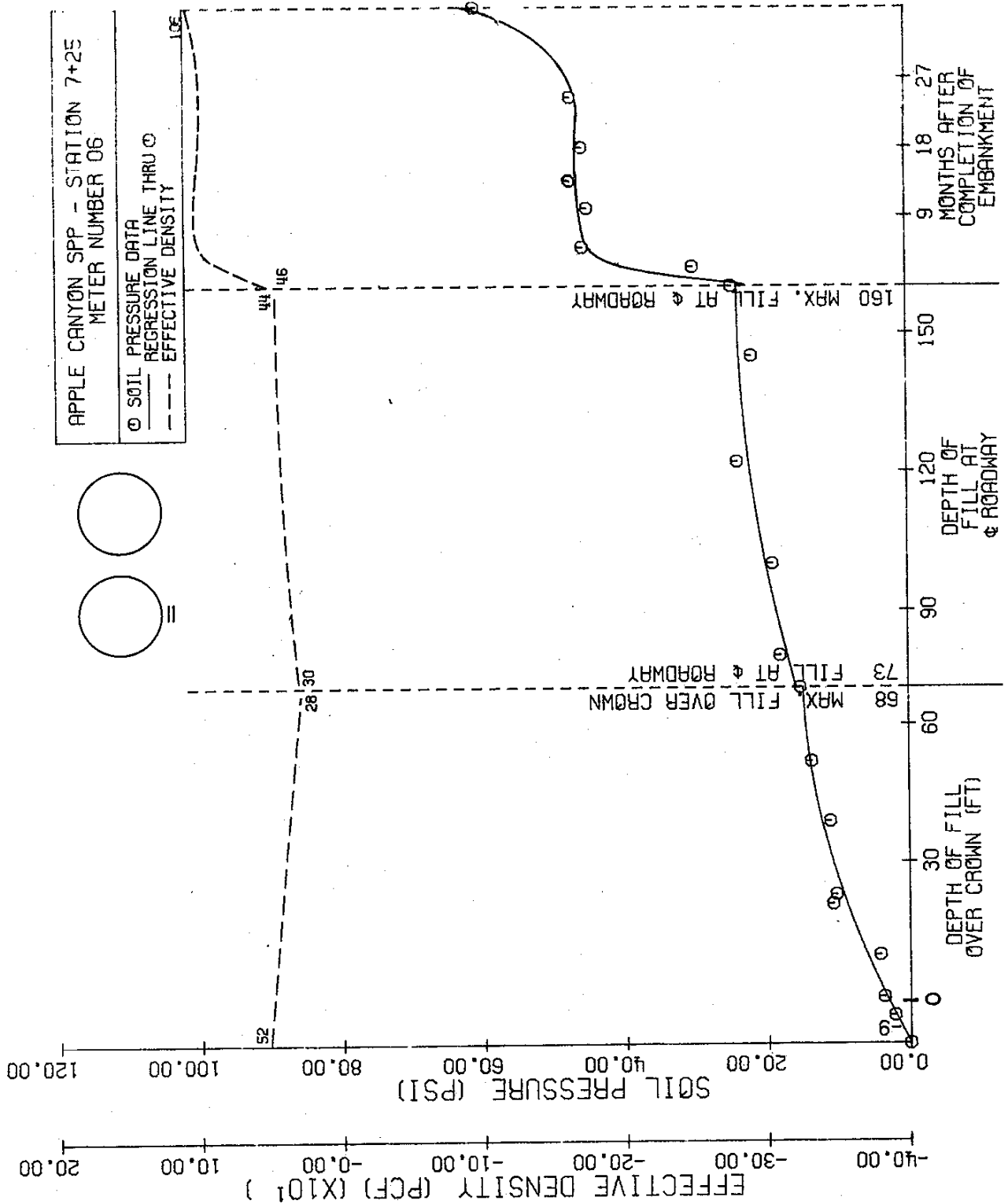


FIGURE 47

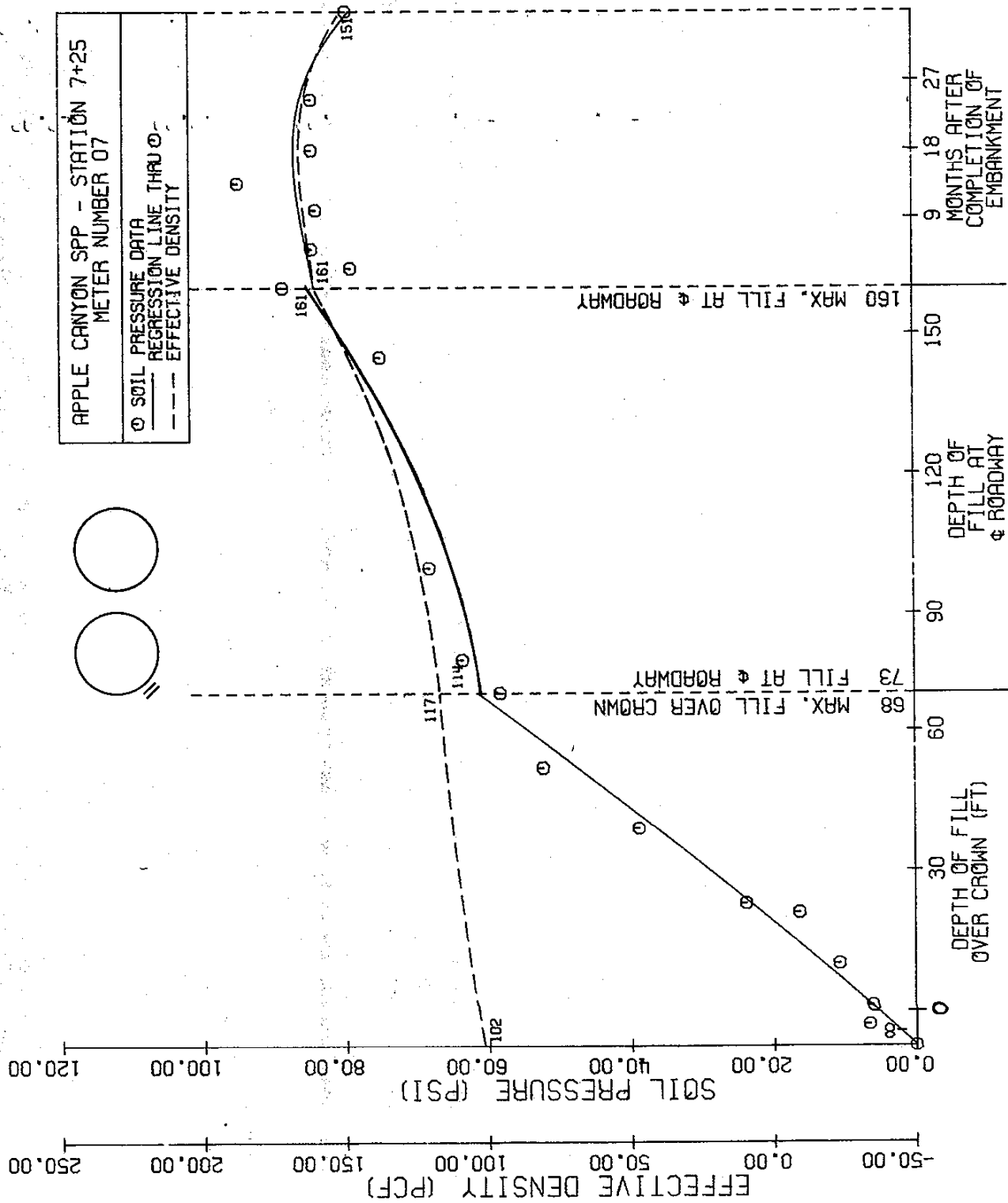


FIGURE 48

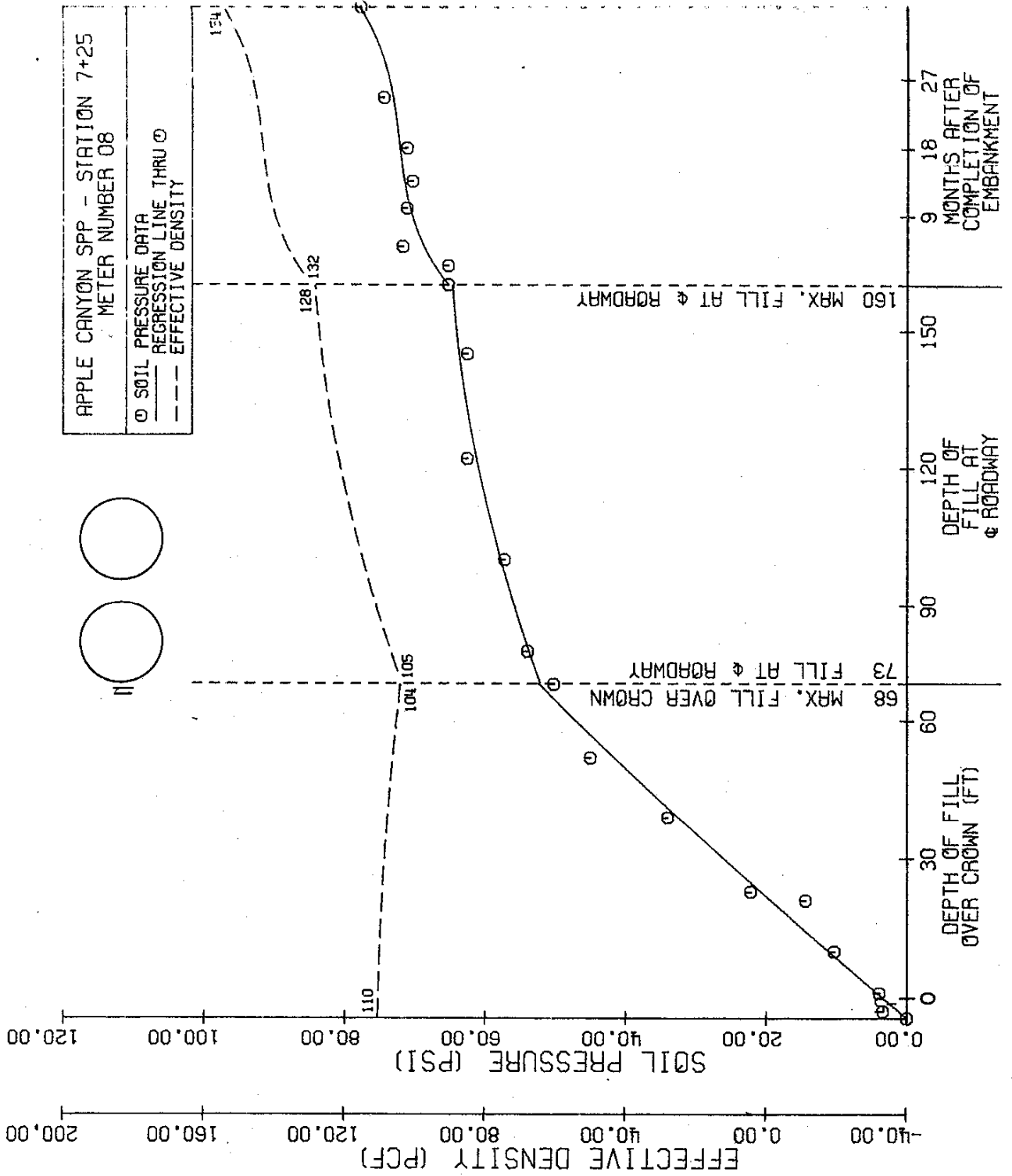


FIGURE 49

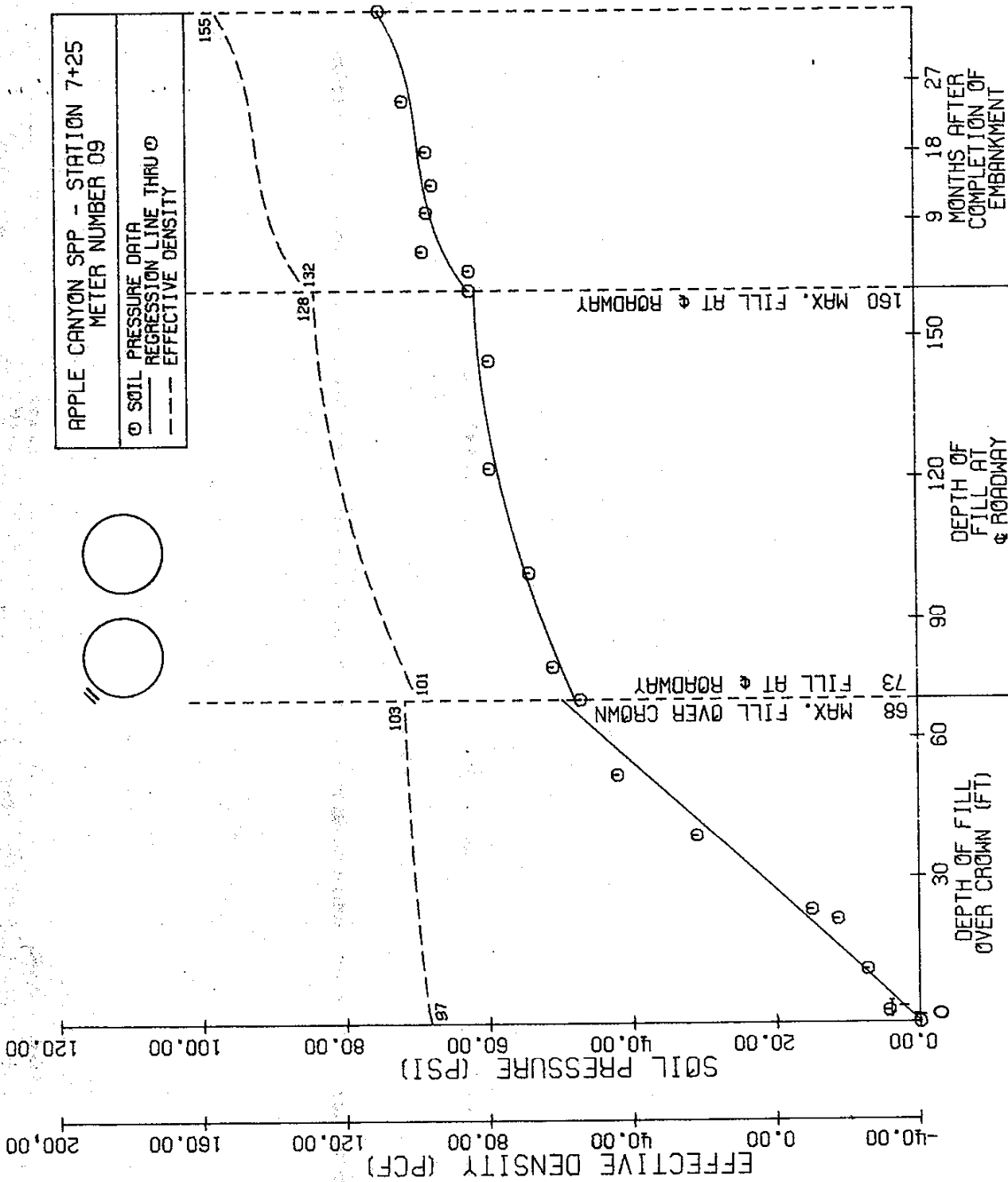


FIGURE 50

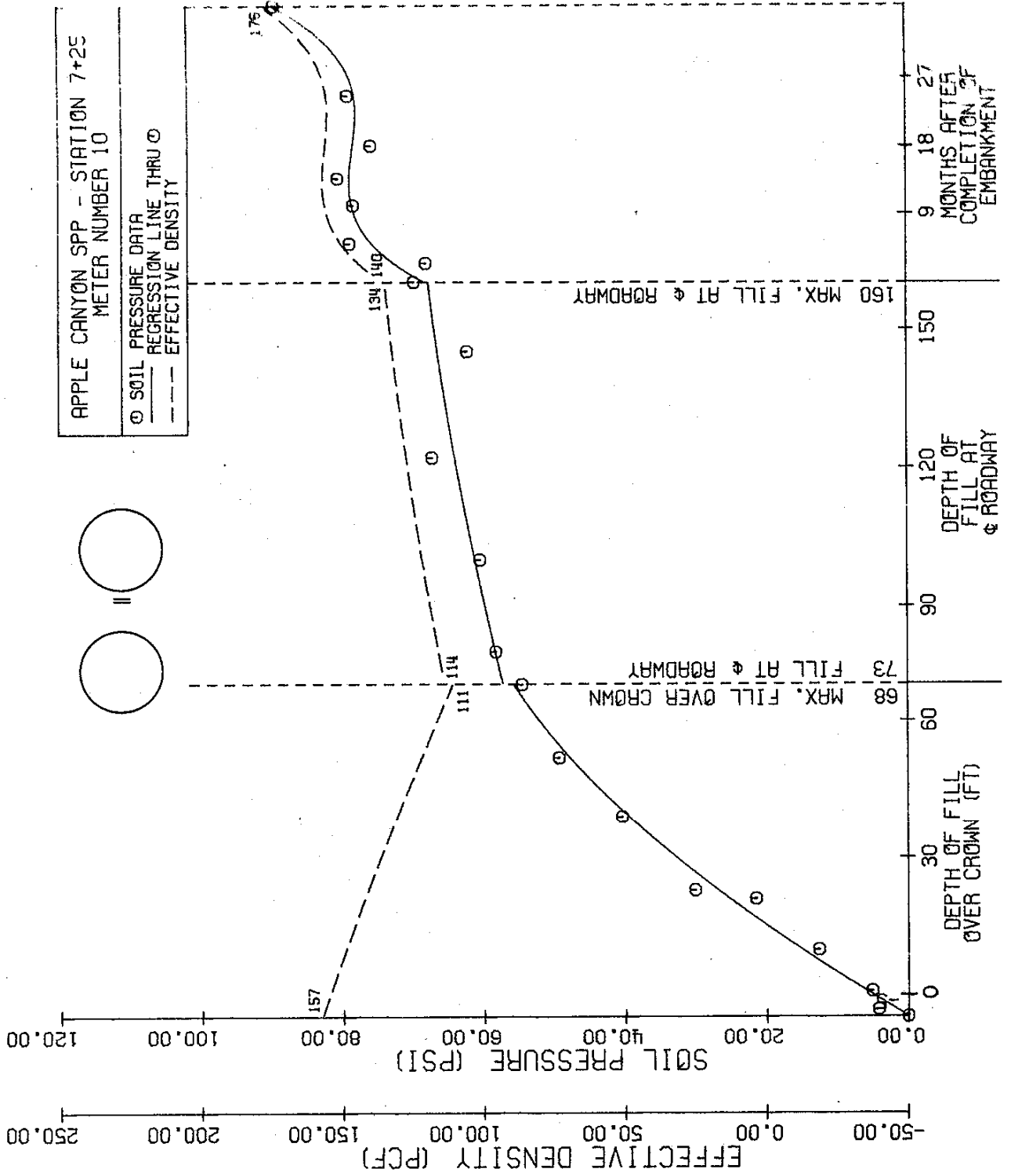


FIGURE 51

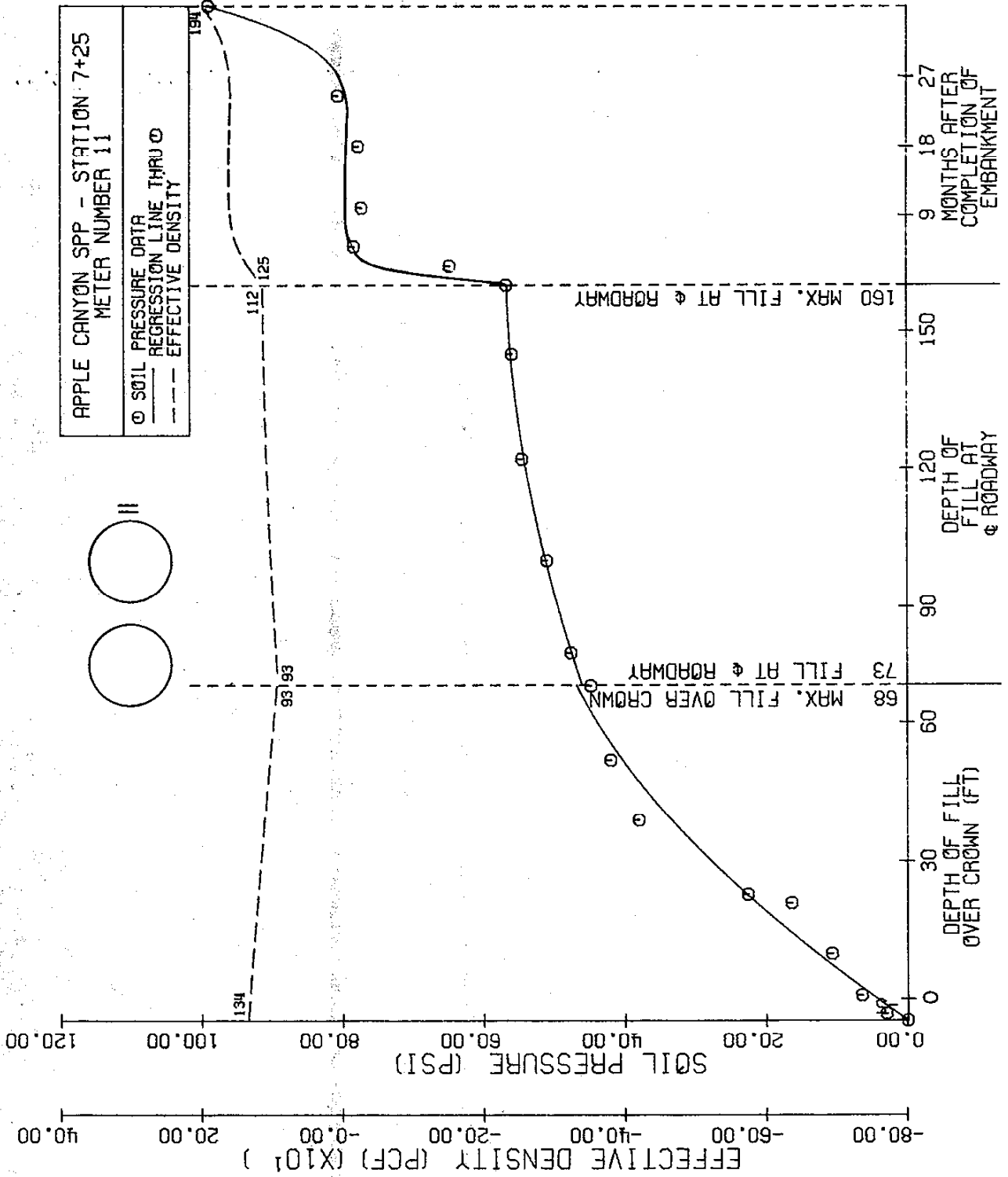


FIGURE 52

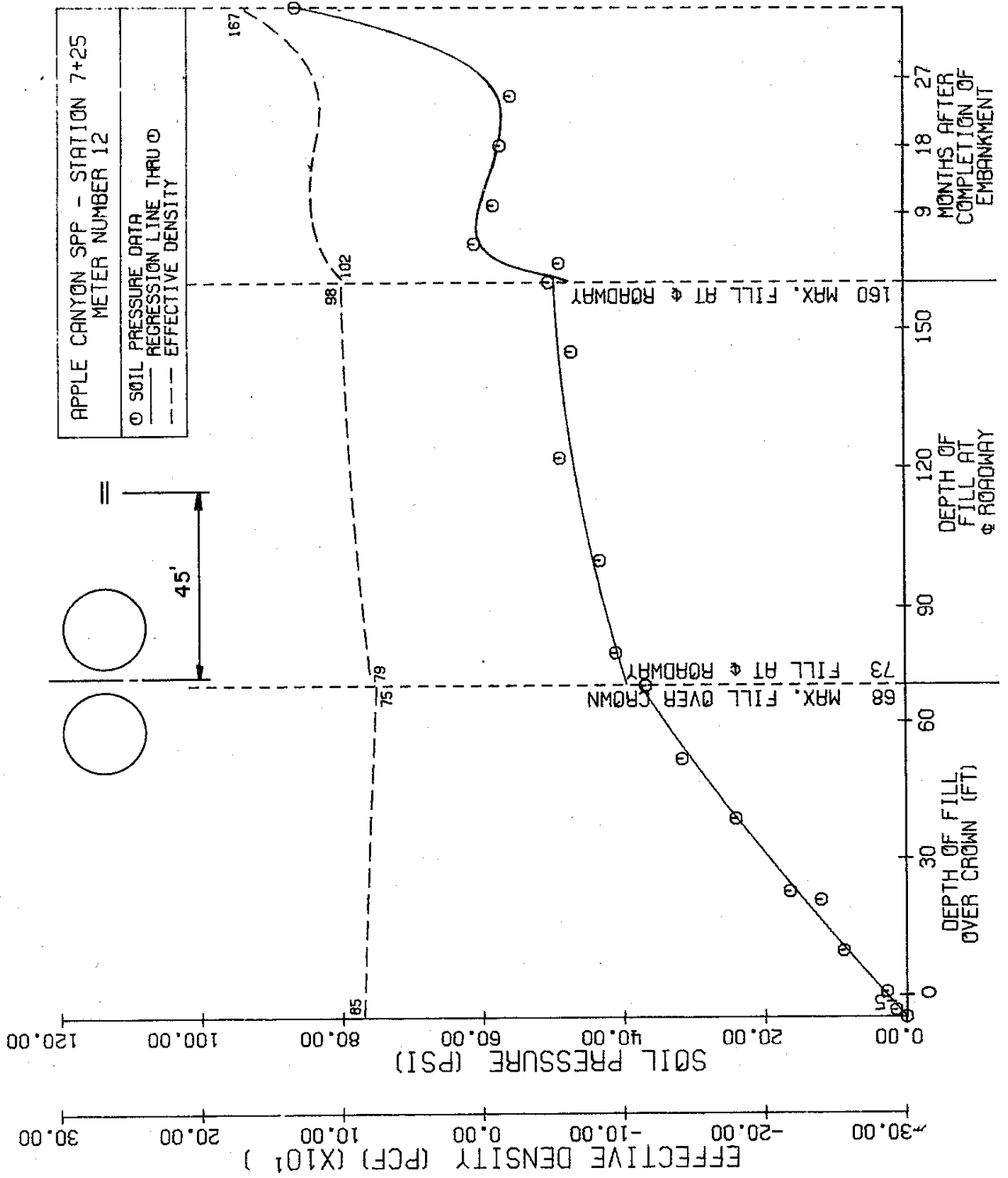


FIGURE 53

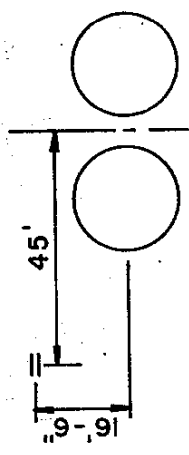
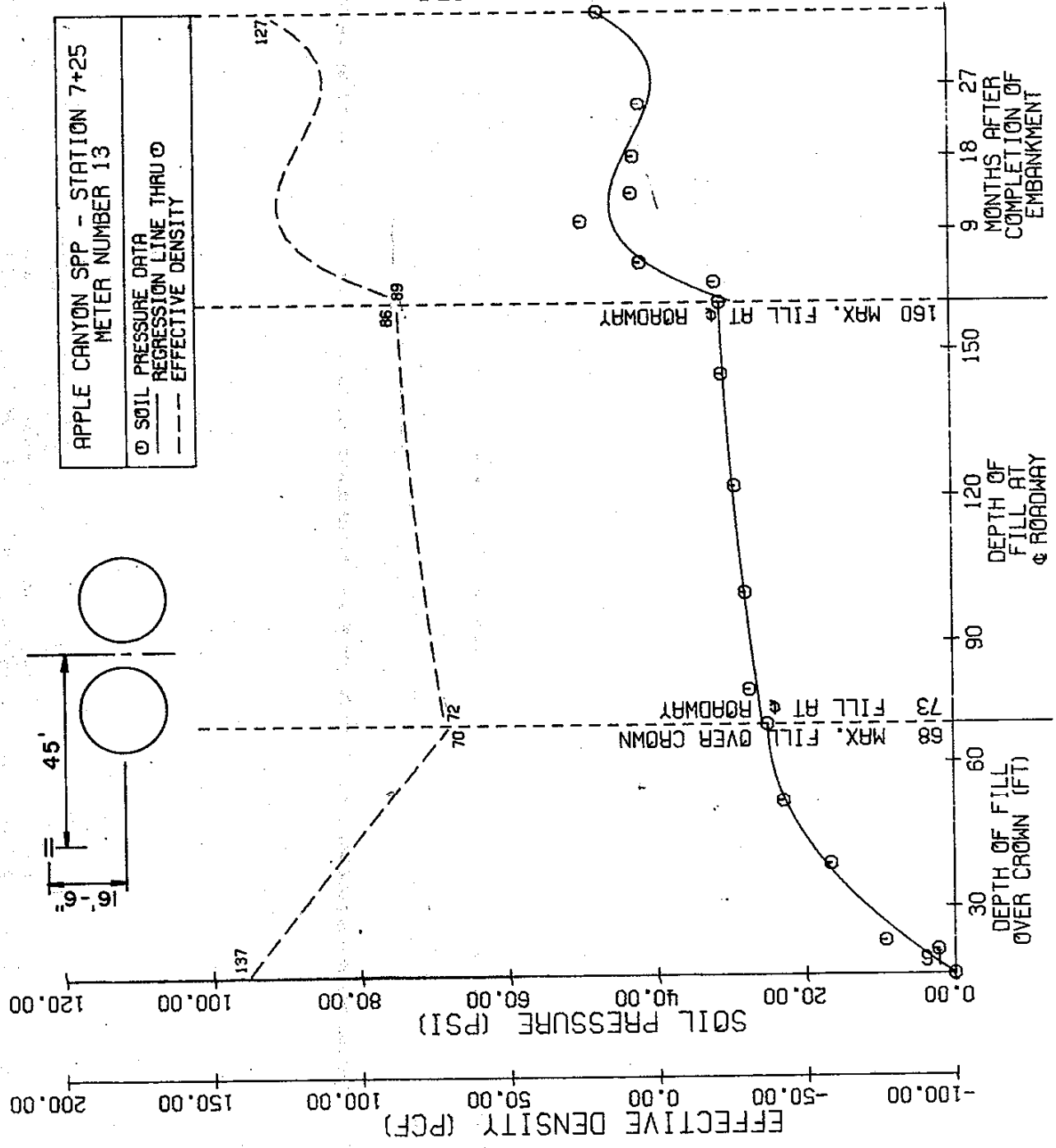


FIGURE 54

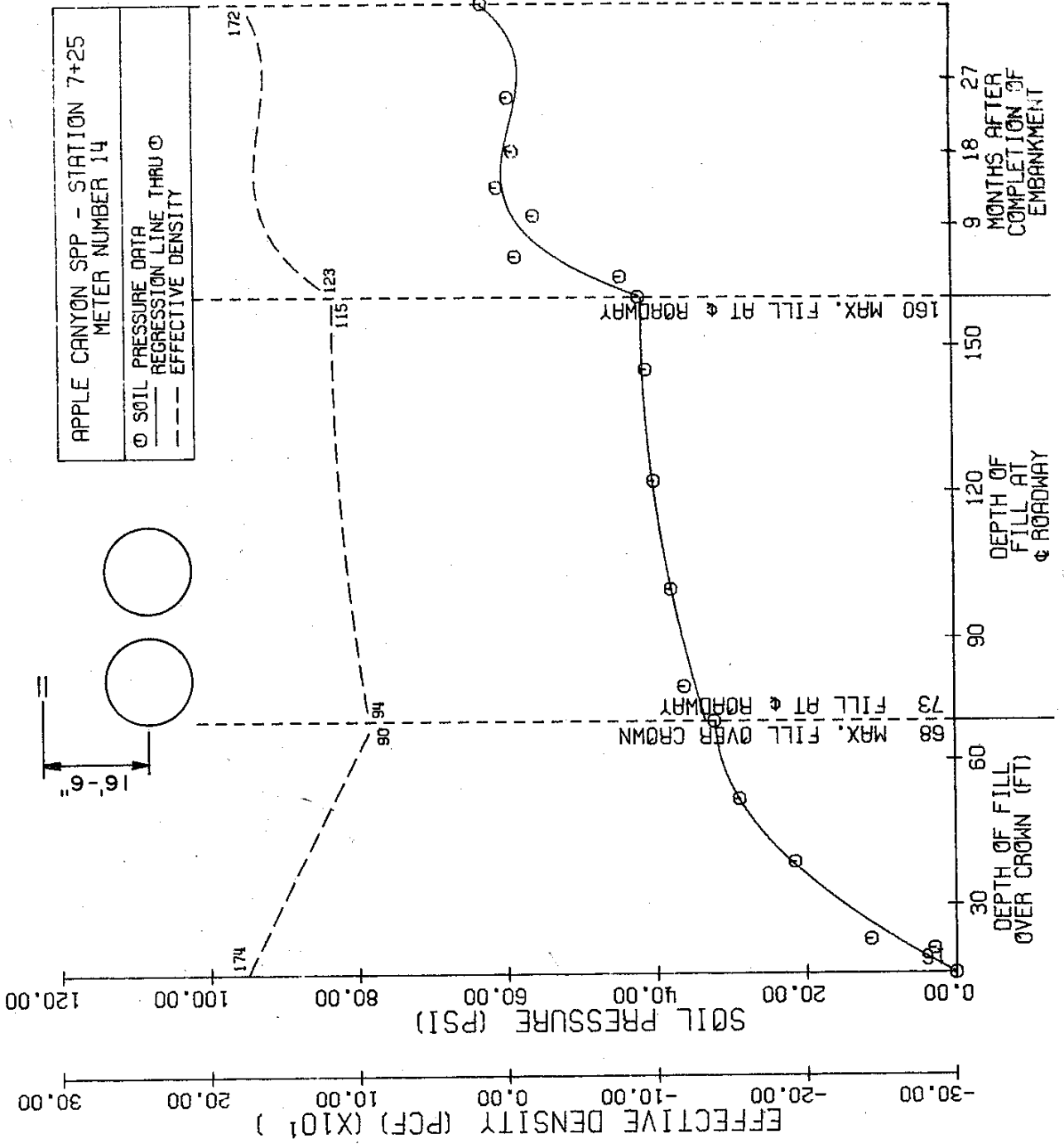


FIGURE 55

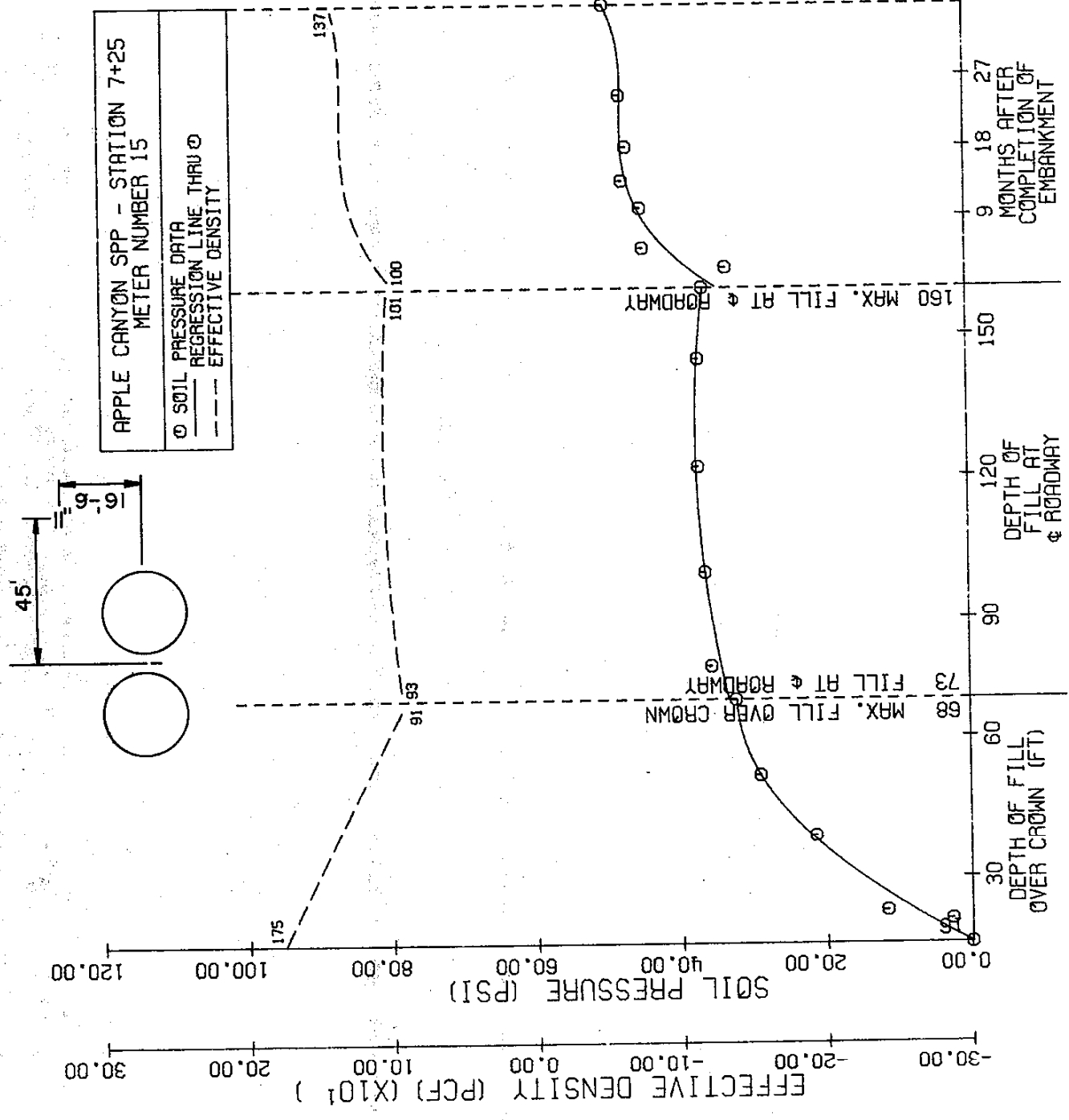
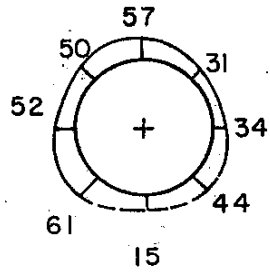
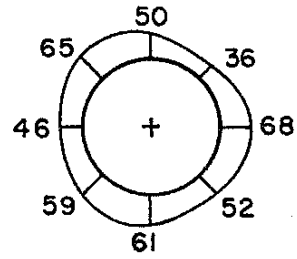


FIGURE 56

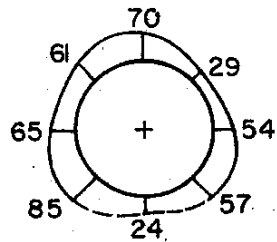
APPLE CANYON SPP
SOIL PRESSURES AT VARIOUS TIMES



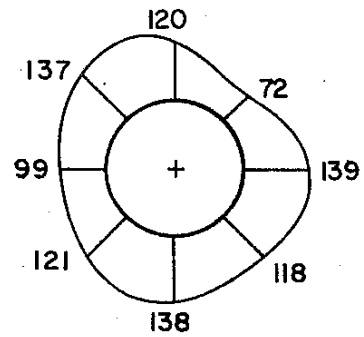
Fill Height = 68'



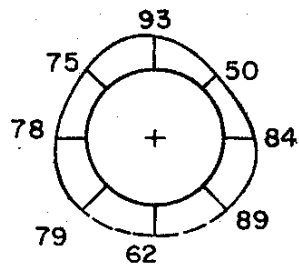
Fill Height = 73'



Fill Height = 68'
Fill Height at Sta. 10+00 = 160'

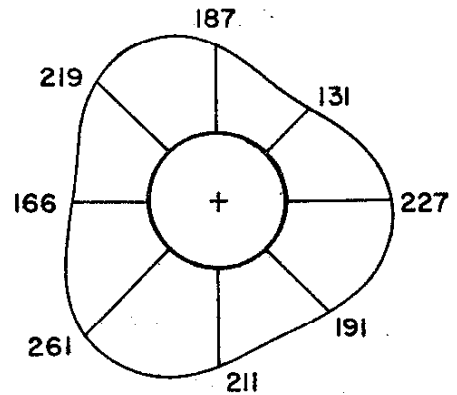


Fill Height = 160'



Fill Height = 68'
Time after fill completion = 36 mo.

STATION 7+25



Fill Height = 68'
Time after fill completion = 36 mo.

STATION 10+00

Scale :

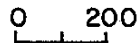
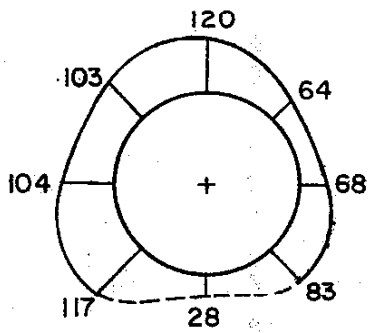
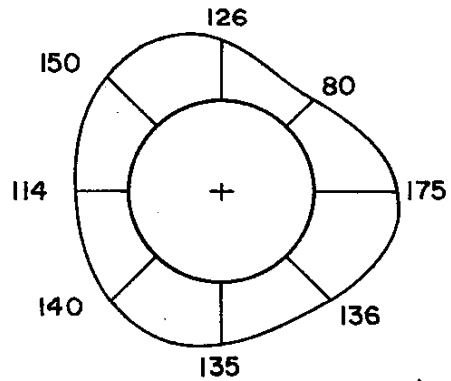


FIGURE 57

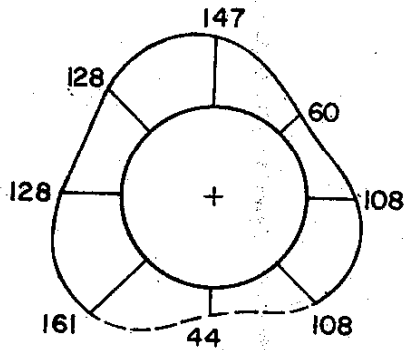
APPLE CANYON SPP EFFECTIVE DENSITY



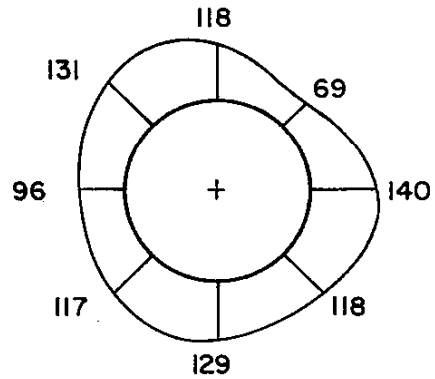
Fill Height Over Crown = 68'



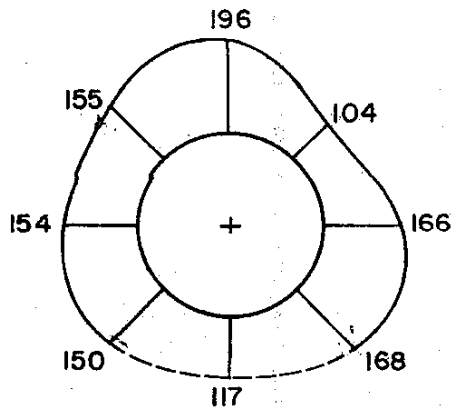
Fill Height Over Crown = 73'



Fill Height Over Crown = 68'
Fill Height at \ominus Roadway = 160'

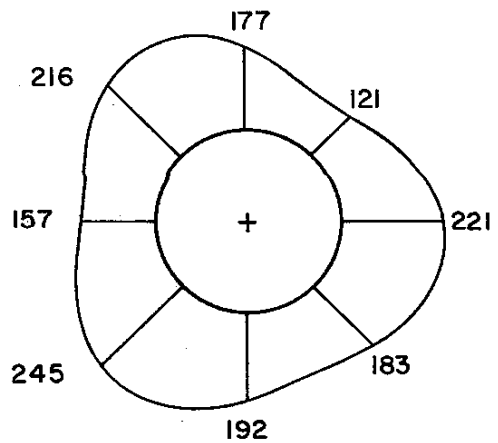


Fill Height Over Crown = 160'



Fill Height Over Crown = 68'
Time After Fill Completion = 36 mo.

STATION 7+25



Fill Height Over Crown = 160'
Time After Fill Completion = 36 mo

STATION 10+00

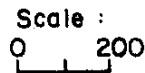


FIGURE 58

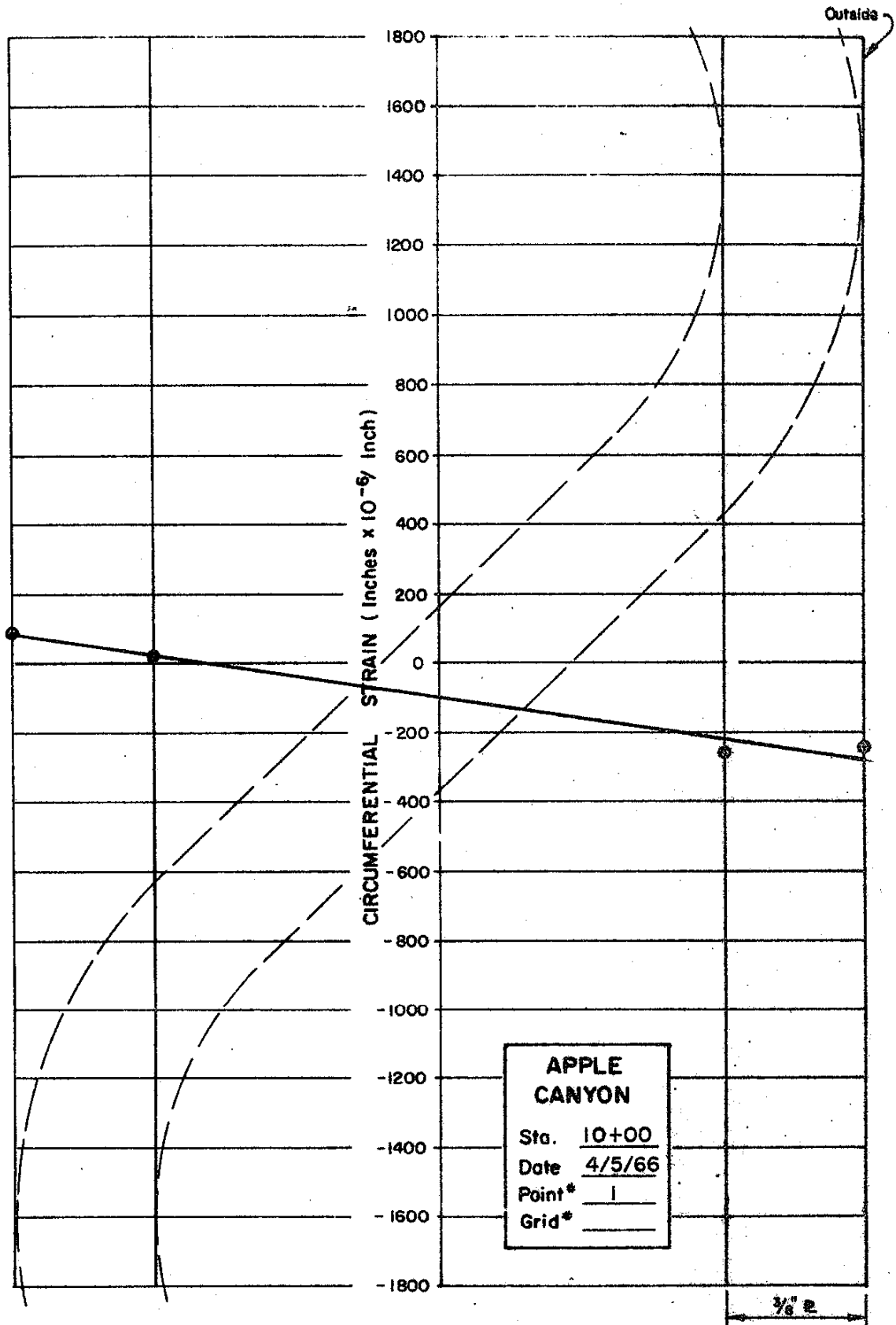


FIGURE 59

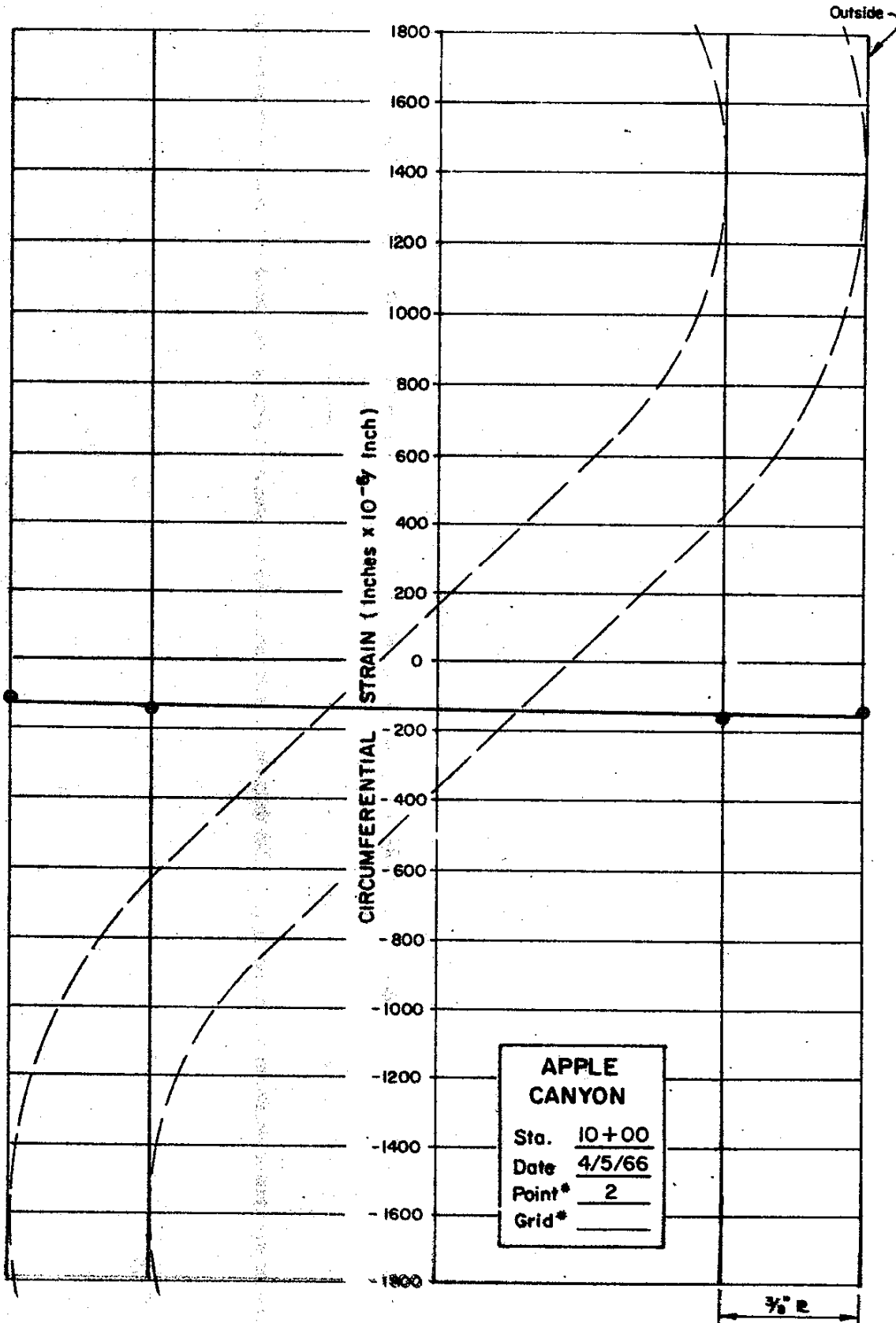


FIGURE 60

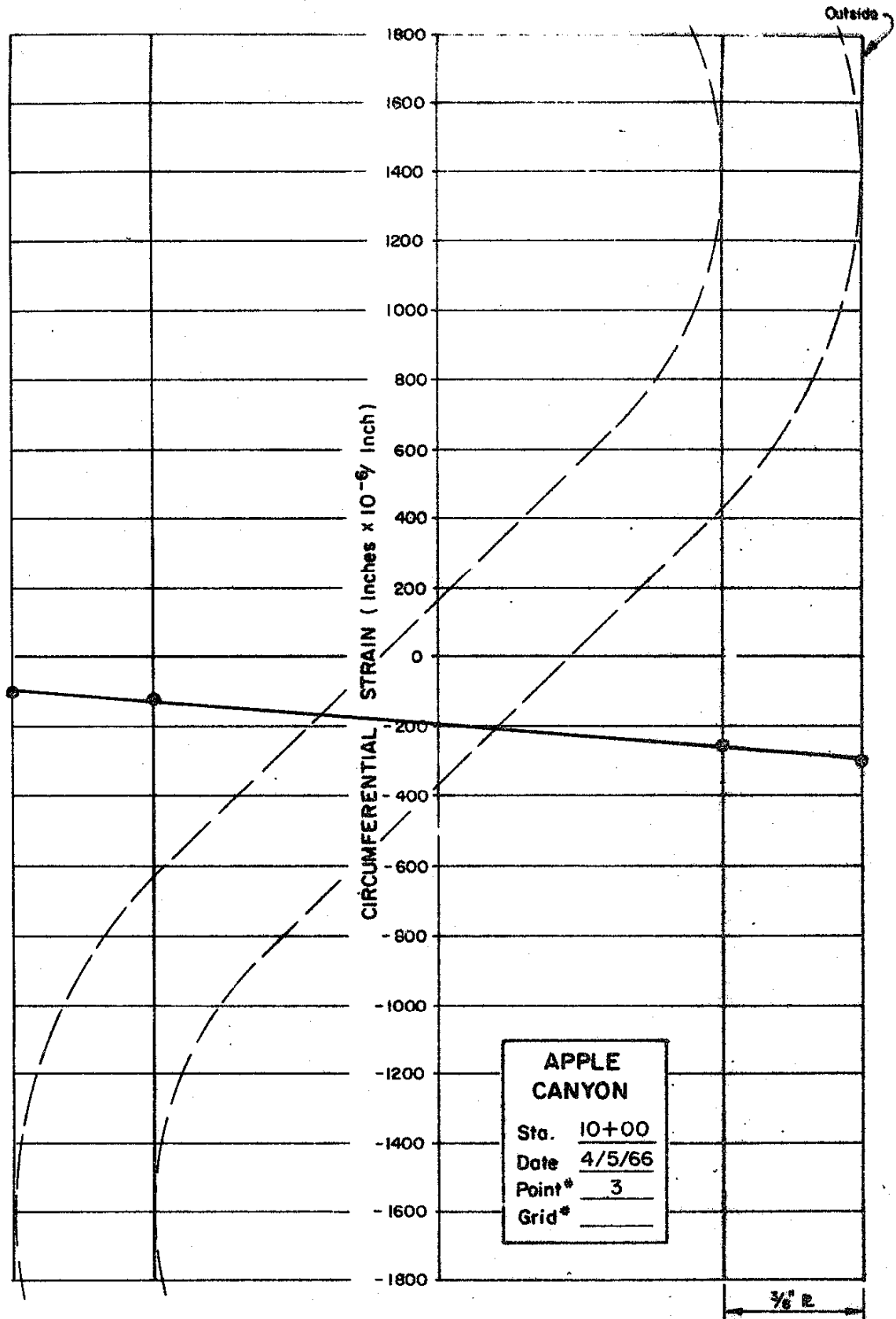


FIGURE 61

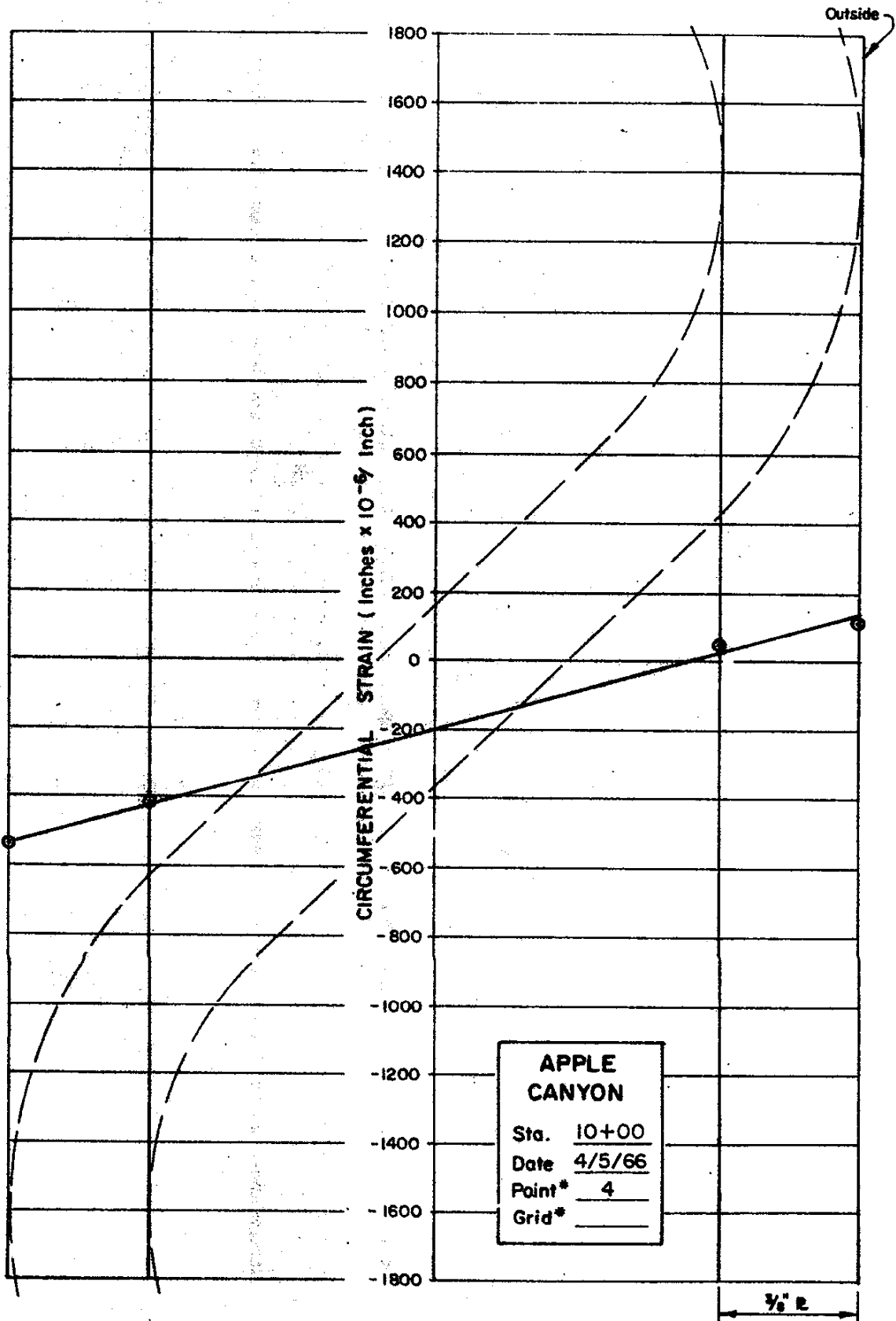


FIGURE 62

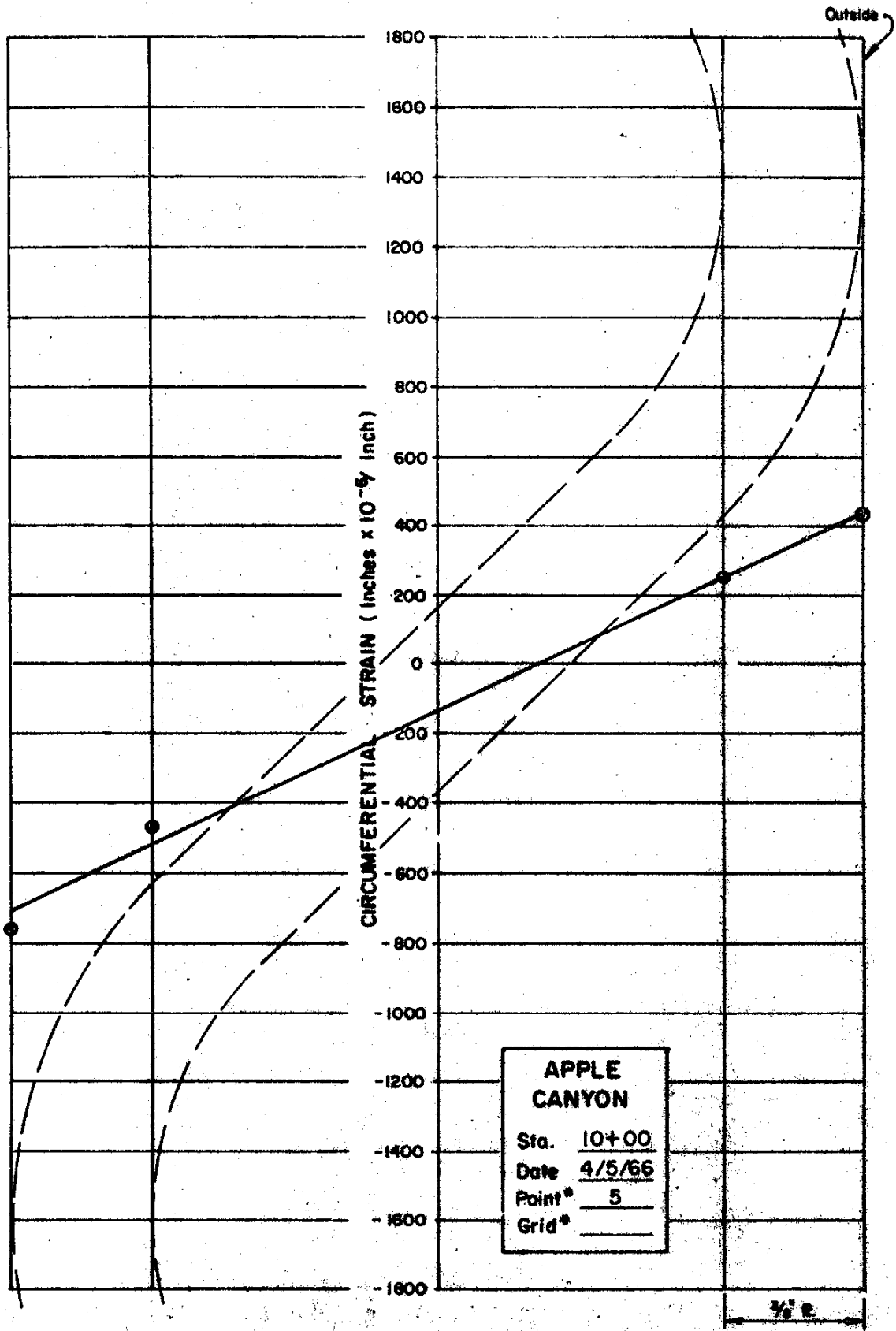


FIGURE 63

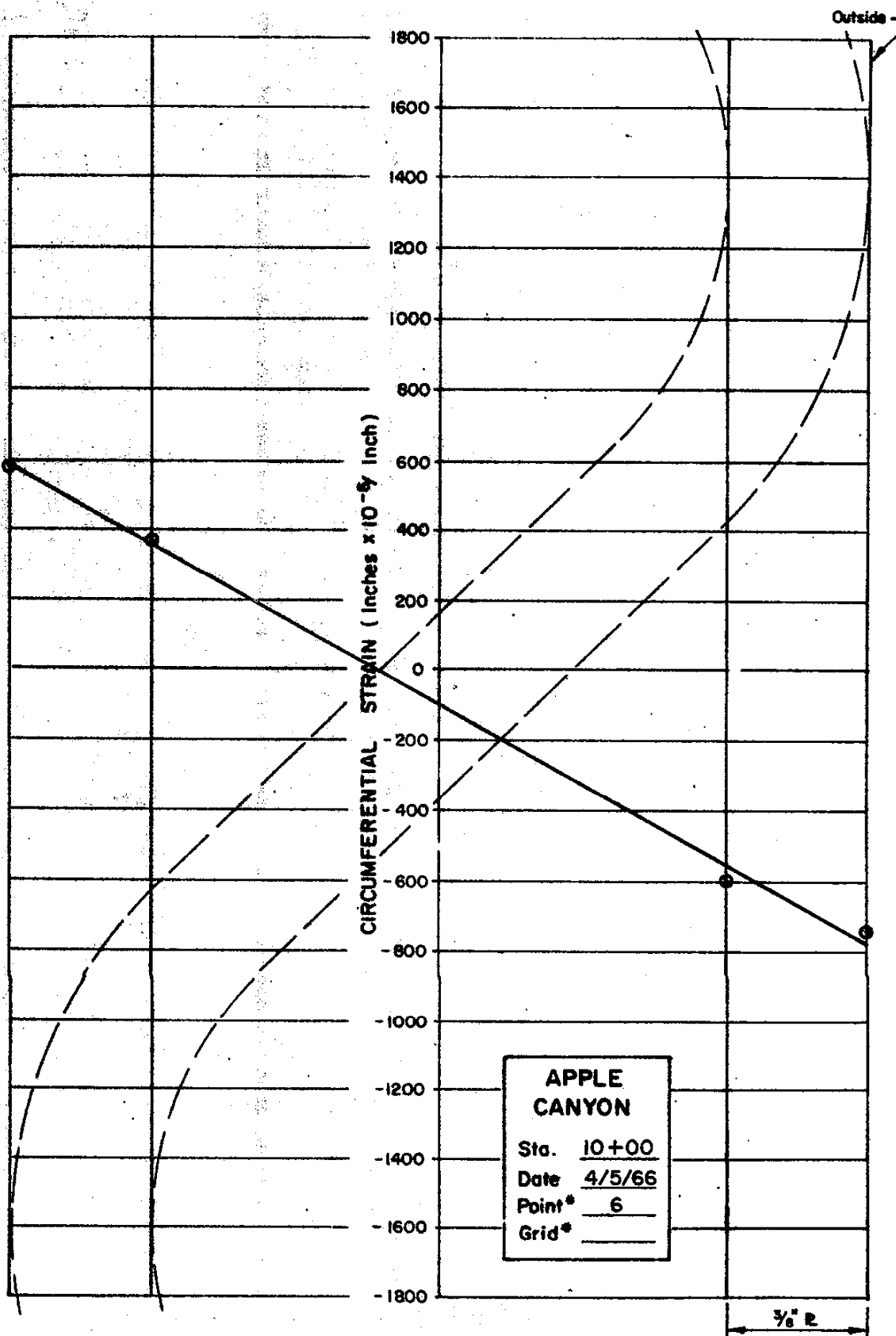


FIGURE 64

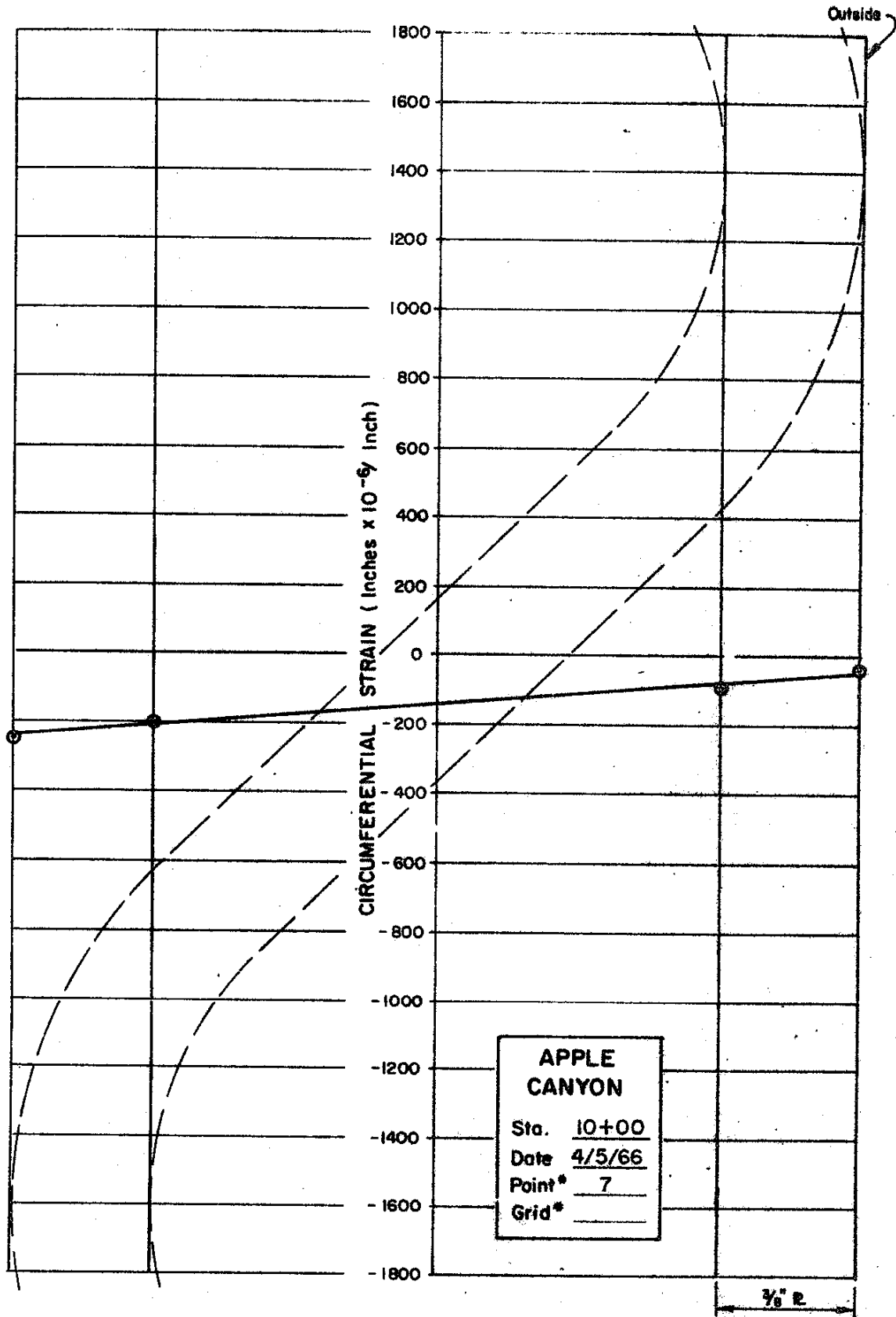


FIGURE 65

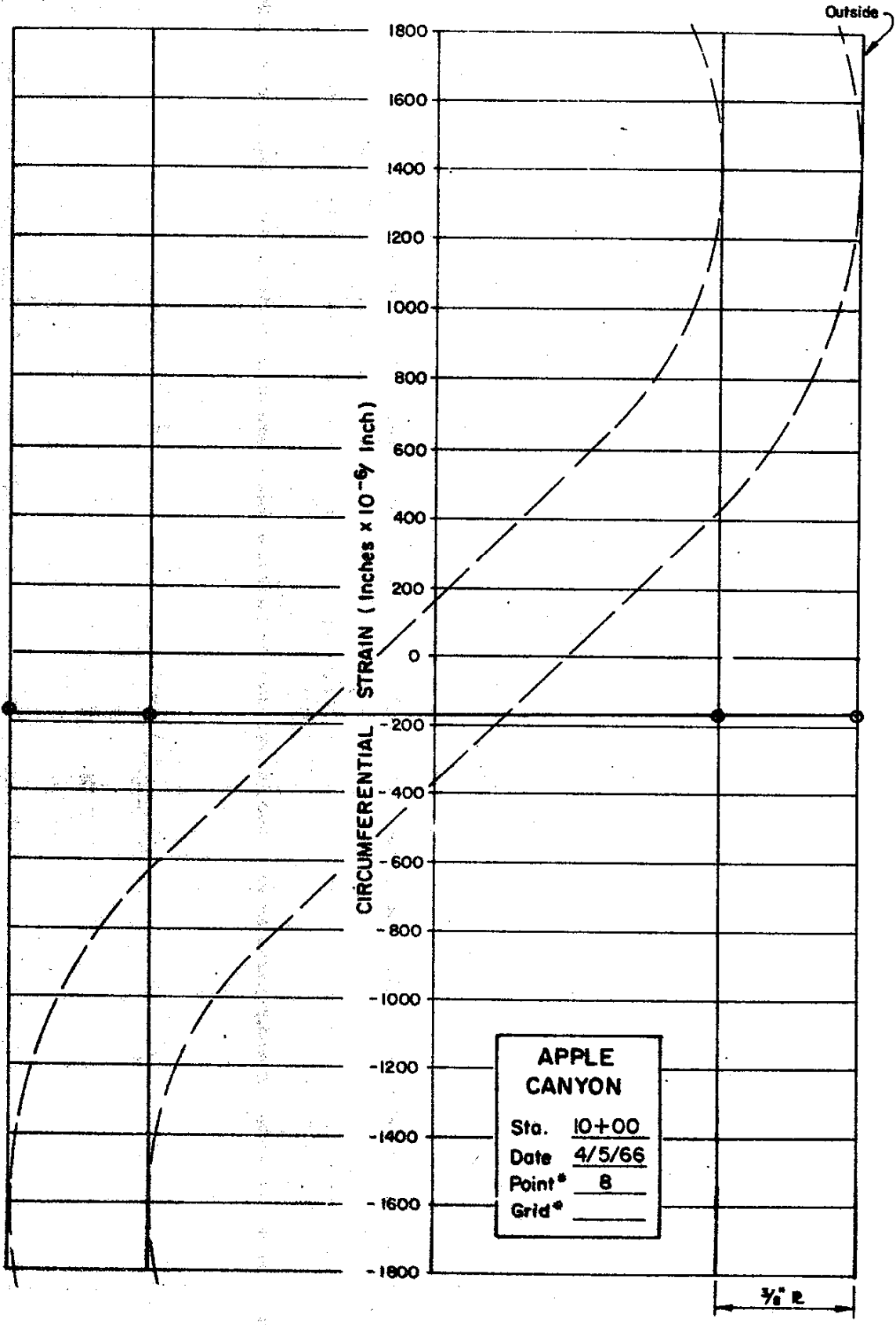


FIGURE 66

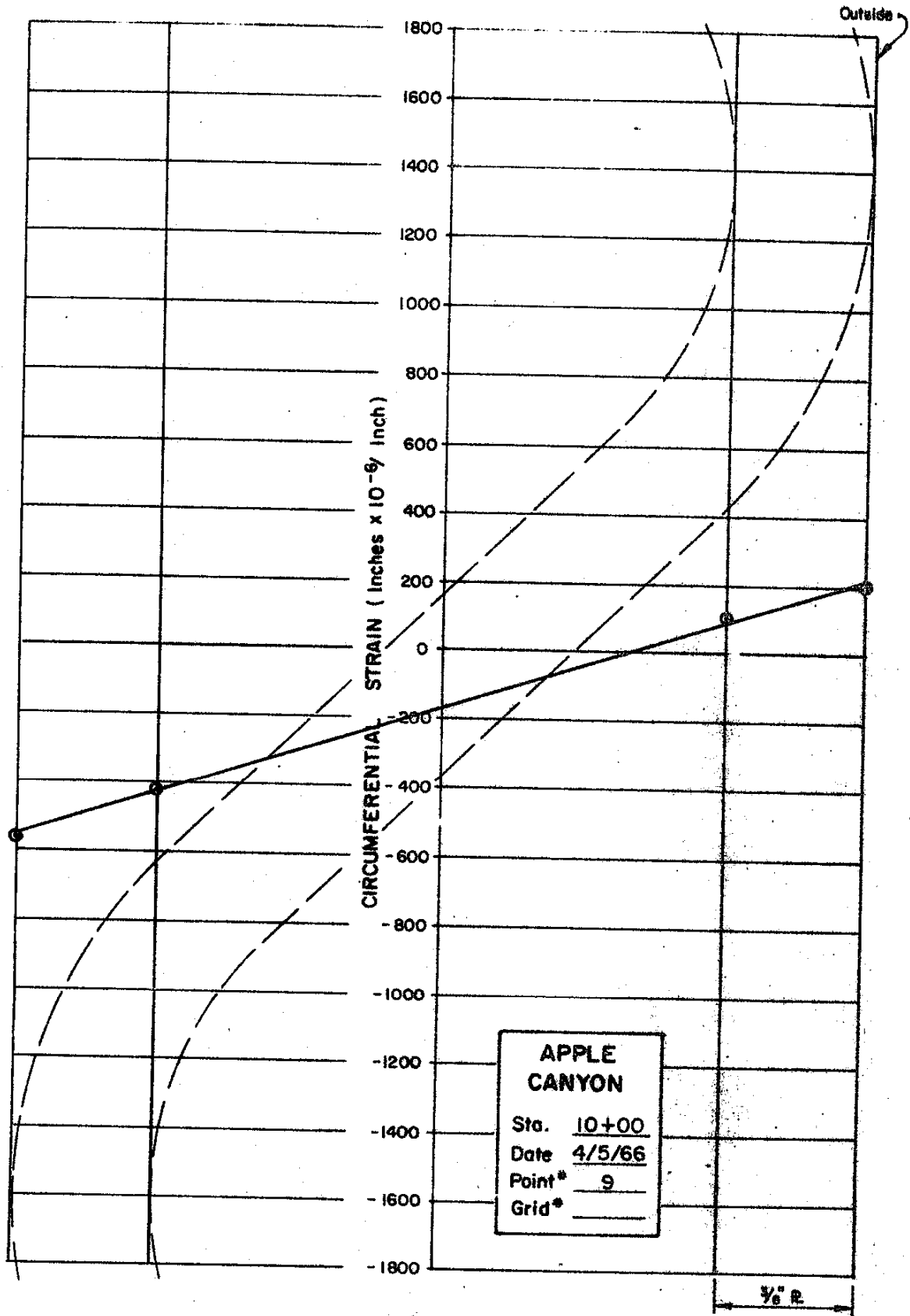


FIGURE 67

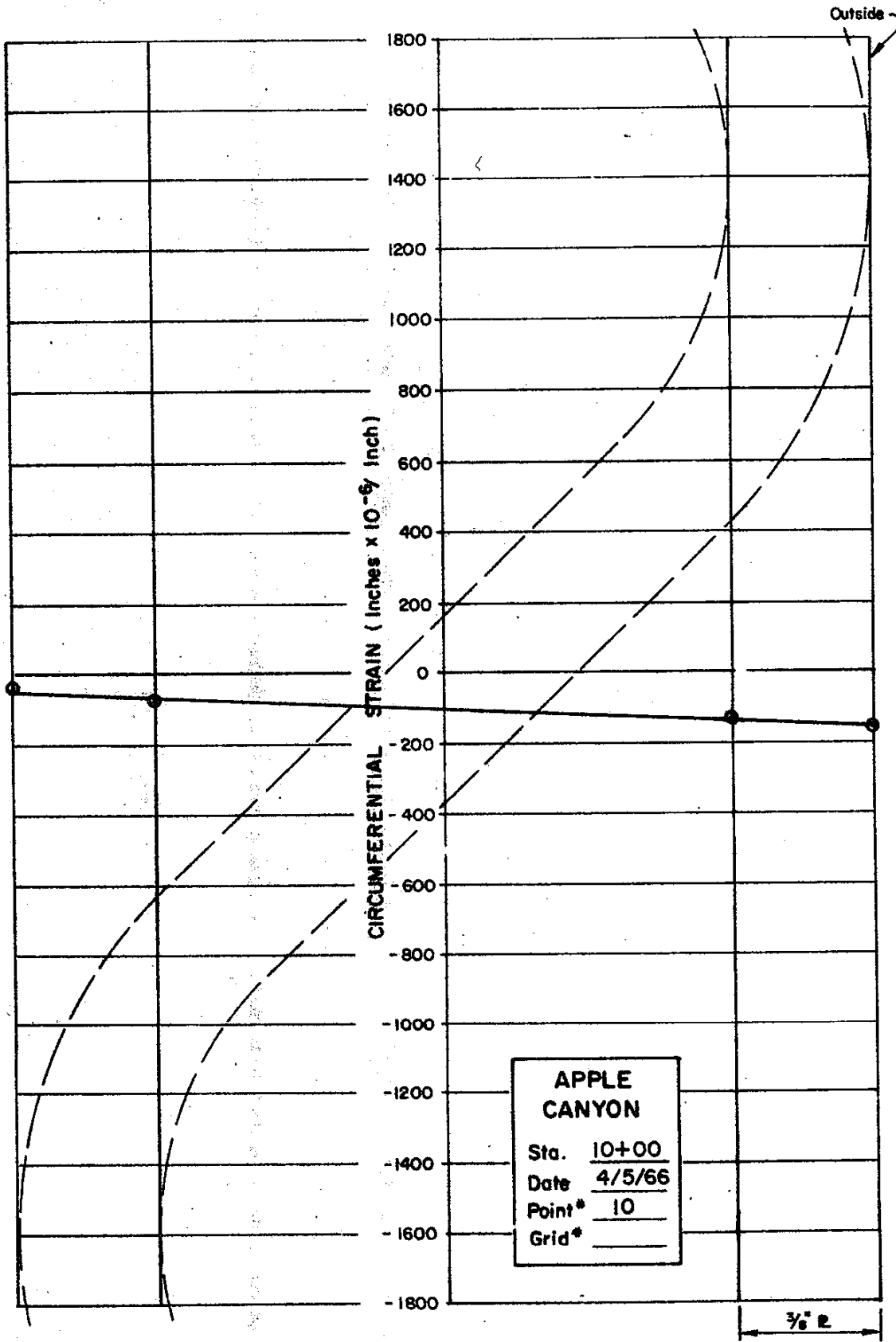


FIGURE 68

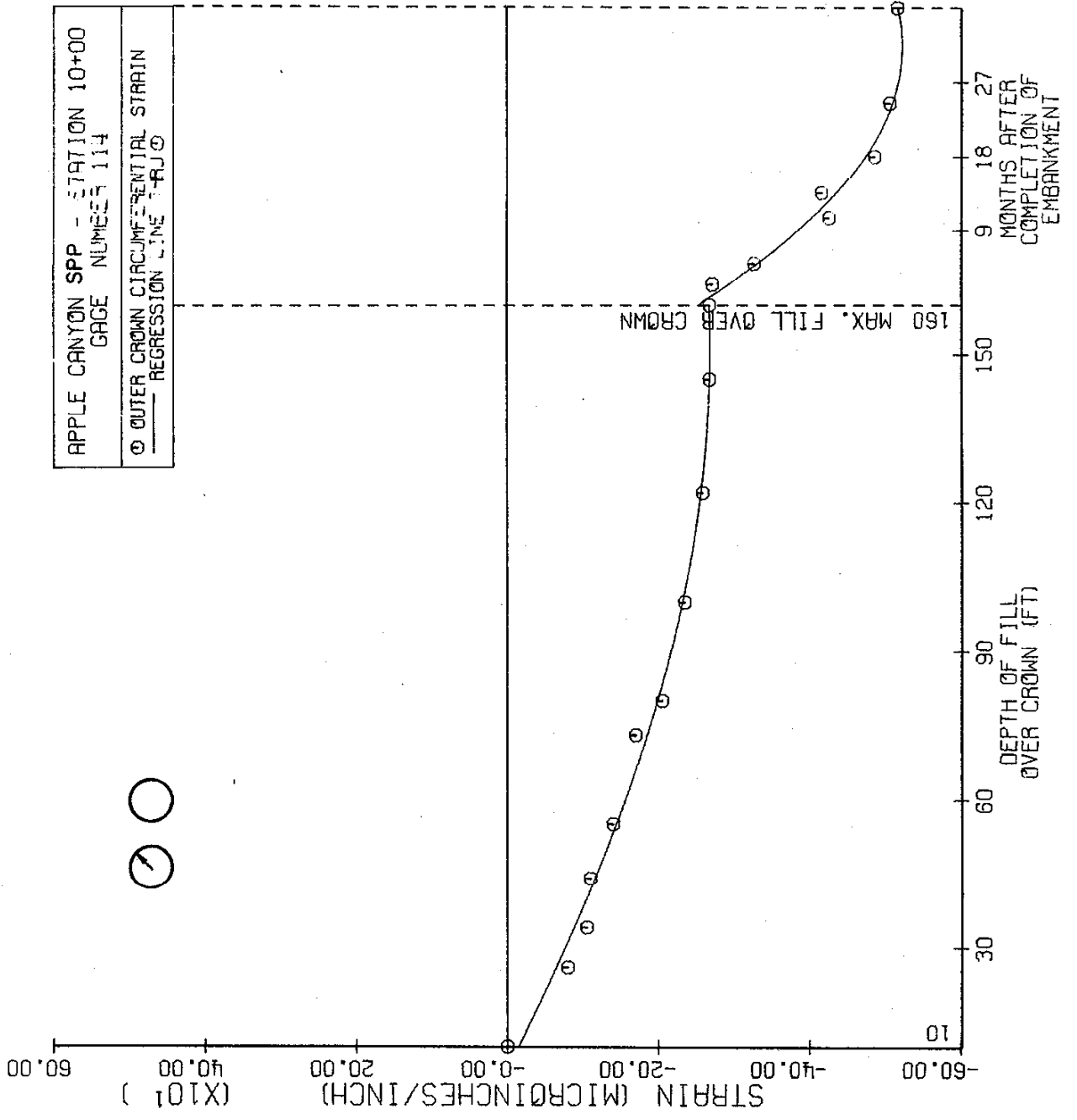


FIGURE 69

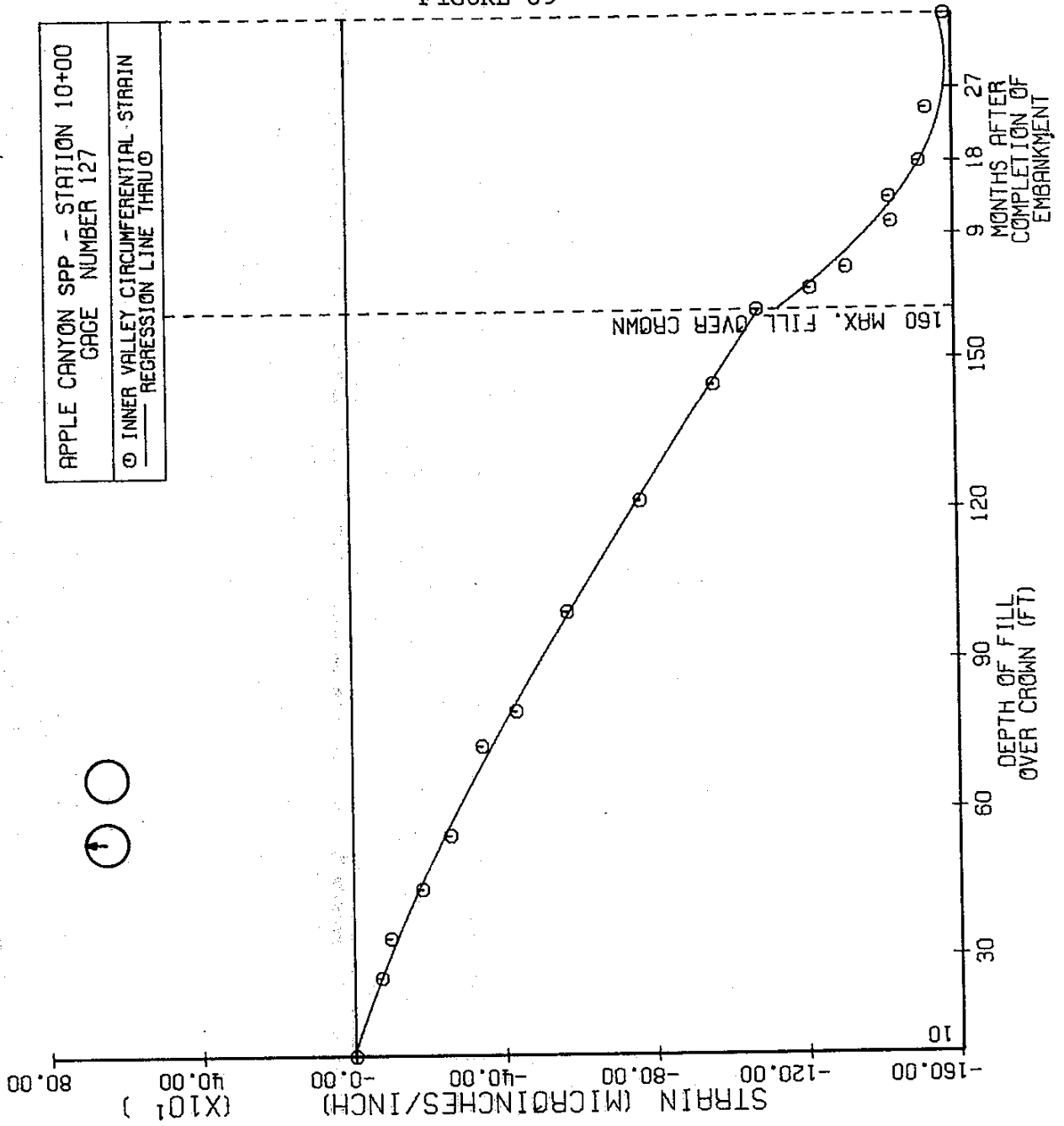


FIGURE 70

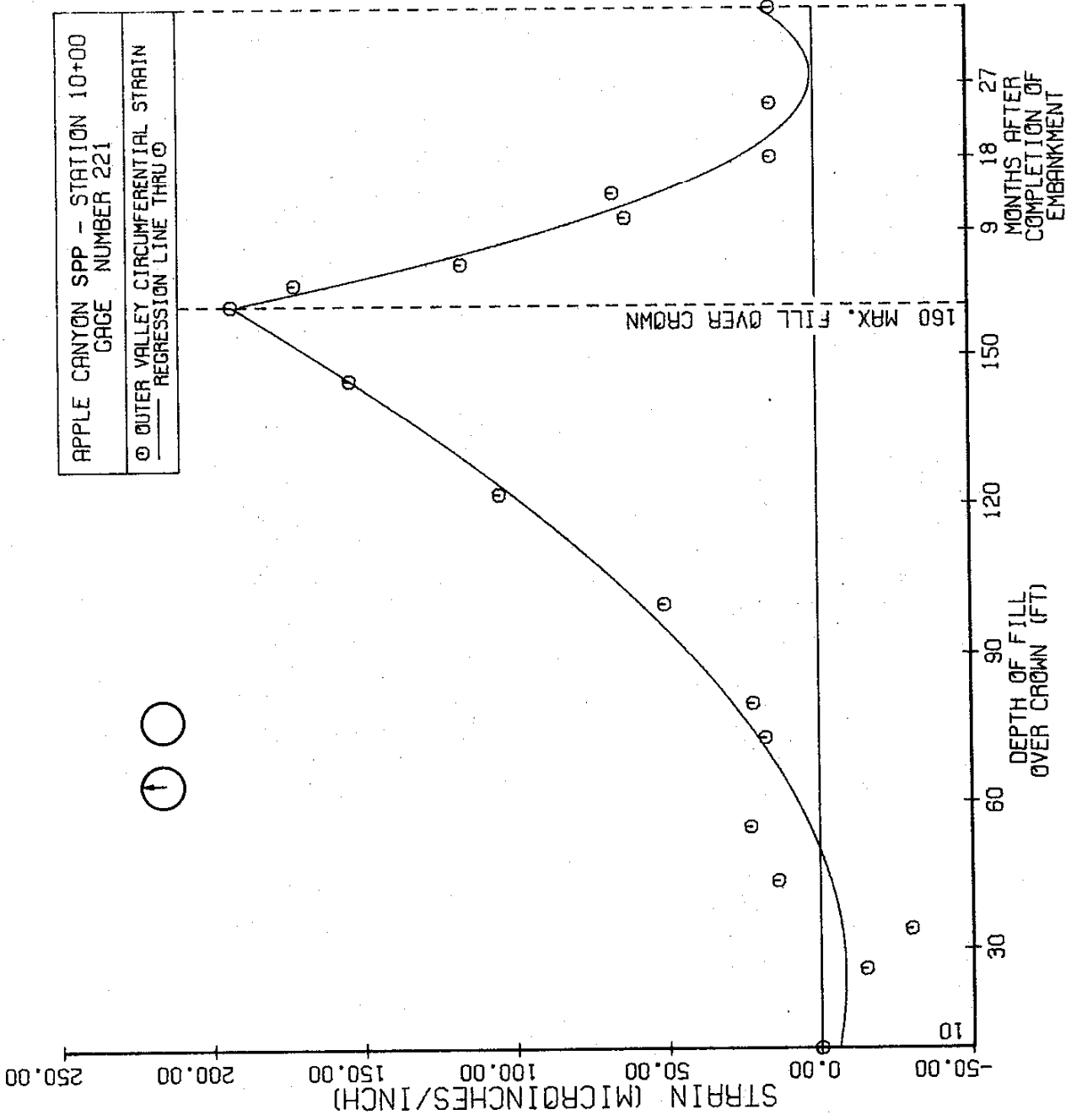


FIGURE 71

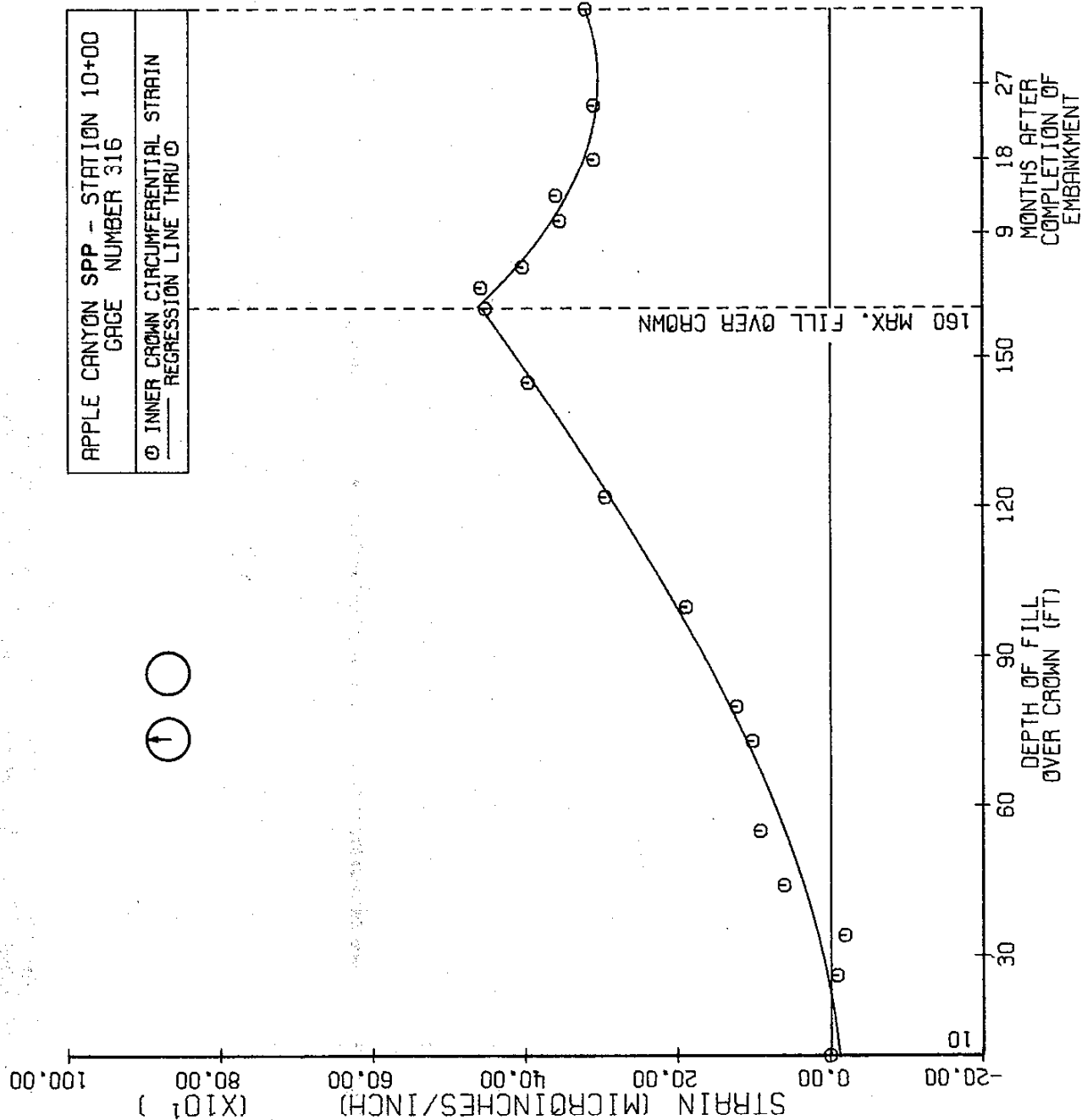


FIGURE 72

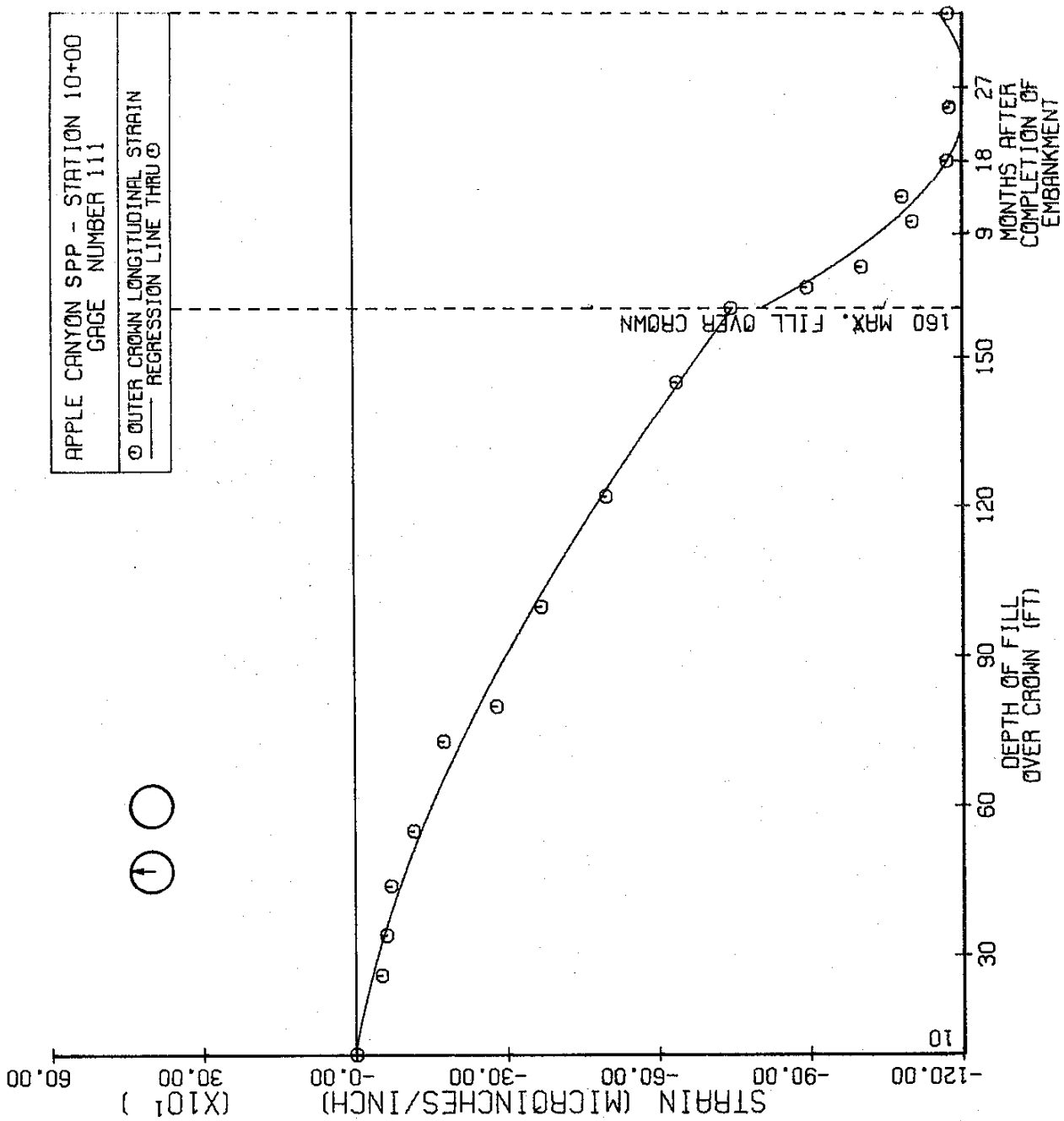


FIGURE 73

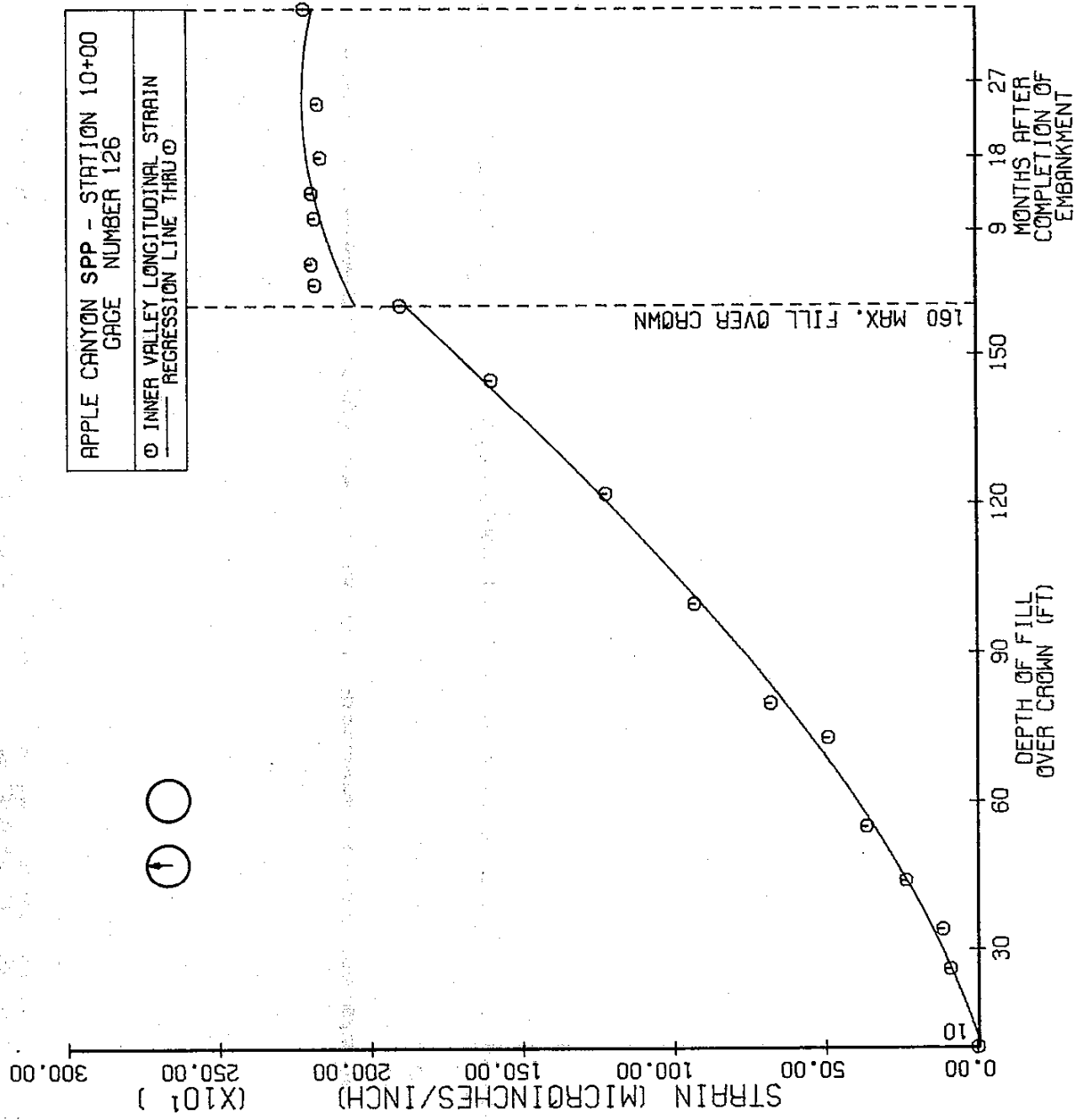


FIGURE 74

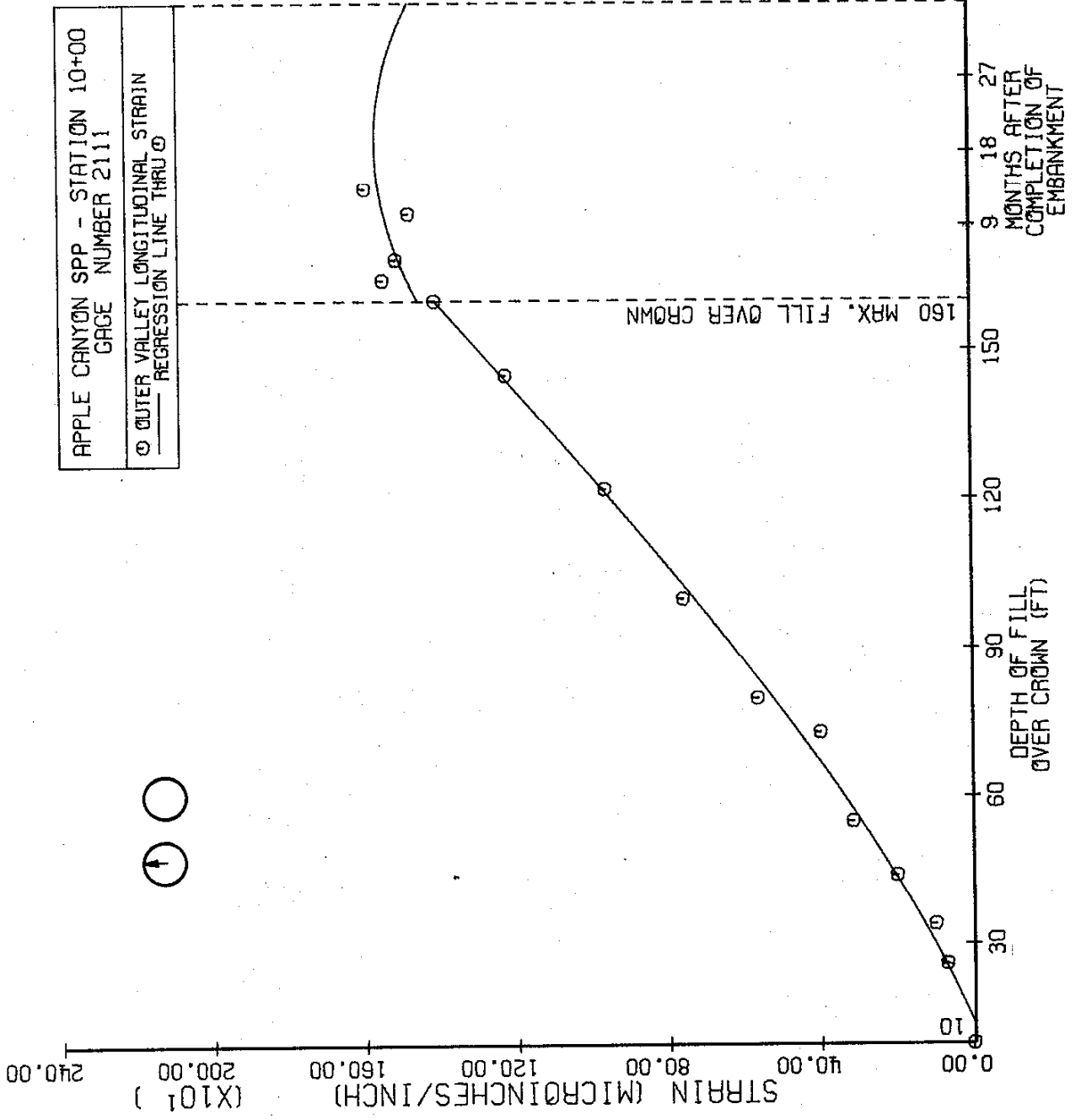


FIGURE 75

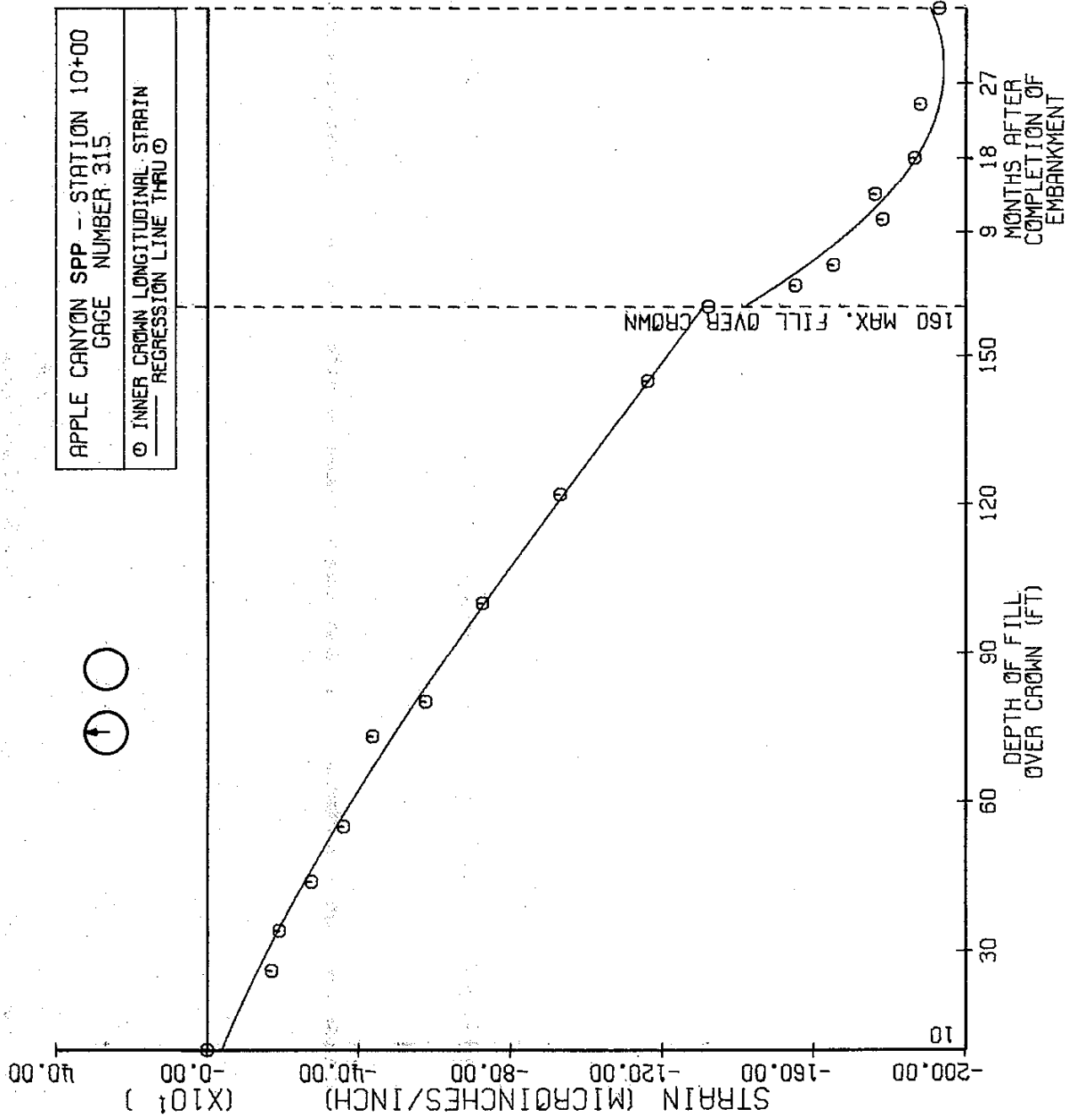


FIGURE 76

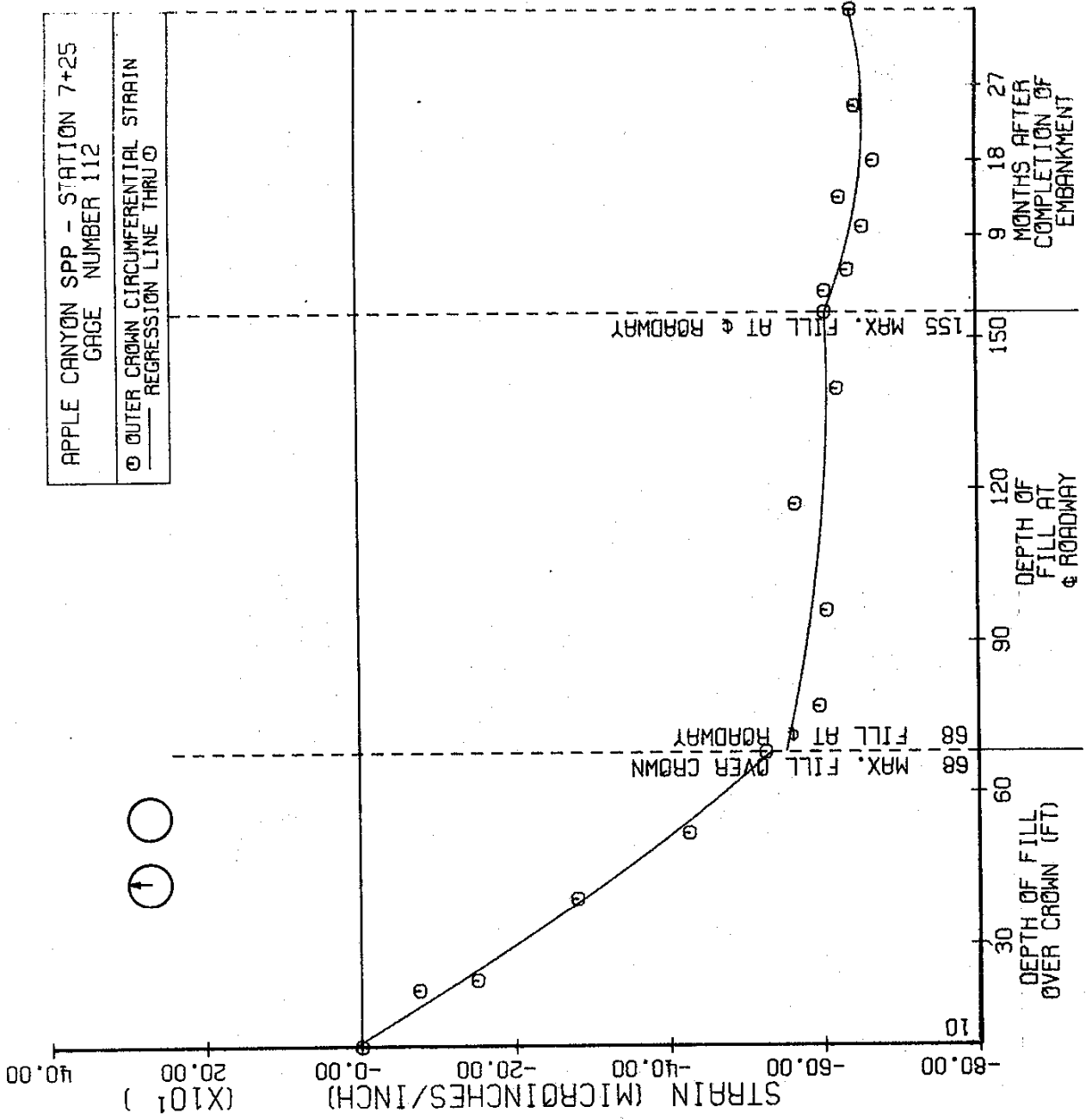


FIGURE 77

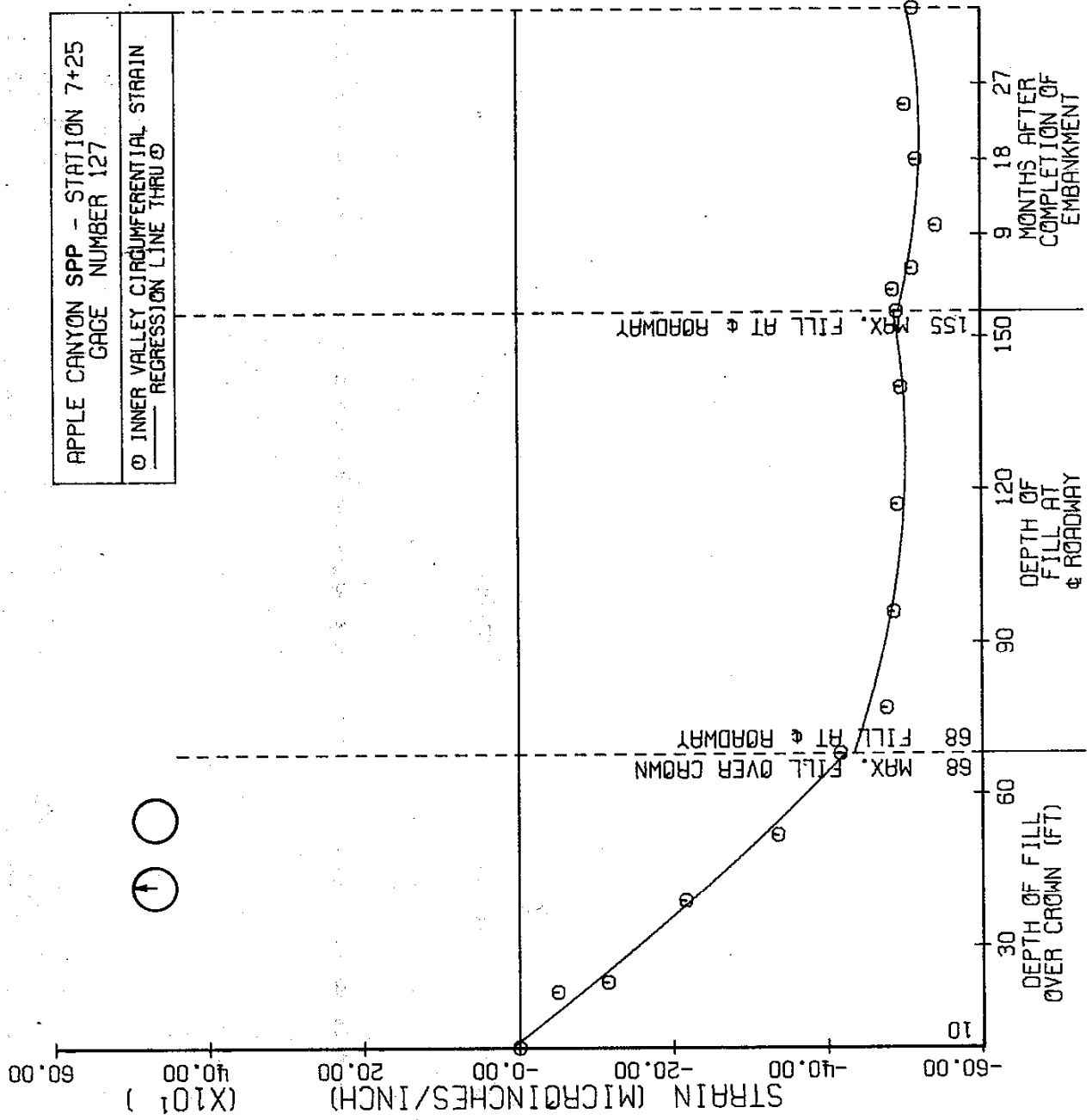


FIGURE 78

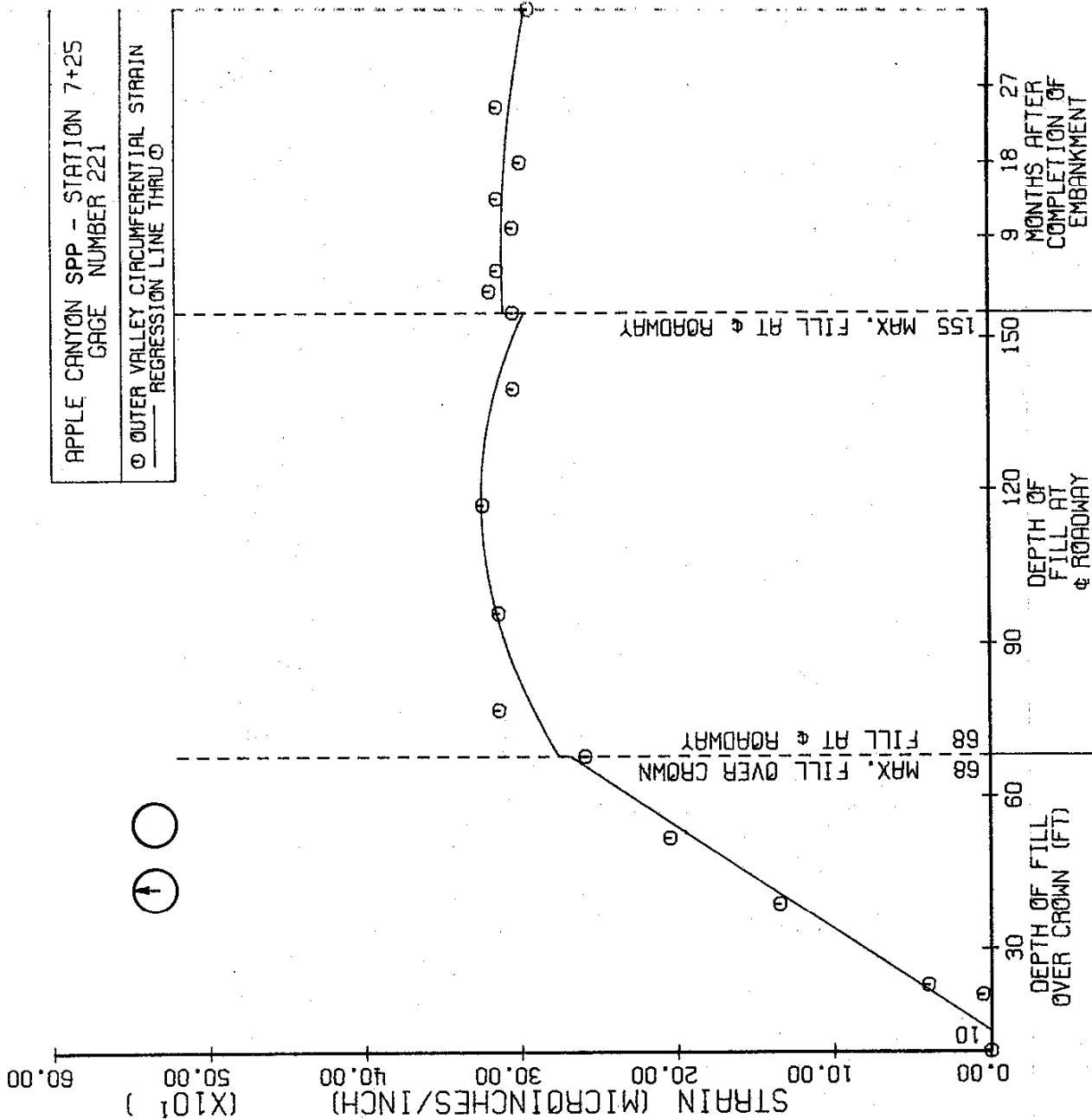


FIGURE 79

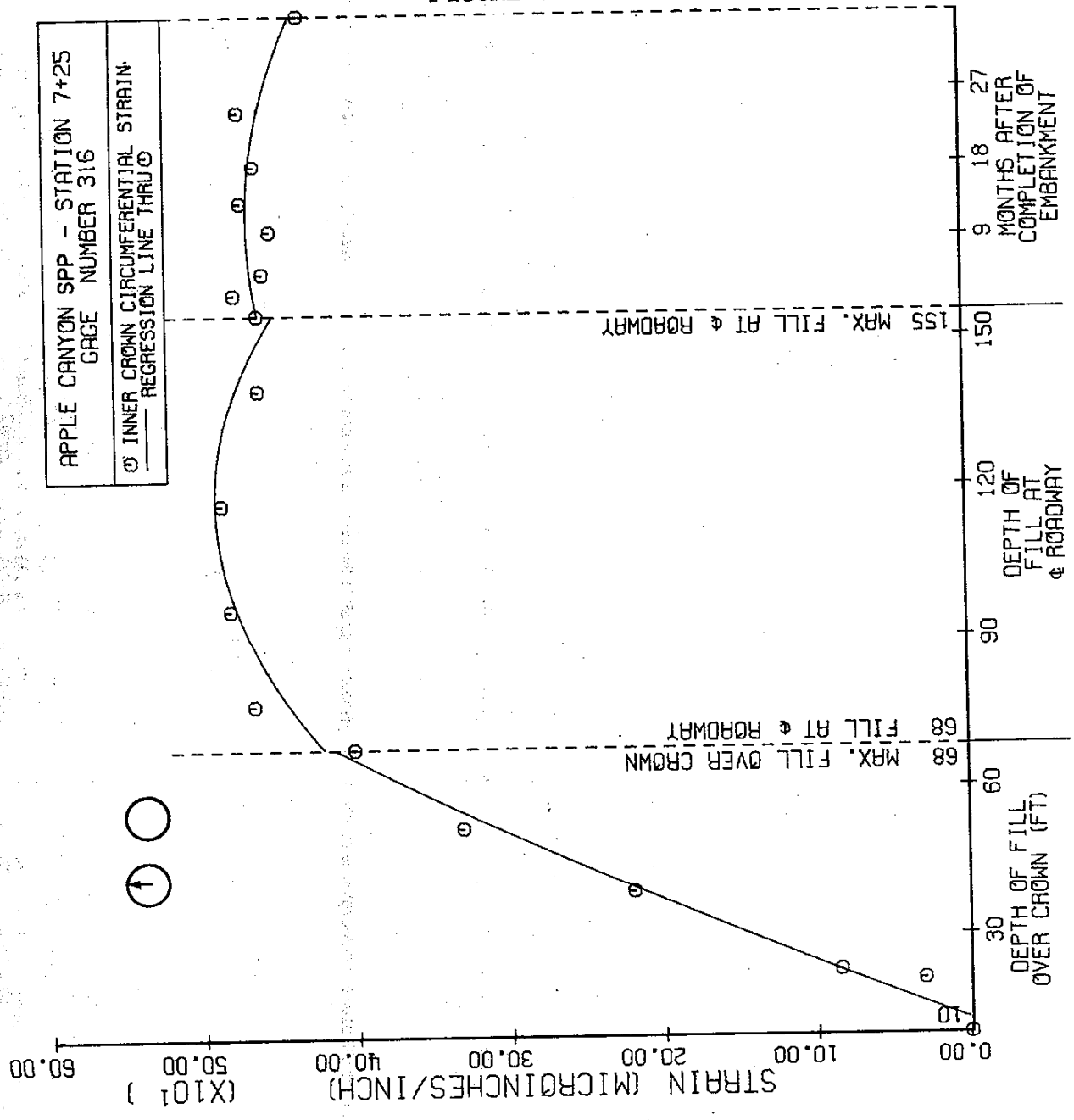


FIGURE 80

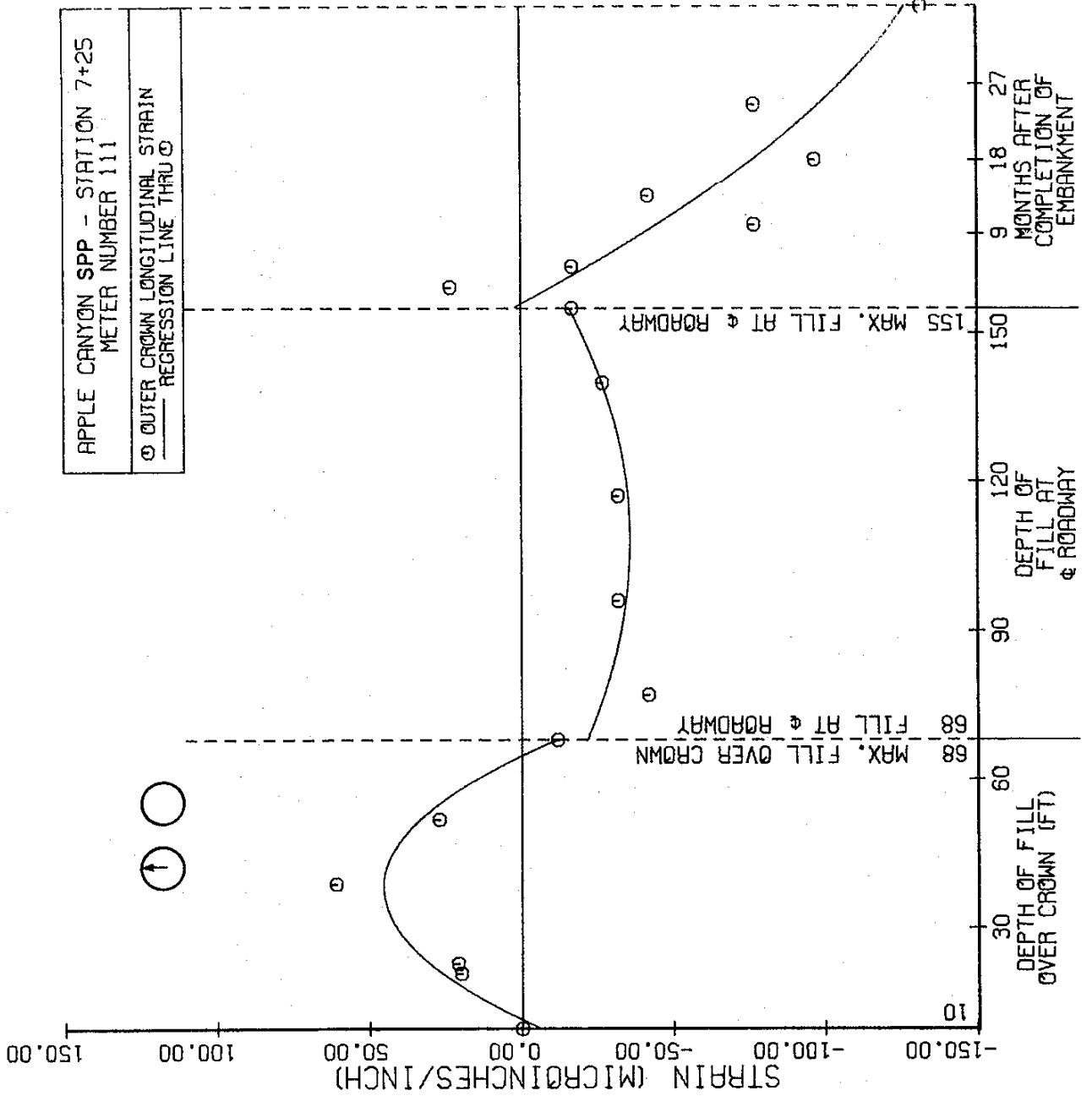


FIGURE 81

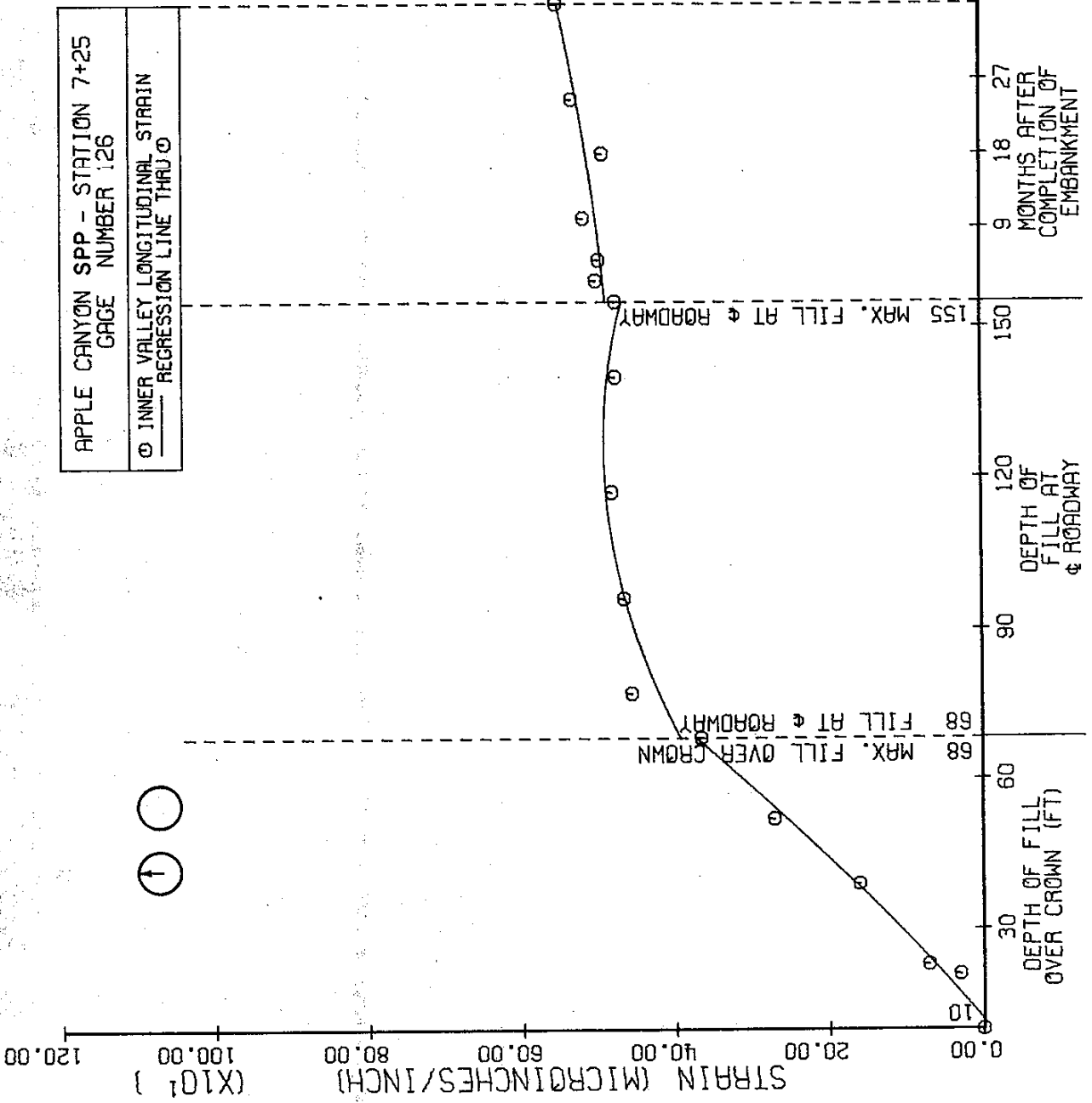


FIGURE 82

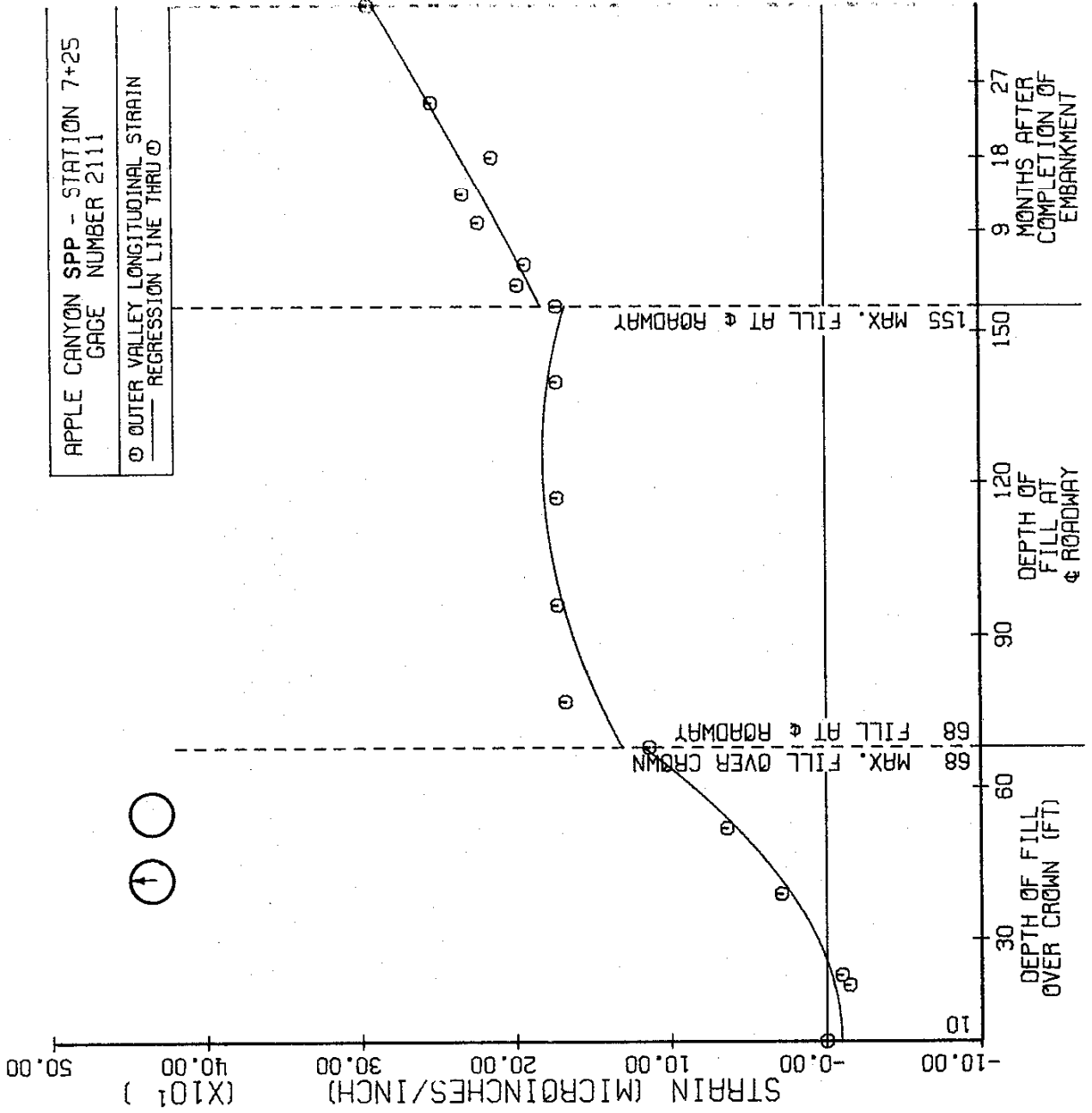


FIGURE 83

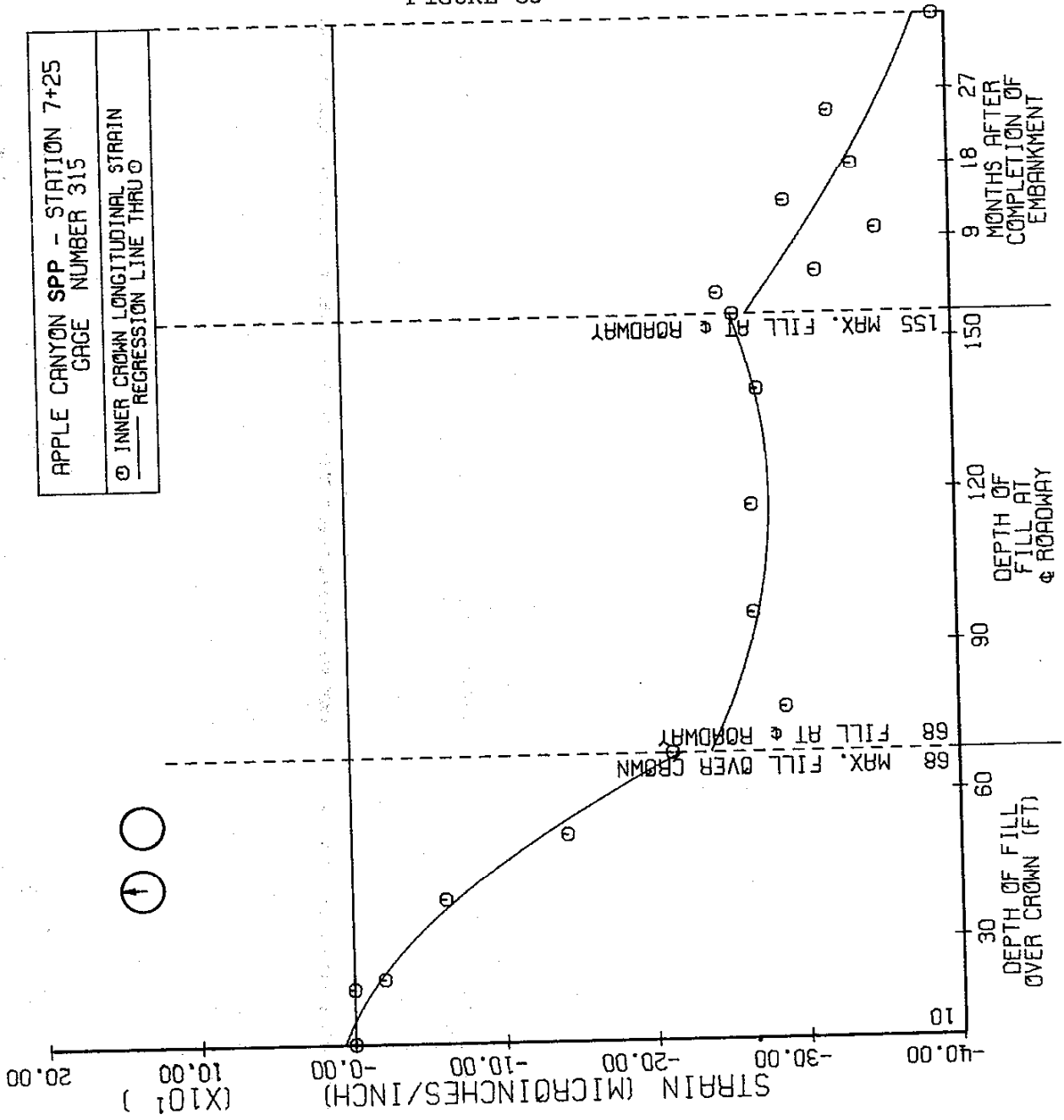
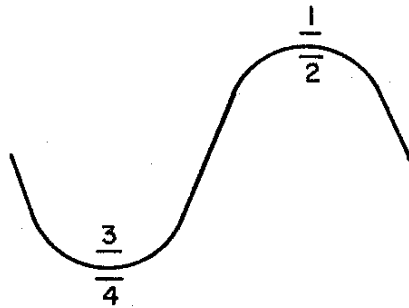


FIGURE 84

APPLE CANYON SPP
CONVERSION OF STRAIN TO STRESS



Stresses

$$\text{Longitudinal: } f_L = \frac{E}{1-\mu^2} (\epsilon_L + \mu \epsilon_C)$$

$$\text{Circumferential: } f_C = \frac{E}{1-\mu^2} (\epsilon_C + \mu \epsilon_L)$$

Quasi - theoretical moments and thrusts

$$f_T = \frac{1}{2} (f_1 + f_2)$$

$$f_B = \frac{1}{2} (f_3 + f_4)$$

$$f_b = \frac{1}{2} (f_T - f_B)$$

$$f_a = \frac{1}{2} (f_T + f_B)$$

$$M = \frac{f_b l}{C}$$

$$T = f_a A$$

FIGURE 85

APPLE CANYON SPP
MARSTON'S THEORY
POSITIVE PROJECTING CONDUIT

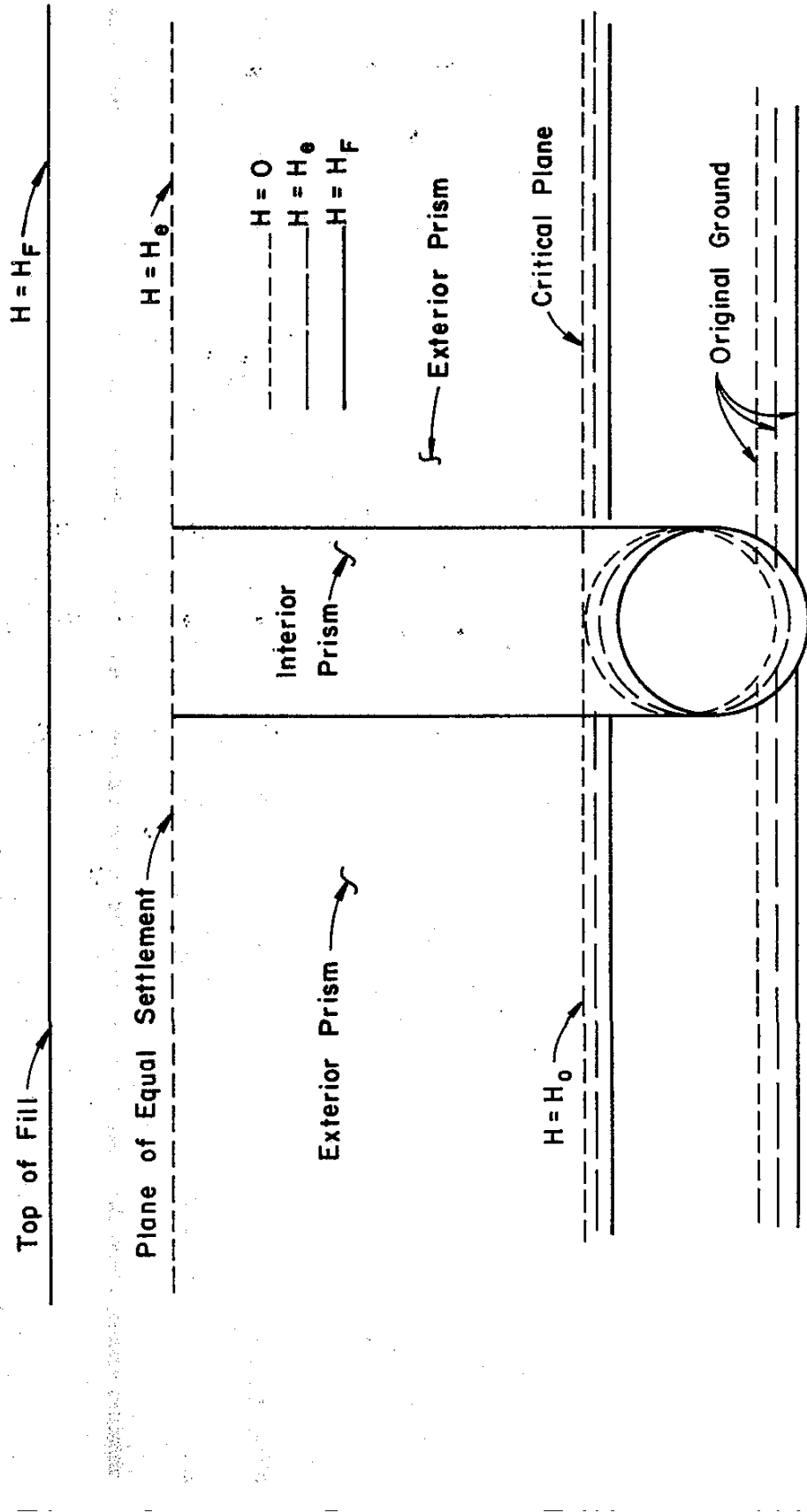


FIGURE 86

APPLE CANYON SPP
MARSTON'S THEORY
NEGATIVE PROJECTING CONDUIT

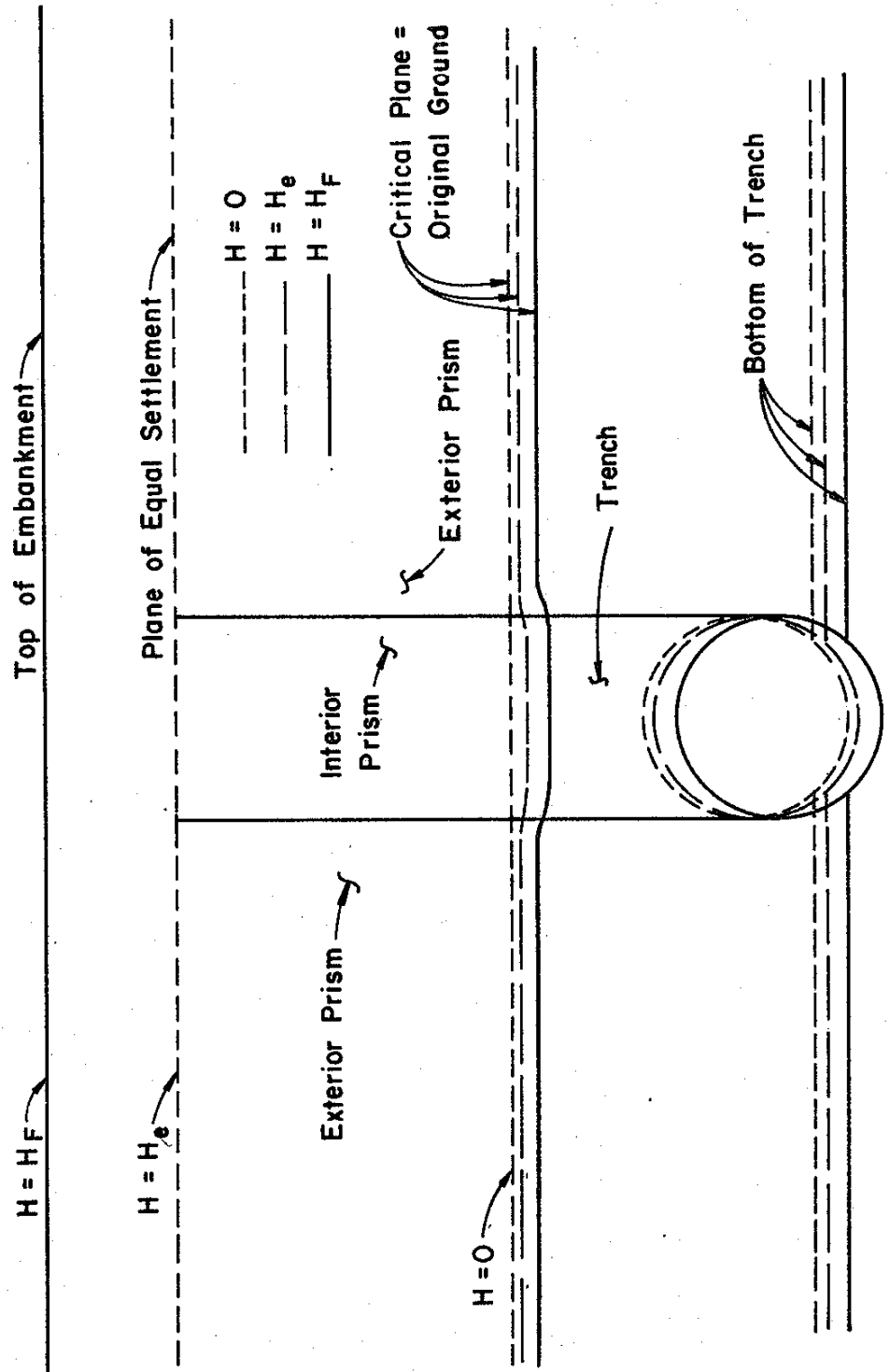


FIGURE 87

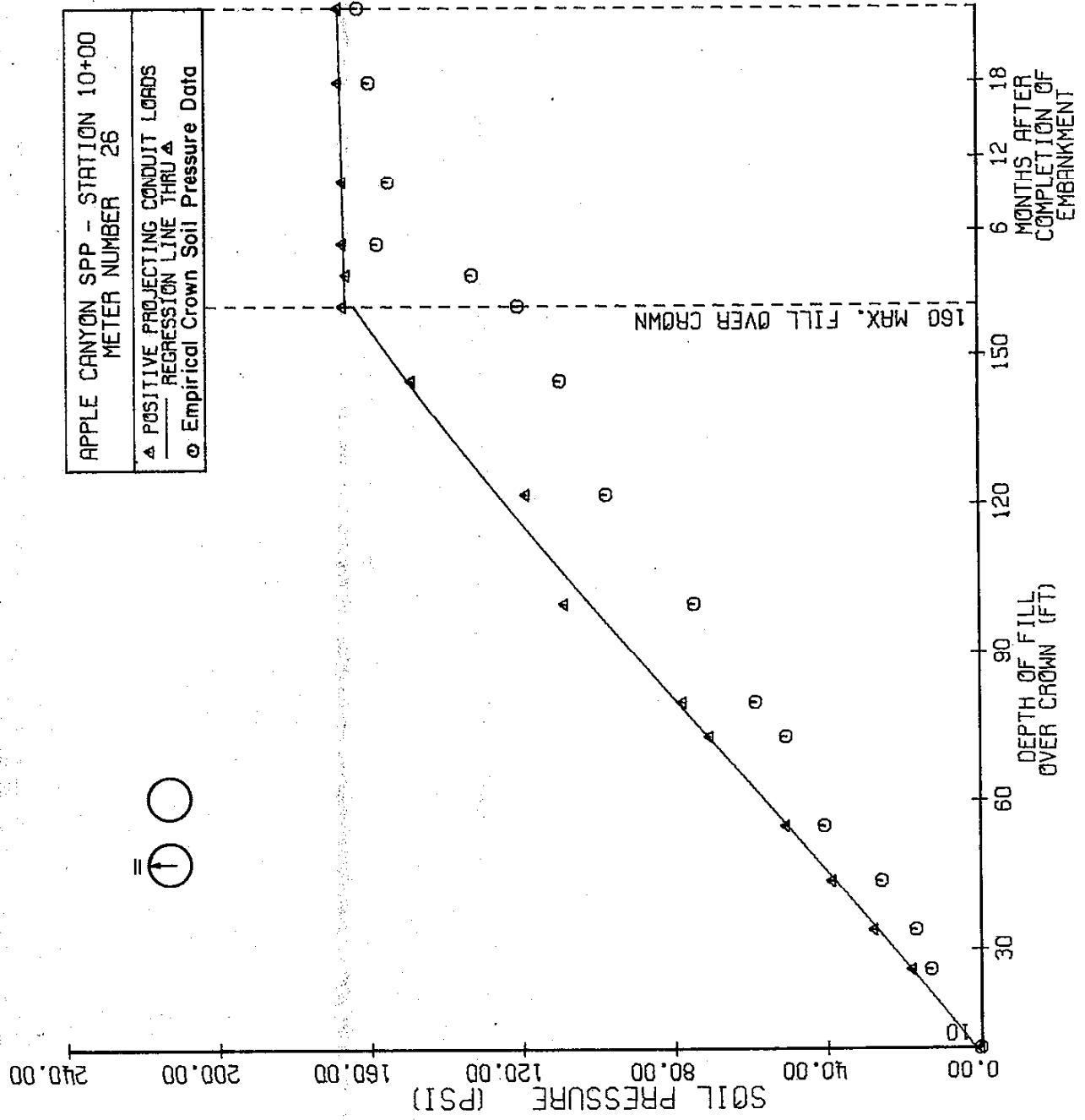
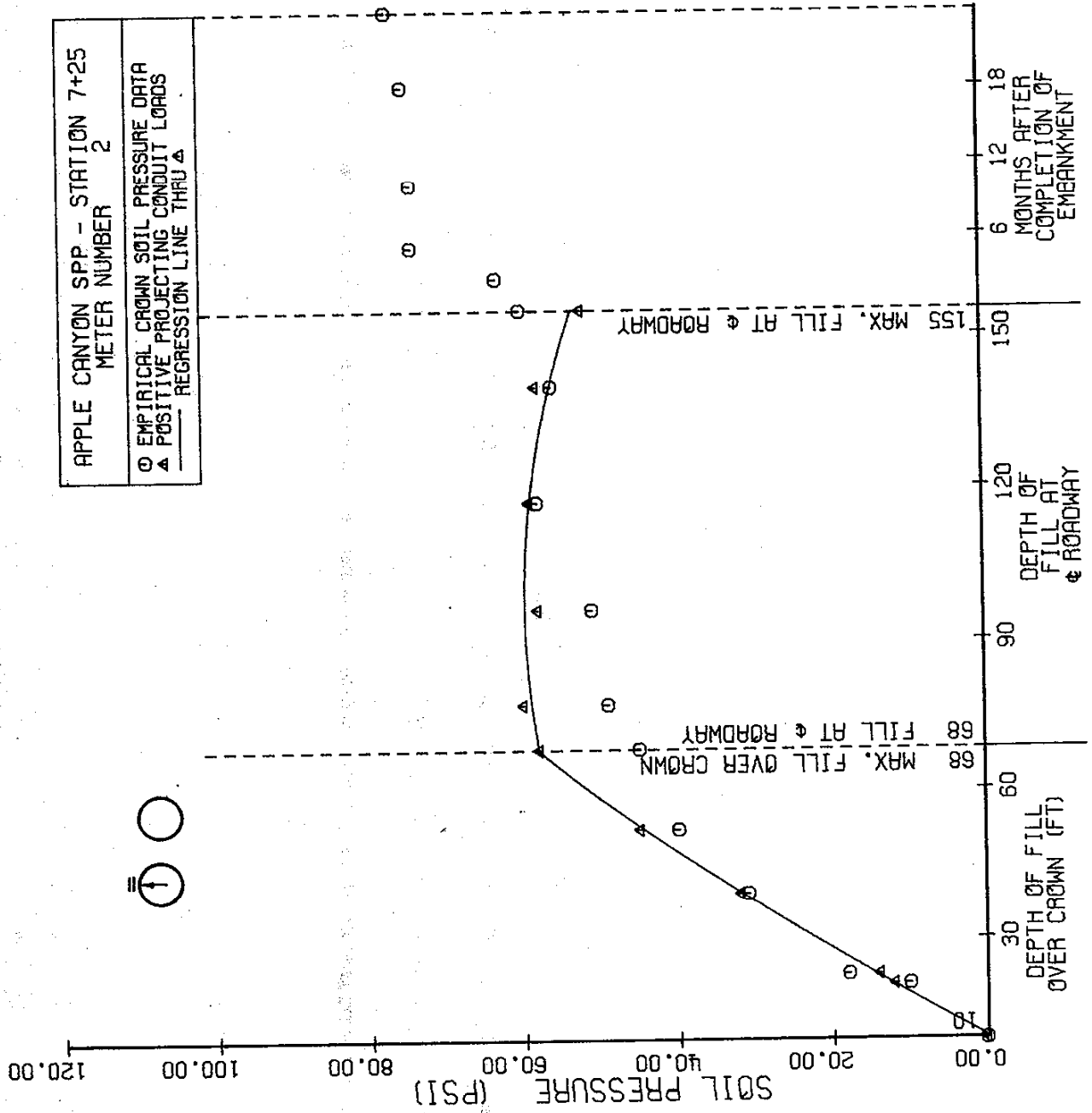


FIGURE 89



APPLE CANYON SPP - STATION 7+25
 METER NUMBER 2

○ EMPIRICAL CROWN SOIL PRESSURE DATA
 ▲ POSITIVE PROJECTING CONDUIT LOADS
 — REGRESSION LINE THRU ▲

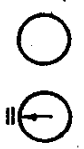


FIGURE 90

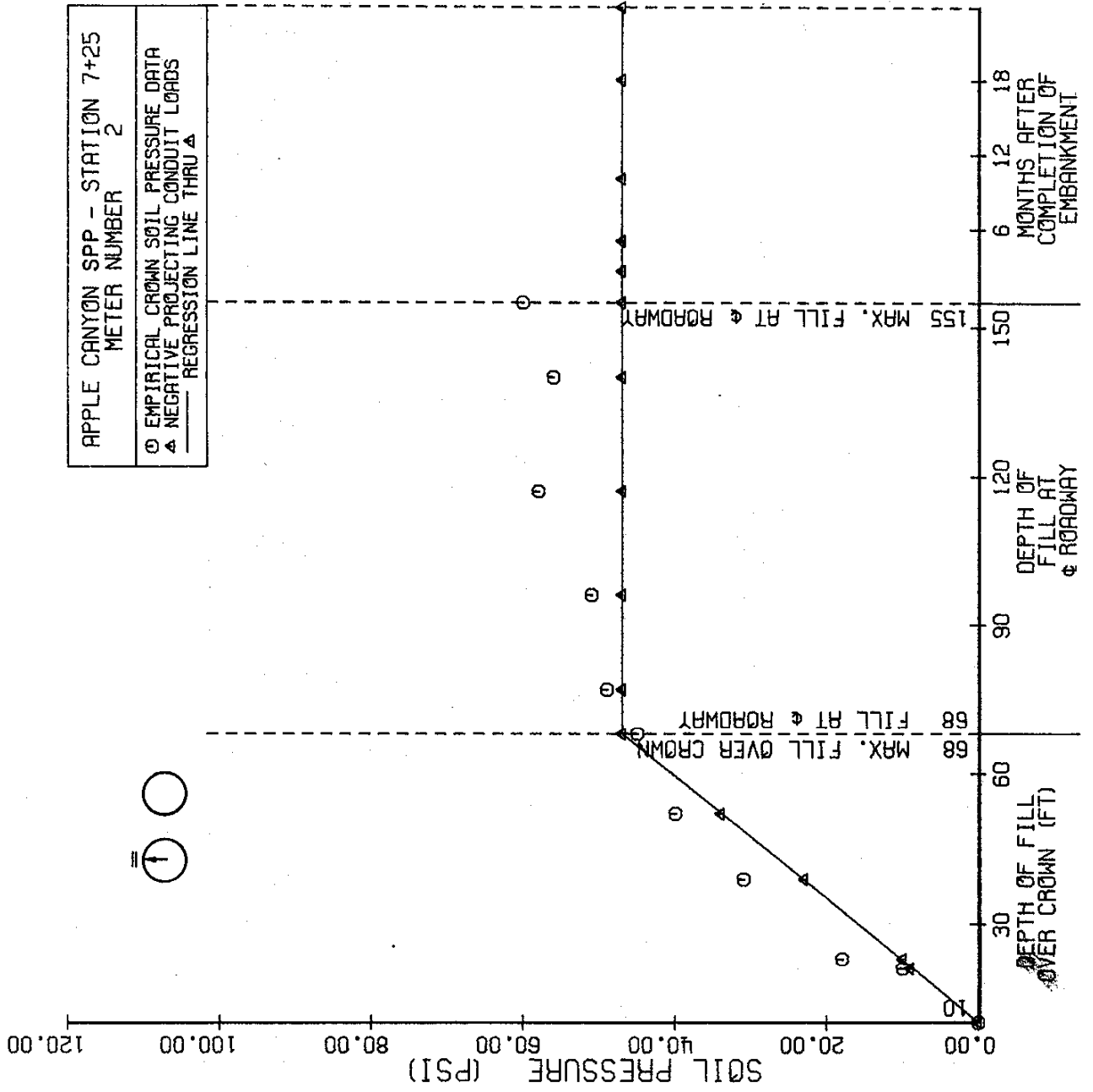


FIGURE 91

APPLE CANYON SPP
SPANGLER'S ASSUMPTION FOR
PRESSURE DISTRIBUTION ON A
FLEXIBLE CULVERT

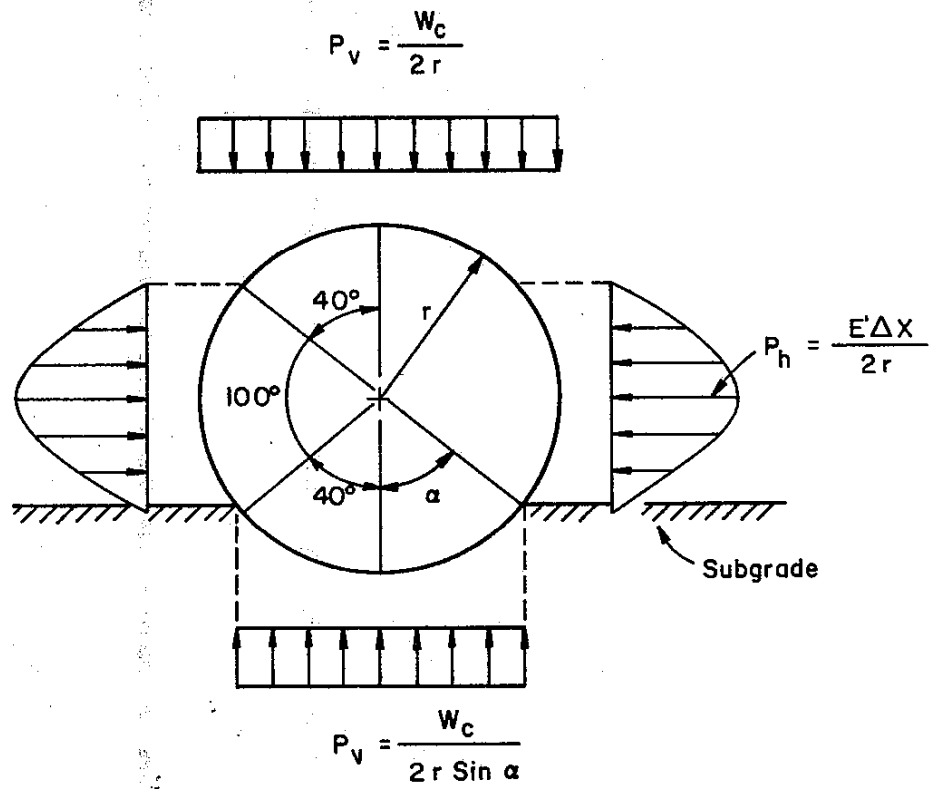


FIGURE 92

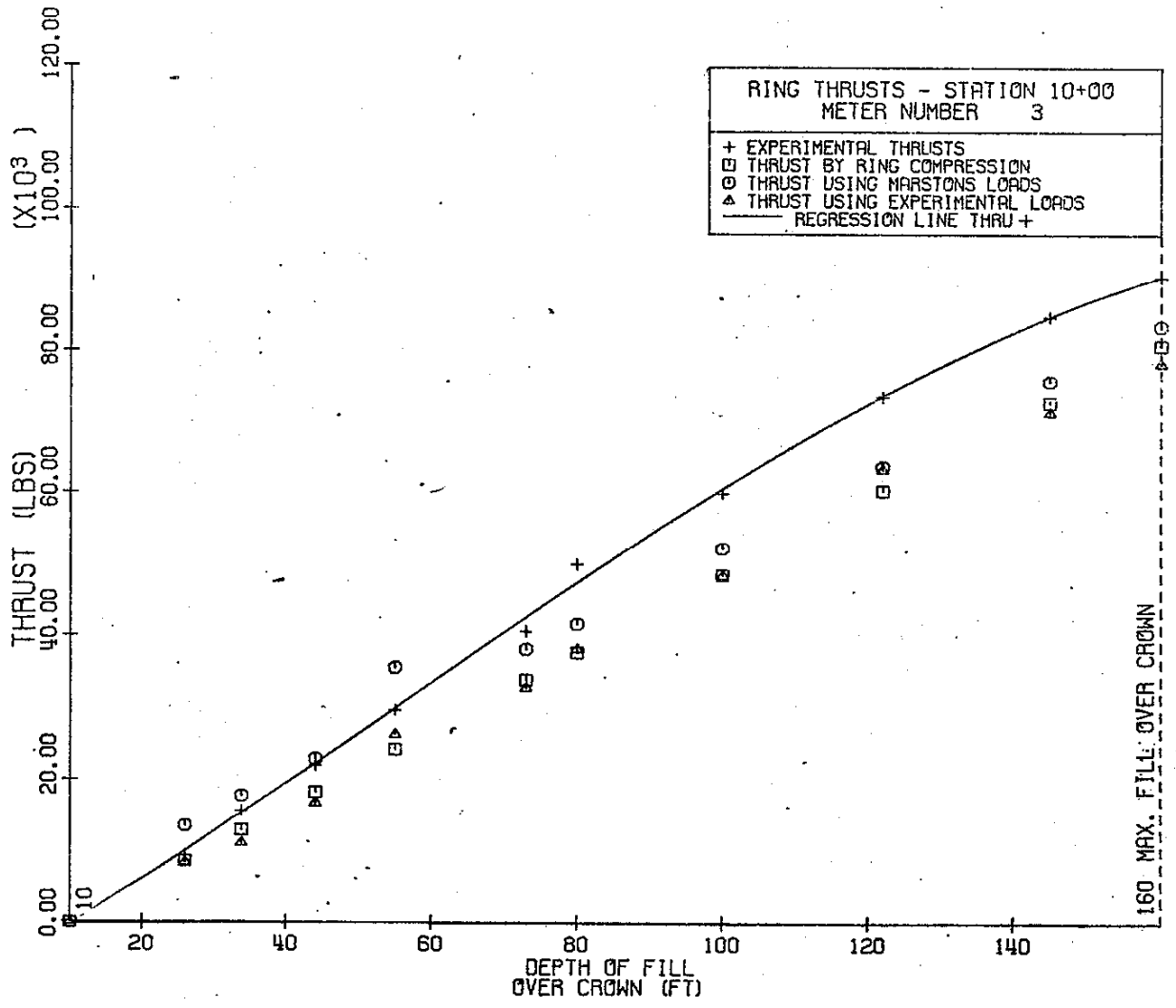


FIGURE 93

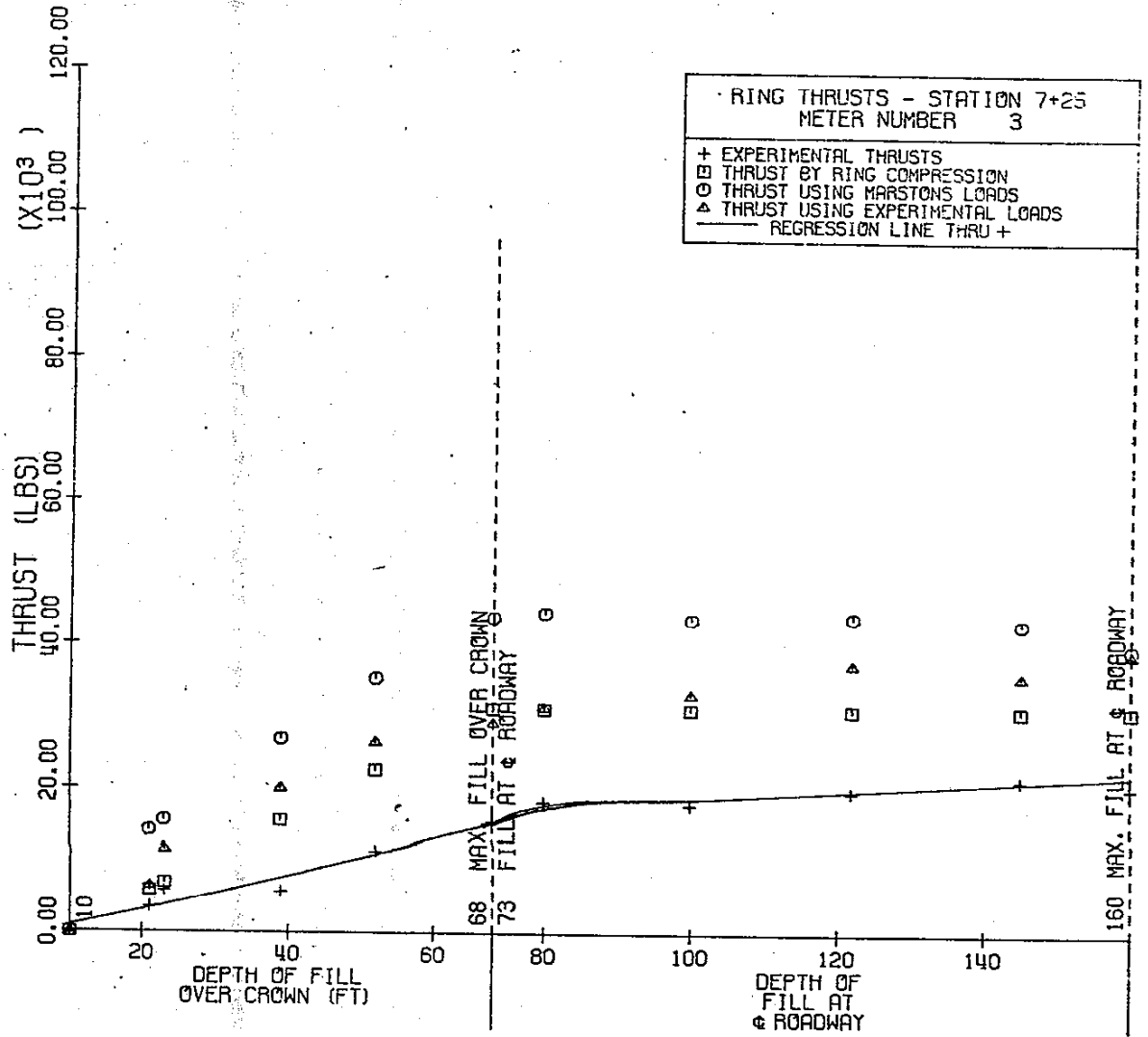
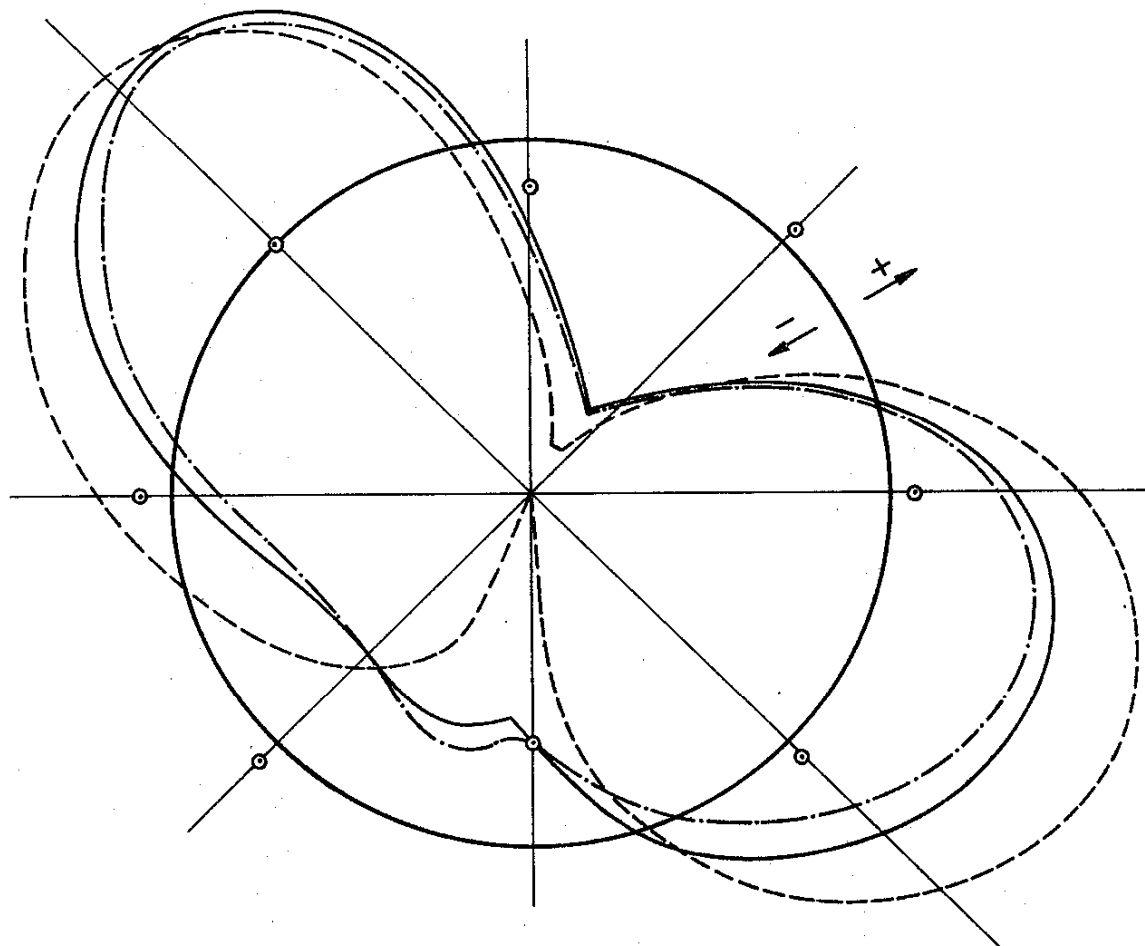


FIGURE 94

APPLE CANYON SPP
NEUTRAL POINT ANALYSIS
MOMENT PROFILE
FILL HEIGHT = 160'



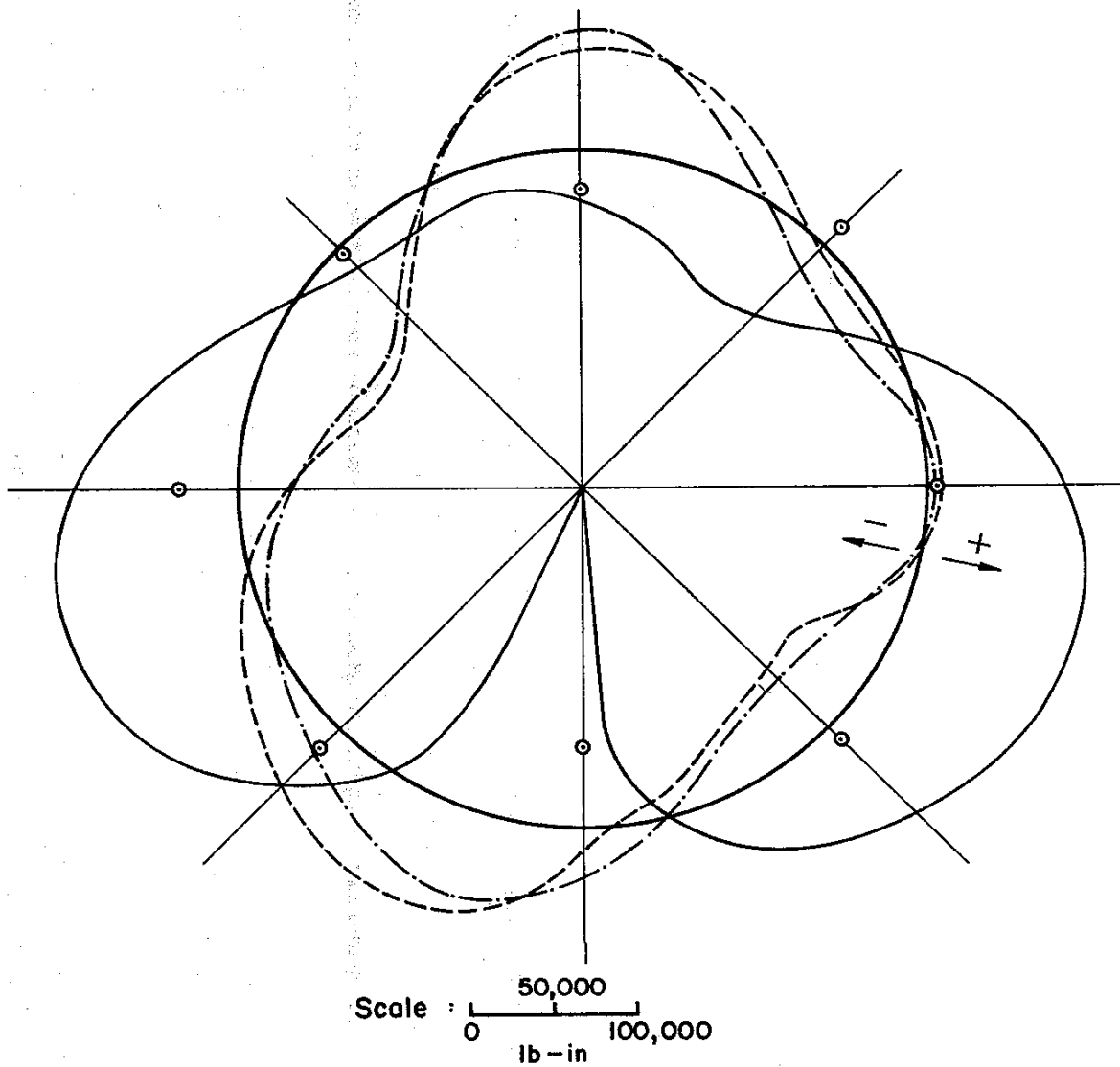
Scale : $\frac{50,000}{100,000}$
0 lb-in

LEGEND

- 1 Layer analysis without approximate lateral force
- 1 Layer analysis with approximate lateral force
- · - · - 9 Layer analysis with approximate lateral force
- ⊙ Quasi-theoretical Moment

FIGURE 95

APPLE CANYON SPP
NEUTRAL POINT ANALYSIS
MOMENT PROFILE
FILL HEIGHT = 68'



LEGEND

- 1 Layer analysis without approximate lateral force
- 1 Layer analysis with approximate lateral force
- · - · 4 Layer analysis with approximate lateral force
- Quasi-theoretical Moment

FIGURE 96

APPLE CANYON SPP
FINITE ELEMENT MESH
STATION 10+00

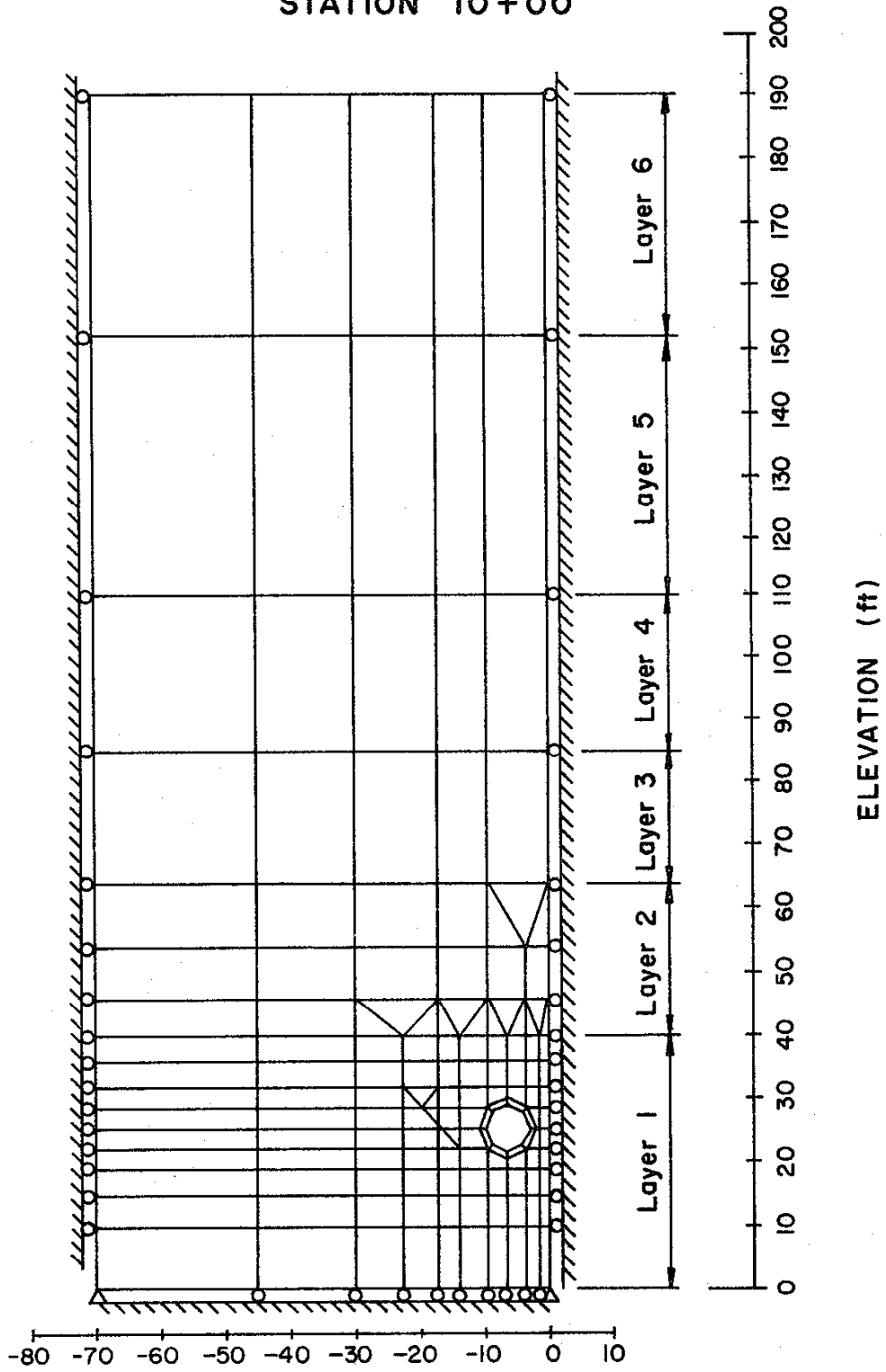


FIGURE 97

APPLE CANYON SPP
FINITE ELEMENT ANALYSIS
PRESSURE PROFILE
FILL HEIGHT = 160'

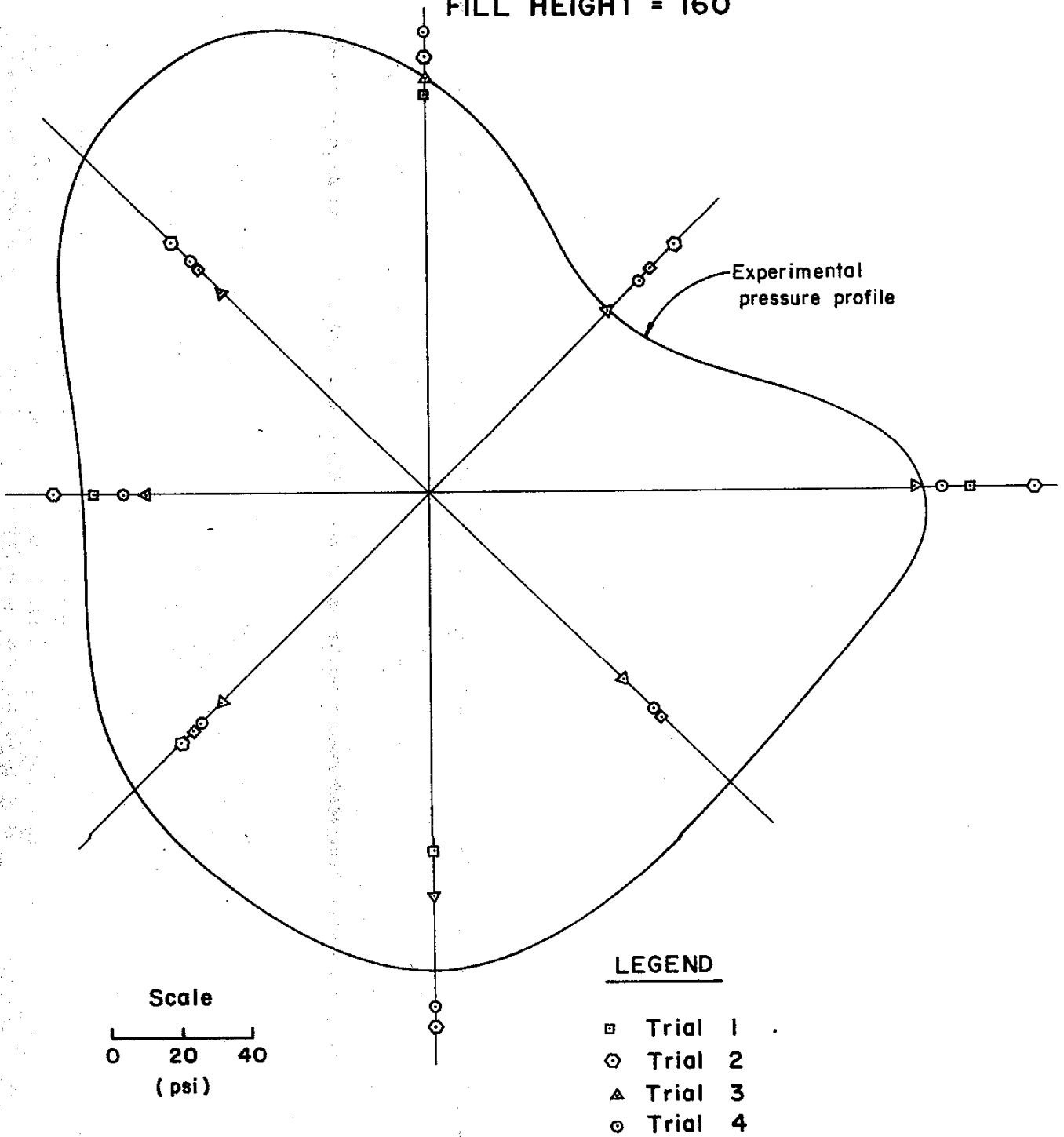
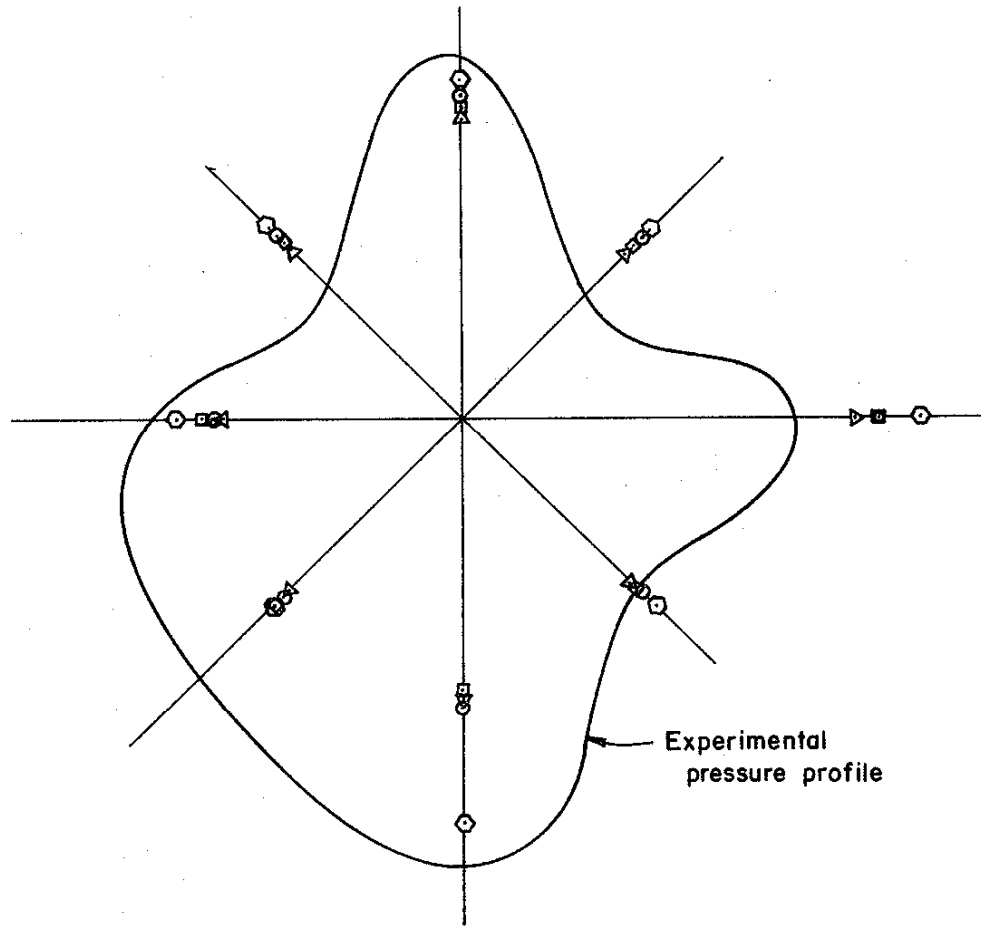
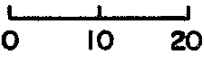


FIGURE 98

APPLE CANYON SPP
FINITE ELEMENT ANALYSIS
PRESSURE PROFILE
FILL HEIGHT = 52'



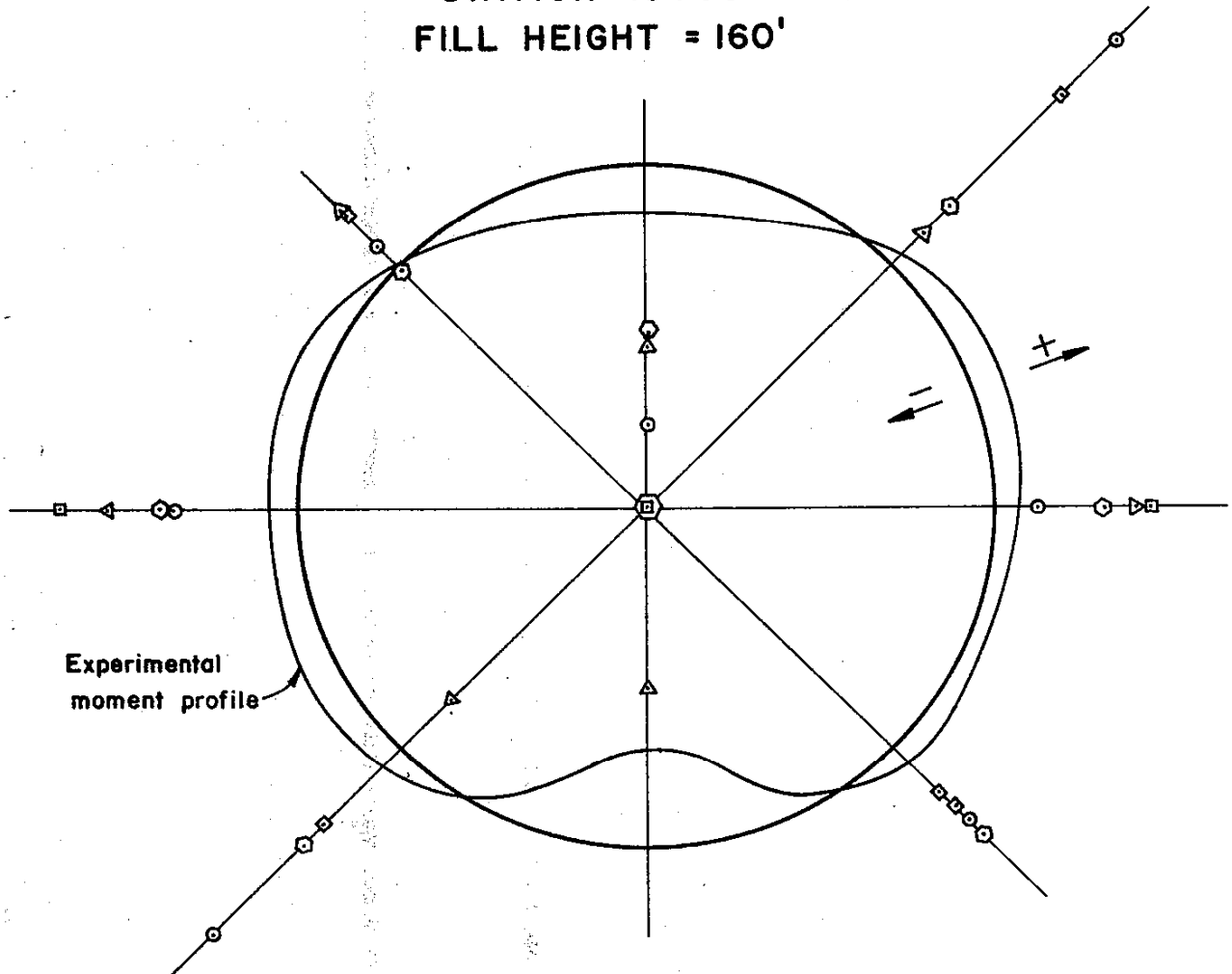
Scale : 
(psi)

LEGEND

- ▣ Trial 1
- Trial 2
- △ Trial 3
- ◇ Trial 4

FIGURE 99

APPLE CANYON SPP
FINITE ELEMENT ANALYSIS
MOMENT PROFILE
STATION 10+00
FILL HEIGHT = 160'



Experimental
moment profile

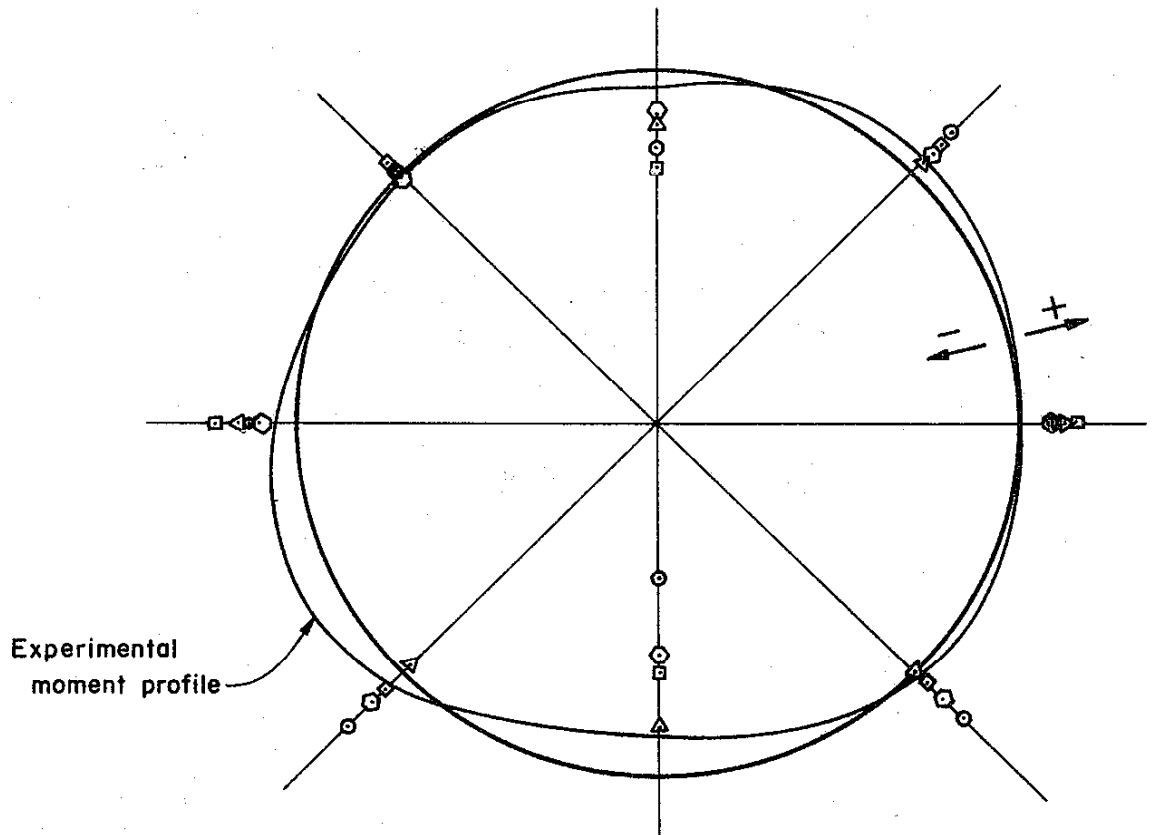
Scale : $\frac{0 \quad 10,000 \quad 20,000}{(lb-in)}$

LEGEND

- ▣ Trial 1
- ⊙ Trial 2
- △ Trial 3
- Trial 4

FIGURE 100

APPLE CANYON SPP
FINITE ELEMENT ANALYSIS
MOMENT PROFILE
STATION 7+25
FILL HEIGHT = 52'



Scale : $\frac{0}{10,000} \frac{20,000}{(lb-in)}$

LEGEND

- ▣ Trial 1
- ⊙ Trial 2
- △ Trial 3
- ⊖ Trial 4

FIGURE 101

INSTALLATION AT CHADD CREEK OF 114" x 598' PIPE CULVERT

01-HUM-101 39.2/47.3

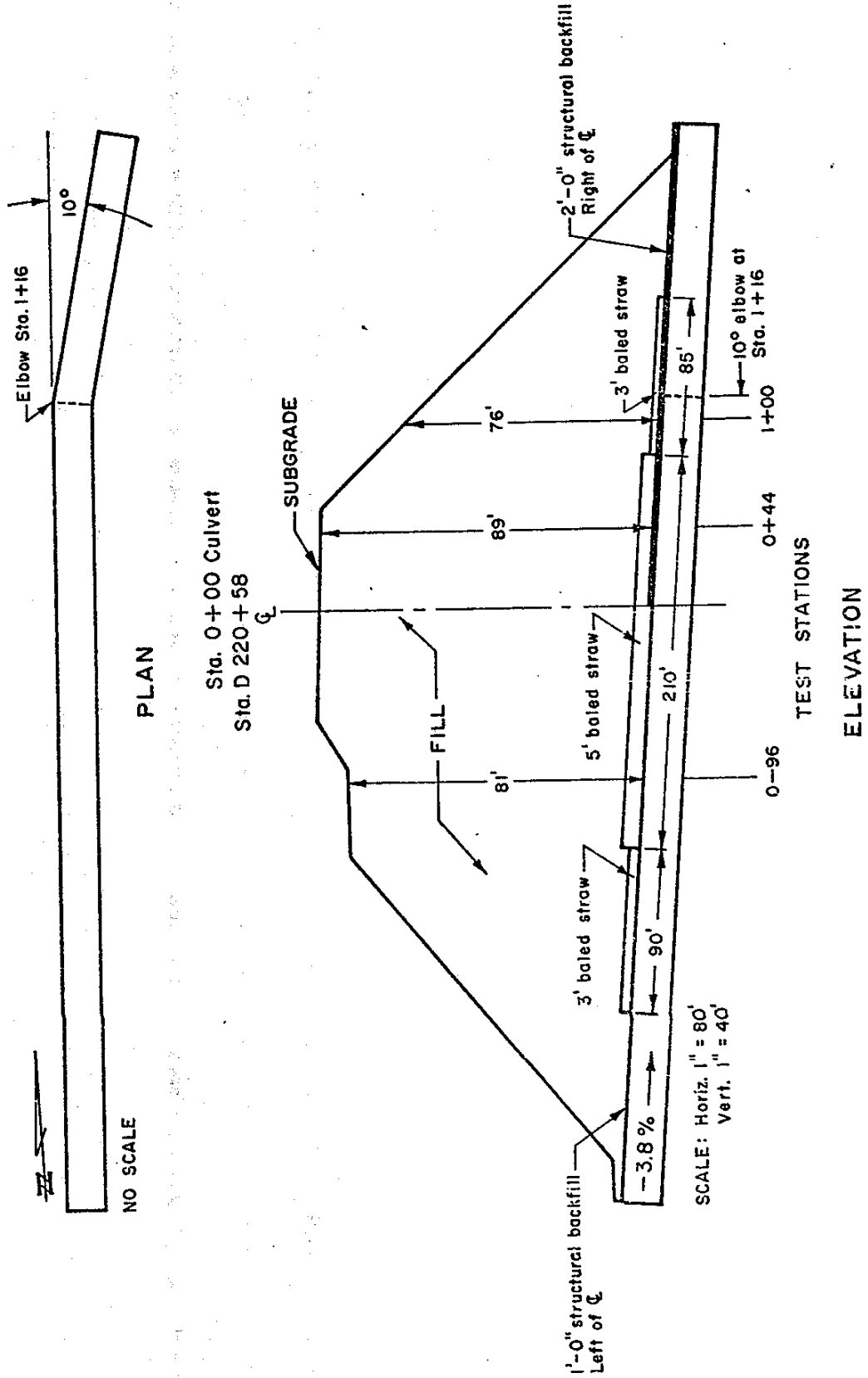


FIGURE 102

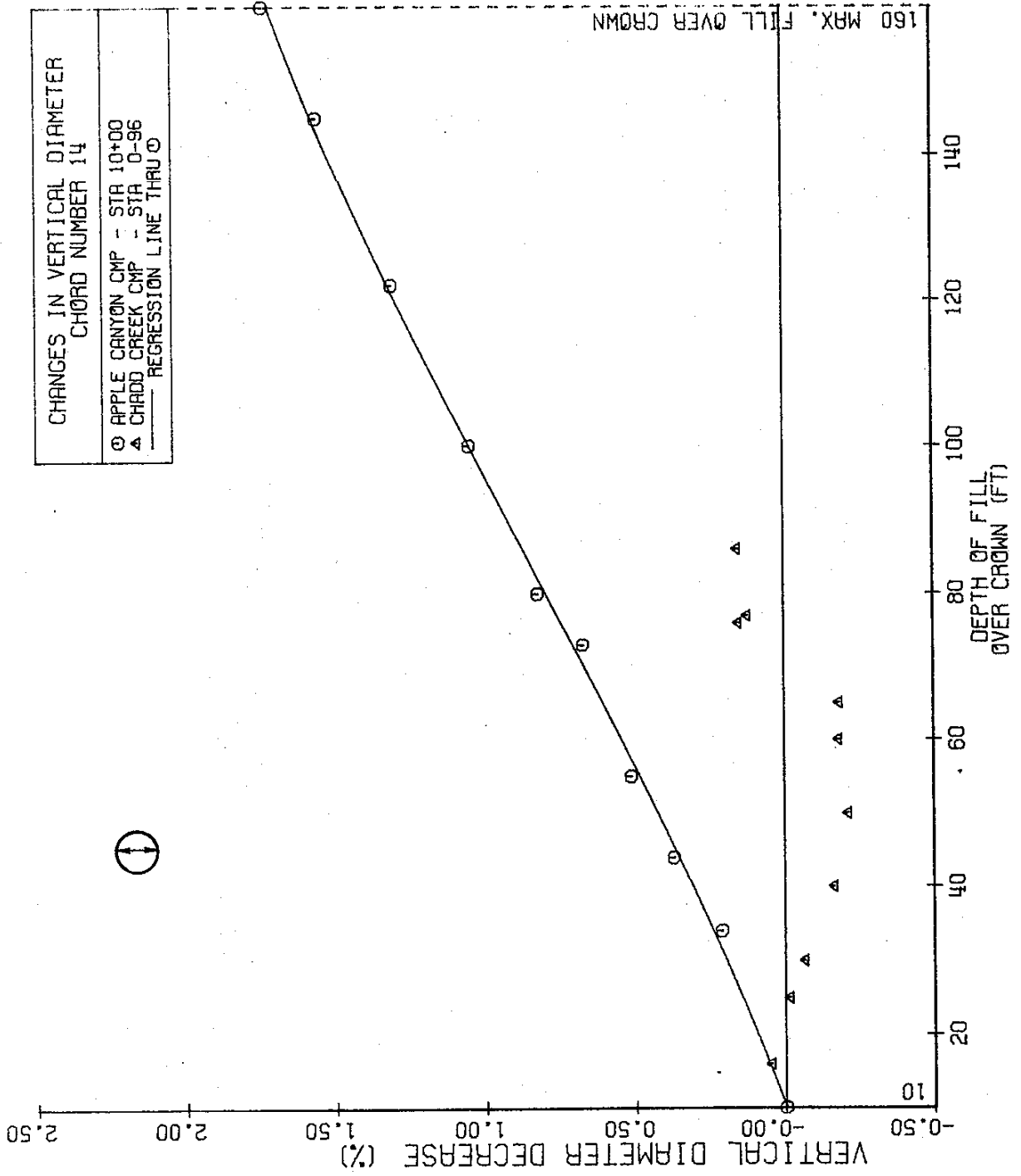
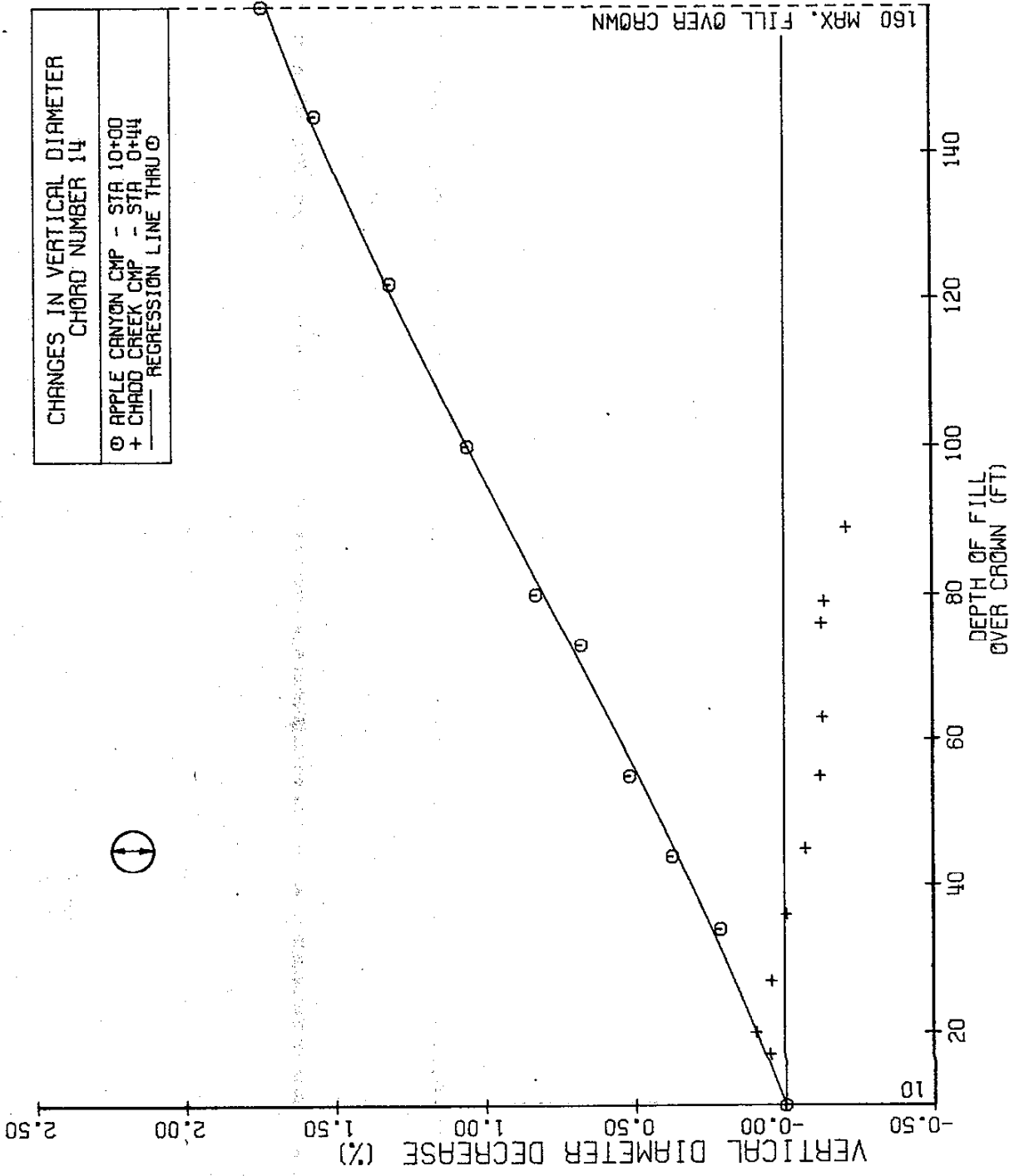


FIGURE 103



CHANGES IN VERTICAL DIAMETER
CHORD NUMBER 14

○ APPLE CANYON CMP - STA 10+00
+ CHADD CREEK CMP - STA 0+44
— REGRESSION LINE THRU ○



160 MAX. FILL OVER CROWN

FIGURE 104

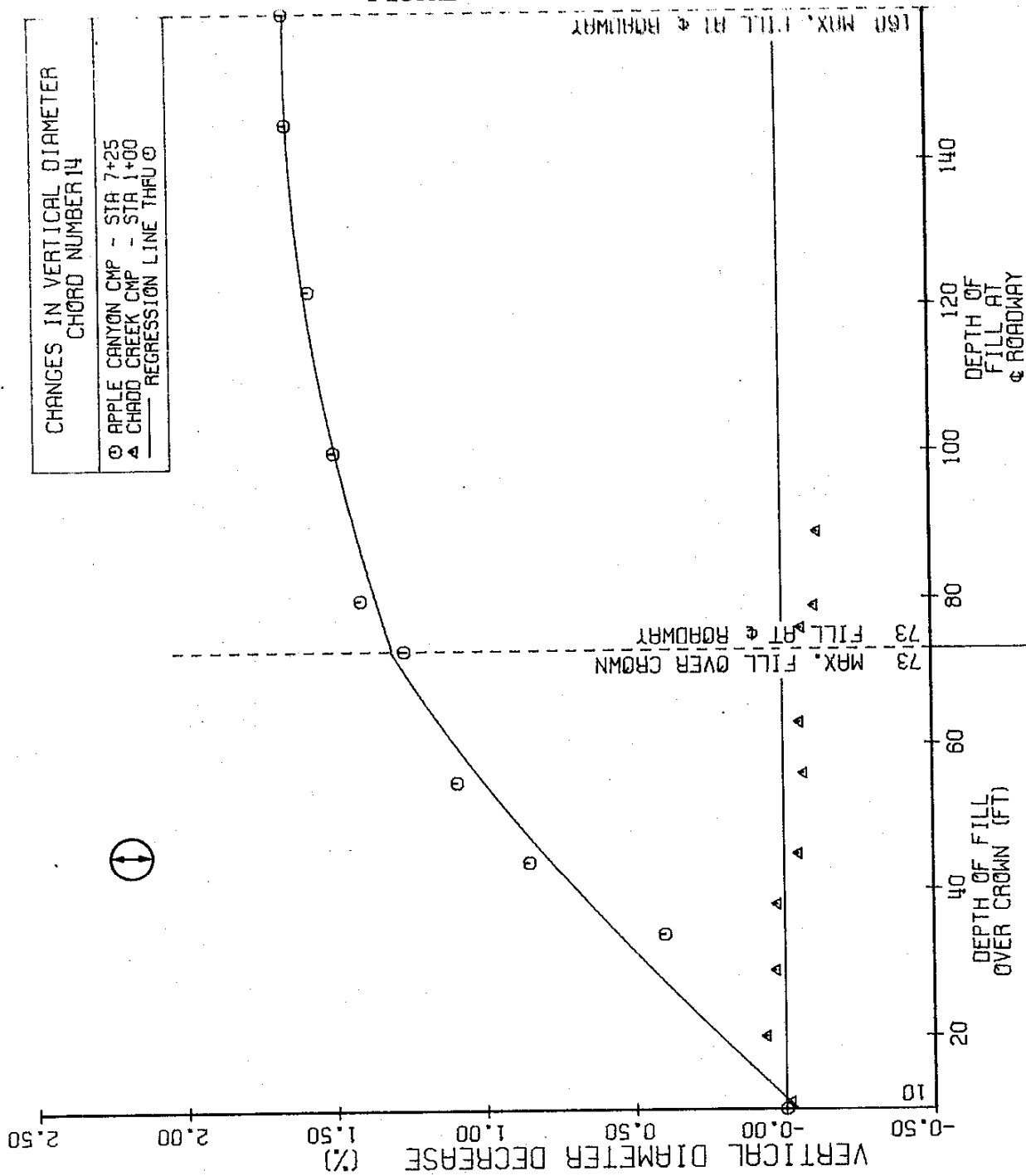


FIGURE 105

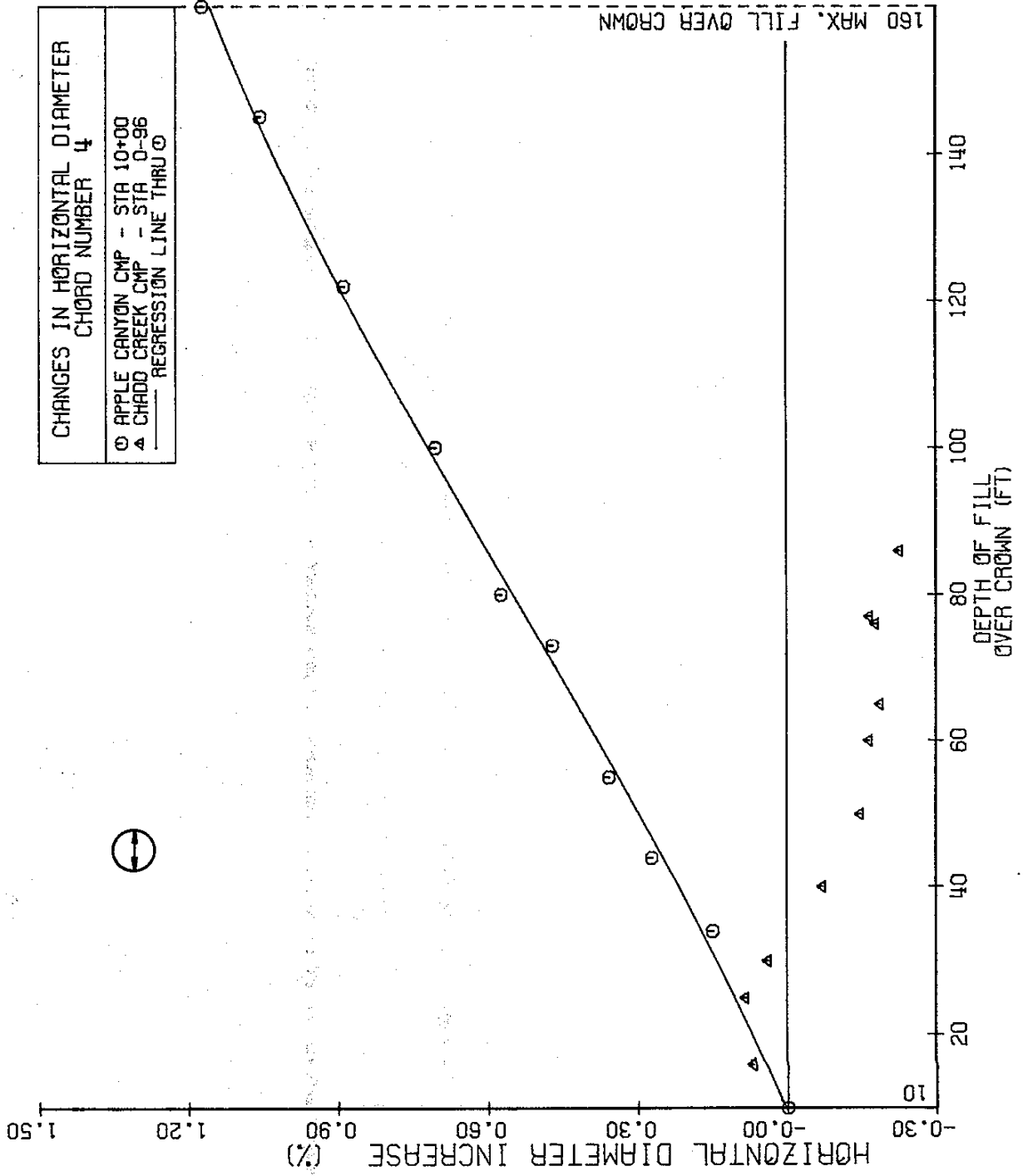


FIGURE 106

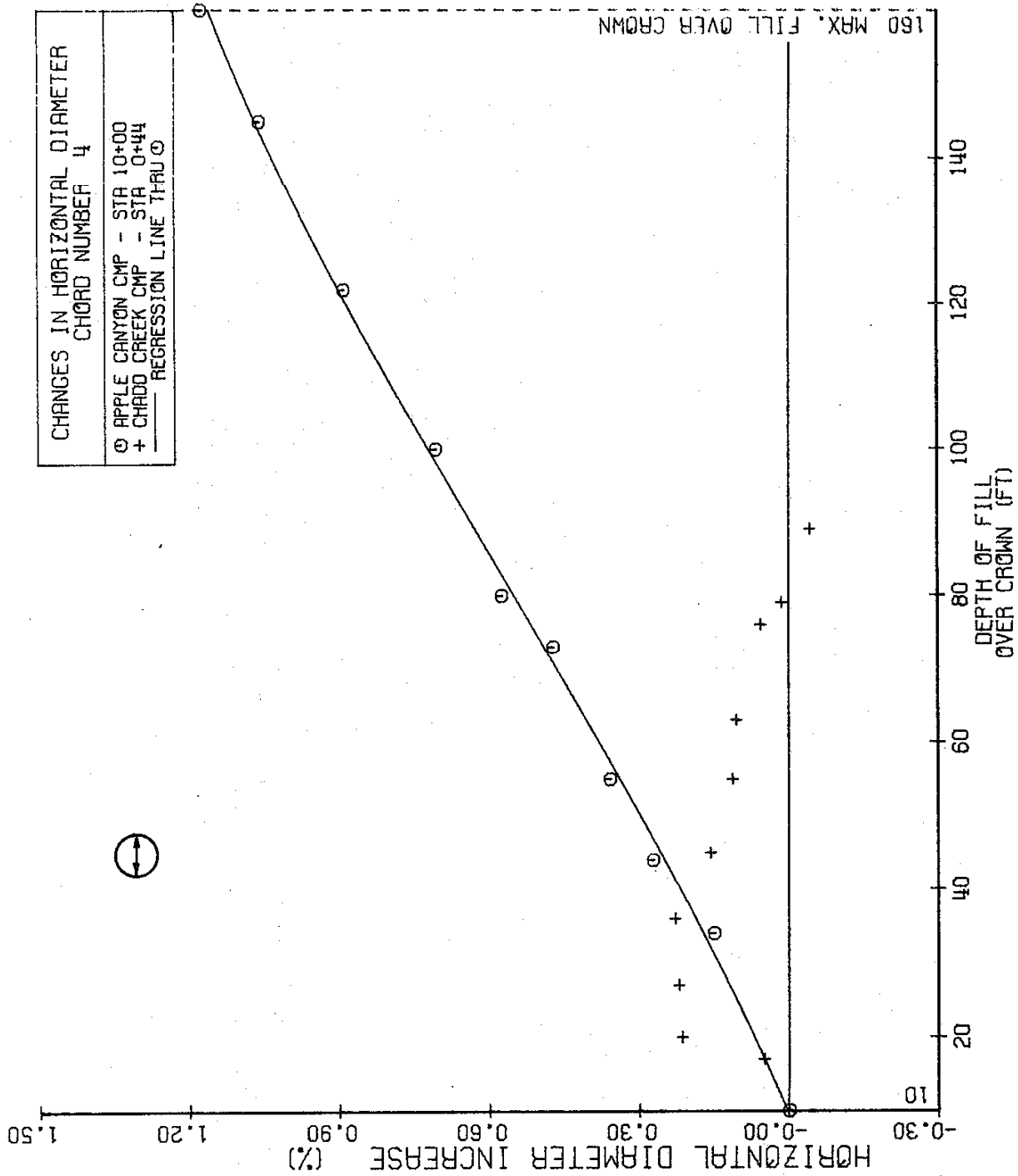


FIGURE 107

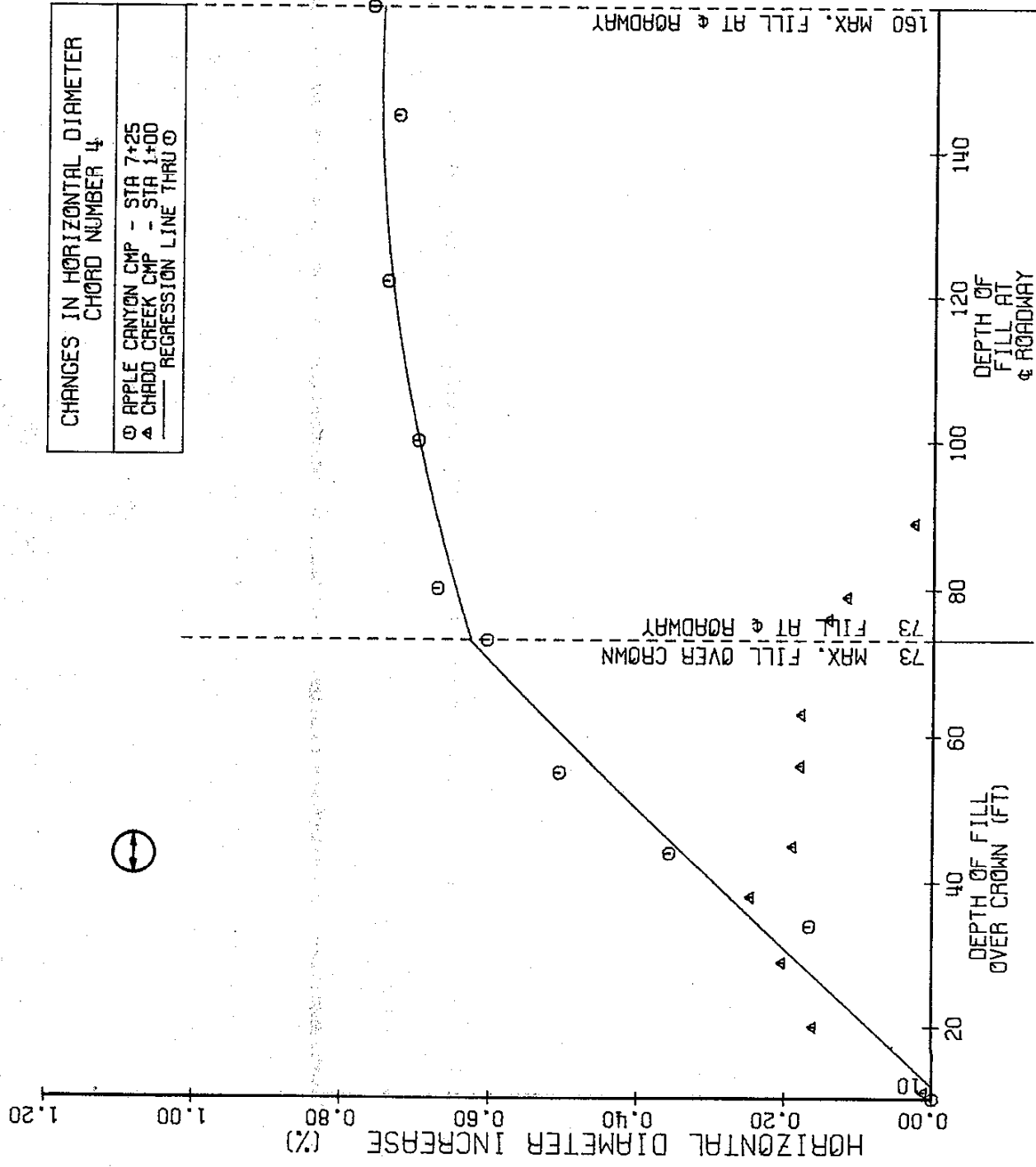
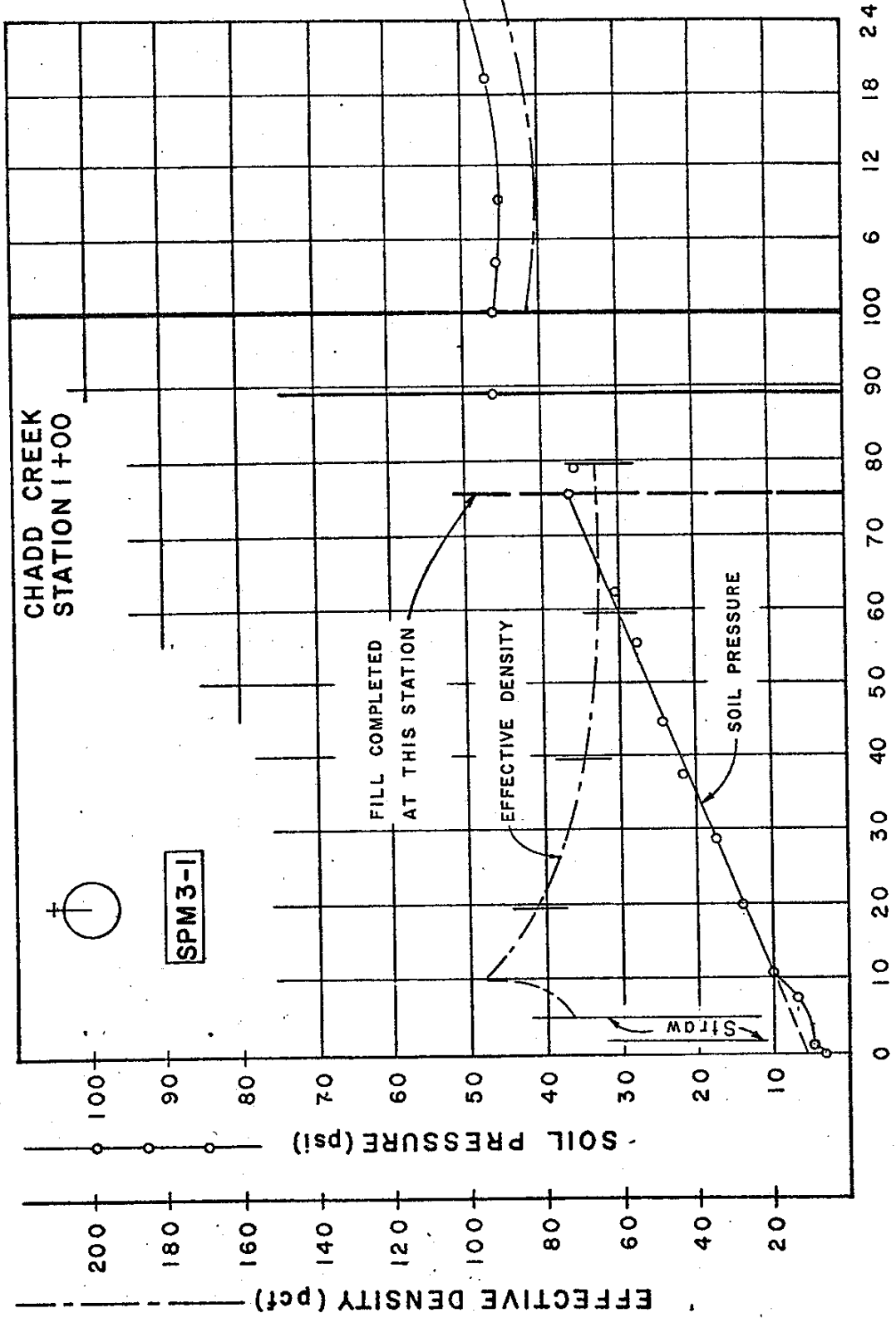


FIGURE 108



CHADD CREEK
STATION 1+00

SPM3-1

FILL COMPLETED
AT THIS STATION

EFFECTIVE DENSITY

SOIL PRESSURE

SITING

DEPTH OF FILL OVER SOIL METER (ft)

After max. fill is reached at designated station,
reference depth used is at culvert
station 0+44

TIME AFTER FILL
COMPLETED (mo)

EFFECTIVE DENSITY (pct)

SOIL PRESSURE (psi)

FIGURE 109

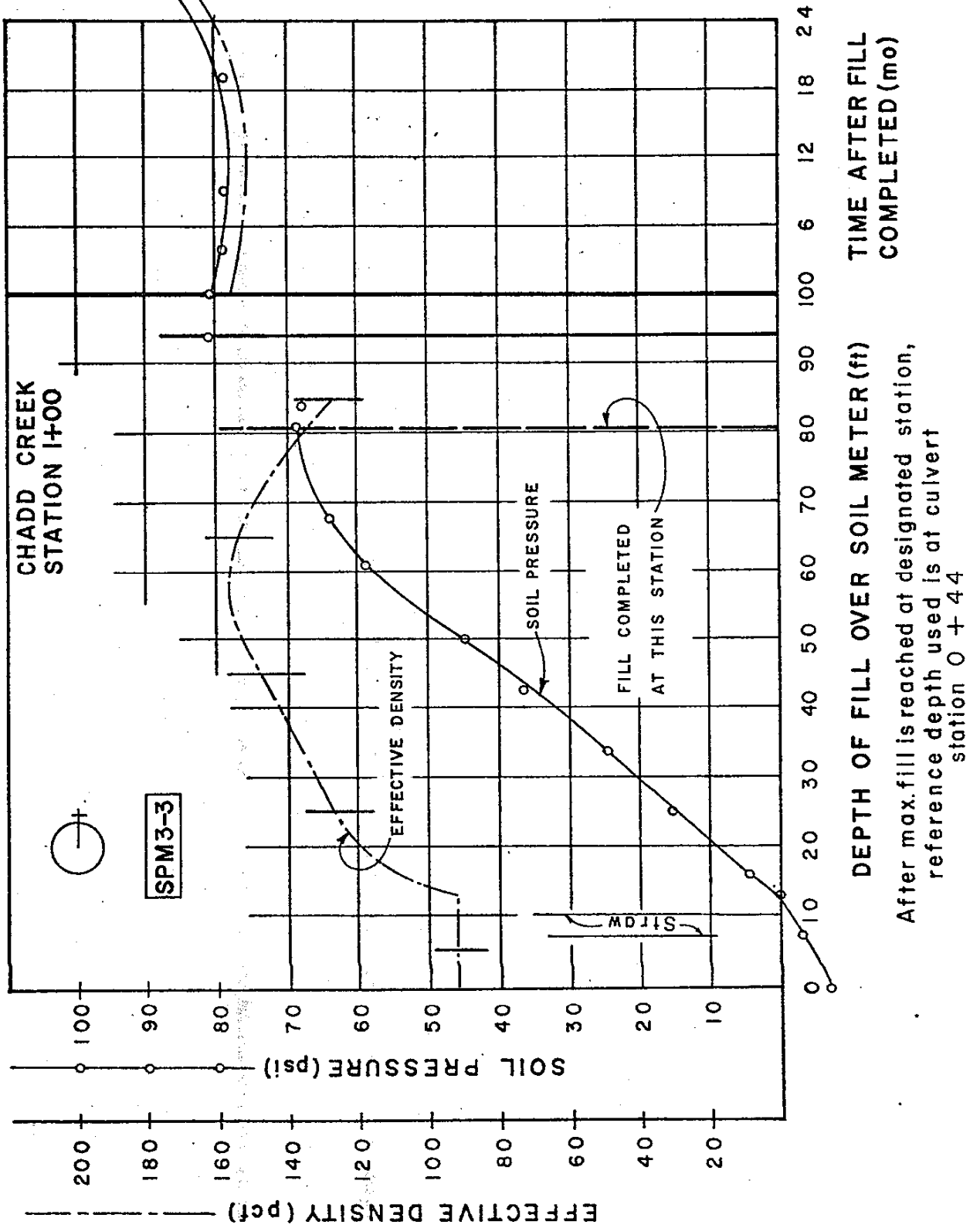
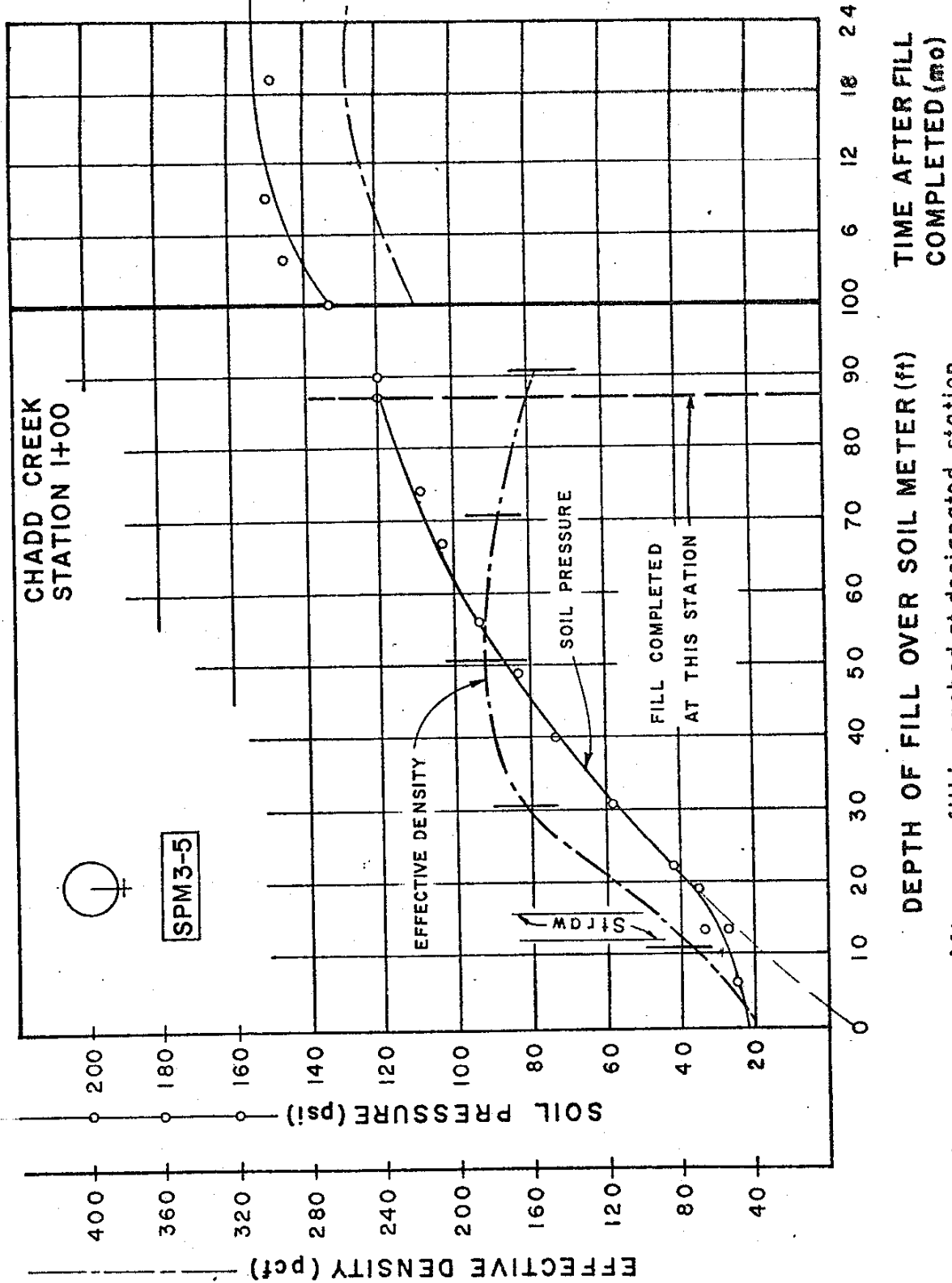
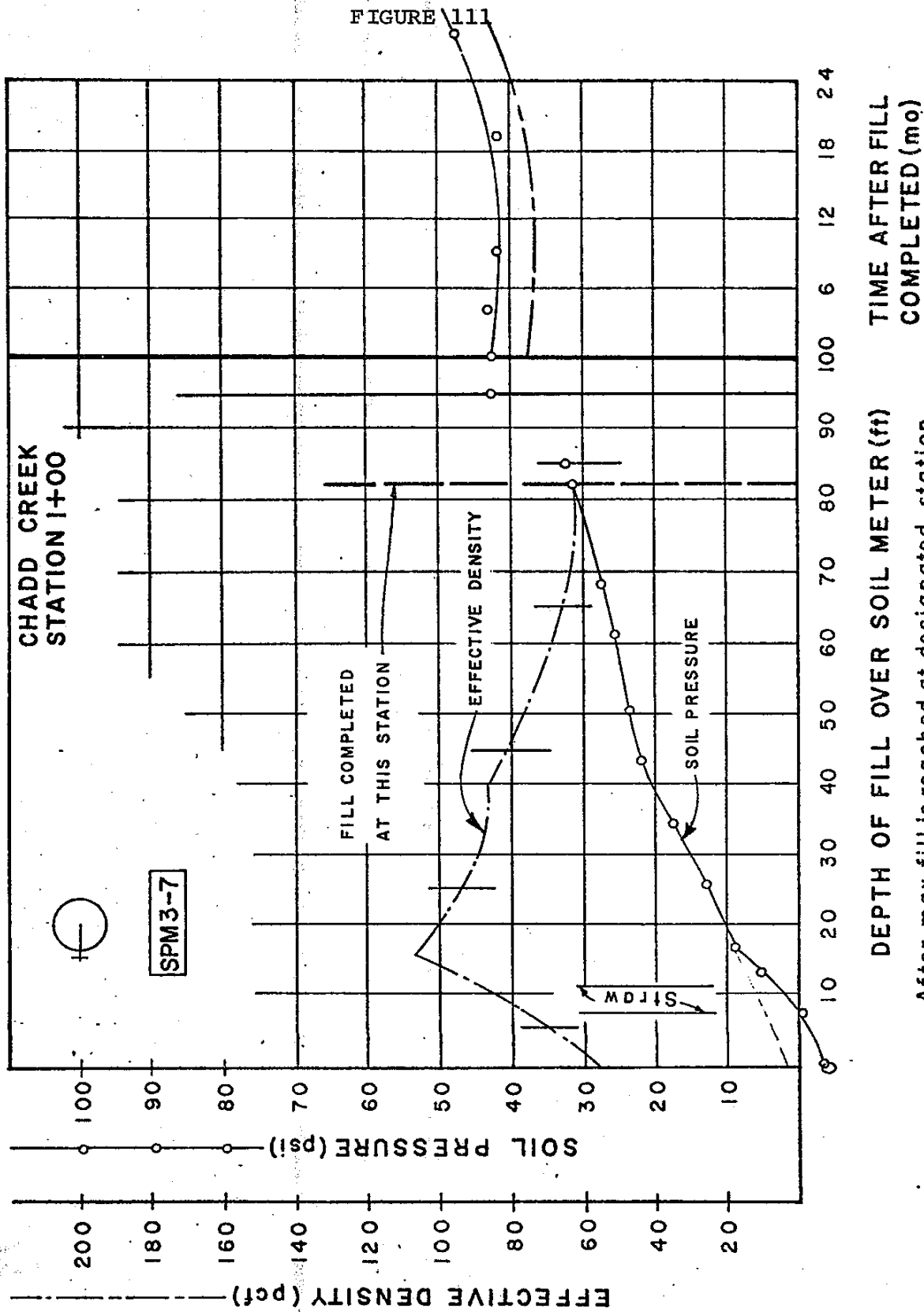


FIGURE 110



After max. fill is reached at designated station, reference depth used is at culvert station 0 + 44



DEPTH OF FILL OVER SOIL METER (ft)

After max. fill is reached at designated station,
reference depth used is at culvert
station 0 + 44

TIME AFTER FILL
COMPLETED (mo)

FIGURE 112

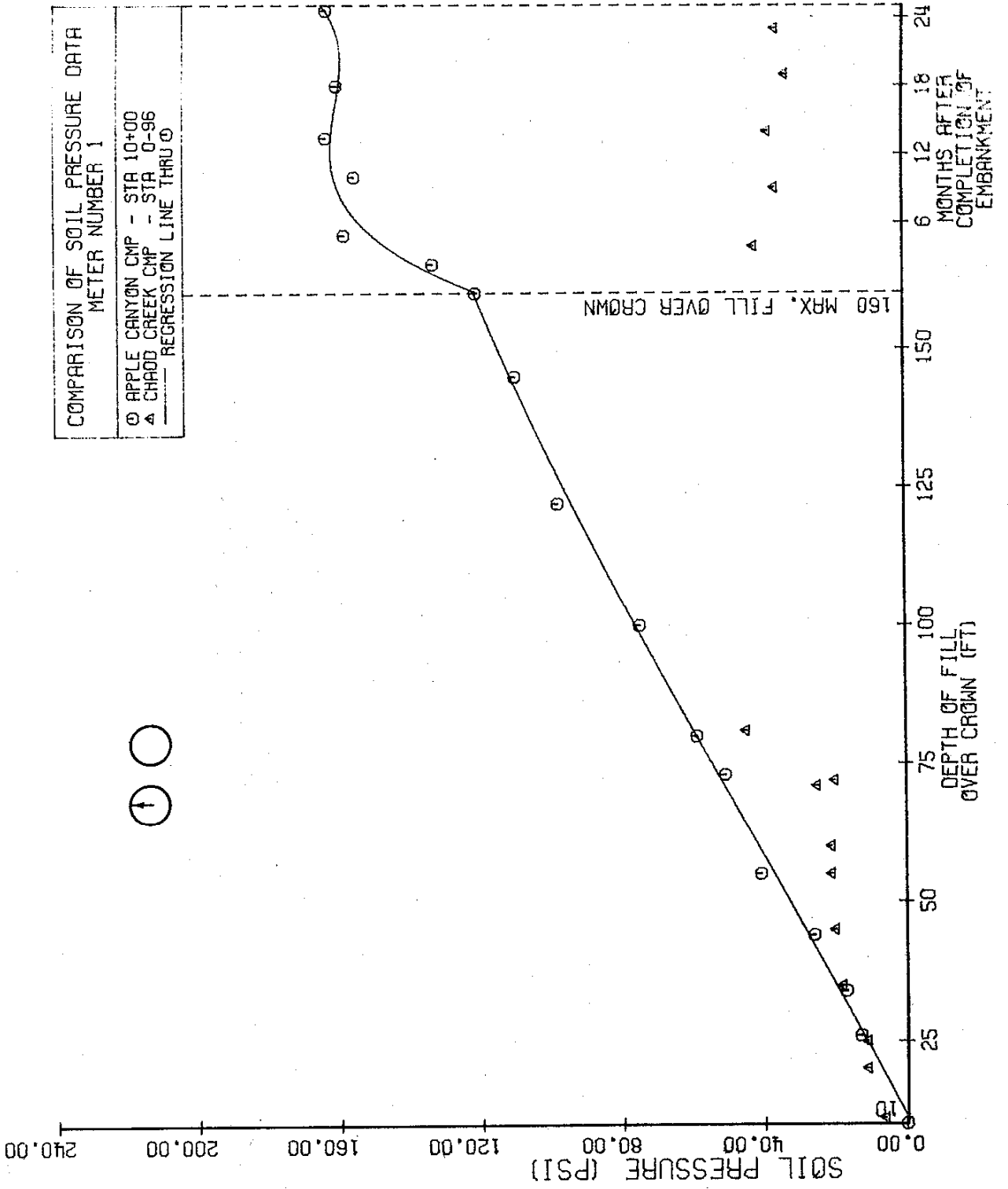


FIGURE 113

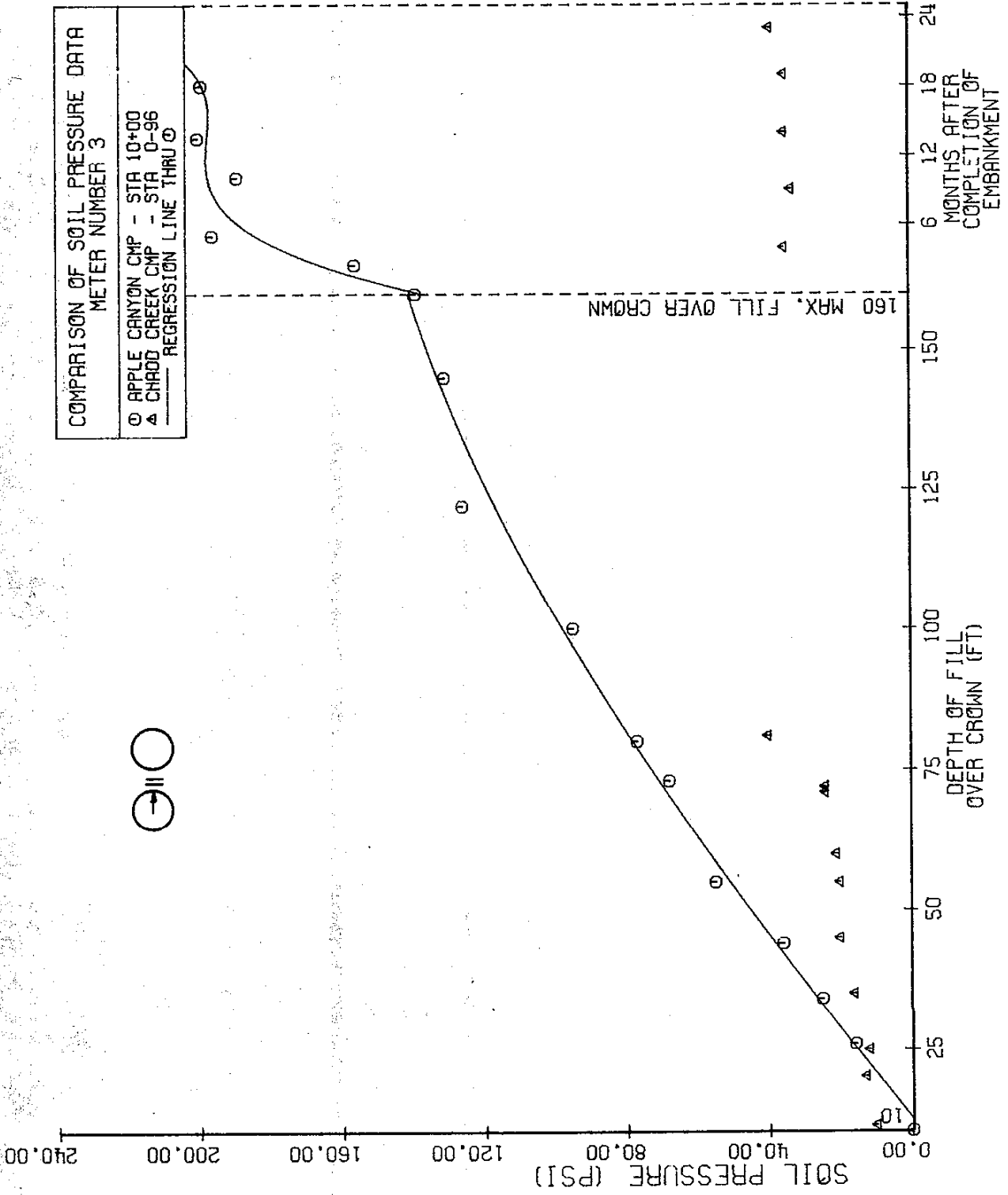


FIGURE 114

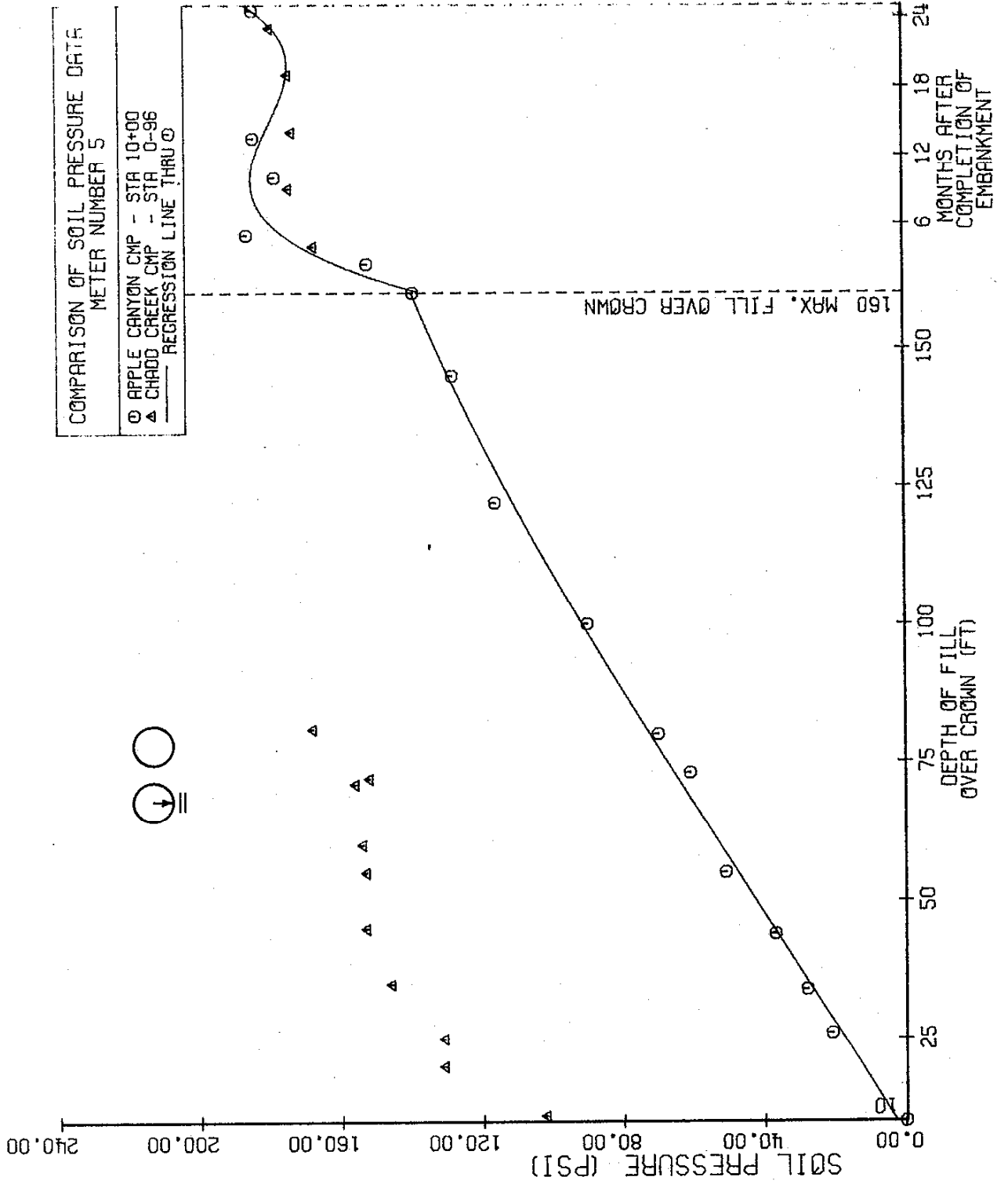


FIGURE 115

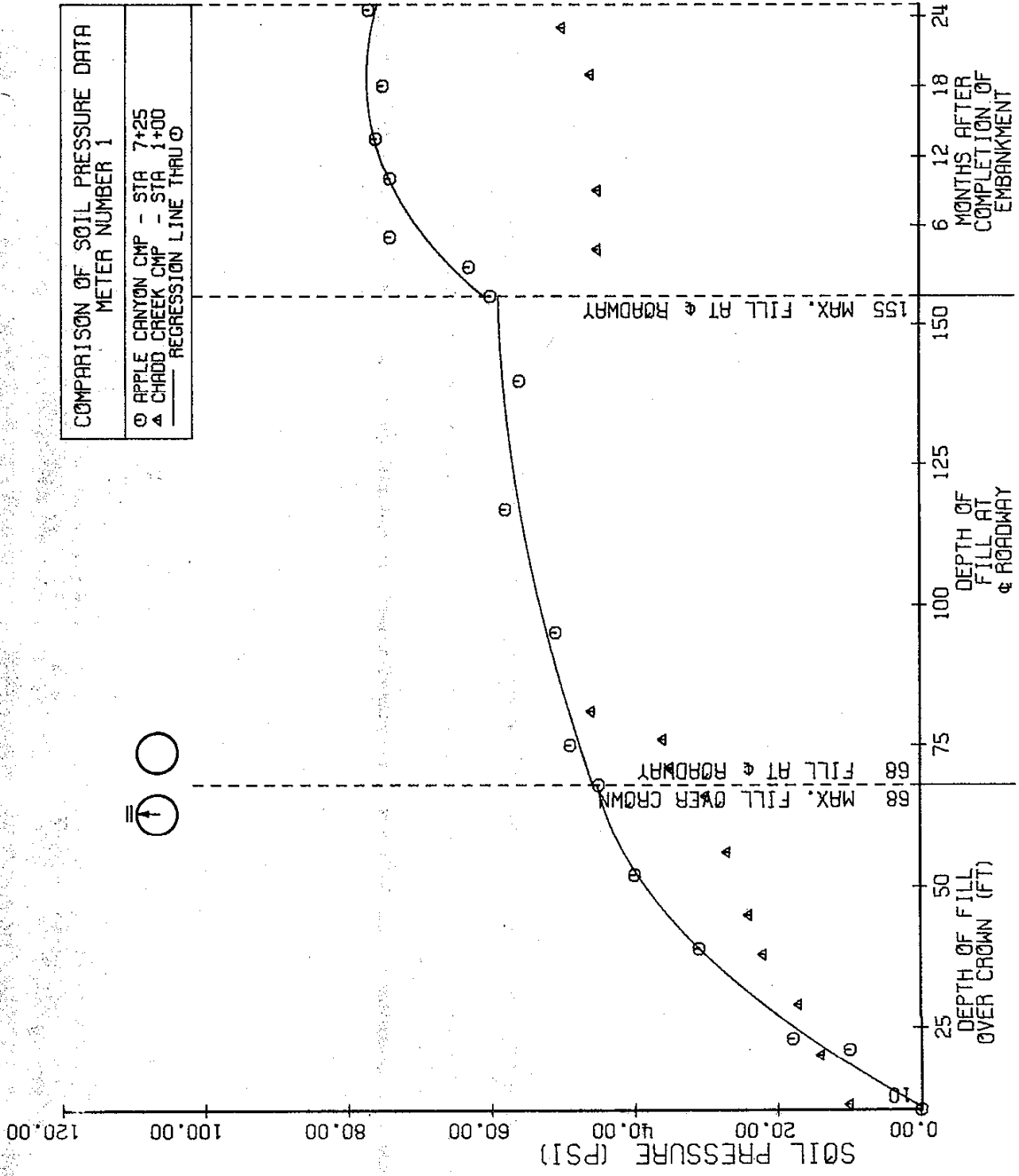


FIGURE 116

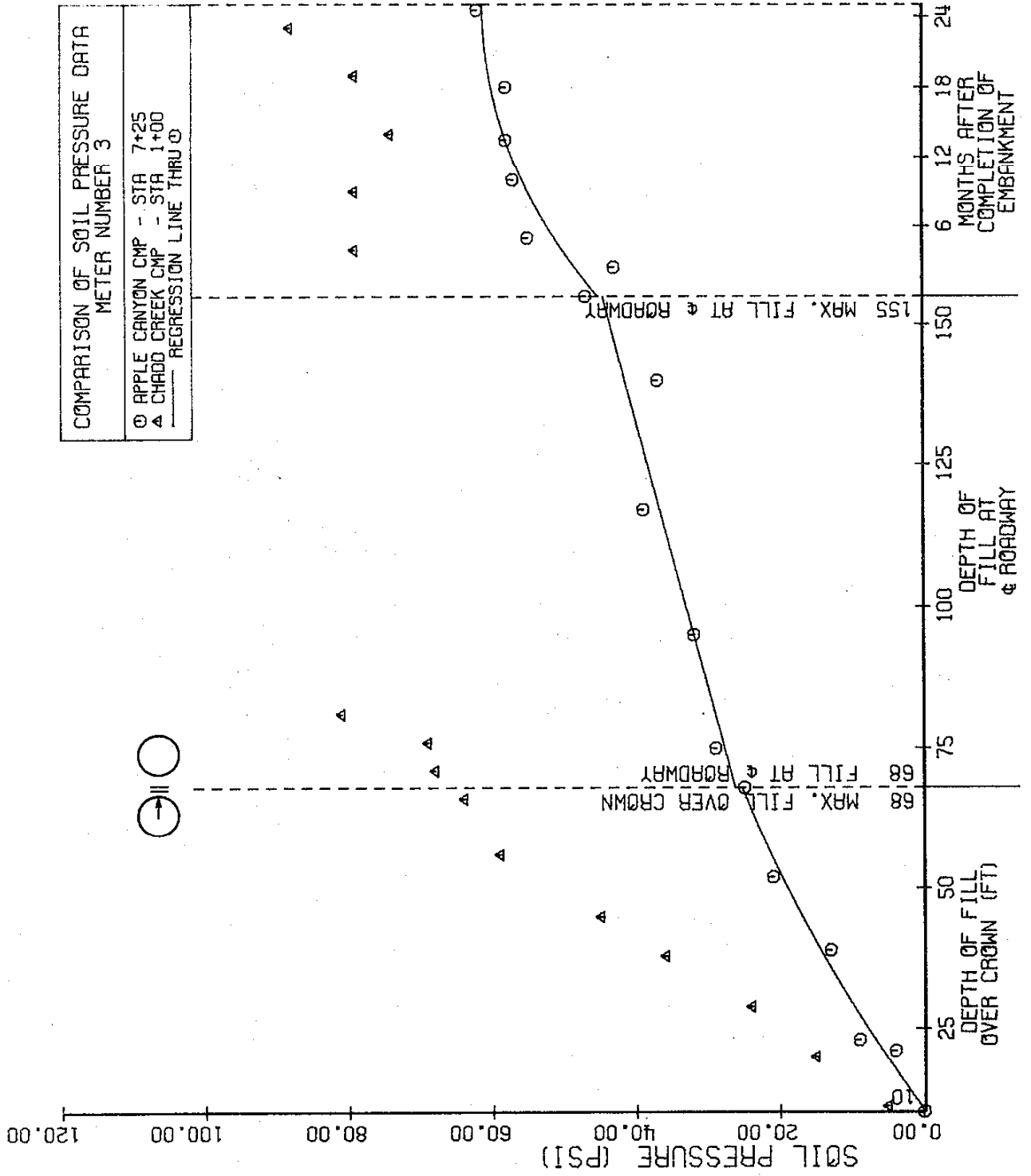


FIGURE 117

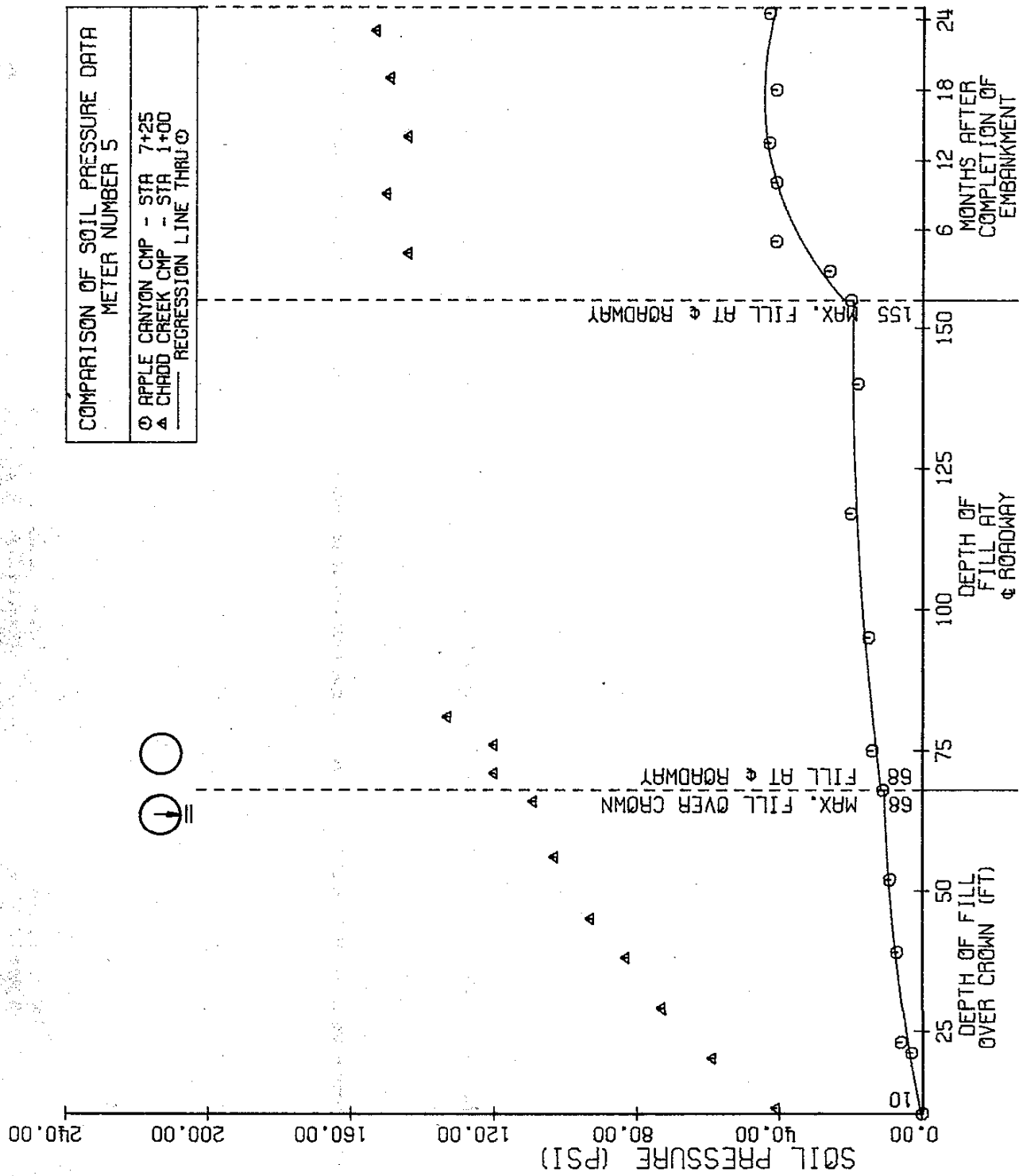
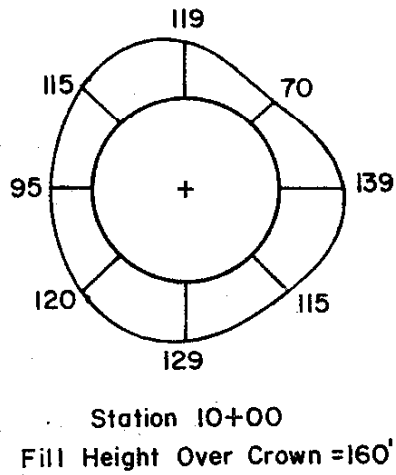
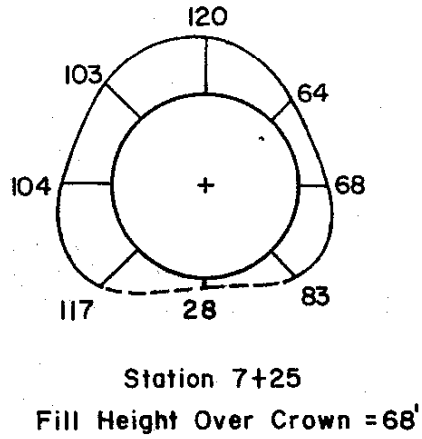
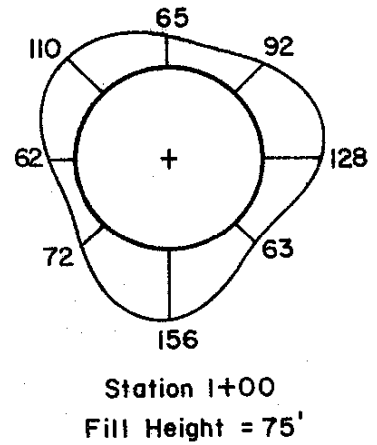
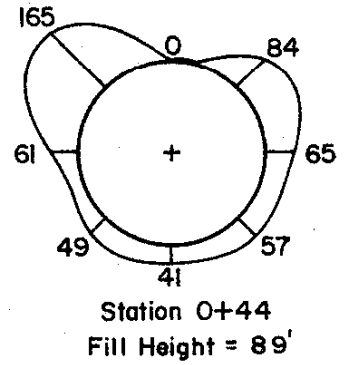
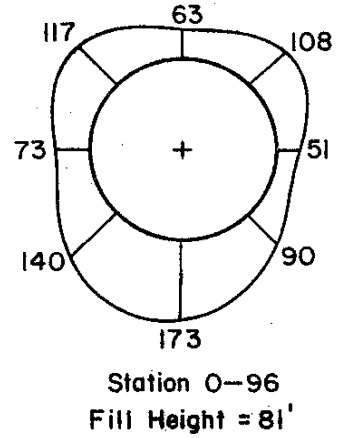


FIGURE 118

APPLE CANYON SPP
COMPARISON OF EFFECTIVE DENSITY PROFILES
AT TIME OF FILL COMPLETION



APPLE CANYON



CHADD CREEK

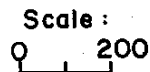
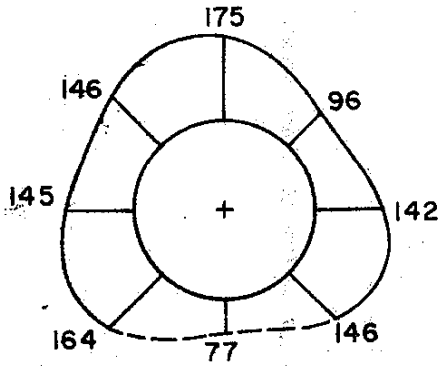
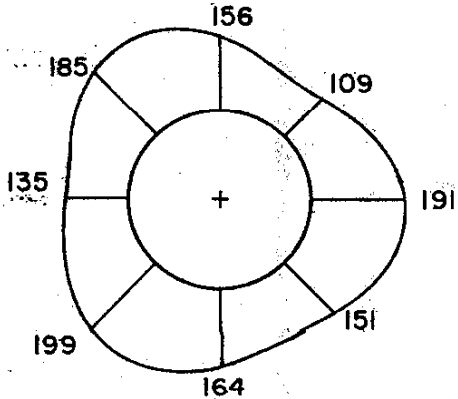


FIGURE 119

APPLE CANYON SPP
COMPARISON OF EFFECTIVE DENSITY PROFILES
AT 24 TO 28 MONTHS AFTER COMPLETION

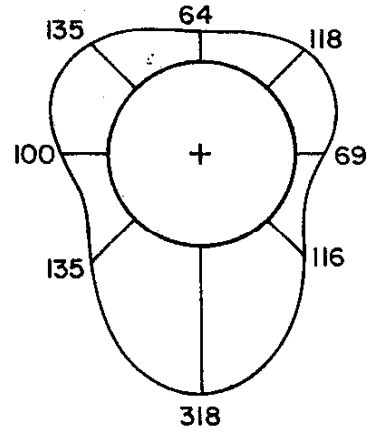


Station 7+25
Fill Height Over Crown = 68'
Time After Fill Completion = 24 mo.

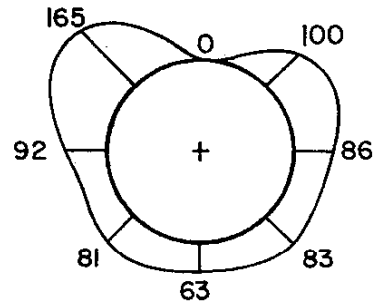


Station 10+00
Fill Height Over Crown = 160'
Time After Fill Completion = 24 mo.

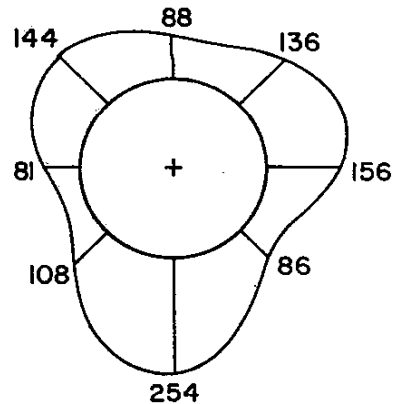
APPLE CANYON



Station 0-96
28 mo. After Fill Completion



Station 0+44
28 mo. After Fill Completion



Station 1+00
28 mo. After Fill Completion

CHADD CREEK

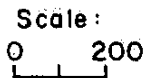
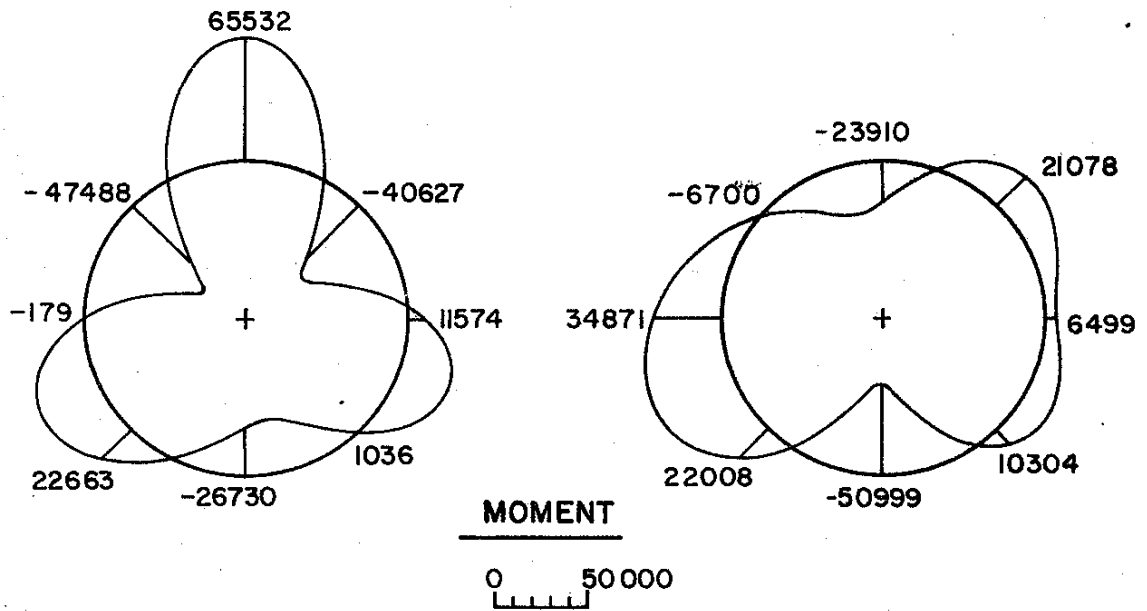
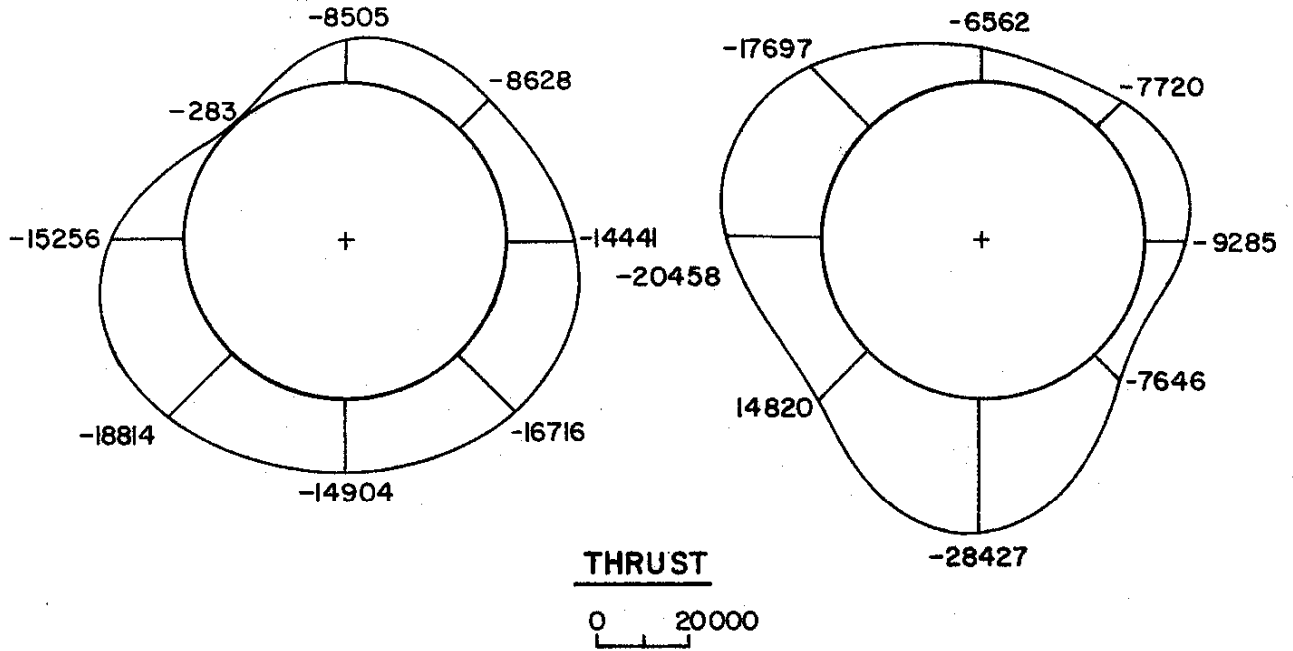


FIGURE 120

APPLE CANYON SPP
COMPARISON OF MOMENTS AND THRUSTS



CHADD CREEK
(AVERAGE)

APPLE CANYON
STATION 7+25

Appendix A

NON-LINEAR STRESS DEPENDENT SOIL PROPERTIES

The stress-strain behavior of soils is dependent on a large number of factors including density, composition, water content, stress history and confining pressure. Even when specimens are selected which duplicate field conditions, their behavior over a range of stresses is often non-linear. A simple method of representing the complex characteristics of soils was developed by Duncan and Chang and has been used successfully by several investigators (2, 12, 14) for various types of soils and placement conditions. This procedure has been used to determine the behavior of the fill at Apple Canyon and is employed in the Finite Element analysis.

The material properties of the Apple Canyon fill were derived from triaxial tests of remolded, unconsolidated, undrained specimens. Volumetric and axial strains were also measured during the tests. Plots of the deviator stress vs. axial strain, volumetric strain vs. axial strain and the Mohr-Coulomb failure envelope are depicted in Figures A-1 through A-3. From these curves, the parameters controlling the determination of Young's Modulus and Poisson's ratio may be determined.

The procedure for determining soil parameters for initial tangent modulus requires that a hyperbola of the form

$$(\sigma_1 - \sigma_3) = \frac{\epsilon_a}{a + b \epsilon_a} \quad (1)$$

be fitted to the triaxial test data. This equation may be transformed to,

$$\frac{\epsilon_a}{(\sigma_1 - \sigma_3)} = a + b\epsilon_a \quad (2)$$

where a and b become the parameters defining a straight line. The intercept, a, represents the reciprocal of the initial tangent modulus, $\frac{1}{E_i}$, and the slope, b, is the reciprocal of the ultimate deviator stress, $1/(\sigma_1 - \sigma_3)_{ult}$. Experiments have shown that a best fit straight line passes through points corresponding to 70 percent and 95 percent of the maximum deviator stress. Figure A-4 depicts the linear representation of the hyperbolae. The asymptotic limit of the hyperbola, $(\sigma_1 - \sigma_3)_{ult}$, is always larger than the maximum deviator stress from triaxial tests. To produce a more precise correlation between the hyperbolic function and empirical data, the function is modified by the failure ratio, R_f , given by,

$$R_f = (\sigma_1 - \sigma_3)_{max} / (\sigma_1 - \sigma_3)_{ult} \quad (3)$$

Soil stress-strain characteristics also depend on confining pressure. The variation of tangent modulus may be expressed as:

$$E_i = K P_a \left(\frac{\sigma_3}{P_a} \right)^n \quad (4)$$

where E_i and σ_3 are the initial tangent modulus and confining pressure, respectively. Atmospheric pressure is denoted by P_a . The variation in E_i with σ_3 is approximated by a straight line on a log-log plot, K and n being the intercept and slope. Such a plot is presented in Figure A-5.

The relationship between compressive strength and confining pressure is expressed in terms of the Mohr-Coulomb failure criterion by:

$$(\sigma_1 - \sigma_3)_{\max} = \frac{2C \cos \phi + 2\sigma_3 \sin \phi}{(1 - \sin \phi)} \quad (5)$$

where c and ϕ are the soil cohesion and angle of internal friction.

The tangent modulus is defined by the differential equation,

$$E_t = \frac{d(\sigma_1 - \sigma_3)}{d\epsilon}$$

After the indicated differentiation and appropriate substitution of equations 1, 3, 4 and 5, the expression for tangent modulus in terms of the stress state becomes,

$$E_t = \left[1 - \frac{R_f (1 - \sin \phi) (\sigma_1 - \sigma_3)}{2C \cos \phi + 2\sigma_3 \sin \phi} \right]^2 K P_a \left(\frac{\sigma_3}{P_a} \right)^n \quad (6)$$

The tangent Poisson's ratio is similarly defined as the rate of change of radial strain with axial strain, under axial compression and without radial restraint. The governing equation becomes,

$$\mu_t = - \frac{d\epsilon_r}{d\epsilon_a} \quad (7)$$

The average value of radial strain, ϵ_r , may be expressed in terms of measured volumetric strain by:

$$\epsilon_r = \frac{1}{2} (\epsilon_v - \epsilon_a)$$

A hyperbolic function of the form:

$$\epsilon_a = \frac{\epsilon_r}{f + d\epsilon_r} \quad (8)$$

may be used to express the non-linear relationship between axial and radial strain. Transformation of this equation into a linear form yields

$$\frac{\epsilon_r}{\epsilon_a} = f + d\epsilon_r \quad (9)$$

The straight line parameters f and d represent the initial Poisson's ratio and rate of variation of ϵ_a with ϵ_r . As for initial modulus, the points representing 70 percent and 95 percent of maximum radial strain yield a best fit line. See Figure A-6.

The stress dependency is expressed by the function,

$$\mu_i = G - F \log \left(\frac{\sigma_3}{P_0} \right) \quad (10)$$

where μ_i is initial Poisson's ratio, G is Poisson's ratio at one atmosphere confining pressure and F represents the rate of decrease in μ_i with σ_3 . Plotting f against $\log \frac{\sigma_3}{P_0}$ yields a straight line from which G and F are found.

Figure A-7 depicts such a plot.

Again appropriate differentiation and substitution into the governing equation yields an expression for Poisson's ratio in terms of the above parameters and the soil stress state.

The equation,

$$\mu_f = \frac{G - F \log \left(\frac{\sigma_3}{P_0} \right)}{\left[1 - \frac{d - (\sigma_1 - \sigma_3)}{\left[1 - \frac{R_f (1 - \sin \phi) (\sigma_1 - \sigma_3)}{2C \cos \phi + 2\sigma_3 \sin \phi} \right] K P_0 \left(\frac{\sigma_3}{P_0} \right)^n} \right]^2} \quad (11)$$

uses the five tangent modulus parameters and three strain parameters.

For the particular data obtained from the Apple Canyon fill, it appears that the test using a confining pressure of 4 k.s.c. may be in error. The stress-strain relationship (Figure A-1) indicates an anomaly in the family of curves at low axial strain.

Similarly, the volumetric vs. axial strain plot, Figure A-2,

reveals a truncated curve prior to reaching maximum volumetric strain. These anomalies are further indicated in Figure A-5 where the initial tangent modulus deviates markedly from a least-squares fit through the remaining points. Based on these observations, the triaxial test data for a confining pressure of 4 ksc were deleted during parameter determination. The soil parameters are shown in Table A-1.

As a check on the soil parameter accuracy, the theoretical stress-strain curves for each triaxial test were constructed. Empirical and theoretical curves are shown in Figure A-8. A close correlation appears between the two families of curves, indicating that the soil parameters accurately model the actual fill behavior.

Of extreme interest is the fact that the tangent modulus does not appear to be a function of confining pressure. This is an idiosyncrasy of this particular soil. Hence, it is expected that non-linear analyses may not deviate significantly from linear-elastic results.

Table A-1

Summary of Soil Parameters

R_f	=	.09378
k	=	1264.2683
n	=	-0.03458
c	=	1.43313
ϕ	=	27.8755 $^\circ$ = 0.48652 rad
d	=	6.971
G	=	0.23798
F	=	0.14676

FIGURE A-1

APPLE CANYON SSP
STRESS - STRAIN RELATIONS
FOR TRIAXIAL TESTS

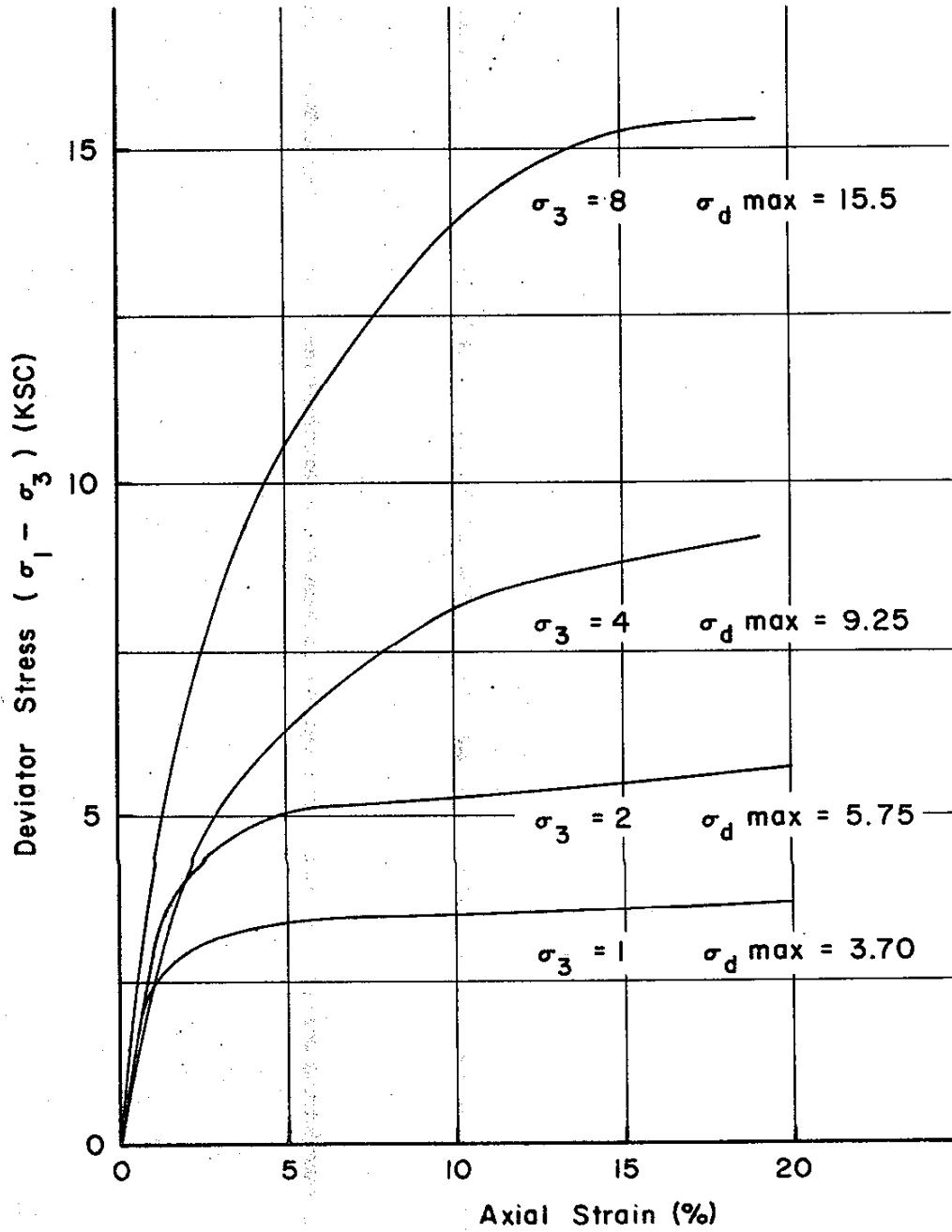
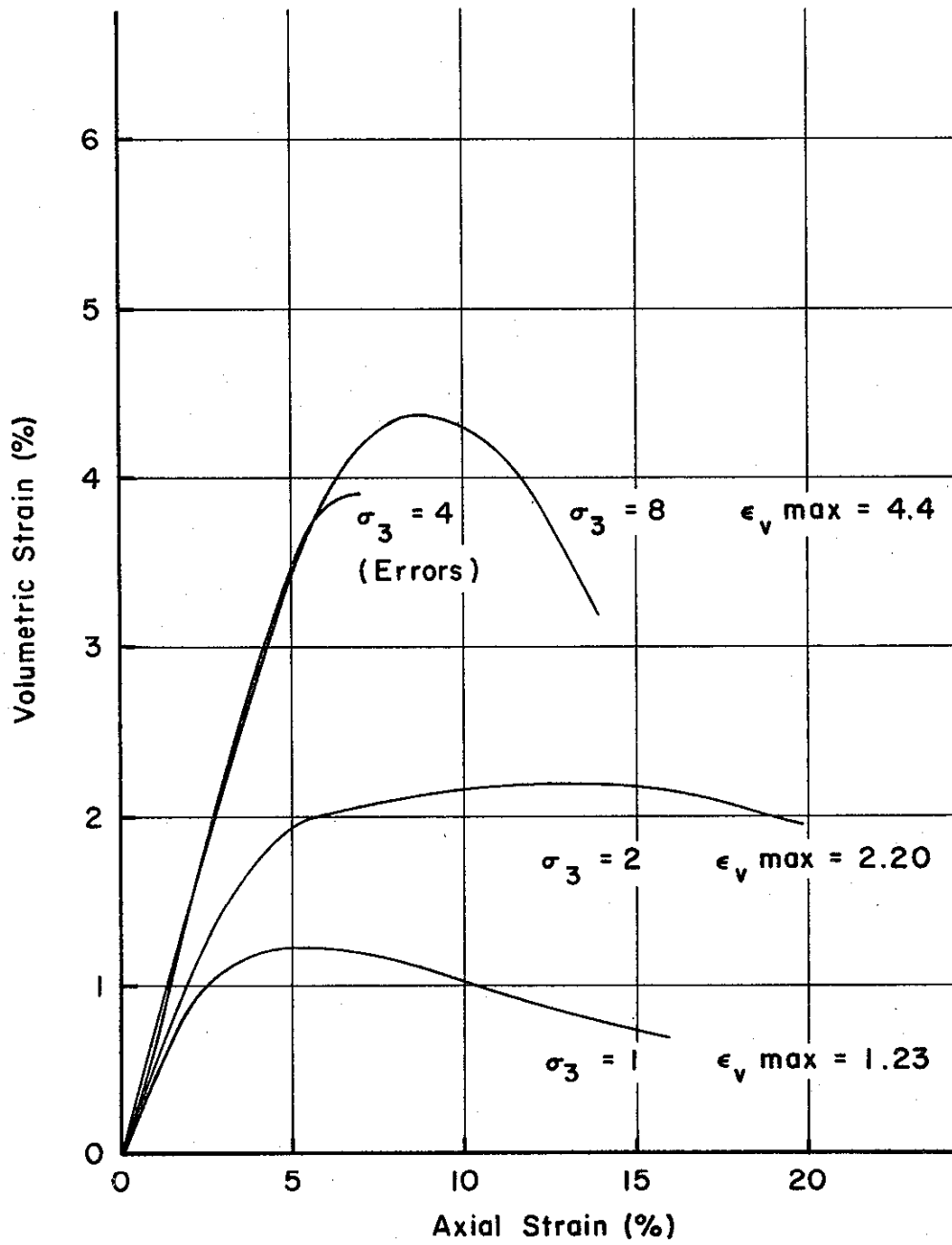


FIGURE A-2

APPLE CANYON SSP
AXIAL-VOLUMETRIC STRAIN
RELATIONS FOR TRIAXIAL TESTS



APPLE CANYON SSP
FAILURE ENVELOPE FOR U-U TRIAXIAL TESTS

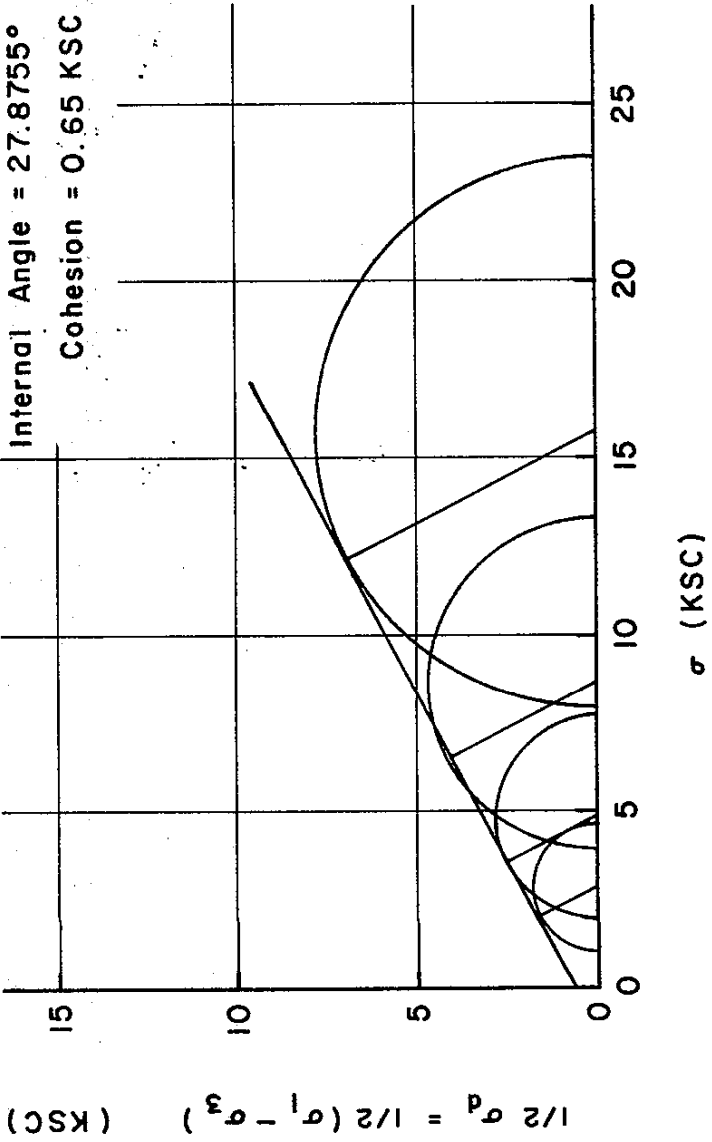


FIGURE A-3

FIGURE A-4

APPLE CANYON SSP
TRANSFORMED HYPERBOLIC REPRESENTATION
OF STRESS - STRAIN CURVE

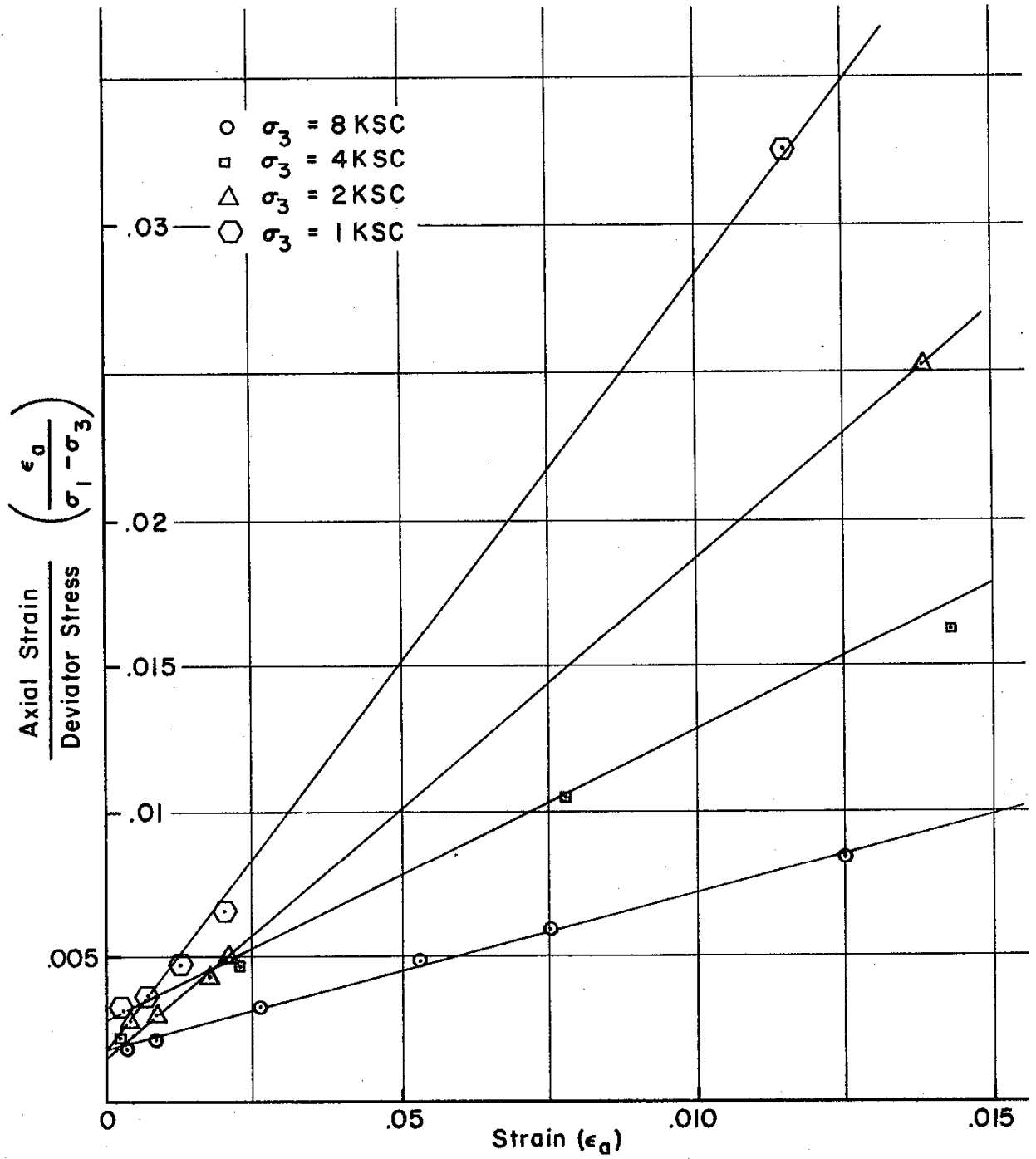


FIGURE A-5

APPLE CANYON SSP
VARIATION IN INITIAL TANGENT MODULUS
WITH CONFINING PRESSURE

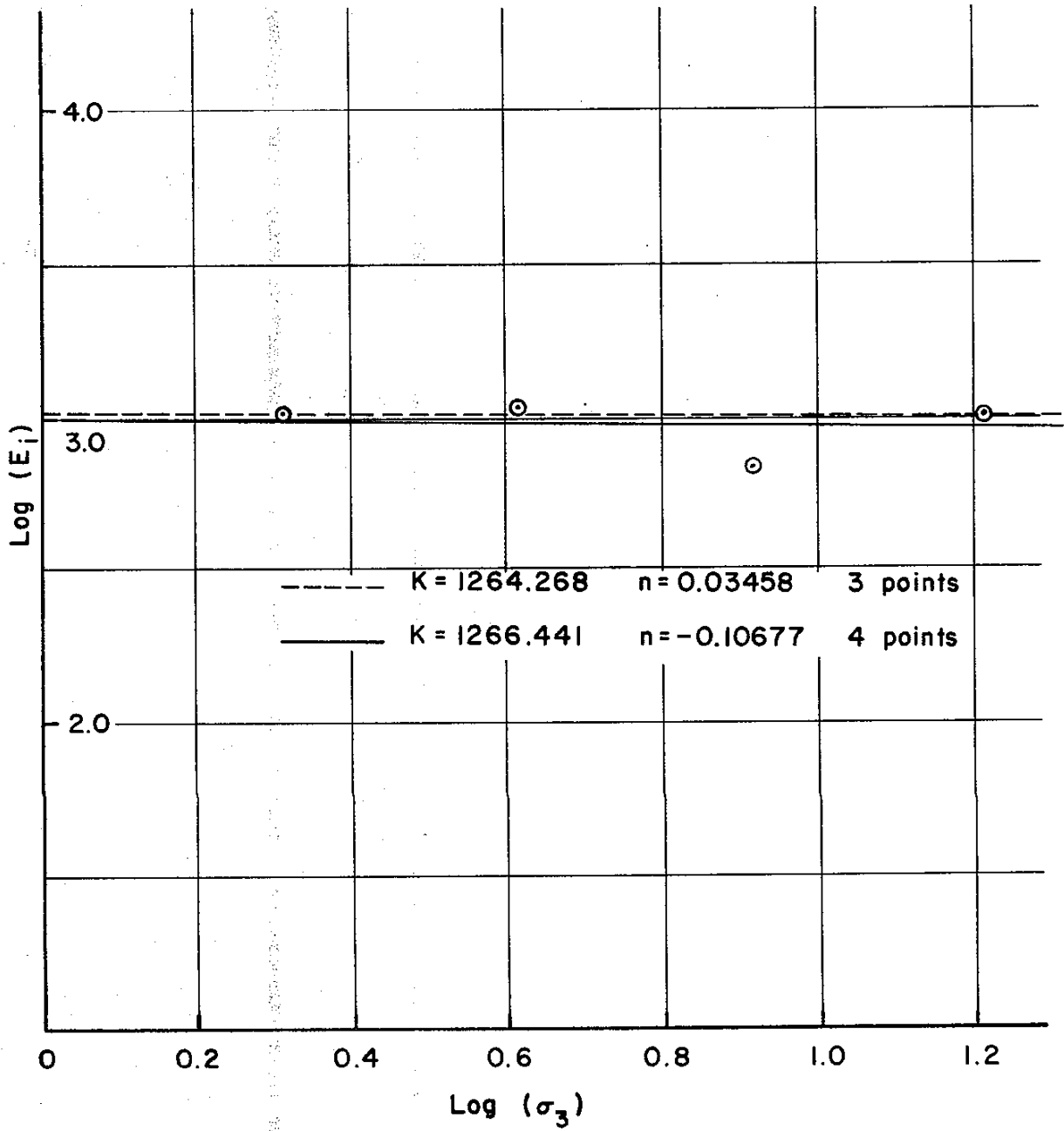


FIGURE A-6

APPLE CANYON SSP
 TRANSFORMED HYPERBOLIC REPRESENTATION
 OF RADIAL STRAIN—AXIAL STRAIN RELATIONS

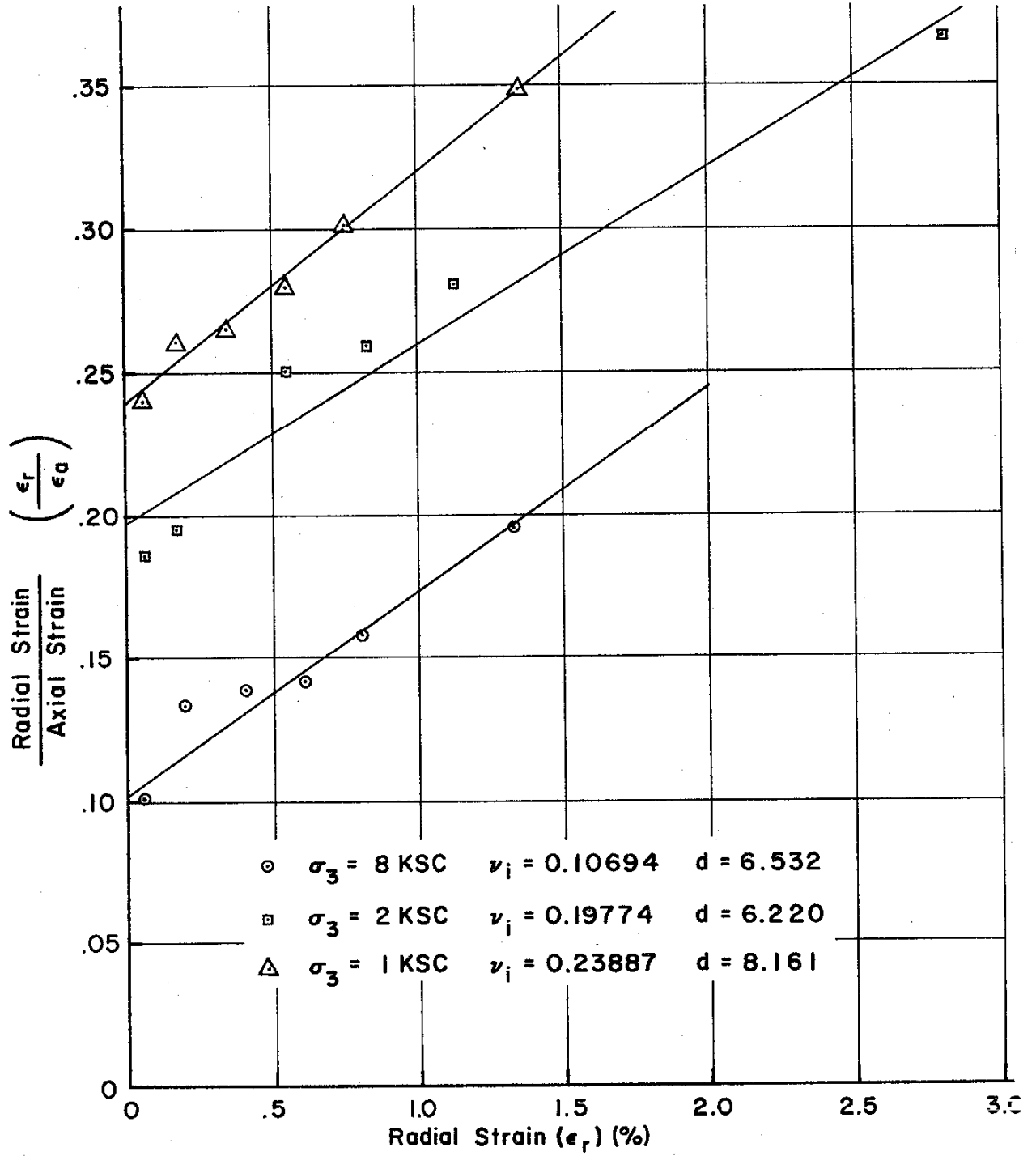


FIGURE A-7

VARIATION IN INITIAL POISSON'S RATIO
WITH CONFINING PRESSURE

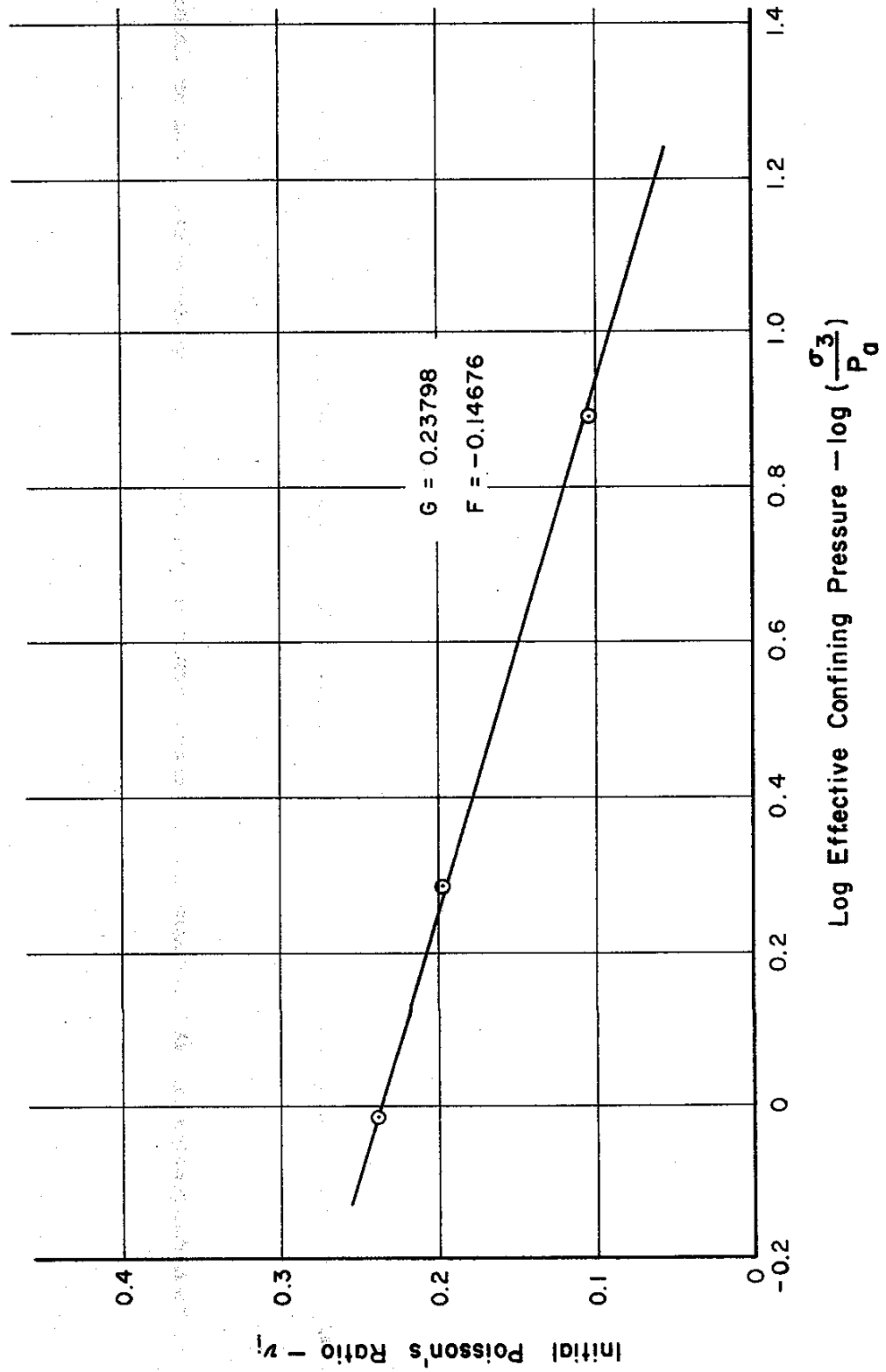


FIGURE A-8

THEORETICAL AND EMPIRICAL STRESS-STRAIN RELATIONS

